Applications and Industry®

N.Y.

November 1959

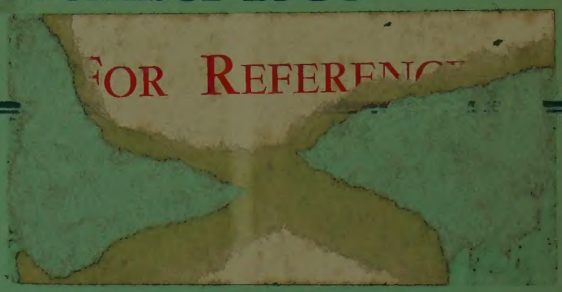

Transactions Papers

NUMBER 45

Published Bimonthly by

AMERICAN INSTITUTE OF ELECTRICAL ENGINEERS

Communication and Electronics—November 1959

(See inside back cover)

Note to Librarians. The six bimonthly issues of "Applications and Industry," March 1959–January 1960, will also be available in a single volume (no. 78) entitled "AIEE Transactions—Part II. Applications and Industry," which includes all technical papers on that subject presented during 1959. Bibliographic references to Applications and Industry and to Part II of the Transactions are therefore equivalent.

Applications and Industry. Published bimonthly by the American Institute of Electrical Engineers, from 20th and Northampton Streets, Easton, Pa. AIEE Headquarters: 33 West 39th Street, New York 18, N. Y. Address changes must be received at AIEE Headquarters by the first of the month to be effective with the succeeding issue. Copies undelivered because of incorrect address cannot be replaced without charge. Editorial and Advertising offices: 33 West 39th Street, New York 18, N. Y. Nonmember subscription $8.00 per year (plus 75 cents extra for foreign postage payable in advance in New York exchange). Member subscriptions: one subscription at $5.00 per year to any one of three divisional publications: Communication and Electronics, Applications and Industry, or Power Apparatus and Systems: additional annual subscriptions $8.00 each. Single copies when available $1.50 each. Second-class mail privileges authorized at Easton, Pa. This publication is authorized to be mailed at the special rates of postage prescribed by Section 132.122.

Printed in United States of America

Number of copies of this issue 5,500

Load Characteristics of a Submerged-Arc Silicon-Smelting Furnace

GEORGE GRANT III
MEMBER AIEE

SUBMERGED-arc furnaces have been in commercial operation for more than 50 years. However, the literature tells little about what they require from the supplier of the electric energy or what effects they have on the supply system. A silicon-smelting furnace is typical of these operations. In fact, this process is generally considered to be one of the most exacting in its demands for precise operation to prevent undesirable performance of the furnace and unreasonable demands on the electricity supplier. This paper presents information on the electrical performance of such a furnace.

Equipment

Fig. 1 outlines the power circuit to the furnace. The utility company's supply of 46 kv is stepped down through a 10-mva (megavolt-ampere) transformer to 14.4 kv. It is then regulated by a step voltage regulator to 14.0 kv to the plant substation delta-connected bus. The circuit to the furnace building goes from this bus through a 500-mva air-magnetic circuit breaker and armored aerial cable. In the building, the auxiliary power transformer is connected directly to this cable while the 6.0-mva furnace transformer is connected through a disconnect and air-magnetic circuit breaker. Built into this transformer is added reactance, adjustable in five steps from the inherent 6.7%, to 31.2%. The low voltage of the transformer is connected to interleaved copper bar. This bus bar is terminated and the delta connection closed at the flexible leads to the electrode clamps. Six electrode voltages may be selected at the operating panel through a remote control no-load tap changer in the transformer.

Control of the electrical load is attained by raising the electrodes to reduce the current and lowering them to increase the load. This is done with reversing electric motors driving hydraulic pumps which activate pistons that support the electrode with cables. Either manual or automatic control is available. The automatic control is piloted by a float-action current relay and each electrode is regulated independently.

Process

Description

The process of smelting silicon consists of heating silica (silicon dioxide) with carbon. Carbon combines with the oxygen in the silica rock to form carbon monoxide and leaves the silicon in a molten state at the bottom of the furnace. The silicon is tapped from the furnace at regular intervals. Fresh mix or charge of silica and carbon is fed into the furnace from the top and banked around and between the electrodes. This is shown as *C* in Fig. 2. As the mix works its way down into the hot reaction zone toward the bottom, the carbon monoxide flows up through it. The carbon reaches the reaction zone to combine with the oxygen of the silica because it is protected from air by this blanket of carbon monoxide.

Conducting paths between electrodes are produced by the carbon in the charge. The conductivity of this path consists of a multitude of contacts and small arcs which continually change as the mix moves toward the bottom of the furnace and as the reduction process proceeds. Electric energy also goes from the electrodes through arcs to the metal in the bottom of the hearth. As a result, several factors affect the electric load in the furnace, with the multiple paths through the mix continually tending to make the load unsteady. By proper control of the mix and by the use of the proper voltage, the variations in conductivity through the multiple paths can be made to cancel one another and produce an over-all conductivity that is relatively steady.

Power Requirements

Ideal scheduling of operations calls for 24-hour operation at 6.0 mva. In practice, a monthly operating time factor of more than 90% is maintained. Most days do 97% or better. Maximum operating time is desirable both because of increased production and because delays upset the furnace.

When the power is shut off, the reaction stops and the reaction zone starts to cool. Carbon then starts to burn out of the charge because there is no protective carbon monoxide. The burning of the carbon disturbs the proportions of the mix and reduces the conductivity. Conductivity is further reduced by the cooling. This reduction in conductivity can become so great that the furnace cannot be restarted with the available voltages.

During the course of a month, shutdowns must be scheduled to make mechanical repairs. It has been found that both the duration of the shutdown and the condition of the furnace at the time of shutdown influence the ability to start up again. When the furnace was in good condition, it was started quite easily after a 48-hour outage. On the other hand, with the furnace in poor condition, an 8-hour delay has made restarting doubtful. Consequently, all scheduled shutdowns are aimed at less than 8 hours to minimize this chance of not getting started. Thus, it is difficult to state a maximum safe period for power discontinuity, but less than 8 hours can always be tolerated.

The process is not particularly sensitive to voltage variations but the electrical performance is. A 5% change causes changes in performance that are noticeable at once and become troublesome if maintained for more than 30 minutes. However, when a change of this nature arises, it is counteracted by changing taps on the transformer. A drop in the supply voltage is more desirable than an increase

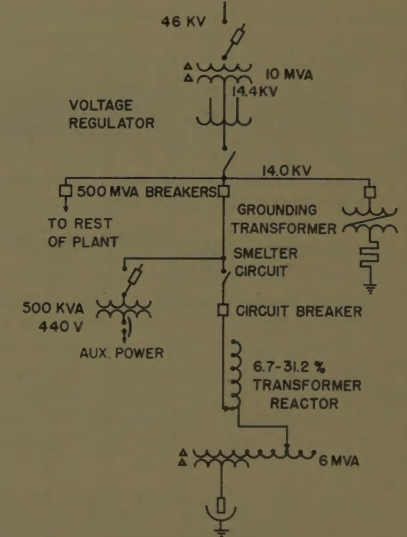

Fig. 1. Power circuit

Paper 58-1259, recommended by the AIEE Industrial and Commercial Power Systems Committee and approved by the AIEE Technical Operations Department for presentation at the AIEE Fall General Meeting, Pittsburgh, Pa., October 26–31, 1958. Manuscript submitted June 25, 1958; made available for printing September 9, 1958.

GEORGE GRANT, III, is with the Dow Corning Corporation, Midland, Mich.

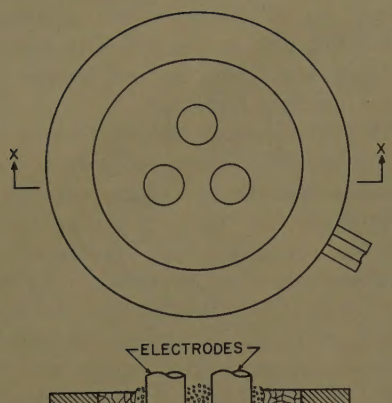

Fig. 2. Idealized section of furnace

A—Arc from electrode to metal
B—Burned-out mix, silica, and ash with no carbon
C—Fresh mix
R—Ceramic refractory
RC—Carbon refractory

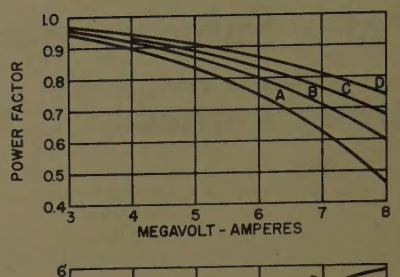

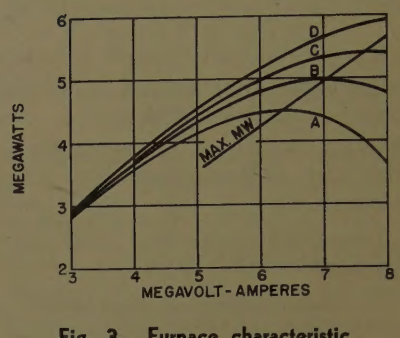

Fig. 3. Furnace characteristic

Transformer = 6.0 mva, 6.7% reactance
High voltage = 13.8 kv, 60 cycles per second
Low voltage = (A) 100, (B) 105, (C) 110, (D) 115

because the tap change is made toward higher furnace voltage which results in a better power factor characteristic. However, voltage variations are not considered a serious problem.

Loads

General

The amount of load delivered for any given volt-ampere demand is determined by the circuit supplying power to the electrodes and the reactance of the furnace transformer is the major factor here. In Fig. 3 the megawatts and power factor of the load are shown as functions of the megavolt-ampere demand. The relationship is shown for the four voltages found to work best in this installation. These show that it is best to operate at as high a voltage as possible because of the higher power and power factor for any specific volt-ampere demand. This also results in a steadier load. Further, it is seen that for each voltage there is a maximum power obtainable and further increases in volt-amperes result in reduced power and power factor. It is also apparent that as this maximum power is approached, there is little increase in power for substantial increases in demand with a corresponding serious drop in power factor.

In order to obtain the greatest production, the load is scheduled to be as high as possible within the limits determined by the electrical characteristics and thermal limitations of the electric equipment. A satisfactory compromise is 6.0 mva, which is the rating of the transformer and of the other electrical design features of the installation. Other loads are occasionally carried, but 6.0 mva is considered the normal load. The load is scheduled by megavolt-ampere demand instead of megawatt load, in order to get full utilization of the electric equipment and to minimize demand peaks, both of which are directly involved in changing voltage taps.

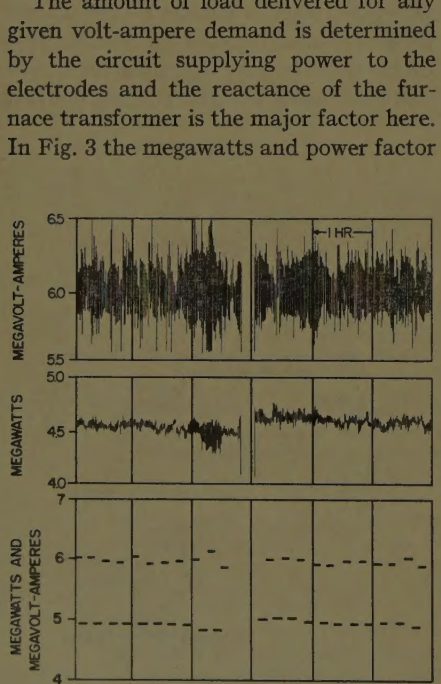

A—Good operation

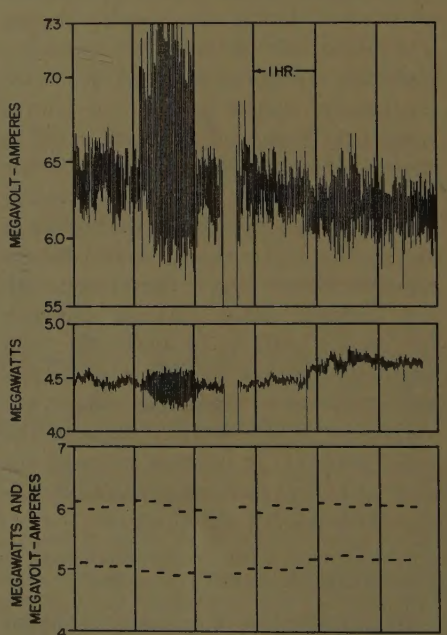

B—Poor operation

Fig. 4. Momentary and 15-minute load charts

Measured Loads

Under normal operating conditions the load is steady with little fluctuation and no definite peak load time. Fig. 4 shows momentary and 15-minute load charts recorded when operation was considered to be good. (Momentary values are from thermal converter instruments having 2-second full-scale travel.) A period including a shutdown was included to show that the full 6.0-mva load is dropped and again picked up with a tapering off or gradual increase. The charts also show that no appreciable

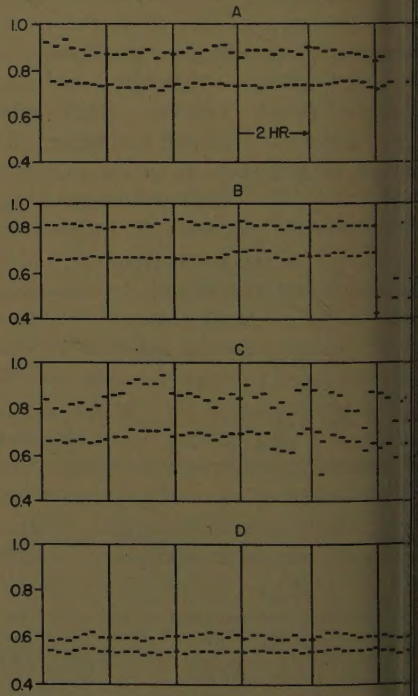

Fig. 5. Fifteen-minute load charts for several load conditions (7,200x), identifications given in Table I

Table I. Identification of Charts in Fig. 5

Chart	Operation	Volts	Megawatts	Megavolt-Amperes	Power Factor
A	Good	110	5.2–5.6	6.2–6.8	0.80–0.87
B	Good	110	4.8–5.0	5.7–6.0	0.80–0.87
C	Bad	105	3.7–5.2	4.8–6.9	0.73–0.86
D	Good	100	3.8–4.0	4.2–4.5	0.87–0.92

rush or surge is experienced from this pe of switching. While operating, the wer factor ranges from 0.80 to 0.87 and e demand has approximately 10% read [per-cent spread = 100(maximum-inimum)/minimum]. In Fig. 5 and able I, the 15-minute load charts *A*, *B*, d *D* demonstrate the same character-ics and spread in values for other loads. nder these conditions no flicker voltage oblem has been noticed.

Unfortunately, these normal steady ads do not always exist and what ight be called poor conditions sometimes esent themselves. There are several ocess difficulties which produce trouble. Such conditions are usually corrected within 2 or 3 days. The momentary and 15-minute load charts in Fig. 4(B) show what happens under these conditions. In this case the problem only lasted 2 hours. Here the thermal demands remain substantially the same as for normal loads. However, the momentary values are distinctly worse with the spread increased to 30%. Slight flicker is sometimes produced. Infrequently, downright bad operation develops. No momentary charts are available to demonstrate this but a spread of more than 60% in demand is produced. Chart *C* of Fig. 5 and Table I shows that under these conditions the 15-minute demand spread goes up to 40% with corresponding large swings in power factor. This is accompanied by a severe flicker voltage problem. The ability of the operating personnel is a major factor in avoiding undesirable operating conditions, in minimizing the magnitude of the swings in load, and in shortening the duration when trouble is encountered.

Conclusions

This 6.0-mva load at 0.83 power factor is normally steady. Its prime requirement is to be able to go on and off the line without creating a disturbance on the power supply system. No surge is involved in direct switching, no flicker problem is present, moderate voltage fluctuations are compensated, and outages up to 8 hours can be tolerated. However, process difficulties may occasionally arise which result in heavy load and power factor swings and in a flicker voltage problem.

Discussion

Tauber (The Detroit Edison Company, etroit, Mich.): The information that the thor presents on the characteristics of a merged-arc silicon-smelting furnace ould be of great interest to those people signing power supplies for furnace loads. The author points out that this load is rmally stable, at good power factor, and nerally free from flicker problems. He o points out that this submerged-arc rnace load tends to be unstable, but rough proper control of the mix and the of the proper voltage, the unstable tend-ies can be cancelled out. He does, how-r, caution that there is the possibility heavy load and power factor swings as ll as a potential flicker problem.

understand that not only is the sub-rged-arc furnace being used in silicon elting, as described by the author, but o for phosphorous, calcium carbide, and roalloy production. Some of these fur-es are very large and even exceed the volt-ampere capacity of the larger direct- furnaces. The nature of the charge and size of the furnace may cause fluctua-ns that could be disturbing to the power pply.

We would expect that the submerged-arc rnace would present a high-power-factor istance-type load that is relatively ady, because the electrodes are sub-rged into the charge. However, since I derstand that part of the current is con-cted through the charge by small arcs ween the granular parts of the charge, would expect that a fluctuating load is sible, depending on the properties of the rge. Although the author describes a ly steady load for the silicon furnace, his rds of caution concerning the possibility fluctuation may become increasingly important when serving other type, or larger submerged-arc furnaces. For example, if the electrodes in a submerged-arc furnace are individually controlled, one would expect that, fairly frequently, one, two, or possibly all three of the electrodes would lose contact with the charge. The associated load fluctuation may be undesirable. In the case of the phosphorous furnace, "cave-ins" have been described by others that may cause a "splash" which changes the level of the charge or even a separation of the charge from an electrode. This, too, is a potential source of fluctuating load.

Unless the electric energy supplier is furnished with complete electrical load characteristics similar to that so carefully described by the author, I am of the opinion that the submerged-arc furnace should be considered as a potential fluctuating load, and should be served with the same caution the electrical supplier uses when serving direct-arc furnaces.

I should like to ask the author about this particular furnace and also about submerged-arc furnaces in general. Although a submerged-arc furnace is generally considered a resistance load under normal conditions, is the reactor in series with this furnace transformer used as a means of controlling load along with the taps on the transformer, or is it possibly used as a buffer to reduce voltage changes to the source? I would expect that, if arc stabilization is not a factor, minimum circuit reactance is desirable to give the best possible power factor. I would also like to know how often "bad" operation is experienced.

In an area where generally little information is available, the author should be complimented for supplying specific data on a submerged-arc furnace. I should like to ask if he has data available on other submerged-arc furnaces, and if he would expect that larger furnaces would undergo the same percentage change between "good" operation and "bad" operation, as does the furnace reported on?

A. M. Killin (Electro Metallurgical Company, Niagara Falls, N. Y.): Mr. Grant in his paper discusses the equipment and process for a 6,000-kva silicon-smelting furnace. The equipment consists of a standard submerged-arc ferroalloy furnace of suitable proportions for the manufacture of silicon metal. Smelting silicon consists of heating silica dioxide with carbon which produces the silicon metal with the release of carbon monoxide. A 6,000-kva transformer is provided for power source. This transformer is equipped with reactors adjustable in five steps from an inherent 6.7% to 31.2%. Controlled electric load of the furnace is obtained by raising and lowering the electrodes. Electrodes are controlled by a hydraulic system either manually or automatically controlled.

Operations of the silicon-smelting furnace are very steady. The monthly operating load factor is around 90%. Maximum operating time is beneficial not only in increased production but in the reaction in the furnace.

In Mr. Grant's paper he has brought out variances and operating conditions due to load changes. In some cases it may be 2 to 3 days in order to correct poor furnace operating conditions. The ability of the operating personnel is a major factor in avoiding undesirable operating conditions and minimizing the magnitude of load swings.

George Grant: I am not associated with any installation other than that presented in the paper and am therefore in no position to discuss such equipment.

Mr. Tauber points out the fact that submerged-arc furnaces are used for phosphorous, calcium carbide, and ferroalloy production. There are many more of these than there are silicon-smelting operations, and the manufacture of some refractories and abrasives can be added to the list. Some of these installations use as much as 35,000 kva.

Individually controlled electrodes can theoretically produce conditions such as suggested by Mr. Tauber. However, in our installation using this type of control, no problem has been experienced that was traceable to such conditions.

The transformer was originally built for an entirely different application. The series reactor was included to fit that job. In this operation it is not used for arc stabilization. Reactance of less than the inherent 6.7% woud give more desirable power, power factor, and voltage regulation characteristics. Added reactance has been tried as a buffer to reduce voltage changes to the source. This produced dubious results.

"Bad" operation has been experienced three times since the furnace was put into service in 1954. These were all encountered during the first year of production while entirely inexperienced personnel were learning the rudiments of such an operation. Generally speaking, bad and poor load demands are produced when more load is impressed on the furnace than its condition will gracefully accept.

It might be expected that bigger furnaces operated poorly will result in somewhat the same percentage change between good and bad load swings.

As pointed out in the paper, there is no question that in smelting silicon the steadiness of the load is primarily a function of the ability and philosophy of the operating personnel.

Electrified Fibrous Air Filters

J. W. THOMAS
NONMEMBER AIEE

E. J. WOODFIN
NONMEMBER AIEE

THERE are two principal methods of separating suspended particles from air: mechanical separation and electrostatic precipitation. Mechanical separation includes dry-type filters, cyclones, water scrubbers, and gravity settling chambers. Dry-type filters are commonly used in air conditioners. Mechanical separators depend on inherent differences in size and density existing between particles and the gas in which the particles are suspended. In contrast, electrostatic precipitators cause a difference between properties of particle and gaseous medium; that is, either the particle is charged in an ionizer[1] or, without an ionizer, the particle undergoes polarization in the field existing between charged plates of the precipitator.

The principal mechanism of removal in mechanical separators of preponderant interest is inertial impingement. In essence, this removal method consists of turning the direction of the air stream, which causes particles to be thrown out by their inertia onto collecting surfaces. Unfortunately, it is necessary to exert force on the entire air stream. Hence, the operation causes a pressure drop which increases monotonically with separation efficiency.

Electrostatic precipitators do not suffer from this defect. It is not necessary to turn the direction of the air stream since the applied field acts directly on the particles alone. Hence electrostatic precipitators have the inherent advantage of high efficiency at very low pressure drop. However, ordinary electrostatic precipitators are not satisfactory where size is at a premium. Size of the precipitator can be reduced without sacrificing efficiency by spacing the plates closer together, but there are definite limits to this process.

However, choice is not limited to pure mechanical filters or electrostatic precipitators. It is possible to insert Fiberglas into an electrostatic precipitator, giving an "electrified fibrous air filter." The principal feature of this combination filter may be seen from the following example. Consider a parallel plate precipitator having a plate spacing of 1 inch, with a particle-laden air stream moving through parallel to the plates. Because of the field gradient between the plates a charged particle will have a velocity component perpendicular to the air flow direction. A particle in the center of the spacing will have to travel 1/2 inch perpendicular to the air flow direction before being deposited on a surface. Consequently if air velocity is too high or the precipitator too short in the direction of air flow the particle will not be collected. However, if the spacing is now packed with low-density fibrous filtering material, the particle will have only a few thousandths of an inch to travel under influence of the field before contacting a collecting surface. Thus much higher efficiency can be expected at some sacrifice in pressure drop.

This investigation of electrified fibrous filters was undertaken because of deficiencies of pure mechanical filters and electrostatic precipitators for air-conditioner application. Principally, it was desired to obtain filters that were relatively small and cheap yet which had low pressure drops and high efficiency in removing cigarette smoke. Efficiencies of electrified fibrous filters were determined without attempting to precharge the test aerosol, using cigarette smoke as a test aerosol. This is a common smoke, and is made conveniently by a cigarette smoking machine. Average size of cigarette smoke is below 1 micron in diameter, probably about 1/2 micron, although authorities differ.[2] Cigarette smoke is much more difficult to filter mechanical

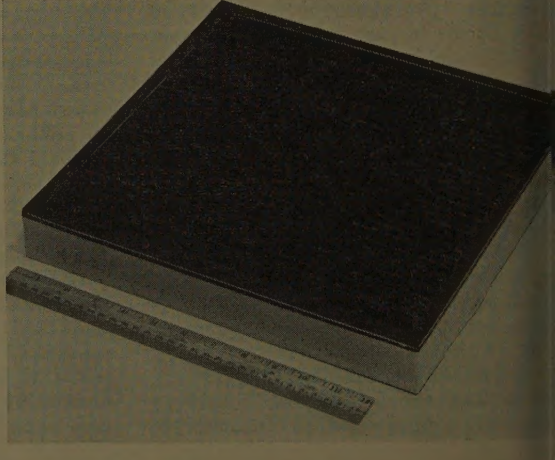

Fig. 1. Electrified pleated filter

Paper 59-680, recommended by the AIEE Domestic and Commercial Applications Committee and approved by the AIEE Technical Operations Department for presentation at the AIEE Appliance Technical Conference, Cleveland, Ohio, May 18–19, 1959. Manuscript submitted September 22, 1958; made available for printing September 10, 1959.

J. W. Thomas and E. J. Woodfin are with the Whirlpool Corporation, St. Joseph, Mich.

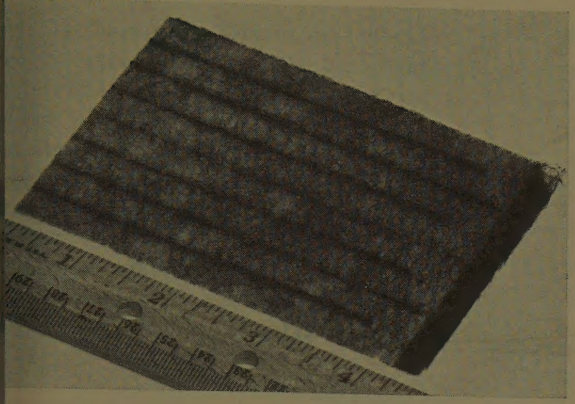

Fig. 2 (left). Section of filter of Fig. 1

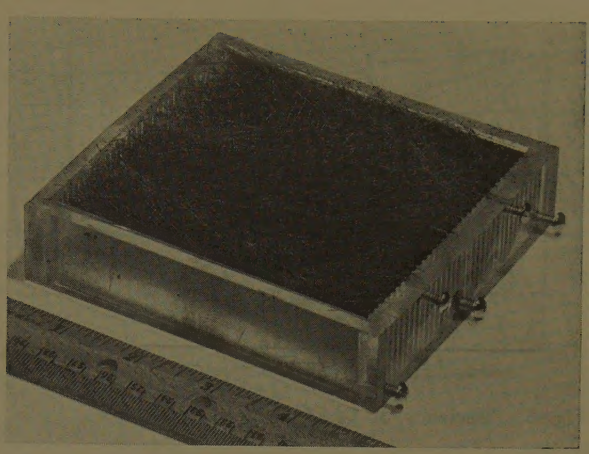

Fig. 3 (right). One-inch precipitator

an larger particles such as ragweed llen, and its is probable that if a filter- g device efficiently removes cigarette noke it will also efficiently remove any her air-borne particulate matter.

est Filters and Precipitators

Fig. 1 shows a commercial-type elec- ified fibrous filter. This filter is of berglas media, electrified, and pleated provide a very large surface area which eatly reduces the pressure drop through e filter. This particular filter has 8 uare feet of filtering area per square ot of superficial area, which is the area closed by the outside edges of the filter. g. 2 shows the unfolded Fiberglas media. ne dark lines spaced 0.31 inch apart, are nducting channels. Alternate channels e at a 3,000-volt potential with respect adjacent channels which are grounded. Two test electrostatic precipitators were ade from a 4- by 4-inch Lucite housing, tted at top and bottom to receive 0.060- ch-thick aluminum or copper plates. ne precipitator was 14.5 inches long in e direction of air flow, and used plates 4 ches wide by 14 inches long spaced 0.91 ch apart. The other precipitator was nilar but was only 1 inch long in the rection of air flow. Fig. 3 shows the 1- ch precipitator. Both precipitators re used empty, and packed with Fiber- as.

Test Procedure

Filters and precipitators were tested in ducts at 50-, 200-, and 400-foot-per-minute superficial face velocity. Concentrations of cigarette smoke influent and effluent from a test filter were determined by sampling about 0.3 cubic foot of smoke through a high-efficiency white filter paper. It was not necessary to sample isokinetically since the particle size of cigarette smoke is sufficiently small that errors do not arise from nonisokinetic conditions.

Relative amounts of cigarette smoke deposited on the white filters were determined by measuring the reflectance of the brown stains caused by the cigarette smoke. From reflectance readings, efficiency of the test filter was determined.

It was necessary to convert the reflectance reading of each sampling filter into a quantity proportional to mass of cigarette smoke on the filter. Since the Kubelka-Munk equation has been used in cloth-soiling studies[3] to convert reflectance readings into quantities proportional to mass of soil of the cloth, it is possible that this equation also could be used for assessing cigarette smoke. The equation is

$$K/S=(1-R)^2/2R$$

Quantity K/S is the ratio of coefficient of reflectivity to coefficient of light scattering. Under certain conditions this quantity is a linear function of mass of discoloring component present on the surface of a white object. Quantity R is fractional reflectance of the sample referred to reflectance of magnesium oxide as unity. If the equation holds for cigarette smoke a plot of $(K/S)_s-(K/S)_o$ against quantity of smoke collected should give a straight line with zero intercepts. Subscript s refers to the sample filter and subscript o to a clean white filter. Two experiments were made to test this relationship.

In each experiment a cloud of cigarette smoke was set up in a 1,200-cubic-foot closed room. This smoke dissipates very slowly. Multiple smoke samples were taken for known, different times, giving known ratios of smoke quantity on the sampling filters. Fig. 4 shows the results. The two curves are at different smoke concentrations. Both curves show that the Kubelka-Munk equation applies fairly well although there is some divergence from proportionality.

Test filter efficiencies were therefore calculated as follows where the subscript A refers to the influent sample, subscript B to the effluent sample, and subscript o to a clean white filter.

$$\text{Per-cent efficiency}=\frac{(K/S)_A-(K/S)_B}{(K/S)_A-(K/S)_o}$$

Results of tests of the pleated filter,

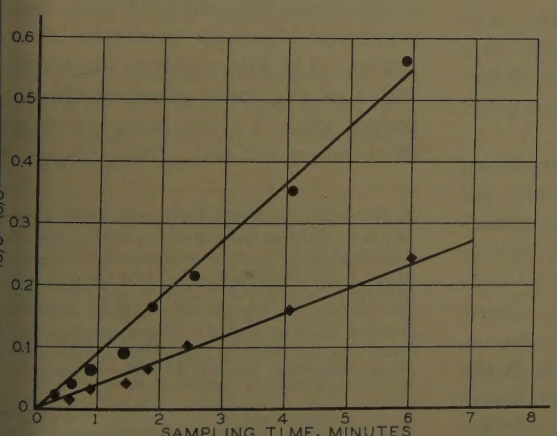

Fig. 4 (left). Test of Kubelka-Munk equation

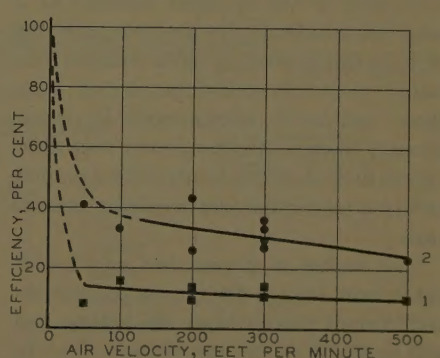

Fig. 5 (right). Efficiency of pleated filter

1—No field
2—9,600-volt-per-inch field

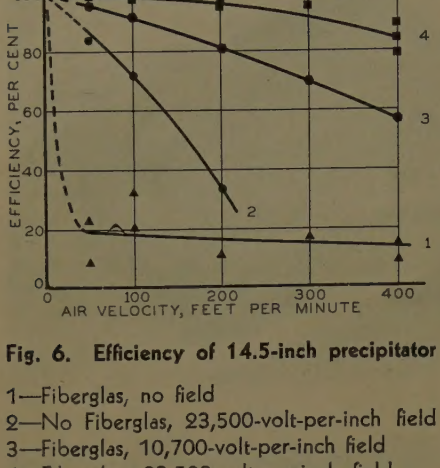

Fig. 6. Efficiency of 14.5-inch precipitator

1—Fiberglas, no field
2—No Fiberglas, 23,500-volt-per-inch field
3—Fiberglas, 10,700-volt-per-inch field
4—Fiberglas, 23,500-volt-per-inch field

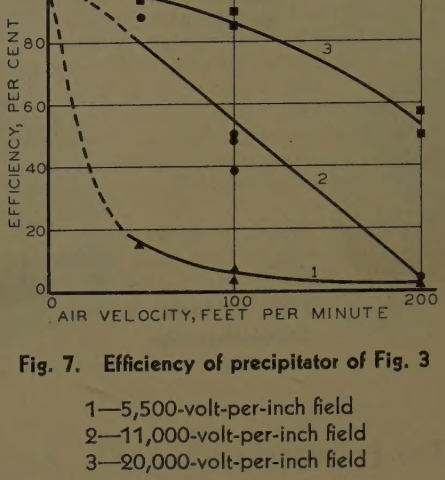

Fig. 7. Efficiency of precipitator of Fig. 3

1—5,500-volt-per-inch field
2—11,000-volt-per-inch field
3—20,000-volt-per-inch field

illustrated in Figs. 1 and 2, are given in Fig. 5. Pressure drop was 0.02 inch of water at 200-foot-per-minute superficial face velocity, and 0.04 inch of water at 400 feet per minute. The curves show that application of the field more than doubled efficiency at flow rates between 50 and 500 feet per minute.

Fig. 6 shows performance data of the 14.5-inch precipitator. Pressure drop when Fiberglas loaded was 0.18 inch of water at 200-foot-per-minute superficial air velocity and 0.55 inch of water at 400 feet per minute. Without Fiberglas, pressure drop was less than 0.01 inch of water at both velocities. Curves *3* and *4* show improved efficiency resulting from impressing a field gradient on Fiberglas packing. Improvement was better than a factor of five, as shown by a comparison of curves *1* and *4*, in the air velocity range of 50–400 feet per minute.

Also, results show that for a precipitator operating on natural cigarette smoke a great improvement in performance may be obtained by packing the precipitator with Fiberglas, at some sacrifice in pressure drop.

Fig. 7 shows performance data of the 1-inch precipitator illustrated in Fig. 3. Pressure drop in this Fiberglas-packed precipitator was 0.03 inch of water at 200-foot-per-minute superficial air velocity and 0.06 inch of water at 400 feet per minute. Curves *1* to *3* show data taken with both Fiberglas packing and an impressed electrical field. Data were not obtained for electrical field only or Fiberglas only as efficiencies were too low to measure accurately, being of the order of 2% or less. Again, the data show great improvement caused by impressing an electrical field on Fiberglas material.

Conclusions

1. Cigarette smoke filtration efficiency of Fiberglas filtering media can be improved greatly by impressing a field gradient on the media.

2. Improvement is synergistic: that is, efficiency of a Fiberglas-packed precipitator is considerably greater than that calculated from efficiency of each effect separately.

3. Air-conditioner filters 1 inch thick can be made to have 50% efficiency in filtering cigarette smoke at 200 feet per minute with less than 0.05-inch pressure drop by using Fiberglas-packed electrostatic precipitator.

References

1. Particle Charging in Electrostatic Precipitation H. J. White. *AIEE Transactions*, v. 70, pt. II, 1951, pp. 1186–91.

2. Concentration and Particle Size Cigarette Smoke Particles, Gerhard Lang, M. A. Fisher. *Archives of Industrial Health*, Chicago, Ill., vol. 13, 1956, pp. 372–78.

3. Detergent Action, O. C. Bacon, J. E. Smith. *Industrial and Engineering Chemistry*, Washington, D. C., vol. 40, 1948, pp. 2361–70.

Deep Ground Beds for Cathodic Protection

S. E. TROUARD
MEMBER AIEE

E. A. WAGNER, JR.
MEMBER AIEE

THE SUCCESSFUL application of cathodic protection to undergound structures in the crowded confines of a large metropolitan city presents problems of cathodic protection co-ordination certainly more acute and perplexing than those ordinarily encountered in cross-country work. It is frequently very difficult to find a suitable location for a ground bed in a particular area requiring protection.

The farther a ground bed can be located from foreign structures, the less direct current pickup from the ground bed will be found on the structures. Yet in a large city it may be impossible, or at least impracticable, to find a spot for a ground bed where more than 20 or 30 feet horizontal separation from foreign structures can be secured.

The radical new concept of introducing cathodic protection currents into the earth from a ground bed located a considerable distance below the earth's surface was originally suggested in 1951 by Robert J. Kuhn, New Orleans, La., Corrosion Consultant. As a result of the cooperative effort of New Orleans Public Service Inc., engineers and of Mr. Kuhn, the designs for deep rail ground beds mentioned in this paper were developed. The first deep rail ground bed in New Orleans was installed on December 21, 19[illegible]. This new idea of deep ground beds has received rather wide public acceptance as evidenced by the fact that a large number of deep ground beds have since been installed by other utilities, particularly in the southern states, and even as far away as Iran.

There are two separate and distinct problems of cathodic protection co-ordination. The first problem, illustrated in Fig. 1, is the anode effect, or the direct pickup effect on the foreign structure from the ground bed. This can be re[illegible]

Paper 59-505, recommended by the AIEE Chemical Industry Committee and approved by the AIEE Technical Operations Department for presentation at the AIEE Southeast and South Central District Meeting, Atlanta, Ga., April 8–10, 1959, and for presentation at the AIEE Summer and Pacific General Meeting and Air Transportation Conference, Seattle, Wash., June 21–26, 1959. Manuscript submitted January 8, 1959; made available for printing May 22, 1959.

S. E. Trouard and E. A. Wagner, Jr., are with New Orleans Public Service Inc., New Orleans, La.

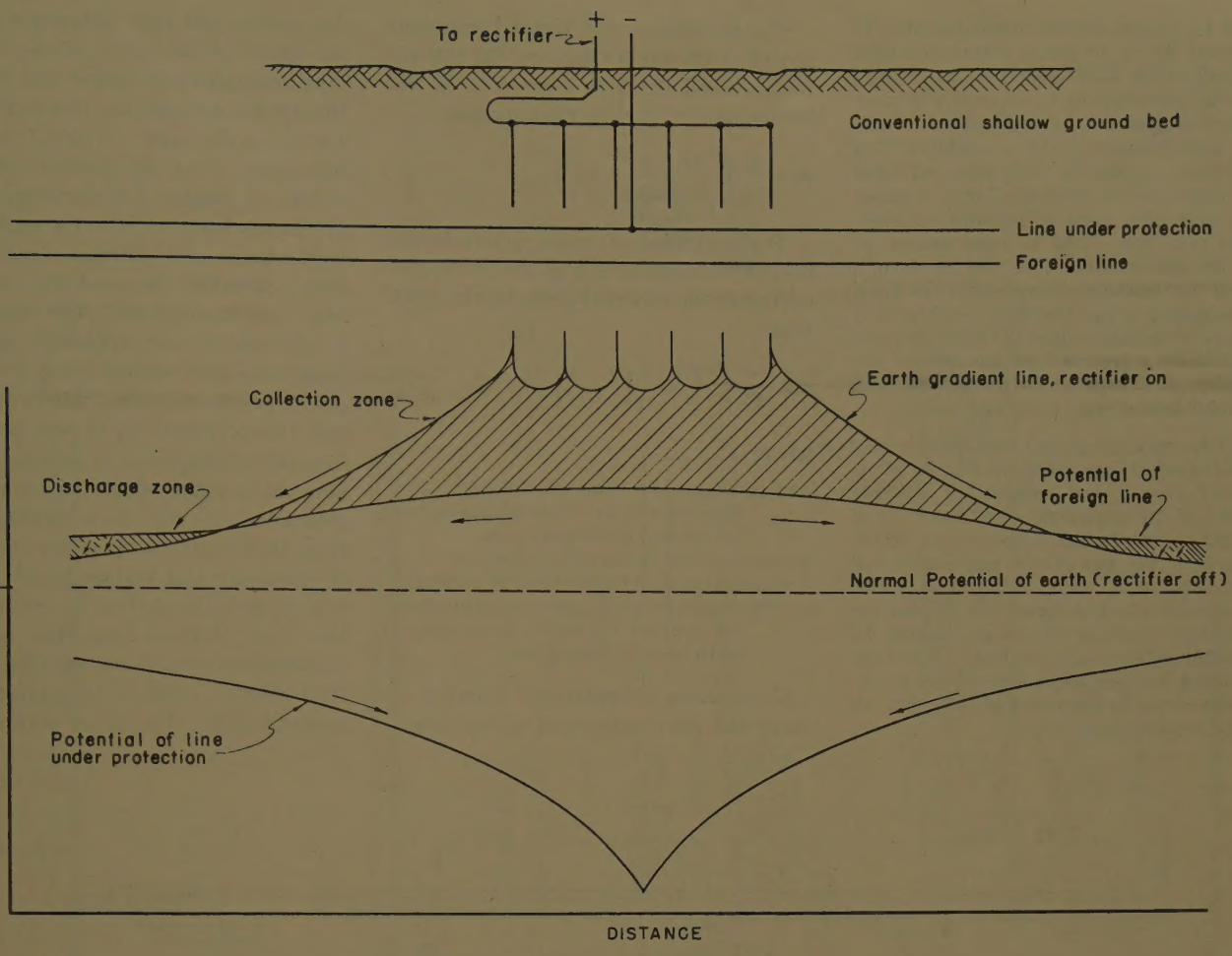

Fig. 1. Direct ground bed effect

Schematic potential relationships of earth, foreign line, and line under protection from conventional shallow ground bed

red so small as to be undetectable by acing the ground bed at a great distance om the foreign lines. With conven-onal shallow ground beds this would be ost difficult to accomplish where the reign lines are in the form of a network th mains on every street and cross reet.

The second problem may be called the thode effect. This effect is independ-t of the location of the ground bed. It beyond the scope of this paper to discuss ys and means of coping with this par-ular phase of the co-ordination prob-n.

For the cathodic protection of the ated steel gas main system in New leans, three different types of ground ds are employed:

1. Conventional shallow rail ground bed as own in Fig. 2. Provided a suitable loca-n can be secured, this type of ground bed generally preferable because it is the least pensive ($250 installed). The used rails igh approximately one ton and such a ound bed is designed conservatively for a -year life with a 5-amp (ampere) current scharge, assuming that only half of the tal would go into solution, and the rest lost by segregation. Actually, in this design the inner faces of the rail webs will discharge but little current because of mutual interference effects. Thus, rather than obtain only 50% use of the metal, closer to 75% would be secured and the losses from segregation would be reduced, hence the actual life of the ground bed would be longer than the 10-year figure mentioned. In 500-ohm-cm (centimeter) soil, the resistance to earth of this type of bed ranges from 0.5 to 1.0 ohm.

2. Deep rail ground bed, construction details of which are shown in Fig. 3. In this type of ground bed, a hole is drilled in the earth nominally 8 inches in diameter, but actually closer to 9 inches in diameter, 250 to 300 ft (feet) in depth. Two 30-ft lengths of 100-pound-per-yard used T-rails are lowered into the hole by means of a 1/4-inch-diameter wire rope. The rails are joined together longitudinally by means of rail joint plates, and a separate wire with no splices is brought from each rail length to the surface of the earth. The resistance to earth of this type of ground bed is in the general order of 0.2 ohm, excluding lead-wire resistance. The installation is de-

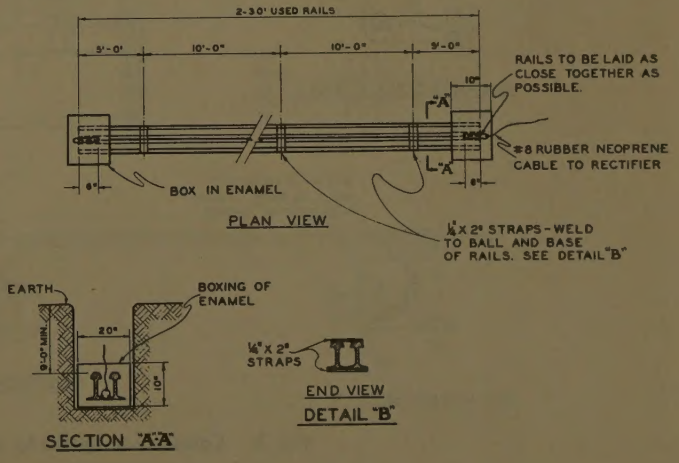

Fig. 2. Typical rail ground bed for cathodic protection

signed for 5-amp current discharge and its estimated life is 10 years, estimating that only half of the 2,000-pound weight of iron would be consumed by the current discharge and the balance lost by segregation. Rails were used because of the availability of a fairly large surplus of used rails, salvaged from discontinued streetcar lines. Various other materials, such as graphite or high-silicon cast iron, could be used instead of rails for the anode. The cost of such a ground bed installed is approximately $750. In congested areas the $750 results in a cheaper installation than the $250 conventional shallow ground bed because of the elimination of expense of trial ground beds and joint testing with other utilities.

3. Deep stalk rail ground bed, construction details of which are shown in Fig. 4. This type of ground bed consists of 12–30-ft lengths of 100-pound-per-yard used T-rail inserted vertically into a drilled hole 360 ft deep, with the top of the uppermost rail practically flush with the ground. The cost of such a bed, designed for 10-year life at 30-amp current discharge, would be approximately $1,750 installed. This type of ground bed has an extremely low resistance to earth, in the order of 0.05 ohm, as will be shown later.

The resistance of a metal hemisphere buried at the earth's surface, flat side up, to any shell of earth concentric to the hemisphere is given by the equation:

$$Rr = \frac{\rho}{2\pi}\int_{r_1}^{r}\frac{dr}{r^2} = \frac{\rho}{2\pi}\left(\frac{1}{r_1} - \frac{1}{r}\right) \qquad (1)$$

The resistance of metal sphere buried deep in the earth to any shell of earth concentric to the sphere is given by the equation:

$$Rr = \frac{\rho}{4\pi}\int_{r_1}^{r}\frac{dr}{r^2} = \frac{\rho}{4\pi}\left(\frac{1}{r_1} - \frac{1}{r}\right) \qquad (2)$$

where

Rr = resistance in ohms of the earth to a distance r from center of hemisphere (or sphere) measured in cm
ρ = uniform soil resistivity in ohm-cm
r_1 = radius in cm of hemisphere (or sphere)
r = distance in cm from center of hemisphere (or sphere) to which resistance to earth is to be computed

Comparison of equations 1 and 2 reveals that the resistance of a deep spherical ground bed to a distance r cm from the center of the sphere is only half that of a hemispherical ground bed buried at the earth's surface, the resistivity of the soil being the same. Table I shows the resistance of a hemisphere of 15-cm radius, or roughly 1 ft diameter to earth at various distances from the center of the hemisphere, and corresponding voltage drops caused by the discharge of 10 amp from the hemisphere. For comparison it also shows corresponding calculated resistances and voltage drops for 10-amp discharge from a deep spherical ground bed, the soil resistivity in each case being for sake of simplicity in calculations 6[illegible] ohm-cm, a value which is commonly encountered in the New Orleans area. Note that for the deep sphere, the values of resistance and voltage drops are only half those of the shallow hemisphere. [illegible] the New Orleans area, the so called Pleistocene Layer is encountered below a 75-ft depth. Soil in this layer is fine textured clay. The upper portion of the

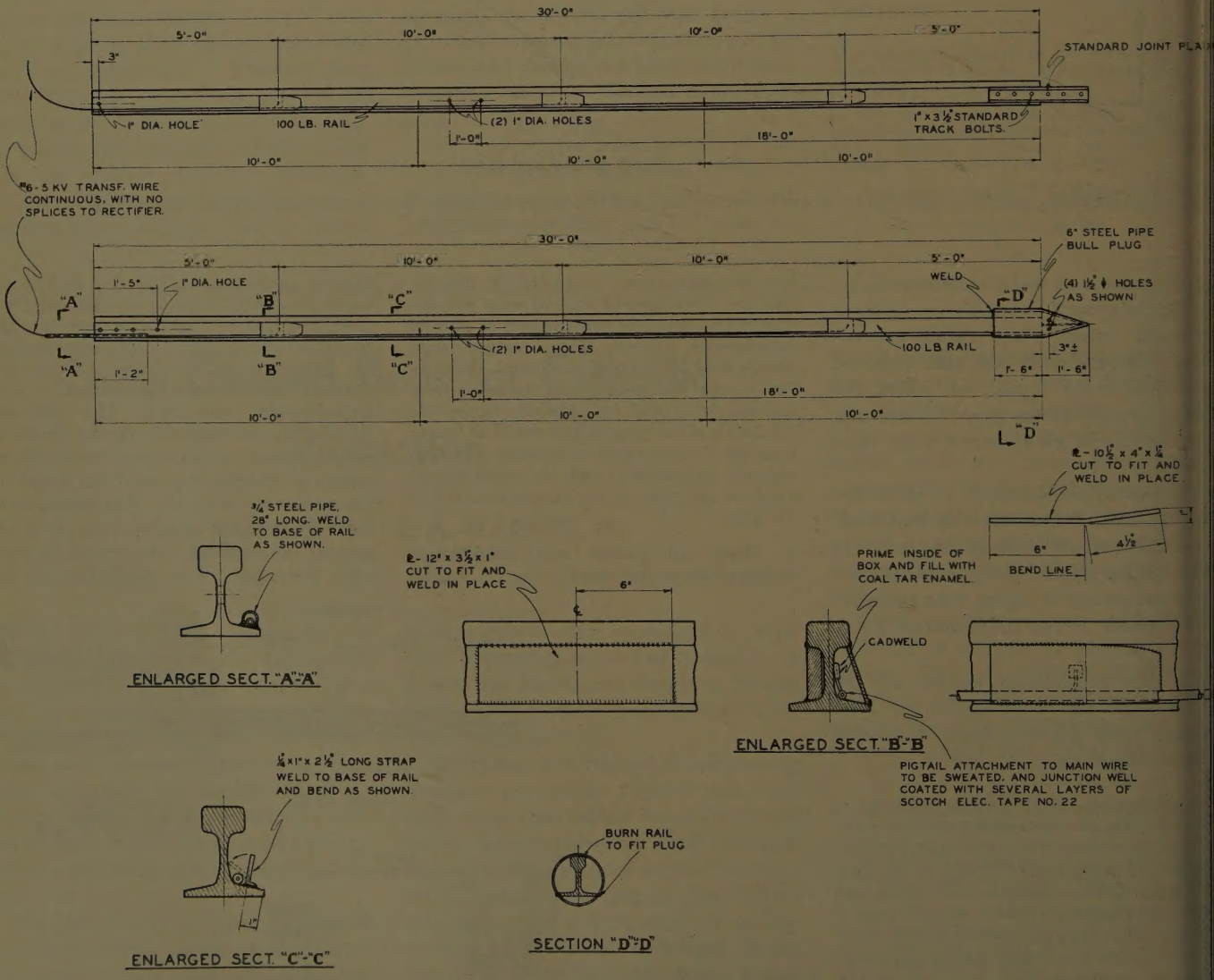

Fig. 3. Construction details for standard deep vertical rail ground bed

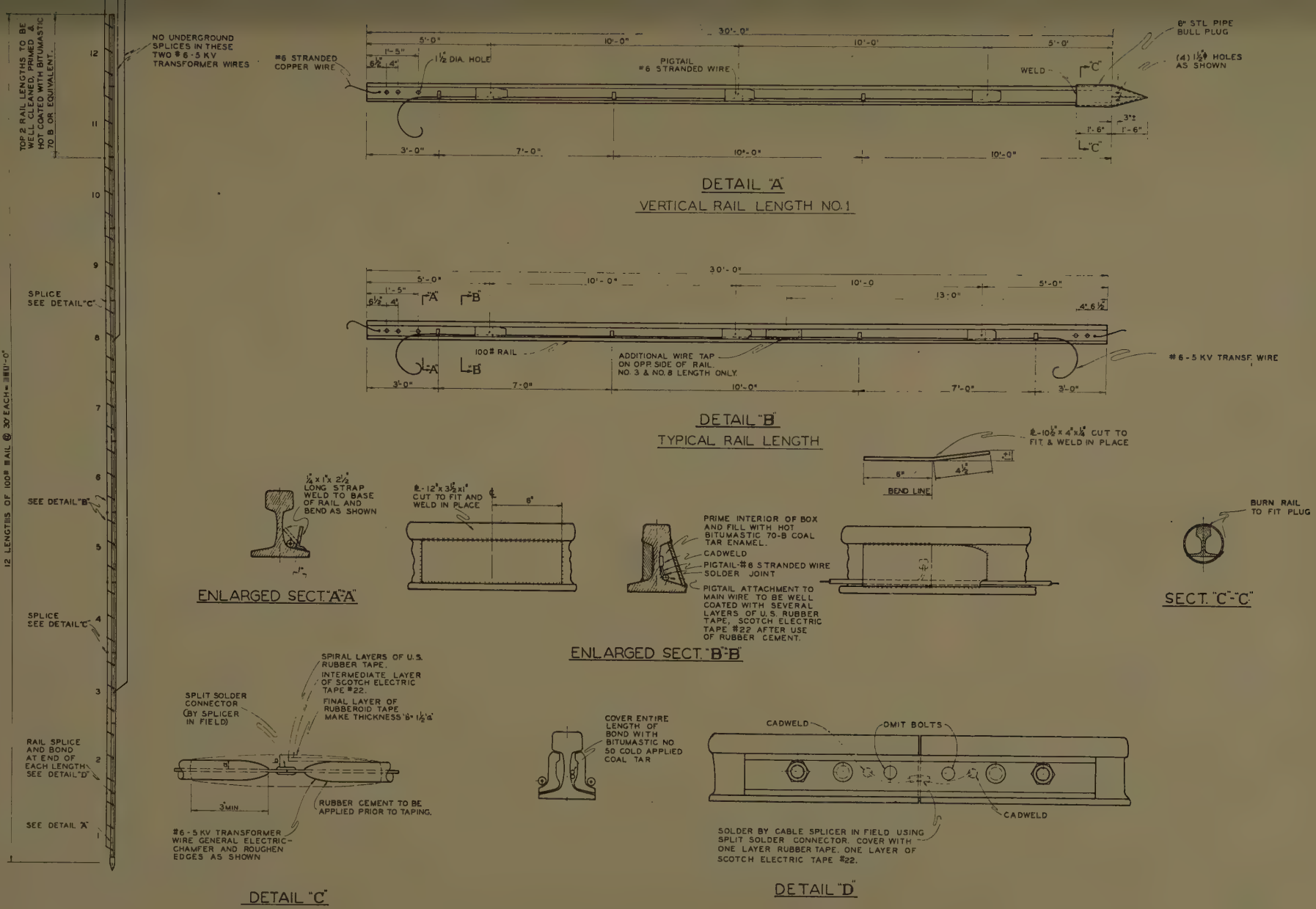

Fig. 4. Construction details for 360-ft length of vertical rail ground bed

Table I. Voltage Values in Earth Surrounding a Hemispherical Ground Bed at Earth Surface and a Deep Spherical Ground Bed, Each Discharging 10 Amp

Distance From Center of Hemisphere or Sphere (r)		Hemisphere*		Sphere*	
Cm	Ft	Resistance, Ohms (Rr)	Voltage Drop from Center, Volts	Resistance, Ohms (Rr)	Voltage Drop from Center, Volts
16		0.42	4.2	0.21	2.10
20		1.67	16.7	0.885	8.85
30	0.98	3.33	33.3	1.665	16.65
60		5.00	50.0	2.5	25.0
90		5.56	55.6	2.78	27.8
120		5.83	58.3	2.965	29.65
150		6.00	60.0	3.000	30.0
180		6.11	61.1	3.055	30.55
210		6.19	61.9	3.095	30.95
300	9.84	6.33	63.3	3.165	31.65
3,000	98.4	6.63	66.3	3.315	33.15
30,000	984.0	6.663	66.63	3.3315	33.315
300,000		6.666	66.66	3.333	33.33
3,000,000		6.6666	66.666	3.33333	33.3333

ρ = 628 ohm-cm.

* Radius of hemisphere and sphere is 15 cm (r_1).

layer is light tan in color due to oxidation and is rather stiff. At the 250–300-ft depth the clay is dull gray in color and less stiff. The soil is wet, being always well below the natural water table. It is not intended to imply that a shallow horizontal ground bed such as shown in Fig. 2 is, in the strictest sense, a hemispherical ground bed, or that the deep vertical ground bed shown in Fig. 3 is a spherical ground bed, but, in the final analysis, each may be thought of as approaching these respective hypothetical types of ground beds in so far as the *IR* drops near the surface of the earth caused by current discharge from them is concerned. Within the approximately 100 ft of earth which would be appreciably influenced by the shallow horizontal ground bed, this type of ground bed would have only a hemisphere of earth 100 ft in radius in which to dissipate its current discharge. But the deep vertical bed would have a sphere of earth, of the same radius, in which to dissipate, hence *IR* drops near the surface of the earth caused by current discharge from the shallow ground bed would be substantially higher than would be *IR* drops near the surface of the earth caused by the same amount of current discharging from the deep vertical ground bed. For all practical purposes, the same net effect could be attained by locating the shallow bed the same distance laterally from the foreign structures as the deep ground bed is separated from the foreign structures vertically. In a city crowded with networks of foreign structures, it is virtually impossible to secure the desired clearances laterally which can easily be attained vertically by use of the deep ground bed.

In Fig. 5 resistance and voltage drop data from Table I are plotted on semilog paper, predicated upon the same soil resistivity at great depth as that encountered at shallow depth. Note that the steepest part of the lower curve would be at points in the earth 250 to 300 ft below the earth's surface and, therefore, 225 to 300 ft from the closest foreign line. Therefore the advantage of the deep ground bed in the solution of the most troublesome part of the cathodic protection co-ordination problem should be obvious.

Fig. 6 shows the location of two deep stalk rail ground beds at a large electric substation. For purposes of gathering field data to demonstrate the earth effects shown in Figs. 7 and 8, the rectifier was temporarily set at 55 amp, 7.0 volts. The negative side of the rectifier was tied to the common neutral system which

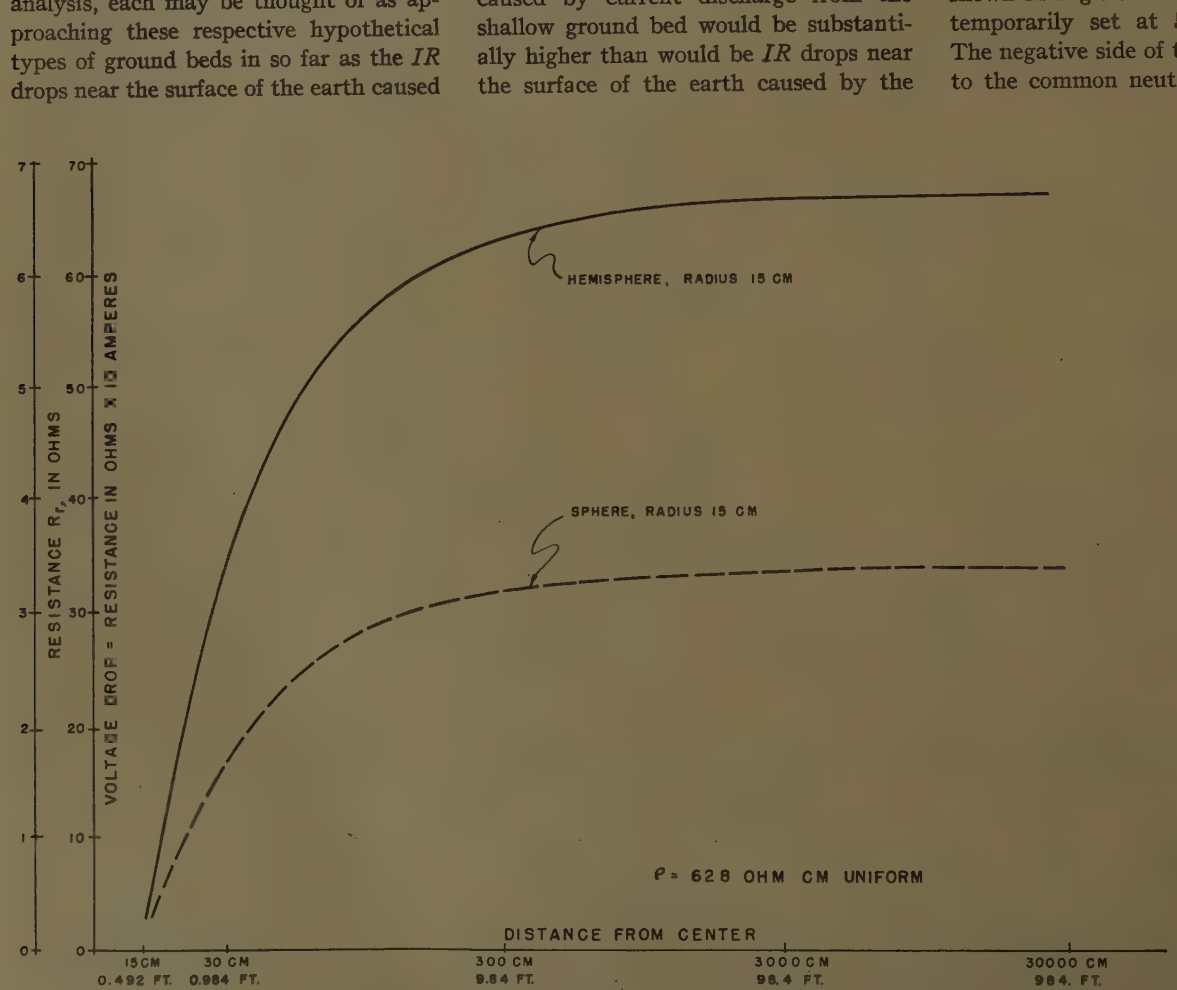

Fig. 5. Resistance to earth of s hemispherical spherical gro beds, and vol drops produced earth by each 10-amp discha

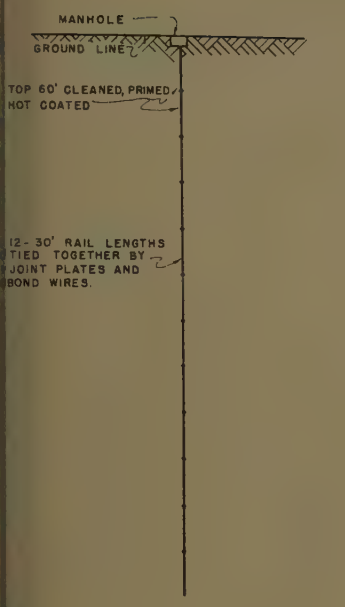

ELEVATION VIEW OF TWO DEEP RAIL GROUND BEDS

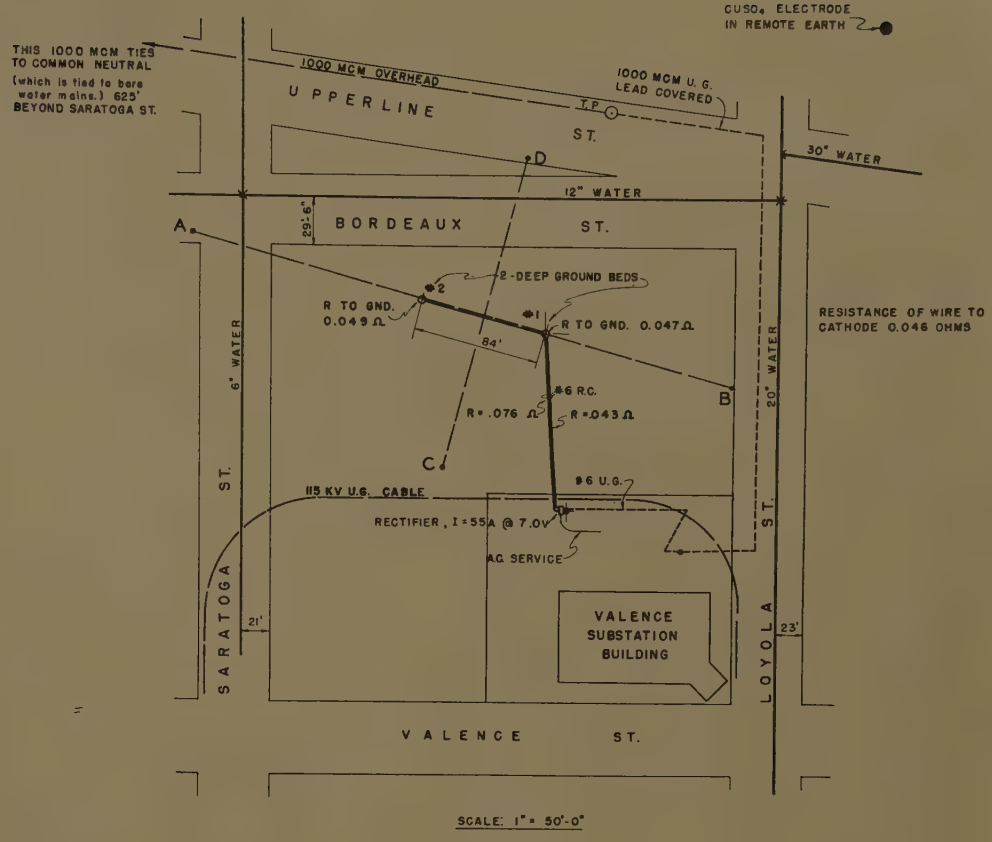

Fig. 6 (above). Location of deep vertical rail ground beds in Valence Substation yard

Fig. 7 (below). Earth gradient in line over two deep ground beds (line AB)

Total current from rectifier to two deep ground beds=55 amp at 7.0 volts

All readings are Δ potential difference measurements in volts between $CuSO_4$ electrodes in earth at points plotted and a $CuSO_4$ electrode in remote earth

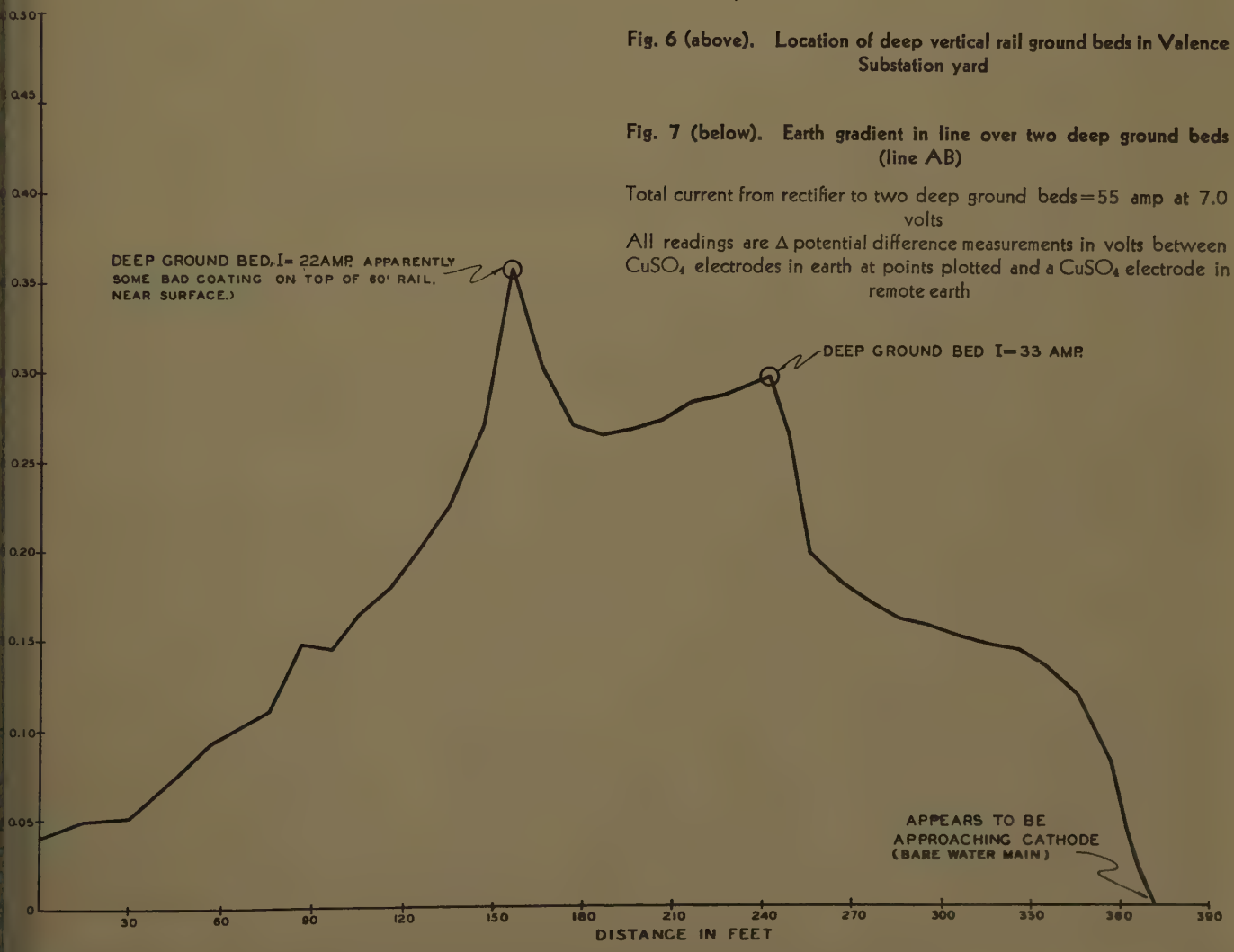

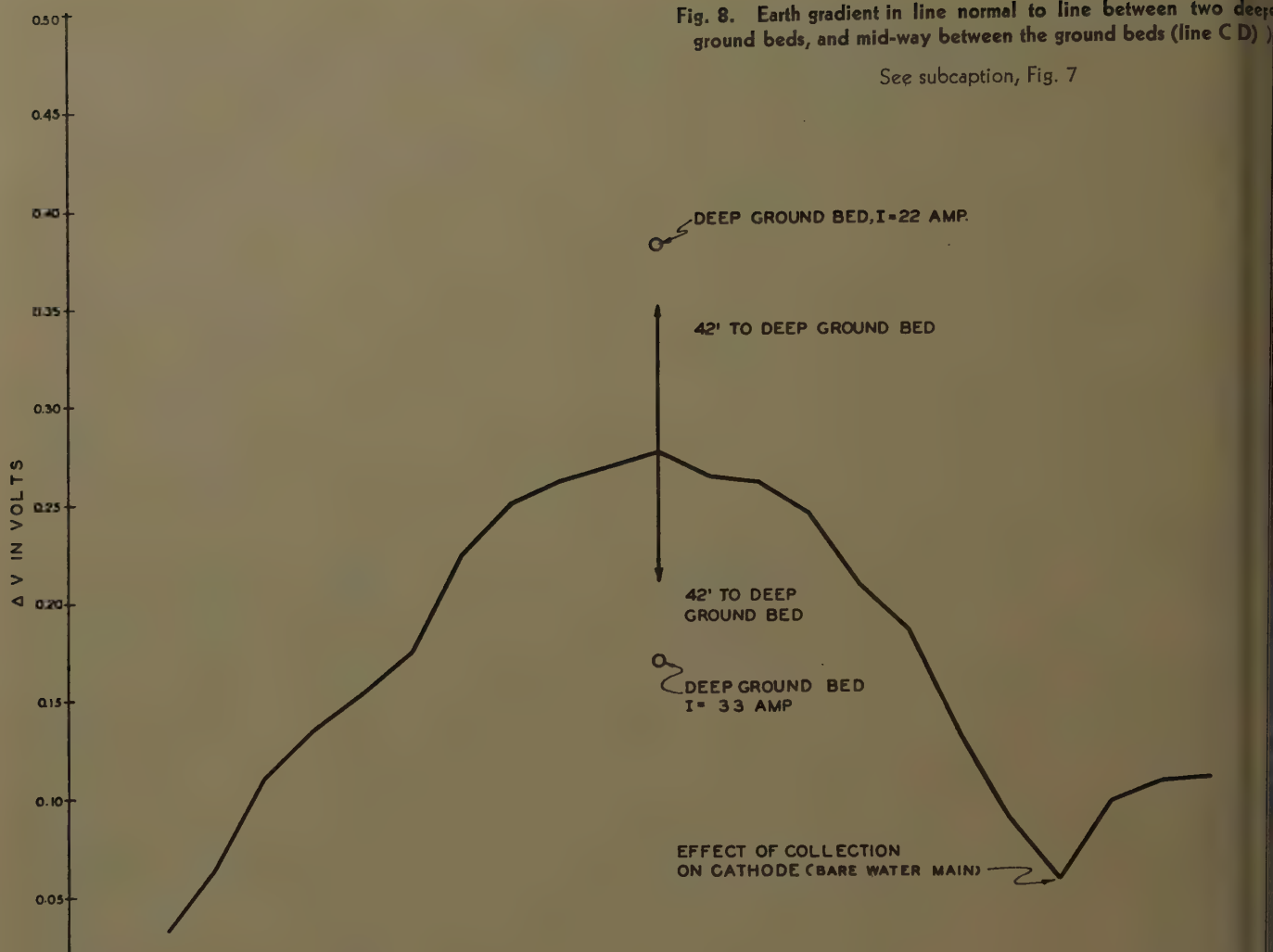

Fig. 8. Earth gradient in line normal to line between two deep ground beds, and mid-way between the ground beds (line C D).

See subcaption, Fig. 7

bonded solidly to the bare cast-iron water pipe system more than 1,000 ft away. A profile of change of earth potentials referred to a remote copper sulfate ($CuSO_4$) electrode was measured at 10-ft intervals along line *AB*, and also along line *CD* which is normal to the first line. Note the position of the bare cast-iron water mains in Fig. 6 for, as shown in Figs. 7 and 8, the collection of current on these bare mains, even though the drainage point is more than 1,000 ft away, causes noticeable earth gradients towards the water mains.

Fig. 7 shows a profile of change of earth potential across line *AB*. Each point plotted is the change of potential between rectifier-off and rectifier-on readings of a $CuSO_4$ electrode placed at each point plotted and a remote $CuSO_4$ electrode. One ground bed was discharging 22 amp and the other 33 amp, at 7.0 volts. Note that the change of earth potential is higher at the ground bed discharging 22 amp than at the ground bed discharging 33 amp. The top 60 ft of each of these particular rail ground beds is coated, but apparently there must have been a bare spot on the coating of the one discharging 22 amp which causes the relatively high peak shown. Actually, however, the values are quite small, but are plotted on a large scale. A total of 55 amp is being introduced into the earth here and the highest point of earth rise is only about 0.35 volt right at the ground bed. Within 100 ft this drops to less than 0.1 volt. Note the sharp drop in the earth potential at the right-hand side of the curve, as the bare water main is approached. On the left-hand end of the curve, another water main is crossed but practically no effect is shown. This indicates high-resistance caulked joints in the water main system, such that this main is not tied in too solidly to the balance of the water main system.

Fig. 8 shows another profile along a line *CD* which is normal to the first line, and mid-way between the two rail stalks. This line passes 42 ft from each grou bed, and the highest rise of earth pote tial is 0.27 volt with 55-amp dischar Note also the dip in the earth potent at the 180-ft mark. This is right o the 12-inch bare cast-iron water ma which is electrically drained about 1,(ft away.

Table II shows the resistance to ea of various deep or vertical rail st ground beds in the New Orleans Pub Service Inc., system.

The 300-ft stalks are very low in sistance, being approximately 0.05 oh as shown by the first, second, and items in Table II. The balance of installations listed include lead-wire sistance which should be subtrac from the values shown in order to obt the true resistance of the ground bed earth. For instance, if the resistance the no. 8 lead wire were subtracted the installation at Roman near Tula which consists of two 30-ft-length r 250 ft in depth, the true resistance

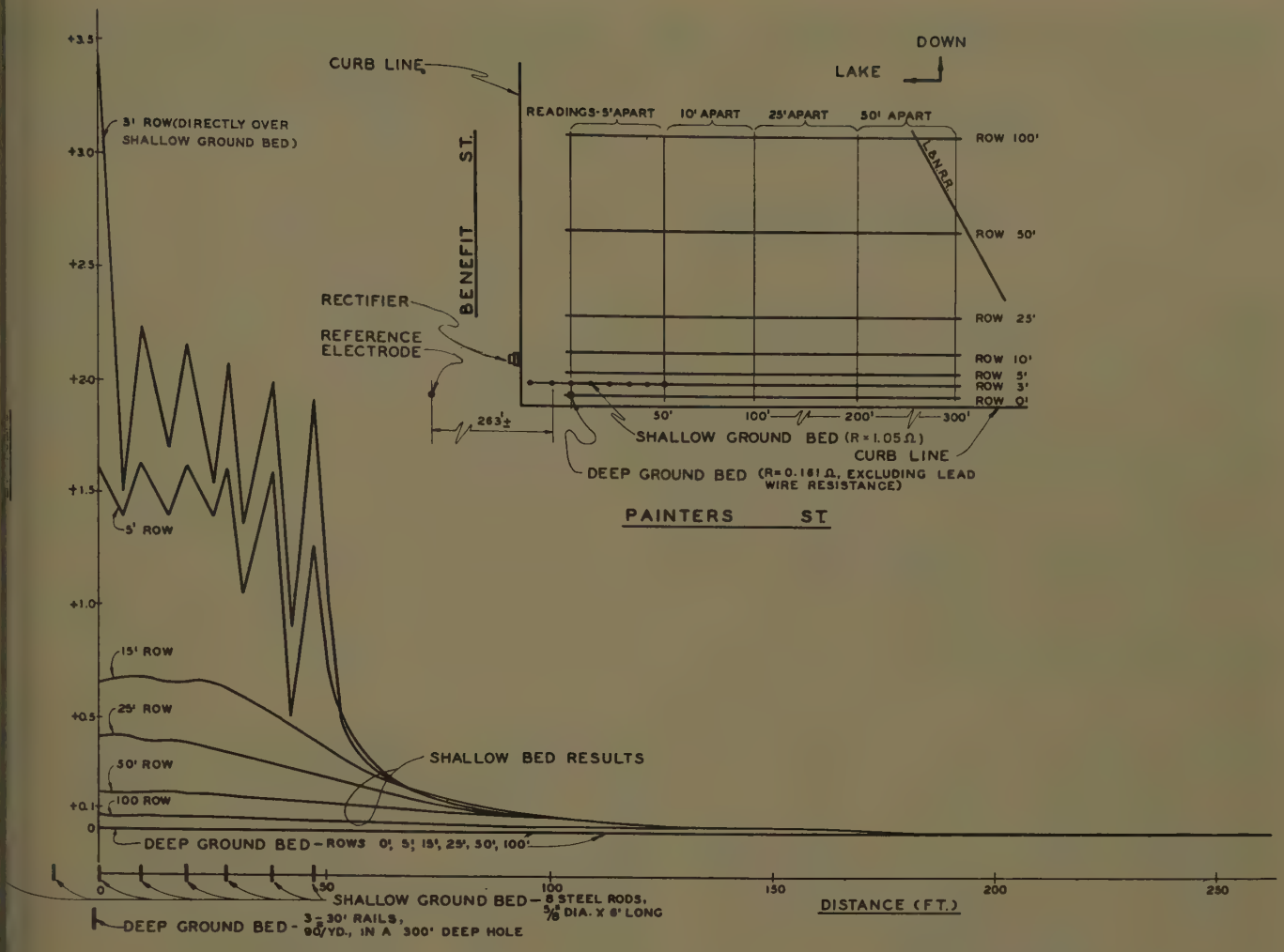

Fig. 9. Voltage gradient comparison of deep and shallow ground beds at Painters and Benefit Streets

Rectifier settings for deep ground bed: I = 9.75 amp; E = 3.0 volts (d-c)
Rectifier settings for shallow ground bed: I = 10.1 amp; E = 10.7 volts (d-c)

ble II. Resistance to Earth of Various Deep Rail Ground Beds

Location and Date Installed	Description*	Resistance to Earth, Ohms
lence Substation no. 1	(A)	0.047
lence Substation no. 2 (4–15–54)	(A)	0.049
neral Pershing near Rendon (12–18–53)	(B)	0.217†
man near Tulane (12–21–52)	(B)	0.251†
nal Boulevard near Robert E. Lee (12–22–52)	(B)	0.233†
enville Plaza no. 1	(C)	0.334†
enville Plaza no. 2	(C)	0.364†
enville Plaza no. 3	(C)	0.251†
mbination of nos. 1, 2, and 3 (9–10–54)		0.110†
ashington Square (5–24–54)	(D)	0.055

A—360 ft of 100-pound-per-yard T-rail, top flush th ground, top 60 ft coated.
B—Two 30-ft lengths of 100-pound-per-yard T-l, bottom 250 ft deep.
C—Four 30-ft lengths of 100-pound-per-yard T-l, bottom 390 ft deep.
D—360 ft of 100-pound-per-yard T-rail, top flush th ground, all bare.
ncludes resistance of no. 6 (or no. 8) wire from tifier to rails (R/1,000 ft no. 6 = 0.394 ohm; 8 = 0.627 ohm).

earth would be 0.17 ohm. Two rails side by side, buried horizontally 9 ft deep, would be 0.5 ohm, so it can be seen that in the New Orleans area extremely low resistance to earth can be secured when the rails are located deep.

Fig. 9 shows, in one illustration, a number of changes of earth potential caused by 10-amp discharge from a shallow bed and later from a deep rail ground bed, the ground beds not being energized simultaneously. Change of potential difference readings between a $CuSO_4$ electrode at various intervals and a remote $CuSO_4$ electrode were measured in a line directly over the shallow bed, and in rows 2, 7, 22, 47, and 97 ft away from and paralleling the shallow ground bed. Another set of readings was made directly over a deep rail ground bed and in rows 5, 10, 25, 50, and 100 ft away from the deep rail ground bed. The results of these tests were plotted as shown, and demonstrate that even for 10-amp discharge in 500-ohm-cm soil, appreciably steep earth gradients are encountered for the shallow bed, whereas for the deep bed, the curve is flat.

Conclusions

The advantages of deep ground beds may be briefly summarized as follows:

1. Full rectifier capacity is available for protection of structure to be cathodically protected. No current need be drained from foreign lines because of direct pickup effect. This means elimination of distributed drainage system for foreign lines, with consequent savings.

2. Lower power costs result because of drastically reduced ground bed to earth resistance.

3. Smaller space is required for a deep ground bed.

4. Deep ground bed can be installed at any convenient location. No right-of-way problems are involved.

5. Cost of cathodic protection coordination tests is practically eliminated since current pickup on foreign lines is negligible.

6. No time is lost in surveys to find suitable locations for conventional shallow ground beds.

D-C Electric Drilling Rigs: Application and Operation

E. E. HOGWOOD, JR.
ASSOCIATE MEMBER AIEE

THE d-c variable voltage drive for diesel or gas-electric drilling rigs has gained considerable popularity since the introduction of lightweight low-cost electric equipment. However, quite often not sufficient advantage has been taken of the intermittent capability of the generators and motors, both from an application and operational standpoint. This paper presents information derived from an analysis of actual operating test data which should assist users, rig builders, and operators in applying and operating electric drives more effectively on drilling rigs.

Electric Equipment Selection

The electric equipment selection for a diesel-electric drilling rig should first recognize the over-all power requirements. Formerly, the hoisting load was predominant and its size influenced the selection. On modern drilling rigs, the mud pumps are the largest single load; thus, their horsepower requirements are a deciding factor in the choice and number of engine-generator sets for the power plant. Two, three, or four sets are usually selected depending on engine size, degree of reliability desired, and the load requirements. Once the engines are selected, the generators, motors, and control should be chosen. This paper starts with the generators since they are the first link in any electric drive system or transmission.

Generators

The first requirement in the selection of the d-c generator is that it have characteristics which will suitably match the engine. An engine is essentially a constant-torque machine from which variable hp (horsepower) can be obtained by speed variation. Its rated horsepower is obtained at maximum rated speed; therefore, it is important that the generator match the maximum continuous hp and speed of the engine. Second, the generator output volts and ampere rating or some multiple of either must also match those of the motors being considered.

Fig. 1 shows the desirable volt-ampere and kw-ampere characteristic for a drilling generator. The engine horsepower is expressed in generator output volts and amperes. The generator voltage is maximum at zero current and decreases or droops with increased load to a minimum when the current is greatest. This generator characteristic fixes the maximum no-load speed and stalled torque developed by a separately excited motor connected to it The motor performance curve is very similar to this curve with volts and amperes being replaced by speed and torque respectively. Also, this characteristic limits the peak engine load to a value which can be preset by simple adjustment of the maximum generator excitation. The product of volts and amperes results in the kw curve shown. As the load amperes increase, the engine loading first increases to a maximum, and then decreases. The engine is unloaded at both low and high currents and is fully loaded on a small portion of the curve. Therefore, the generator should be selected so that its peak kw exceeds slightly the continuous engine output. Five- to ten-per-cent overload on the engine at peak kw is permissible and desirable when required. Overloading allows the system to operate at or near peak power over a wide load range.

The electrical rating of the generator is established on the basis of a continuous ampere load and a permissible temperature rise. It is usually not possible to take advantage of the full intermittent capability of the generator even on cyclic loads because it is desirable to limit the maximum loading on the engine. The generator kilowatt rating converted to horsepower should match the continuous output of the engine.

During recent years available generator frames and ratings have led to the application of one or two types of generators to a wide range of engine sizes. This procedure has many advantages for both the user and the electric equipment manufacturers. First, it offers low-cost low-weight electric equipment on a short delivery basis. Second, it is possible to adjust the generator peak output so that a number of different oil field engines can be matched. Third, the motors and generators are practically duplicates which minimize spare parts requirements. Fourth, any necessary repairs can be handled quickly in the repair shops because of available standardized parts.

Motors

Consideration must be given to the drive requirements when selection of the motor is made. Consider the drawworks. This load is intermittent, essentially constant hp in the operating range, and requires a certain maximum pull for stuck bit and a certain maximum speed for light hook operation. Fig. 2 shows a typical curve for a large drawworks specifically designed for an electric drive. This curve shows the performance of two 1,000 hp motors receiving power from three 800 hp engine-generator sets. The drawworks has only four forward gear ratios and no reverse gear since reversing is accomplished electrically.

The drawworks is usually rated in input hp (while hoisting) based on the load and resultant hoisting speed. This rating may be expressed as hoisting power and is calculated by the following equation.

$$\text{Hoisting Power} = \frac{P_L \times N_L}{33{,}000 \times E_{DW}}$$

where

P_L = fast line pull in pounds
N_L = fast line speed in fpm (feet per minute)
E_{DW} = efficiency of drawworks

Since the load requires this hoisting power for a variable length of time after which there is a semifixed interval of time of no-load for "breaking-out" the stand and setting it aside, the drawworks motor may be applied with a continuous hp rating considerably below the drawworks hp rating.

The amount of power that the motor can transmit to the drawworks on an intermittent basis depends on: its design capabilities from a maximum torque and maximum speed standpoint and the amount of power available from the engine-generator sets. The motor is designed to carry a continuous current under load conditions without exceeding a maximum safe temperature. Applied to the drawworks, it does not carry current for the entire hoisting cycle; the

---

Paper 59-1103, recommended by the AIEE Petroleum Industry Committee and approved by the AIEE Technical Operations Department for presentation at the AIEE Petroleum Industry Conference, Long Beach, Calif., August 23–26, 1959. Manuscript submitted November 10, 1958; made available for printing July 3, 1959.

E. E. Hogwood, Jr. is with Westinghouse Electric Corporation, East Pittsburgh, Pa.

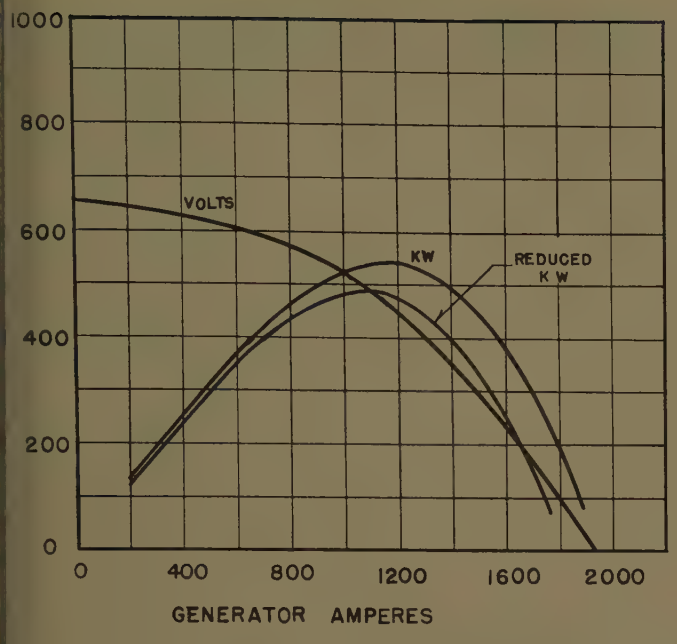

g. 1. Performance curves of one 550-kw d-c generator for use on drilling rigs

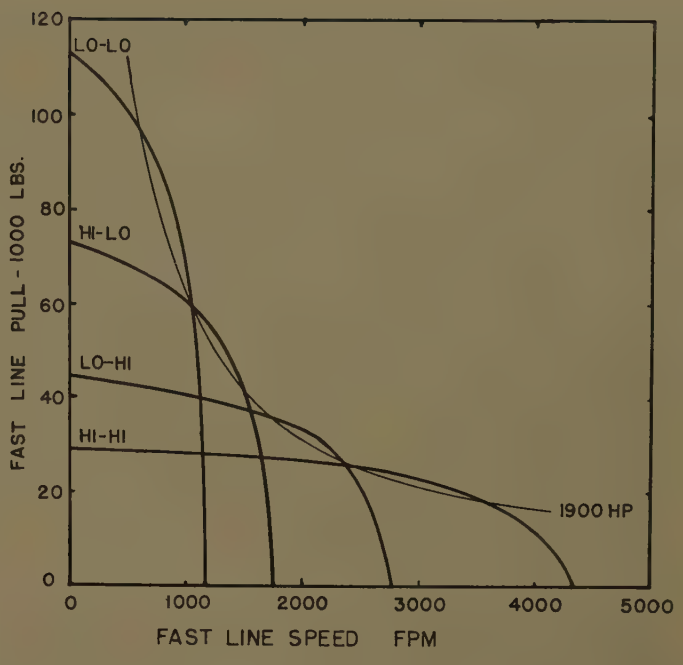

Fig. 2. Performance of two 1,000-hp motors on a large drawworks

re, it can carry considerably more than ted current during the hoisting portion ithout causing any thermal damage to ie insulation. The maximum current iat a given motor can carry, regardless the duty cycle, is determined by com- utation. Also, the maximum voltage hich can be applied to the motor is etermined by the point where either ashing-over or serious overspeeding ccurs. Both of which are undesirable.

A motor then can receive power from ie or several engine-generator sets and eliver more output to the drawworks n a short time basis, as long as the safe iaximum current and voltage ratings are ot exceeded and the effective current held to rated amperes or less.

The effective current which establishes ie amount of heating that the motor an withstand is defined as the rms of the istantaneous currents for a given duty ycle. For instance, Fig. 3 shows the urrent trace of two drawworks motors onnected in series for two successive oists. Hoist no. 1 is in Low-High gear oisting 5-inch drill pipe from 5,590 feet. loist no. 2 is in High-High gear hoisting ssentially the same load from 5,500 feet. he rms amperes for each cycle is deter- ined by using a mean value of current $_m$ and assuming this current is required uring the hoisting portion of the cycle. his is an approximation, but is close nough for application purposes.

$$\text{rms } I = \sqrt{\frac{I_m^2 \times t_h}{t_h + t_r}}$$

here

I_m = mean amperes during hoisting portion of cycle
rms I = effective current in amperes
t_h = hoisting time in seconds
t_r = rest time in seconds

For hoisting cycle no. 2 of Fig. 4:

$$\text{rms } I = \sqrt{\frac{(1{,}300)^2 \times 23.3}{23.3 + 33.3}}$$

$$= \sqrt{692{,}000}$$

rms I = 832 amperes

This calculation is based on force-ventilated motors. If the motors were self-ventilated, the rest time would be reduced by a factor of 4 because the heat cannot dissipate as rapidly.

Each motor on which this data was taken is rated 960 amperes continuous; therefore, the peak current of 1,470 amperes and the "running" current of approximately 1,350 amperes for this hoist is satisfactory.

On the rms-ampere basis, higher currents could have been taken during this hoist, because the rms is less than rated amperes; however, it will be shown later that the driller obtained approximately maximum hp transfer to the drawworks by using a running current of 1,350 amperes.

Motor Application Factor for Drawworks

An analysis of test data taken over a period of many years indicates that approximately 85–90% of the hoisting cycles are in the 20–60% "on" classification. In other words, the motor is delivering power to the drawworks from 20% to 60% of the total time per stand and is resting from 80% to 40% of the total time. Of course, the time "on" per stand varies with the amount of power on the rig, the load, and the gear ratio; however, a conservative cycle is estimated to be 50% on and 50% off. The hoisting motor gains additional cooling after completing a round trip because it is usually at rest with full ventilation

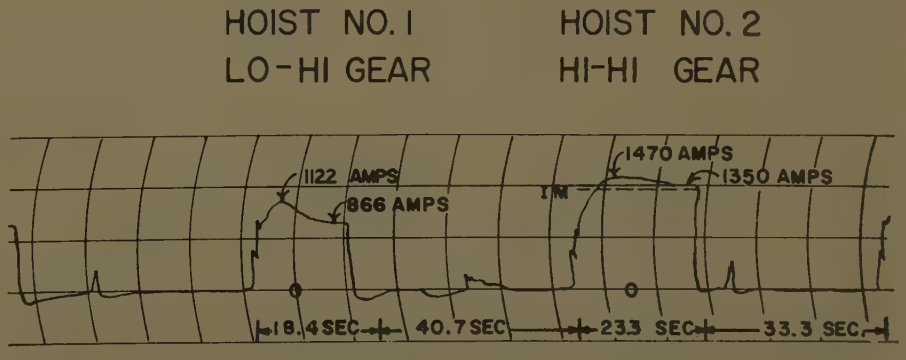

Fig. 3. Amperes versus time for two successive hoists by two 1,000-hp motors

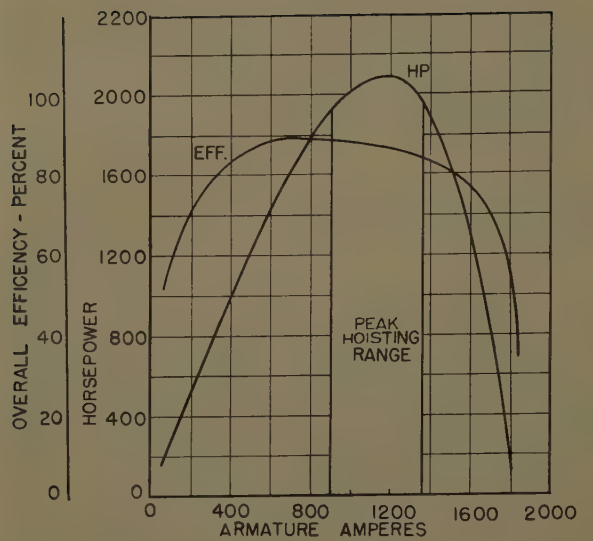

Fig. 4. Peak hoisting range for two 1,000-hp motors

or else rotating the bit at light load. This adds conservatism to the factors used in determining the actual hp rating of the motor for the drive.

Based on the preceding, it is standard practice to apply drawworks motors so that they develop approximately 140–145 % of their continuous rating on a 50-50 hoisting cycle. This is conservative enough to handle normal hoisting without allowing the rms current to exceed rated current. An application factor of 1.4–1.45 for the drawworks motor means that one 1,000-hp continuous-rated electric motor can drive a drawworks with a rating of approximately 1,400–1,450 hp if the chain ratios are properly selected and sufficient power is provided.

Motor Application Factor for Mud Pumps

The mud pumps are designed for an input hp based on a maximum speed in strokes per minute and a maximum force in pounds. Built-in protection in the form of a pressure relief valve or shear pin is usually provided by the pump builder to protect the pump against overstressing the mechanical parts when high loads exist. Since this pressure relief is usually set at approximately 25-30% above rated pressure, the electric drive system should have built-in torque limit to prevent unnecessary operation of the pump protective device under these conditions. This is accomplished by the generator characteristics as previously discussed.

The running load of the mud pump is sufficiently continuous to warrant an application factor of 1 for the mud pump motor. This means that a 1,000 hp motor should be applied on a pump requiring 1,000 hp rated input. For reasonably long periods the pump will be operated at full load and speed. Strictly speaking, however, the pump is not running on a continuous basis for longer than approximately 2 hours; therefore, by applying an electric motor at the same rating as the pump input rating, a conservative margin exists to provide extra capacity when an emergency demanding an overload arises.

It is usually more economical to apply one motor than two on any large drilling rig drive. In some instances a motor has been applied to a pump whose rating is higher than the motor. If the difference in rating is not too great and it is recognized that the motor rms current must not exceed rated amperes during overloads, this application is justified for the economical gain. One motor and one chain drive is more economical than two

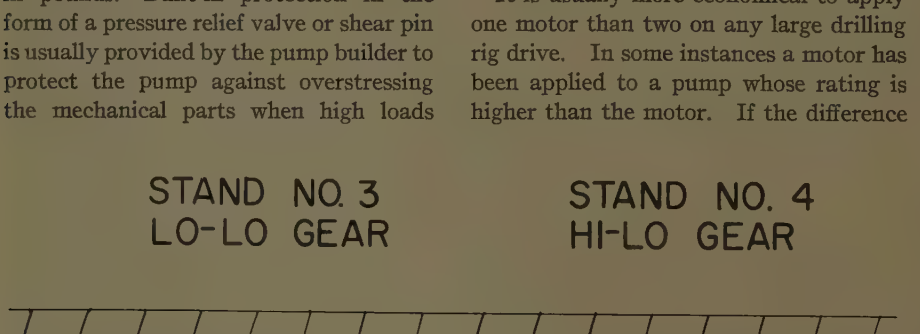

Fig. 5. Amperes versus time for stands 3 and 4 from 10,000 feet

Motor Application Factor for Rotary Table

The maximum torque delivered to the drill pipe by the rotary table must be controlled to prevent it from twisting off. Likewise, it is desirable to limit the maximum rotating speed to provide adequate control when "fishing" or drilling in peculiar formations. Variable speed is important to provide the correct speed for best penetration rate. Therefore, from a speed and torque standpoint, the requirements of the rotary table are very similar to the mud pump.

The running load of the table, like the mud pump, is sufficiently continuous to warrant an application factor of 1. It may be driven directly by a separate motor or from the drawworks. If separately driven, the maximum torque supplied by the motor and the chain ratio from the motor to the table may be selected so that the torsional limit of the drill pipe will not be exceeded. If the table is driven from the drawworks some means of torque adjustment on the drawworks motors must be provided to provide this protection because the rotary table load is relatively low in comparison to the hoisting load. This can be accomplished automatically when the driller operates the "Drill-Hoist" selector switch by reducing the number of generators available to the drawworks motor while drilling or by inserting resistance in the generator field circuit to limit the excitation.

Control

The selection of the control system depends on several considerations. The first is the degree of power flexibility required on the rig. The control can be arranged so that the generators may be switched to any motor on the rig or to only one motor. Of course, these are extreme examples of flexibility; however, some operators have deemed it justifiable to provide 100% flexibility. For most applications some intermediate degree of flexibility is usually satisfactory.

Certainly, all or almost all the generators on the rig should be connectable to the drawworks motor(s) and perhaps to one large pump. This will provide full power should any one of the engine-generator sets fail. Of course, the degree selected depends on the user's desire and

e amount of insurance required. For stance, offshore, the additional expense having each motor connectable to all nerators is usually justified as is extra nerating capacity in the power plant the basis that down-time is much more pensive than the additional investment. A second consideration is the over-all nplicity of the control system. Most erating and maintenance personnel are t sufficiently trained as yet to handle e more complex schemes available to e electrical design engineer today. r that reason the control system should as simple as possible and yet provide e necessary operational and protective tures for the equipment and personnel. Simplicity means the desirability of ving the control and machine character-ics as much a part of the inherent stem as possible without additional tating machines, relays, regulators, air stems, slide valves, air actuators, and stems requiring critical adjustment. ith characteristics built in the main gen-tors or into static, easily-adjusted sys-ns, the operating personnel have a nimum of concern about how to find d fix a trouble because troubles are nimized. With the saturable reactor, gnetic amplifier, silicon rectifiers, and ner "no-moving-parts" devices, simple, sily understood control systems can and e being built today to minimize down-ne due to component failures in the con-l system. The machine tool industry s found these systems invaluable from maintenance standpoint and there is no ason why such systems cannot be plied on drilling rigs to provide im-oved control systems.

nprovement of Operation

Since the motors and generators serve an electric torque converter between e engine and driven equipment, it is ll to analyze their performance for thods of improved operation. As ted earlier the d-c generator auto-tically limits the peak loading on the gine by limiting its own maximum out-t.

Fig. 4 shows the over-all electrical efficiency from generator input to motor output and hp output for two 1,000-hp motors receiving power from three 550-kw generators. It will be noted that the efficiency of the system is highest through the range of maximum hp, and is similar in many respects to the efficiency curve of a hydraulic torque converter. This indicates that the optimum operating range is near the peak kw output of the generator or peak hp output of the motor, where maximum power will be transmitted to the drive. This range is shown between 900–1,350 amperes and is intended to be used only on an intermittent basis. It is not to say that higher amperes should not be used, for if the load requires 1,700–1,800 amperes for high torque pulling, then it can be supplied on a momentary basis. However, for maximum hp transfer to the hoist, the running current should be between 900 and 1,350 amperes for the motors in this example.

This is particularly important on the drawworks during hoist because a significant saving in time can be made if the driller changes to a higher speed gear ratio at the right time. Not only will the equipment be operated near peak efficiency but it will also transmit peak hp from the engines which will result in minimum hoisting times. Such operation is best for the electric equipment, because it will not be overloaded on an rms basis, but will allow full utilization of its intermittent capacity at peak performance on intermittent loads.

A suggested method of operation for the driller is to have the drawworks ammeter marked in green for the peak hp range of currents, red above peak hp marked "Shift Down" and yellow below peak hp marked "Shift Up." In this manner, the driller will not have to make a test shift when he thinks the hoisting speed can be improved. It can definitely be improved with one shift if the ammeter markings are made taking into consideration the motor performance and the gear ratios of the drawworks.

On some recent tests in the Gulf of Mexico, it was noted that the driller hoisted the first three stands in Low-Low gear from approximately 10,000 feet with 2,000 hp available to the drawworks. From the data shown in Fig. 5 of stands 3 and 4 for this hoist, it is evident that stand 3 could have been hoisted in High-Low or even Low-High gear from an ampere and maximum hp standpoint. Also, later in the same "round-trip" the driller made two test shifts trying to get into a higher speed ratio, whereby some lost time was incurred. Finally, the shift to High-High gear was made approximately 10 stands too early, losing an additional minute. Although the total time lost was only a few per cent of the total, a number of round trips could account for a considerable length of time.

Conclusions

In summary, the application of electric equipment to drilling rig drives can be made more economical if closer consideration of the engine, load, and electrical equipment is made. The generator should provide as close a match as possible with the engine to transmit maximum hp at highest efficiency. The motors should be selected on the basis of the load so that in cases such as the drawworks, the intermittent capability of the motor can be used. On the mud pumps and the rotary table, the maximum torque and continuous hp requirements must be considered. Selection of the control system should be made on the basis of simplicity with a minimum of parts which provides the desired degree of flexibility and protective features.

Consideration should also be given to the method of operation used by the driller. For peak hp transfer and optimum operating efficiency, the driller should shift gears on the drawworks at the time where maximum benefit can be gained. This point will be considered when the application is made if the rms capacity of the motor is utilized. By recognizing these points and taking advantage of them, the builder, user, and operator of modern electric rigs can all benefit.

Discussion

. E. Withers (Sun Oil Company, Beaumont, Tex.): I want to compliment Mr. ogwood on his investigation and analysis the various loads on d-c electric drilling gs. We are in complete agreement that e user has not realized the full advantage the electric drive as far as the intermittent pabilities are concerned. Too many ers do not understand the theory, operation, and flexibility of electric drives; thus, when installing equipment to drive a drawworks, the installed capacity of the motors are equal to or closely approaches the rated capacity of the drawworks. This way of thinking has stemmed from the use of internal combustion engines for these drives. The manufacturer as well as personnel within the user's organization is responsible for recommending the proper sized equipment.

The author points out that the generator kilowatt rating converted to horsepower should match the continuous output of the engine. This is the ideal condition but somewhat impractical economically. When using the Ward-Leonard system of control with five separate loads, it would be necessary to have five engine generator sets. All of these could be the same size but would have to be reasonably large to accommodate the mud pump loads. I believe an installation with two generators on each engine can be used very successfully if proper con-

sideration is given to the division of load. This arrangement will reduce the number of engines and consequently the area required for this equipment.

The point made by the author concerning standardized parts, fast delivery, and quick repairs for the equipment is very necessary in the petroleum industry inasmuch as time is very costly.

Mr. Hogwood uses the term effective current (rms amperes) in determining the load on the drawworks motors. This method of calculating the effective current gives some meaning to the term "intermittent duty" which so many manufacturers use. Inasmuch as the loading of a motor is primarily governed by the ability of the motor to dissipate the heat generated within it, the quantity of forced ventilation is also a factor that must be considered. However, with ventilation as supplied by the manufacturer, Mr. Hogwood's calculations of the rms current to determine maximum loads for cyclic loading is quite satisfactory.

The rotary table load is the smallest drilling load encountered, but a very important one. The size of this load is influenced by the drilling program, subsurface formation, and hole condition. A close approximation for the rotary table load is one horsepower per revolution of the rotary table; however, with a high rate of penetration and a large hole (18 inches) the table motor can be stalled. Further investigation of this load is needed by both the manufacturer and the user.

The author's discussion of control simplicity is of utmost importance. Any and all control circuitry should be as simple and straight forward as possible with a minimum of equipment requiring critical adjustment.

A. H. Candee (The White Motor Company, Pittsburgh, Pa.): Mr. Hogwood has presented a paper which is worthy of considerable thought. His analyses and conclusions are based upon a background of experience with all types of electric drives, backed by actual field tests. It is upon such foundations that progressive evolution rests, and it is to be deplored that many rather recent applications of electric drives have been made hastily under the pressure of competition, and by their shortcomings and failures have done much to cast undeserved discredit on electric drives as a whole.

There is little in Mr. Hogwood's paper which warrants adverse criticism, but there are a few points which, perhaps, may be expanded or emphasized.

The paper indicates the need for control simplicity and practicality, but it is thought that this deserves added emphasis. Mention is made of the flexibility of electric drives which permit any generator or combination of generators to be used to feed any motor. While this is true, the designers of electric drives often go too far in this respect, for each time a different combination is added, control apparatus and electric contact-making devices must be added, yet the failure of any control circuit device to make an electrical contact when it is supposed to do so may leave the driller and his crew completely lost if the electric control circuits become too complicated. For this reason, the electric circuits must be kept severely simple. While it is true that protection must be arranged to take care against the loss of one or more engines, the degree of protection against the loss of a generator need not be nearly as broad, for the modern electric generator or motor is far more reliable than any gas or diesel reciprocating engine now in use for the drilling of oil wells. In addition to keeping the electric circuitry to its simplest terms, the designer must also avoid any and all apparatus which will not stand up without question in the extremely rough service encountered under normal drilling conditions. Flimsy contact arrangements, fine-wire devices, fragile mechanical structures, and devices which need careful adjustment are to be shunned.

In Fig. 1, Mr. Hogwood shows a typical volt-ampere curve for an electric drive, with the corresponding kilowatt (or horsepower) curve. Fig. 2 then shows how an electric drive requires but four gear ratios in the drawworks. To some of us this points out the need for further work toward utilization of the available engine power over a much wider range of speed so that the number of speed ratios which must be built into the drawworks may be still further reduced, with resultant reductions in first costs and maintenance expenses and with an improved reliability factor.

The paper, as well as Figs. 1, 3, 4, and 5, is specific as to ampere values. It should, of course, be fully understood that these values apply only to the Westinghouse Type *371* generators and motors and not to motors of other manufacture. If competitive motors are compared on an ampere basis, the results may be very misleading. This is due, of course, to the fact that without a fixed voltage or frequency to shape the design, the designer may choose the voltage and ampere capacity best suited to his manufacturing facilities. Thus, motors of equal capacity and stamina built by different builders may differ 20 to 30% in ampere ratings.

There is much work which may yet be done to improve diesel-electric drive systems. It is papers such as this which will assist materially in pointing the way toward increased reliability and efficiency.

G. W. Webb (General Electric Company, Dallas, Tex.): Mr. Hogwood's paper presents a sound approach to the subject of application of d-c drives to drilling rigs. The basic principles covered have been widely accepted in the industry, particularly since the advent in 1955, of low-cost, lightweight, short-delivery modified traction machines.

Such machines by their nature emphasize the principles stated by the author of:

1. Standardization on fewer ratings
2. Engine overload protection
3. Motor torque and speed limits
4. Simple controls
5. Utilization of intermittent capabilities.

By way of comment on these principles, some 15 manufacturers offer about 30 different horsepower ratings of drawworks from 100 hp to 2,500 hp, and about 40 different horsepower ratings of mud pumps from 100 to 1,700 hp. The inherent inefficiencies of such an equipment supply situation are obvious when considered on an industry basis. All these models must be redesigned periodically to keep up with competition and advancing technology. As a result, few units of any one make and model can be sold to the limited market available. The economic advantages of mass production are seldom obtained and much of the equipment cost goes to cover development and engineering.

The electrical manufacturers so far have each offered only two or three ratings of motors to drive the wide range of drilling machinery and two or three ratings of generators to be driven by the even wider range of engine horsepower ratings and speeds available. The economic benefits of this approach must be sold to the drilling contractors and oil companies who specify equipment. It could result in future savings to all parties involved.

The author points out that peak engine loads are limited by the differential generator characteristic, but recommends that the generator kw rating should closely match the continuous output of the engine. It has been demonstrated that a 3-field generator, including a self-excited shunt field, can be applied to engines of much lower horsepower capability than the generator rating and still prevent engine overloading or stalling. By flattening the top of the hp-versus-motor-rpm curve, this device enables the electric transmission to transmit full engine horsepower to the load over a wider range of load speeds.

The author mentioned the inherent torque and speed limits on separately excited motors by virtue of the generator characteristic. He indicated that the torque limit could be changed by limiting generator excitation or reducing the number of generators available to a motor. One other device which can be used to limit torque applied to a pump or rotary is to weaken the fixed motor field. This trades torque for speed without reducing horsepower, but the drive ratio must be selected accordingly.

We concur with the author's remarks regarding control simplicity. Basic drilling performance should be inherent in the rotary machine characteristics. We feel that complicated voltage and current regulating systems are best avoided by using a differential generator and that this electrical characteristic is best translated into controlled speed and torque by the separately excited shunt motor. We would like to inquire about the author's experience regarding the long term reliability of rectifiers in view of the a-c voltage fluctuation sometimes encountered on drilling rig light plants.

Regarding application factors for drilling motors, we note that the author recommends a factor of 1.4–1.45 for the drawworks whereas his company's advertisement specify a 1.6 factor. We have found the 1.4 factor to be conservative for this application. Referring to the section of the paper on "Motor Application Factor for Mud Pumps," I would emphasize the last paragraph which implies that economic consideration may dictate an application factor exceeding unity. Where experience is available to predict accurately the pumping load cycle, a factor in the order of magnitude of 1.1 or 1.2 may apply. This usually is justified on the basis of possibly increased motor maintenance versus increased initial investment.

In closing, I would like to comment on the general aspects of the application of electric transmission to drilling machinery.

thor describes a drawworks with four ward mechanical ratios and no reverse ar as being "specifically designed for ctric drive." This is true when compared conventional, straight mechanical draw-rks which normally provides 6 or 8 for-rd ratios plus reverse gear and friction tches. However, by more fully utilizing e torque conversion characteristics of the transmission system, the drawworks can further simplified. It is quite feasible to sign a drawworks specifically for electric ve with positive clutches and two chanical ratios to the drum shaft without crificing essential hoisting performance. ch a drawworks could offer the user sav-gs in weight, size and initial cost which uld provide the economic and perform-ce benefits of electric rigs at no greater st cost than mechanically driven rigs.

E. Hogwood, Jr. The author wishes to ank Mr. Withers, Mr. Webb, and Mr. ndee for their discussions and comments. This paper principally outlines applica-n procedures that are presently used in ner industries where electric power is more dely used. As the drilling industry be-nes more familiar with diesel-electric wer, it is expected that the users and sup-ers will learn to use these principles to lize fully the electric equipment. The ult will be a reduction in first cost and erating expenses of drilling oil wells using ctric drives.

First, I want to answer the specific ques-ns that were asked and then, briefly, com-nt on some of the points common to more an one of the discussions.

This paper was presented as a confer-ce paper at the 1958 Petroleum Industry nference and since that writing, a con-erable amount of development work and dy of field test data have been made. the basis of these data, we have initiated d completed development work on a new tic excitation and control system for oil ll drilling. It is still agreed that the use of inherent machine characteristics is a good, simple method of obtaining the required drive performance. We have used the 3-field generator or exciter and the separately excited shunt motor for more than 20 years to obtain this performance for drilling; however, the static excitation system has been developed in an effort to minimize cost further, to increase the output of a given generator and motor frame, to simplify the system, and also to maintain the over-all system reliability. This system utilizes static components such as magnetic amplifiers, saturable reactors, and silicon diodes which need no attention once the system is set. This system is considered to be a definite improvement over the already proved system which relies on inherent machine characteristics.

2. As for the long term reliability of rectifiers considering fluctuation of a-c power on the rig, we have not experienced any difficulty attributable to this cause. However, selenium rectifier applications should be made rather conservatively to avoid excessive aging. Some of the factors affecting aging that should be considered are high ambient temperatures, corrosive atmospheres, cyclic overloads, and long cable runs to the loads. Where silicon rectifiers and diodes have been used, no aging difficulties have been encountered and they are proving to be quite reliable.

It is apparent also that all a-c auxiliary power sets used on drilling rigs should be equipped with reasonably good voltage regulators to operate motors, controls, lamps and other loads within rated tolerances.

3. The 1.6 application factor for the drawworks drive was published by us after this paper was originally written including the 1.4 to 1.45 factor. The application factor depends on the length of the hoisting cycle to rest cycle ratio which is based on the rms current not exceeding the rated current of the motor. It should be noted that a shorter hoisting cycle than that mentioned in the paper is required for the 1.6 factor than for the 1.45 factor. It has been found that the 1.6 ratio is conservative for this application. It is suggested that the Petroleum Industry Committee consider establishing standards for the presently used "intermittent rating" based on rms current and an acceptable hoisting cycle. The basic need is for a standard hoisting cycle which could be used to determine the drawworks application factor for various manufacturers equipment.

I concur with Mr. Withers that applications of two generators per engine offer an economic means of dividing engine horsepower; however, the maximum rating of either generator should still not exceed the horsepower capabilities of the engine. Some engine manufacturers prefer each generator to be capable of absorbing the full output of the engine, even though both never could do so simultaneously. This allows utilization of the full engine output through one generator when required.

Mr. Webb has stated that a 3-field generator, including a self-excited field, can be applied to engines of much lower horsepower capability than the generator rating. This is basically true, depending on the ratio of separately excited field strength to self-excited field strength in the generator design; however, it is felt that a wider range of constant horsepower can be accomplished more economically in the control system than in oversizing the generator.

One more point in closing. Mr. Webb and Mr. Candee both discussed the point concerning a 4-speed drawworks specifically designed for electric drilling. To their comments, I would add that I fully agree and that I hope we may soon be requested to study and build an electric drawworks as Mr. Webb described with some major rig builder. By reducing the mechanical equipment required and fully utilizing the electric drive, certainly the first cost of the electric rig will be approximately equal to the mechanical rig. With the first cost equal, the user will be more desirous of having the electric drive with its additional advantages.

Three-Phase Induction Heating Coils

N. V. ROSS
AFFILIATE AIEE

N THE 60-cycle field of induction heating a 3-phase system is desirable. The dvantages of 3-phase power is fairly vious. In most cases a large amount of wer is required and a balanced 3-phase ad is very practical. Hence, 3-phase duction heating coils have been used to arge extent in 60-cycle heating of alumi-m and brass. Since the size of stock to heated is large in cross section, which the primary reason for 60 cycle, the ount of energy required to heat the terial because of its large mass is, in ny cases, quite high. In the past, large billets, 4 inches to 30 inches diameter of aluminum, as well as brass, 4 inches to 10 inches in diameter, have been heated primarily for extrusion. Temperature uniformity is mandatory for high-quality results. In the case of special brass alloys, the temperature must be maintained at ±10 F (degrees Fahrenheit) throughout the billet. Induction heating is primarily a very rapid heating process taking seconds or minutes to heat, while other methods of heating require hours. Because of this rapid heating, temperature patterns follow closely magnetic flux patterns; also due to the rapid heating, sufficient time is often lacking for equalizing.

As is well known, the magnetic flux pattern described by Fig. 1 is fairly uniform throughout most of its length for long coils. The field intensity H diminishes at the ends to one half the value at the center of a closely spaced solenoidal coil. If a long cylindrical billet is placed inside the coil, the temperature or heat pattern will follow the field intensity pattern, that is, if the billet is longer than the

Paper 59-256, recommended by the AIEE Electric Heating Committee and approved by the AIEE Technical Operations Department for presentation at the AIEE Winter General Meeting, New York, N. Y., February 1–6, 1959. Manuscript submitted November 26, 1958; made available for printing January 28, 1959.

N. V. Ross is with the Magnethermic Corporation, Youngstown, Ohio.

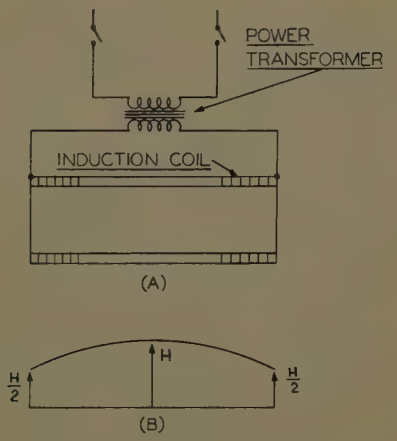

Fig. 1. A—Single phase coil. B—Corresponding field intensity

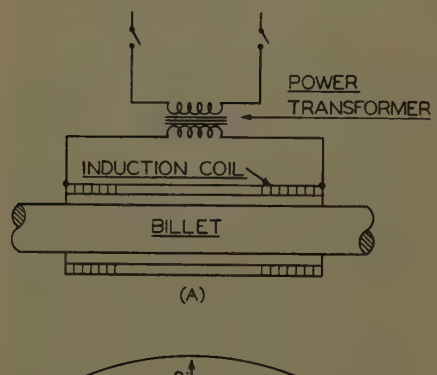

Fig. 2. A—Single phase coil with long billet. B—Corresponding temperature pattern

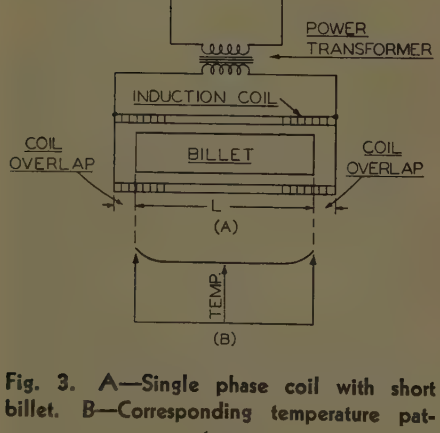

Fig. 3. A—Single phase coil with short billet. B—Corresponding temperature pattern

coil; see Fig. 2. If the billet is shorter than the coil, the ends will tend to overheat as shown in Fig. 3, because of the concentration of flux lines at the ends. The excess coil length is known as coil overlap. The coil overlap depends upon several factors; the material of the coil (in most cases copper), the coil space factor, the material of which the billet is composed, the frequency applied to the induction coil, the inside diameter of the coil, and the diameter of the billet. At present the amount of coil overlap using 60 cycles per second is determined primarily by experiment and varies from 3/4 inch to 2 inches for aluminum billets, and $1^1/_2$ inches to 3 inches for brass. It is fairly easy to obtain a uniformly heated billet with a coil as illustrated in Fig. 3 with single-phase power. The ends are purposely overheated during the heat stage to compensate for radiation losses from the edges as the billet travels from the heater to the press.

In the case of 3-phase coils a phase dip occurs in the flux pattern as shown by Fig. 4. Since the heat pattern is a function of the field intensity squared, the phase dip is quite pronounced. The first improvement was realized by reversing the phase of the center coil section to obtain 60 electrical degrees displacement between phases instead of 120 degrees. This is shown in Fig. 5. The dip in field intensity H at the phase points became less and the corresponding temperature pattern was improved. The results were still not good enough and a better solution was sought. The answer was one of phase overlapping as illustrated by Fig. 6. At the phase points, a small number of turns were simultaneously energized by adjacent phases. The number of turns or phase region overlapped allowed one to obtain nearly uniform flux pattern throughout a 3-phase coil approximating the single-phase coil. The corresponding temperature pattern was improved to such a degree that a billet can be heated within ± 10 F throughout its entire length. The amount of phase overlap required depends upon several factors as in the case of coil overlap. It varies with coil diameter, billet diameter, frequency, billet, and coil conductor material. The phase overlap can be calculated by the following equation:

$$\phi_{OL} = 1/4[(b+d_1)-(a-d_2)] \qquad (1)$$

where

ϕ_{OL} = phase overlap
b = coil inside diameter
a = billet outside diameter
d_1 = penetration depth of coil conductor
d_2 = penetration depth of the billet

If b and a are measured in inches, then d_1 and d_2 for nonmagnetic materials are calculated by:

$$d_1 = 3{,}160\sqrt{\frac{\rho_1}{sf}} \text{ and } d_2 = 3{,}160\sqrt{\frac{\rho_2}{f}} \qquad (2)$$

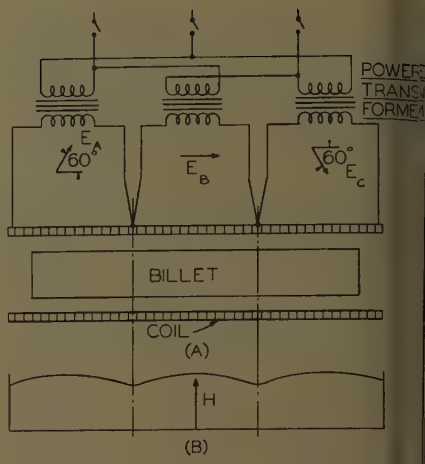

Fig. 4. A—Transformer and coil connectio 3-phase nonreversed center section. B Corresponding field intensity for coil as in (A

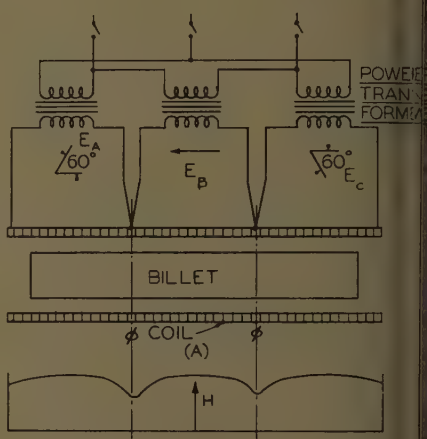

Fig. 5. A—Transformer and coil connecti 3-phase reversed center section. B—Coo sponding field intensity for coil as in (A

where

ρ_1 = resistivity of coil conductor in ohm in
ρ_2 = resistivity of billet material in ohm in
s = coil space factor
f = frequency cycles per second

Equation 1 holds for 3-phase coils on Since an integral number of turns can contained within an overlapped ph region, the nearest whole number of t widths is usually used for the phase ov lap calculated by equation 1.

Example: Calculate the phase over of an aluminum billet of 5-inch diame and length 24 inches, coil dimensio 6-inch inside diameter and 26-inch leng The copper turn width is 3/8 inch w 1/32-inch turn insulation. Coil space f tor = 0.92. Mean temperature of alu num to be 850 F, with 60-cycle 3-ph power supplied to the coil.

Solution: First calculate the penet tion depths for the coil copper and aluminum load. Use average resistiv

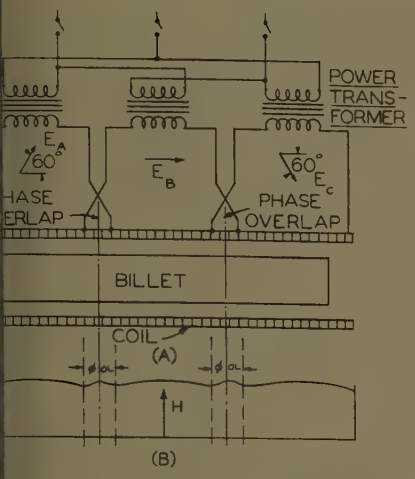

. 6. A—Transformer and coil connections hase reversed center section with phase rlap sections. B—Corresponding field intensity for coil as in (A)

ues over the temperature range. The rage resistivity of copper is 0.8×10^{-6} m-inch.

nce:

$$=3{,}160\sqrt{\frac{0.8\times10^{-6}}{0.92\times60}}=0.380 \text{ inch}$$

i

$$=3{,}160\sqrt{\frac{2.24\times10^{-6}}{60}}=0.611 \text{ inch}$$

$$_2=1/4[(6+0.38)-(5-0.611)]$$

$$_2=1/4[(6.38-4.39)]=0.498 \text{ inch}$$

The total turn width is $0.375+0.0314=$ 06 inch. Hence, two turn widths would e 0.812 inch. In this case either one or o turns could be chosen but for physical ace reasons, two turns would be ed.

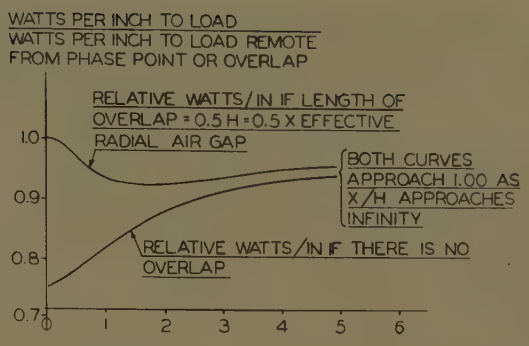

Conclusions

One may conclude from the preceding that it is possible to obtain a uniform temperature pattern over the length of an inductively heated billet using a 3-phase coil. A slight dip or rise in temperature, approximately ±10 F, still exists at the phase points due to the necessity of using an integral number of turns approximately equal to the calculated phase overlap. In Fig. 7 the relative watts per inch for phase overlap is plotted along the billet length and is compared to that without phase overlap.

Appendix I. Calculation of Field Intensity Near End of Long Cylindrical Coil at Load Surface

Refer to Fig. 8 and the following assumptions:

1. Ratio of radial air gap to radius of load small enough such that curvature effects may be neglected.
2. Reference depth d small in relation to h and radiuses.
3. Constant coil ampere-turn per inch.

With the above assumptions the field intensity $H/(NI/L)$ is given by the following equation:

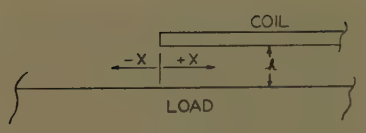

Fig. 7 (left). Ratio x/h of distance from phase point or center of overlap to effective radial air gap

Fig. 8 (above). Diagram for calculating field intensity near end of long cylindrical coil

$$H/NI/L=1/2+1/\pi \tan^{-1}(x/h) \qquad (3)$$

Equation 3 is plotted in Fig. 9 for values $+x/h$ and for values $(-x/h)$; see reference 1.

Appendix II. Effect of Total Field Intensity in Phase Overlapped Region

With reference to Fig. 10 where the vectors $\mathbf{H}_1$ and $\mathbf{H}_2$ represent the components of magnetic intensity at x produced by left and right hand coil segments and where the real axis is taken as the resultant of $\mathbf{H}_1+\mathbf{H}_2$ at $x=0$, and where H_1' and H_2' are the real components of $\mathbf{H}_1$ and $\mathbf{H}_2$ and H_1'' and H_2'' are imaginary components, the magnitude of the axial component of $\mathbf{H}$ at x is:

$$H=\sqrt{(H_1'+H_2')^2+(H_1''-H_2'')^2} \qquad (4)$$

$$H=\sqrt{H_1^2+H_2^2+H_1H_2}$$

Substituting equation 3 into 4 for corresponding points and replacing

$1/2+1/\pi \tan^{-1} x/h$ by $f(x/h+\phi/2h)$

$1/2+1/\pi \tan^{-1}-x/h$ by $f(-x/h+\phi/2h)$

$$H^2/(NI/L)^2=f^2(x/h+\phi/2h)+f^2(-x/h+\phi/2h)+f(x/h+\phi/2h)f(-x/h+\phi/2h) \qquad (5)$$

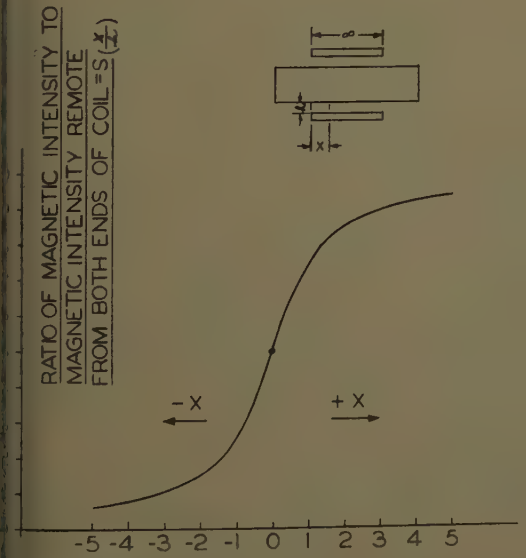

Fig. 9 (left). Ratio x/h of distance in coil to radial air gap

Fig. 10 (below). Cross section of coil and billet at an overlapped phase point

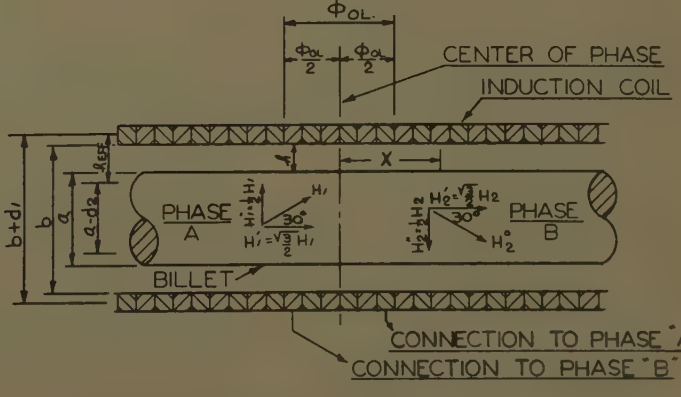

In equation 5 in order to have the same heating at $x=0$ as at $x=\infty\phi/2h$ must be chosen such that:

$$^3\int^2(\phi/2h)=1 \qquad (6)$$

Writing equation 6 in the form of equation 3 it follows that

$$(\phi/2h)=\sqrt{1/3}=1/2+1/\pi\tan^{-1}(\phi/2h) \qquad (7)$$

Solving equation 7: $\phi/2h=0.247$. Hence the phase overlap ϕ should be equal to 0.494 h or approximately half of the effective radial air gap. The effective radial air gap is defined by

$$h=(b+d_1/2)-(a-d_2/2)$$
$$h=1/2[(b+d_1)-(a-d_2)]$$

Therefore, the phase overlap is given by the equation

$$\phi_{OS}=1/4[(b+d_1)-(a-d_2)]$$

Reference

1. Radio Frequency Heating, G. H. Brown, C. N. Hoyler, R. A. Bierworth. D. Van Nostrand Company, Inc., Princeton, N. J., 1947, chap. 8, 90.

Stability Criteria for Instrument Servomechanisms with Coulomb Friction and Stiction

M. P. PASTEL
NONMEMBER AIEE

G. J. THALER
MEMBER AIEE

IT IS WELL KNOWN that relative motion between rubbing surfaces is opposed by friction forces. In general, a force directly proportional to velocity is produced by a component known as "viscous friction." Normally, another component, the coulomb friction force C, produces a force that is essentially constant regardless of velocity. In addition, if the surfaces are initially stationary, the force required to start motion is greater than the coulomb friction force. Since the surfaces seem to adhere, the effect is called "stiction" and the magnitude of the required starting force is called the stiction force S. These effects are illustrated graphically in Fig. 1. Note that the ordinate may be force or torque, and the dimensions of C or S obviously must be adjusted as needed.

The effect known as stiction is frequently considered to be a static (zero velocity) phenomenon, which postulates that as soon as motion is initiated the stiction disappears and only the coulomb friction remains. This is a reasonably accurate assumption since the retarding force is normally reduced to the coulomb friction level at very low velocities. For some surfaces the stiction effect may decrease gradually as the velocity increases; see Fig. 1.

Paper 59-649, recommended by the AIEE Feedback Control Systems Committee and approved by the AIEE Technical Operations Department for presentation at the AIEE Middle Eastern District Meeting, Baltimore, Md., May 19–21, 1959. Manuscript submitted February 10, 1959; made available for printing April 3, 1959.

M. P. Pastel and G. J. Thaler are with the U. S. Naval Postgraduate School, Monterey, Calif.

Phase Plane Analysis

Step Function Response of a Second-Order Servo

For a second-order proportional-error servomechanism with coulomb friction, the torque equilibrium equation is

$$J\ddot{\theta}_c+f\dot{\theta}_c+C \text{ sign } \dot{\theta}_c=KE \qquad (1)$$

where

J = polar moment of inertia
F = coefficient of viscous friction
C = coulomb friction torque
K = torque constant
θ_c = output position angle
E = error $=\theta_R-\theta_c$

For a step displacement input equation 1 becomes

$$J\ddot{E}+f\dot{E}+KE+C \text{ sign } \dot{E}=0 \qquad (2)$$

To analyze the system on the phase plane the isocline equation is obtained from equation 2 and is

$$\dot{E}=-\frac{KE}{NJ+f}-\frac{C \text{ sign } \dot{E}}{NJ+f} \qquad (3)$$

where $0<N<\mp\infty$ and N is the slope of phase trajectory where it crosses the designated isocline. Equation 3 is the equation of two families of straight lines in the $\dot{E}$ versus E plane, as shown in Fig. 2(A), emanating from $E=\mp C/K$. These isoclines are identically the isoclines of the linear system (without C) except for a translation of the upper and lower half-planes with respect to the origin. For a step displacement input to initiate motion, the amplitude of the step must be such that $E>C/K$. The trajectory then follows the path dictated by the isoclines until it terminates on the E-axis betwe the foci. If discontinuous stiction present the step must be such th $E>S/K$ to initiate motion, the trajecto still follows the isoclines emanating fr the foci at $\mp C/K$, but the trajecto terminates (system sticks) if it hits t E-axis between $\mp S/K$. This is illustrat in Fig. 2(A). A step displacement magnitude such as to cause $E=A$ Fig. 2) would start a trajectory for co lomb friction without stiction, but it do not initiate motion when stiction present. For a step large enough to $E=A'$ motion is always initiated. T trajectory $A'BD$ is produced for C wit out S, but is terminated at B if stictio present. Note that in either case $E_{ss}\neq$ Coulomb friction and stiction are alw stabilizing when a step displacement inp is used. This can be used to stabili unstable systems partially, if some sta error is acceptable.

Ramp Function Response of Second-Order System With Coulomb Friction Only

When the input is a suddenly appli ramp function and only coulomb frict is present, equation 1 still applies, and

$$J\ddot{E}+f\dot{E}+KE=f\omega_t+C \text{ sign } (\dot{\theta}_R-\dot{E})$$

where $\omega_t=\dot{\theta}_R=$ input velocity. T isocline equation becomes

$$\dot{E}=-\frac{KE}{NJ+f}+\frac{f\omega_t+C \text{ sign } (\dot{\theta}_R-\dot{E})}{NJ+f}$$

Equation 5 also defines two families s radial lines intersecting the E-axis

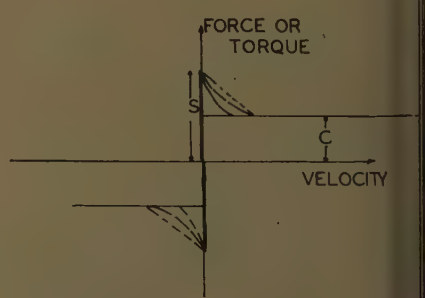

Fig. 1. Definition of coulomb friction stiction

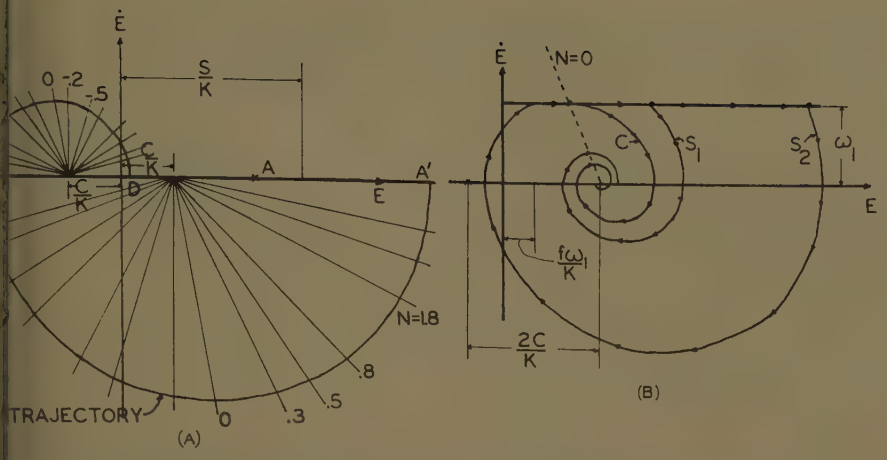

2. A—Phase trajectory of second-order servo with coulomb friction and stiction. B—Phase trajectories as in A, plus ramp input

$= (f\omega_t \mp C)/K$. The foci are again separated by 2 C/K, but the origin of coordinates is not midway between these i; it is displaced from this mid-point an amount $f\omega_t/K$. Also, the term sign $\dot{\theta}_R$ − sign $\dot{E}$) designates the set of clines to be used, and thus defines a iding line at $\dot{E}=\omega_t$. This is shown in g. 3 for an arbitrarily selected ω_t. The ase trajectory for a ramp input has tial conditions $E=0$, $E=\omega_t$, and thus rts at point P. Motion is initiated en $KE=C$, corresponding to a horintal displacement from point P of nount $E=C/K$. This is precisely the int at which the $N=0$ isocline crosses dividing line. After one complete ral about the focus, the trajectory must ss the $N=0$ isocline below the dividing e if the linear system has $\zeta>0$. The ase trajectory spirals into the focus and e steady-state condition provides a locity lag error

$$_s = \frac{f\omega_t + C}{K} \qquad (6)$$

te that the phase plane of Fig. 3 is justed to only one input velocity. For ch new ω_t the dividing line and the

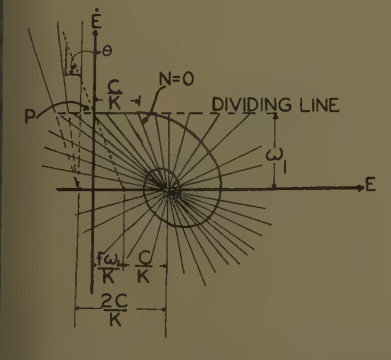

g. 3. Isoclines, dividing line, and phase jectory of second-order servo with coulomb friction and ramp input: $\theta = \tan^{-1} K/f$

origin must be shifted. The displacement of the origin from the point midway between the foci is $-(f\omega_t)/K$, and the vertical displacement of the dividing line is $+\omega_t$. Thus, as ω_t varies from zero to infinity, the intersection of the dividing line with the $\dot{E}$-axis moves along a line with slope $-K/f$. This is precisely the slope of the $N=0$ isocline, and the displacement between these lines is C/K. Thus for any ω_t the system is stable, if the linear system is stable.

Ramp Function Response of a Second-Order System With Coulomb Friction and Discontinuous Stiction

When stiction is present but discontinuous (disappearing for $\dot{\theta}_c \neq 0$) the basic isocline configuration of Fig. 3 is unchanged, but motion is not initiated until the error is such that $KE=S$. This makes a limit cycle possible when a ramp function is suddenly applied, providing that ω_t is sufficiently low. Fig. 2(B) shows the phase plane for a ramp input ω_t, and 3-phase trajectories, for C only, for S_1 slightly greater than C, and for S_2 much greater than C. The first two are seen to be stable, but for S_2 the phase trajectory is a spiral of such dimensions that it intersects the dividing line, the output member sticks, and a limit cycle results.

Stability Criterion for a Second Order System With Discontinuous Stiction When a Ramp is Suddenly Applied

Knowing the system parameters, the values of C and of S, and the value of ω_t, makes it possible to predict whether a limit cycle will exist when the ramp is suddenly applied. Note that the phase trajectory is defined by the isoclines of the linear system, since the only effect of C is to translate the focus. Thus a linear equation can be derived for the phase portrait. Furthermore, the specific trajectory can be designated by inserting the co-ordinates of the starting point of the trajectory when the constant of integration is to be evaluated. The necessary condition for the existence of a limit cycle is apparent from the phase portrait: as the trajectory spirals around the focus the first time, it must pass through a maximum velocity; and if this value of $\dot{E}$ equals or exceeds ω_t, the system sticks and a limit cycle is started. To derive a stability criterion from these conditions, the equation for the phase trajectory is given by

$$\dot{E}^2 + 2\zeta\omega_n E\dot{E} - 4\zeta^2\omega_t\dot{E} + \omega_n^2 E^2 - 4\zeta\omega_n\omega_t E + 4\zeta^2\omega_t^2 = D\epsilon^{\frac{2\zeta}{\sqrt{1-\zeta^2}}\tan^{-1}\frac{\omega_n E + \zeta\dot{E} - 2\zeta\omega_t}{\dot{E}\sqrt{1-\zeta^2}}} \qquad (7)$$

where $\zeta = f/2\sqrt{KJ}$; $\omega_n = \sqrt{K/J}$; D = constant of integration. The specific phase trajectory may be defined by substituting the co-ordinates of the point at which the system pulls free of the stiction, evaluating $D=D_1$. Equation 7 is then completely defined, and it is possible to evaluate the maximum velocity reached on the first spiral. A simpler procedure is to note that the maximum velocity must be a point somewhere on the $N=0$ isocline. The critical phase trajectory is the one which passes through the point of intersection between the $N=0$ isocline and the dividing line. If the value of D associated with this critical trajectory is computed as D_2, then the system has a limit cycle if $D_1 \geqq D_2$. By proper manipulation the stability criteria is obtained as

$$[1 \geqq -b(b - 2\zeta)]\epsilon^{\frac{a}{-2\zeta a'}\tan^{-1}\frac{1-2\zeta^2}{-2\zeta a'} - \tan^{-1}\frac{1+\zeta(b-2\zeta)}{a'(b-2\zeta)}} \qquad (8)$$

where a, a', and b are as defined in the Appendix. Fig. 4 presents the stability criterion as a curve.

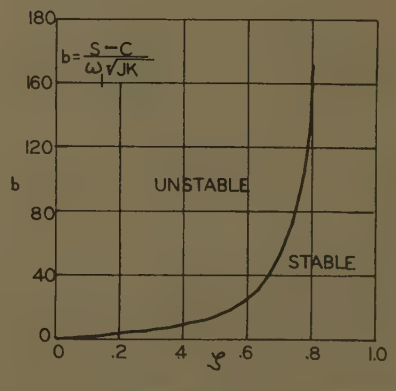

Fig. 4. Graph of stability criterion for second-order servos with stiction and ramp input

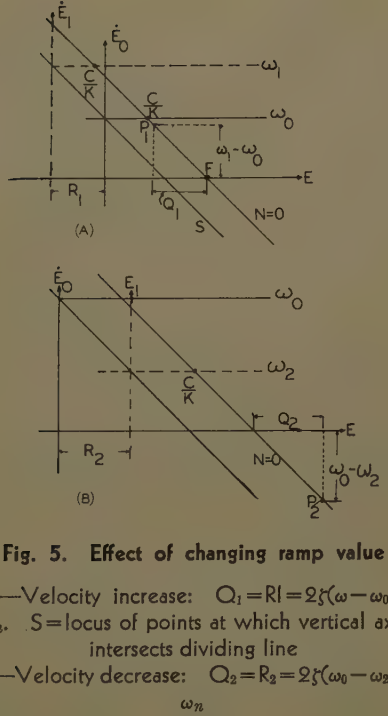

Fig. 5. Effect of changing ramp value

A—Velocity increase: $Q_1=RI=2\zeta(\omega-\omega_0)/\omega_n$. S=locus of points at which vertical axis intersects dividing line

B—Velocity decrease: $Q_2=R_2=2\zeta(\omega_0-\omega_2)/\omega_n$

Effect of a Change in Input Velocity: Stability Criteria

For any given system in which stiction is present a limit cycle must result if the system is started from rest with a sufficiently small ramp ω_i, and a limit cycle cannot result if ω_i is sufficiently large. If stiction produces limit cycles at useful speeds, the limit cycle can be avoided by starting with a large ω_i and reducing the input velocity slowly. If the reduction in speed is accomplished too rapidly the limit cycle may be initiated. Once the system has been adjusted to operate stably at a low speed, the speed may be increased as rapidly as desired without initiating a limit cycle, but speed decreases must be made slowly. This section presents an explanation of these phenomena, and develops certain stability criteria for the speed adjustments.

Fig. 5 shows the effect of changing ω_i on certain important characteristics of the phase plane. When the system is operating stably at velocity ω_0, the operating conditions are described on the phase plane by a point located at the focus F_1; see Fig. 5(A). When the velocity input is increased suddenly from ω_0 to ω_i, the origin of co-ordinates and the dividing line are both displaced. The critical sticking point C/K moves out along the $N=0$ isocline, as shown in Fig. 5(A). The instantaneous conditions may be described as follows: no change in output position or velocity; no change in input position; but a change $(\omega_i-\omega_0)$ in input velocity. The instantaneous error is unchanged, but $\dot{E}=\omega_i-\omega_0$. The operating point is therefore displaced on the phase plane; it is displaced horizontally because of the shift in co-ordinate origin, and vertically because of the sudden change in $\dot{E}$. These displacements are such that the new operating point is on the $N=0$ isocline and below the new dividing line, so it is impossible for the output to stick (if $\zeta>0$). Thus, one stability criterion may be stated: if the system is operating at any steady-state velocity without limit cycle, any desired velocity increase may be made without initiating a limit cycle.

If the velocity is decreased, the operating point moves in a similar fashion but in the opposite direction to point P_2 in Fig. 5(B). Since P_2 and the critical point C/K are both on the $N=0$ isocline, and the limit of stability is reached if the trajectory from P_2 passes through C/K, then the system is stable if

$$\omega_2>(\omega_0-\omega_2)\epsilon^{-\pi\zeta} \tag{9}$$

from which

$$\omega_2>\frac{\omega_0}{1+\epsilon^{\pi\zeta}} \tag{10}$$

Note that equation 10 states the stability criterion for a sudden decrease in input velocity.

Effect of Variable Stiction

When the stiction-coulomb friction characteristic is variable rather than discontinuous, as shown by the broken lines in Fig. 1, the analysis of the preceding paragraphs is not complete. The stability criterion of Fig. 4 is only partially correct in the sense that if Fig. 4 denotes an unstable system it is surely unstable, but some systems which appear to be barely stable may actually be unstable if the stiction is variable rather than discontinuous. For variable stiction the location of the focal point on the E-axis is given by

$$E=\frac{2\zeta\omega_i}{\omega_n}+\frac{S_x}{K} \tag{11}$$

where S_x is the value of stiction specified by the instantaneous velocity. Thus the focal point moves along the E-axis as $\dot{E}$ changes. A step-by-step construction may be used to determine the phase trajectory. First, the stiction versus velocity characteristic must be known, and it is convenient to use a sliding overlay on a base drawing of the isoclines. As indicated in Fig. 6, the breakaway point is located at S_0/K, for which the focal point is at zero. An increment of the trajectory is constructed to point A. One then refers to the stiction versus velocity characteristic to evaluate S_x and equation 11 is used to locate a new focal point at a. The curve is then constructed from A to B to new focal point located at b, the trajectory constructed from B to C, a new focal point located at C, etc. The trajectory for discontinuous stiction is also shown in Fig. 6. Since the focal point for this case is fixed at X, it is obvious that variable stiction has a greater destabilization effect than discontinuous stiction.

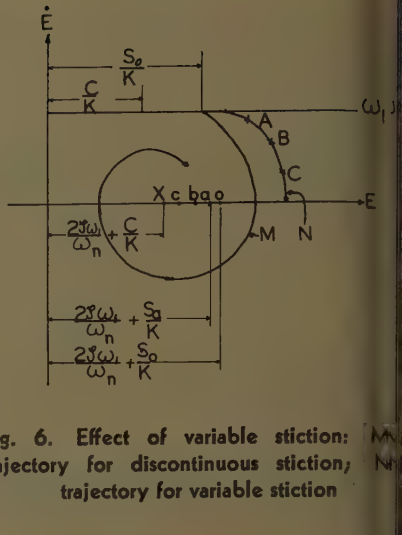

Fig. 6. Effect of variable stiction: M... trajectory for discontinuous stiction; N... trajectory for variable stiction

Conclusions

The effect of coulomb friction, (c... continuous stiction, and variable stict... have been explained with regard ... second-order servos. The conditio... which lead to a limit cycle with ra... input have been determined and stabili... criteria have been developed for the ... missible magnitude of a suddenly appl... ramp and for the permissible variatio... of input velocity during operation.

Appendix. Derivation of Stability Criterion for Sudden... Applied Ramp Input

Definitions:

$$a=2\zeta/\sqrt{1-\zeta^2},\ a'=\sqrt{1-\zeta^2},\ R=\omega_i/\omega_n$$

$$b=(S-C)/KR,\ E_r=E-(2\zeta R+C/K)$$

Equation 7 gives the phase trajectory ... a linear system in response to a ramp inp... If the origin of co-ordinates is shifted to ... focal point so that the relative error quant... is designated E_r, then the equation of ... phase trajectory with respect to this ori... is

$$\dot{E}^2+2\zeta\omega_n\dot{E}E_r+\omega_n^2E_r^2=D\epsilon^{a\tan^{-1}\frac{\dot{E}+\zeta\omega_nE_r}{a'\omega_nE_r}}$$

To evaluate D_1 and D_2 for the phase traj... tory from the break-free point and for ... phase trajectory through the intersect...

the $N=0$ isocline with the dividing line, te that the co-ordinates of point 1 are $=\omega_i=R\omega_n$; $E_r=bR-2\zeta R$; and for point $\dot{E}=R\omega_n$; $E_r=-2\zeta R$. Substituting these lues yields

$$=[R^2\omega^2{}_n+2\zeta\omega_n{}^2R^2(b-2\zeta)+$$

$$\omega_n{}^2R^2(b-2\zeta)^2]\epsilon^{-a\tan^{-1}\frac{R\omega_n+\zeta\omega_nR(b-2\zeta)}{a'\omega_nR(b-2\zeta)}}$$

$$=[R^2\omega_n{}^2-4\zeta^2\omega_n{}^2R^2+4\zeta^2\omega_n{}^2R^2]$$

$$\epsilon^{-a\tan^{-1}\frac{R\omega_n-2\zeta^2\omega_nR}{-2a'\omega_n\zeta R}}$$

and

$$\frac{D_1}{D_2}=[1+b(b-2\zeta)]$$

$$\epsilon^{a\left(\tan^{-1}\frac{1-2\zeta^2}{-2\zeta a'}-\tan^{-1}\frac{1+\zeta(b-2\zeta)}{a'(b-2\zeta)}\right)}$$

The system goes into a limit cycle if $D_1=D_2$; therefore the stability criterion is

$$1\leqq[1+b(b-2\zeta)]$$

$$\epsilon^{a\left(\tan^{-1}\frac{1-2\zeta^2}{-2\zeta a'}-\tan^{-1}\frac{1+\zeta(b-2\zeta)}{a'(b-2\zeta)}\right)}$$

Since the only variables are b and ζ, a curve may be obtained on the b versus ζ plane in such a way that all points on the curve satisfy the condition $D_1/D_2\equiv1.0$, and this curve divides the plane into stable and unstable regions.

Reference

1. Operating Modes of a Servomechanism with Nonlinear Friction, H. Lauer. *Journal*, Franklin Institute, Philadelphia, Pa., 1955.

Constant-Frequency Variable-Speed Frequency-Make-Up Generators

BERT V. HOARD
MEMBER AIEE

XPERIENCE obtained on constant- frequency generation systems which e installed in jet aircraft has indicated eas where improvements are needed. xamples are:

Unpredictable failures, such as carbon ush dusting.

Relatively short life of parts subject to ar.

Poor quality of frequency supply.

Always present also are the needs for luctions in weight, volume, mainte- nce, and rebuilding costs; for improve- nt in efficiency; and for increased avail- le time for operation.

Elimination of brushes on the generator d use of static controls, recently used on ne jet aircraft, have approximately ubled the mean-time-between-failure of nerator and drive unit. However, the ve has a number of wearing parts, and the wear progresses a part may fail. due to increased hydraulic leakage the ality of frequency control deteriorates. fficient improvement in frequency con- l can eliminate special high-quality wer supplies otherwise needed for sensi- e loads. This also improves the per- mance of the electric system as a whole.

ne Frequency-Make-Up Generator System

By replacement of the generator and echanical constant-speed drive with a nerator system designated hereafter as frequency-make-up generator, it is imated that the mean time between lure can be perhaps 4 times that of the orginal brush system or about twice that of the brushless system. The quality of frequency control will be improved and will not be subject to wear of parts. If in addition an improvement in bearing life and a decrease in unpredictable bearing failures can be attained, much better reliability will result.

It is predicted that weight, volume, efficiency, and maintenance for the new system will be either equal to or improved over the existing brushless generator with mechanical constant-speed drive.

Theory and Operation

The frequency-make-up generator has a standard 3-phase stator but has a wound-rotor type field. A 3-phase field will be used for descriptive purposes. The principle of operation used is to supply a correct value of a make-up or slip-frequency power to the polyphase wound field of the generator. By this means, the algebraic sum of; (a) the variable frequency provided from shaft rotational speed, and (b) the electrical make-up frequency introduced into the field windings; together, provide an air gap flux rotating with respect to the stator at constant speed. Under these conditions the stator output frequency is always constant.

A generator of this type may be designed to operate all below synchronous speed; all above synchronous speed; or below, through, and above synchronous speed.

Induction machine theory, for a generator of this type,[1] states in effect that if there is no shaft speed, the slip is 1.0 and all stator output power must be transferred from the rotor through the air gap by transformer action. At half synchronous speed the slip is 0.5, one half of the stator power is received by transformer action from the rotor and one half mechanically from shaft rotation. At synchronous speed the slip is zero, and all stator power is obtained from shaft rotation. Only d-c power is supplied to the rotor at synchronous speed for resistance losses, which of course are present at any speed.

At 1.5 times synchronous speed, the slip frequency in the rotor has reversed (−0.5 slip) the shaft is supplying 1.5 times stator output power, and the excess, 0.5 of the stator power, is flowing out of the rotor and must be recovered or the efficiency becomes very low. For all these cases, the stator frequency multiplied by the slip determines the required rotor frequency.

At a constant stator voltage, and a constant stator output power and power factor, but a varying shaft speed:

1. The shaft torque remains essentially constant, but shaft power input increases directly with shaft speed.
2. The rotor excitation current remains essentially constant.
3. Rotor input power increases directly with the slip below synchronous speed. I^2R rotor losses must be added.
4. Rotor output power increases directly with slip above synchronous speed. I^2R rotor losses reduce the rotor output.
5. Rotor voltage increases with slip either above or below synchronous speed to provide for increased reactance drop and increased power.
6. Friction, windage, and rotor iron losses modify these results slightly with change

Paper 59-773, recommended by the AIEE Air Transportation Committee and approved by the AIEE Technical Operations Department for presentation at the AIEE Summer and Pacific General Meeting and Air Transportation Conference, Seattle, Wash., June 21–26, 1959. Manuscript submitted March 16, 1959; made available for printing April 8, 1959.

Bert V. Hoard is with the Boeing Airplane Company, Seattle, Wash.

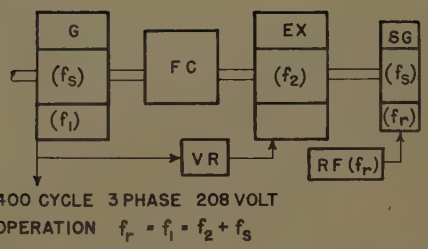

Fig. 1. Frequency-make-up generator with variable speed shaft

SG = signal generator
FC = frequency changer
RF = reference frequency
VR = voltage regulator
G = generator
Ex = exciter

in speed. Stator iron and copper losses are essentially constant.

For machines operating in parallel at any speed and constant total load:

1. An increase in rotor current magnitude will increase reactive power supplied to the system by a generator.

2. An advance in rotor current phase angle will increase real power supplied by a generator to the system. Below synchronous speed this requires more power input to the rotor but above synchronous speed this requires recovery of more power from the rotor.

Selection of a Generator System

The frequency-make-up system selected for modern aircraft should have no brushes and a minimum number of parts subject to wear. Weight and relative complexity become important comparison factors when considering different systems of this type.

The generator system shown in Fig. 1 will be described and discussed and then a weight comparison will be made. As shown, the generator is in its simplest form for operation all below synchronous speed. With added complication it can be made to operate all above synchronous speed or below through and above synchronous speed.

The system components shown in Fig. 1 consist of:

1. A generator having a 3-phase 400-cycle stator and a 3-phase wound rotating field. (Stator frequency $f_1 = 400$ cycles.)

2. An exciter with stationary d-c field and a 3-phase wound rotor. The rotor output supplies power at a variable frequency, f_2, equivalent to shaft speed.

3. A reference frequency source, f_r, 2-phase, for excitation supply to a signal generator. The main generator output frequency f_1 will equal f_r.

4. A signal generator with 2-phase stator and 3-phase rotor. The reference frequency f_r is supplied to the stator. The rotational speed of the shaft provides an equivalent f_2 frequency. The rotor output provides gating signals at slip frequency f_s.

5. A 3-phase frequency changer or rectifier-inverter made of static components (transistors or controlled rectifiers) but rotating to eliminate the need for brushes and commutator or slip rings. This frequency changer accepts variable frequency f_2 power from the exciter rotor and converts it into slip frequency f_s power for supply to the generator rotor. Slip frequency signals for frequency changer control are obtained from isolated windings on the signal generator rotor.

6. A voltage regulator which varies the d-c field excitation of the exciter, hence the magnitude of slip-frequency current in the generator field. This keeps the output voltage of the generator constant.

For parallel operation of generators, a phase shift in the reference frequency supply to the signal generator or in the signal generator stator windings will provide for proper sharing of the load between generators.

This generator, operating all below synchronous speed, will meet the following conditions:

1. Operates efficiently over an engine input shaft speed ratio of 0.5 minimum to 1.0 maximum. This speed range is compatil for most jet-type aircraft engines in use planned.

2. In terms of synchronous speed the ran will be 0.45 minimum and 0.9 maximu For any speeds closer than 0.95 of sy chronous speed the signal generator ou put signal becomes too low for reliab gating of the transistors or controll diodes in the frequency changer.

3. Synchronous speed selected is 12,0 rpm, so maximum shaft speed at 0.9 sy chronous speed will be 10,800 rpm.

4. It has minimum complexity for cont of the frequency changer.

The generator operating through a above synchronous speed requires a ba cally different and more complicat method for obtaining gating signa These can be obtained by adding a subtracting two equal magnitude voltag see Appendix. One of these volta varies at the reference or system freque rate f_1, the other varying at the shaft f quency rate f_2. The resultant, when pro erly rectified and filtered, will prov slip-frequency signals for supplying exci power modified to slip frequency to generator rotor.

When operating above synchron speed, the rotor output power must efficiently recovered. This requires c trolled inversion, in that the low frequency f_s wave must be chopped up provide higher frequency f_2 for feedb into the exciter. When operating bel synchronous speed, controlled rectifi tion, a simpler process, is used.

Weight Comparison

In Table I there is shown, for a 60-k generator, a weight comparison for an below system, *AB*, an all-above syst *AA*, and two below-through-above s tems, *BTA*-8 for 8,000 rpm and *BTA*-6 6,000 rpm synchronous speeds resp tively. In making these comparis

Table I. Weight Comparison of 60-Kva Frequency-Make-Up Generators

	System Designation			
	AB	AA	BTA-8	BTA-6
	Generator Synchronous Speed, RPM			
	12,000	6,000	8,000	6,000
Per cent of minimum and maximum speed range	45 90	110 220	75 150	75 1
Speed range, minimum and maximum rpm	5,400 10,800	6,600 13,200	6,000 12,000	4,500 9,0
Generator rotor power (sK)	0.55K 0.10K	−0.10K ..... −1.20K	0.25K ..... −0.5K	0.25K ..... −0.5
Exciter Rating*				
Power out (1.08×1.06×sK)	0.63K	0.286K	0.286K	
Power in (0.92×0.94×sK)		−1.04K	−0.433K	−0.4
Relative weight — Generator	0.615	1.0 ..... 0.82	0.82 ..... 1.0	1.0
Relative weight — Exciter	0.78	0.592 ..... 0.42	0.342 ..... 0.51	0.4
Relative weight — Exciter and generator	1.395	1.592 ..... 1.24	1.162 ..... 1.51	1.4
Weight 60-kva exciter and generator†	126 lbs.	143 lbs. ..... 111.7 lbs.	136 lbs.	

* Includes 6% I^2R loss in generator rotor and 8% loss in frequency changer.

† Generator kva at synchronous rpm
Exciter kva at minimum or maximum rpm
Weight = $90[\text{kva}/60 \times 6{,}000/\text{rpm}]^{0.7}$ lbs

s = slip in per unit
K = generator rating kva

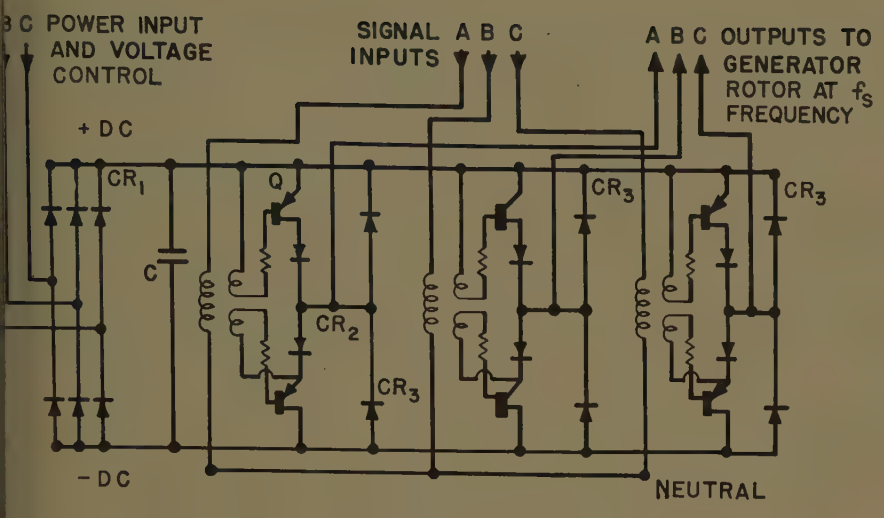

Fig. 2. Transistorized frequency changer

CR_1 = input rectifier
CR_2 = blocking rectifier
CR_3 = by-pass rectifier
Q = transistor
C = capacitor

y the two major weight components are d. These are the generator and the iter. These weights change materially h assumed shaft speeds and generator ings. Fixed weight components are included as they are equal in all tems. Any weight comparison must made on the basis of approximately al maximum values of shaft speed and trifugal force stresses in the generator exciter rotor. Exciter weight is deter- ed, except for the *AA* system, at mini- m shaft speed when maximum output required.

or 400-cycle generators the syn- onous speeds available are limited to 00, 8,000, 12,000, or 24,000 rpm. erators operating at speeds below 00 rpm will definitely be too heavy for 0-kva size and a speed of 24,000 rpm bably is too high because of centrif- l stresses. With wound-rotor con- ction as compared to salient-pole con- ction, for a 60-kva generator, it is believed that lowest weight generators can be built with a maximum shaft speed in the neighborhood of 10,000 to 12,000 rpm.

In Table I the weight of the *AA* system is heavier and its maximum speed is higher than for any of the other systems. Also, for most aircraft flight requirements it will operate at high slip for most of the flight time, hence at relatively lower average efficiency. For these reasons subsequent comparisons will not include the *AA* system.

The weight of the *AB* system is lighter than the *BTA*-6 system and heavier than the *BTA*-8 system. This appears to depend mostly on maximum shaft operating speed plus the fact that only certain values for synchronous speed can be selected.

The power which the exciter and frequency changer must handle on the *BTA* systems is about 70% of that required in the *AB* system. The frequency changer will tend to be lighter because of less power handling requirements but may actually be heavier because of more complicated control and signal requirements, including the provision for absorbing power through the exciter when operating above synchronous speed. It is assumed here that the weights of frequency changer and controls will be essentially the same in both systems. However, there will be less complicated controls in the *AB* system. The average efficiency of the *AB* system will be somewhat better because more engine operating time will occur during flight when the slip is low and efficiency high.

Test Machine

A schematic of a 3-phase transistorized frequency changer, used in a small test generator of about 1 kva, is shown in Fig. 2. The generator was assembled from commercially available components and operated at 60 cycles output. The frequency changer did not rotate, which facilitated making test measurements. Limited tests were made to establish "proof of principle."

The frequency changer operates as follows. The 60-cycle power, equivalent to exciter power, is rectified by CR_1 input rectifiers and direct current and voltage are obtained. Rotor output from the signal generator supplies slip frequency signals f_s to the transistors Q through insulating signal transformers. In each phase the two transistors act like a double-throw switch which changes position each half cycle. The transistors operate in respective phases with a phase displacement of 120 degrees at the slip-frequency rate. By this means they supply pulsating direct current to the respective phases of the generator rotor at slip frequency. Rectifiers CR_2 are used to prevent possible failure of transistors due to excessive back voltage. Rectifiers CR_3 are used to make it easier for the transistors to turn off and allow the inverter to

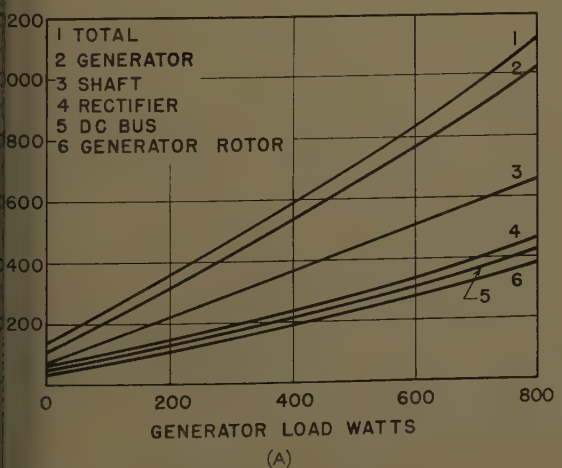

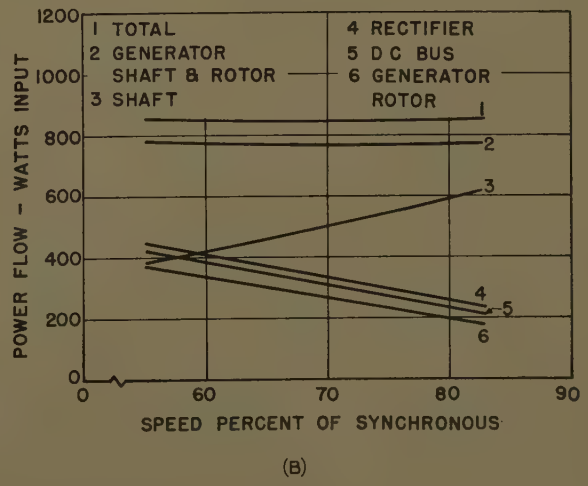

Fig. 3. Power inputs

A—For variable load at 70% synchronous speed
B—For variable speed at 600-watt load

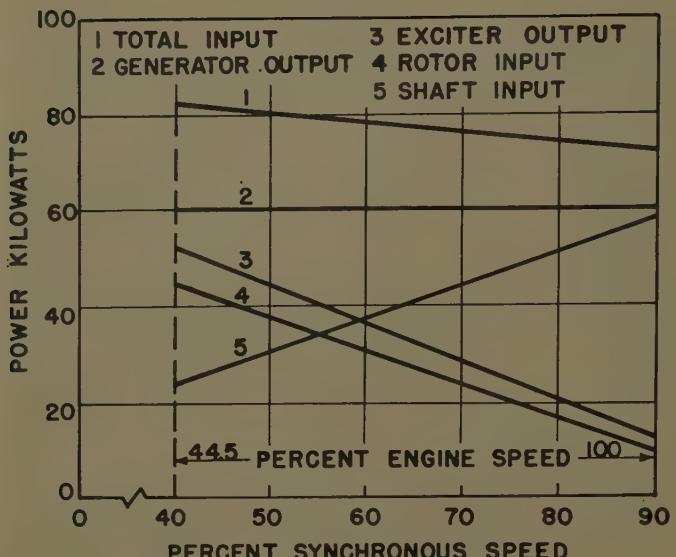

Fig. 4. Calculated power at 60-kw load speed range 40% to 90% of synchronous speed

carry reactive power in an efficient manner. For example, when transistor Q in rotor phase A turns off, the current in phase A rotor flows for a short additional period in the same direction, but through CR_3 rectifier of phase A. There is a slightly higher induced voltage, just enough to return the stored energy in the rotor phase back into the positive d-c through CR_3 rectifiers in the other phases.

Test Results

Power Relations

The curves in Fig. 3(A) show test generator power inputs for external loads from 0 to 800 watts, unity power factor, at 70% of synchronous speed. These curves show power to rectifiers, to the d-c bus, to the generator rotor, to the shaft, and total input over the load range. Shaft and rotor inputs practically straight lines over the range of generator loads shown. Higher test loads could not be carried because transistor temperature ratings were exceeded and a number failed.

The curves of Fig. 3(B) show test generator power inputs for an external load of 600 watts over a speed range from 55% to 85% of synchronous speed. Speeds closer to synchronous speed could not be obtained because of wrong taps on the signal transformers. Shaft speeds lower than those shown caused transistor temperatures to increase above rated values and again a number failed. In Fig. 3(B) it is of interest to note that, while total input (exciter losses excluded) remains nearly constant at any speed, the power supplied by the shaft decreases with speed and increased generator rotor power is required. If these curves are projected to 100% synchronous speed, only electric power input to supply d-c excitation losses would be required by the rotor; and shaft input would supply all other losses plus the load.

Harmonics and Unbalanced Loads

Harmonics in the output voltage are important but were not thoroughly investigated in the "proof of principle" tests. However, inspection of oscilloscope traces show generator stator voltages that appear close to sine waves.

It has been proposed that a floating synchronous condenser across the generator terminals will be needed to meet military specifications with respect to unbalanced voltages when unbalanced loads occur and to meet specification harmonic requirements. Unfortunately, in addition to the weight increase, two added bearings are introduced, that are subject to unpredictable failure, hence there will be reduced reliability and greater maintenance.

It is felt that all other possibilities should be investigated first, including a re-evaluation of military specification requirements, before a synchronous condenser having bearings is added to the system.

Semiconductor Failures and Ratings

The tests prove that if adequately rated semiconductors can be produced commercially, a frequency-make-up system with generator ratings up to 60 kva is practical. It is believed that this will occur in the near future. Germanium transistors were used in the tests and failures occurred, probably chiefly due to deterioration from junction temperatures higher than rated value but also from added effects of transient voltages and currents. Unlike the generator, transistors have little if any overload capabili in current, voltage, or temperature, ev for a few milliseconds above what designated by one manufacturer as th absolute maximum ratings. Power-ty controlled rectifiers were not availab when the tests were started. Higher tem erature silicon controlled rectifiers a now available in larger ratings than transistors, and with some circuit modi cation they can be used. They ha better overload characteristics th transistors. Before practical applicati can be made for generator service, t maximum voltage and current to whi the semiconductors will be subjected a given generator rating must first determined. This will have to inclu generator overload, fault, overvoltage, a operational temperature conditions. addition, for inverter or frequen changer operation, repetitive peak v ages and currents which each semicondu tor must handle are greater than r rotor values indicate for any given loa ing condition on the generator. Wh these special conditions have all b satisfied to prevent failure during unus operating conditions, then with norm loads on the semiconductors the perce age of their absolute maximum rating be small, and very reliable operat should result.

Frequency Control

The frequency-make-up genera shows excellent frequency control wh step loads are added or subtract When a step load is added, only a crease in phase angle occurs because the load addition. This phase an decrease is recovered when the load removed. These changes are much than mechanical constant-speed dri can attain. If oven-controlled cryst are used as frequency reference, integra error in frequency can be less than cycle out of 10^5 cycles.

Calculated Performance, 60-Kva Generator

The curves of Fig. 4 show calcula input-output power flow curves for a kva frequency-make-up generator op ating at unity power factor. The cur are plotted with per-cent synchron speed as abscissa, and for operation at output from 40% to 90% of synchron speed. The efficiency of this genera is several points better than can achieved by a constant-speed drive generator system in the important sp range from 60% to 90% of synchron speed, where most in-flight operat usually occurs.

nclusions

The following conclusions are obtained n the evaluation of frequency make- systems studied, and their comparison h mechanical constant-speed drive l generator systems.

The *AB* synchronous speed system is ferred over a *BTA* system for a speed ge of two to one or less because of less plicated signals, and controls. The ghts of the two systems are estimated to essentially the same, provided that al maximum rotor speeds are used. average operational efficiency of the system is slightly better than for the *A* system. Due to less complication, intenance will be lower in the *AB* system. rating of the frequency changer on *BTA* system is about 70% of the rat- of the frequency changer in the *AB* tem.

If greater speed ranges than two to one required, the weight of the *AB* system ins to exceed that of the *BTA* system the *BTA* system might therefore be cted, although reliability would still be ajor consideration.

Higher temperature and higher voltage current ratings in controlled diodes l/or transistors are needed to build large s *C*-type generators at this time. velopment of these semiconductors is gressing rapidly. It is probable, if de- pment of such a generator is started at s time, that adequate semiconductors will ome available by the time other gen- tor development problems have been ved.

When comparing a 60-kva *AB* fre- ncy-make-up system with a mechanical stant-speed drive and generator system, h having two-to-one speed ratio:

The *AB* system weight is estimated to 15 to 20% less.

The volume and total length will be

The efficiency will be about 3 to 5 nts higher at cruise and maximum engine eds.

Maintenance and rebuilding costs will materially less.

Frequency deviation for step load nges will be reduced essentially to zero.

(f) In-flight failures will be reduced and reliability improved.

Appendix

To obtain a slip frequency signal through synchronous speed:

Using Sum and Difference Relationships[2] for two voltage waves e_1 and e_2, of equal peak magnitude E_0, but of different frequencies f_1 and f_2.

$$e_1 = E_m \sin 2\pi t f_1$$

$$e_2 = E_m \sin 2\pi t f_2$$

$$e_1 - e_2 = 2E_0 \sin \pi t(f_1 - f_2) \cos \pi t(f_1 + f_2)$$

$$e_1 + e_2 = 2E_0 \cos \pi t(f_1 - f_2) \sin \pi t(f_1 + f_2)$$

If $e_1 - e_2$ is rectified full wave and $e_1 + e_2$ is similarly rectified; and the results are subtracted and filtered; a resultant fundamental frequency $f_1 - f_2 = f_s$ is obtained where f_s equals slip frequency. Several high frequencies are also present before they are filtered out. This process is not efficient since a considerable portion of the power is lost in the transformation and filtering. If half wave rectification of the sum and difference equations is used, the proportion of signal output over input power is less than for full wave rectification. It will be observed that the magnitude of either the sum or the difference equation is identical, only the phase position is different.

Another area of investigation for obtaining a slip frequency signal through synchronous speed is suggested in the following manner:

If two voltages c_{a1} and c_{b2} can be made available by electronic means; for example, by modulation, variable impedance, etc. They are expressed as

$$e_{a1} = kf_2 I_0 \sin 2\pi t f_1 \sin 2\pi t f_2$$

$$e_{b2} = kf_2 I_0 \cos 2\pi t f_1 \cos 2\pi t f_2$$

$$e_{a1} = \frac{kf_2 I_0}{2} \cos 2\pi t(f_1 - f_2) - \cos 2\pi t(f_1 + f_2)$$

$$e_{b2} = \frac{kf_2 I_0}{2} \cos 2\pi t(f_1 - f_2) + \cos 2\pi t(f_1 + f_2)$$

$$e_{a1} + e_{b2} = kf_2 I_0 \cos 2\pi t f_s$$

Since

$f_s = f_1 - f_2$ is the needed slip frequency.

References

1. Alternating Current Machines (book), **T. C. McFarland.** D. Van Nostrand Company, Inc., Princeton, N. J., "Polyphase Induction Machines," pp. 143–216; "Impulse Method of Control of Grids," p. 71, p. 432; "Inverters," pp. 457–61, 1948.

2. Fundamentals of Vacuum Tubes (book), **A. V. Eastman.** McGraw-Hill Book Company, Inc., New York, N. Y., "Modulators and Demodulators," chaps. 13 and 14, 1949.

3. Mercury-Arc Power Converters in North America, **AIEE Committee Report.** *AIEE Transactions*, vol. 67, pt. II, 1948, pp. 1031–59.

4. Ignitor Excitation Circuits and Misfire Indication Circuits, **A. H. Mittag, A. Schmidt, Jr.** *Ibid.*, vol. 61, Aug. 1942, pp. 574–77.

5. Grid Controlled Rectifiers and Inverters, **C. C. Hershind.** *Electrical Engineering*, June 1934, pp. 926–35.

6. Design of an Electronic Frequency Changer, **C. H. Willis, R. W. Kuenning, E. F. Christensen, B. D. Bedford.** *AIEE Transactions*, vol. 63, 1944, pp. 1070–78.

7. The Electronic Converter for Exchange of Power, **F. W. Cramer, L. W. Mortin, A. G. Darling.** *Ibid.*, pp. 1059–69.

8. Analysis of Rectifier Circuits, **E. F. Christensen, C. H. Willis, C. C. Herskind.** *Ibid.*, pp. 1048–58.

9. Harmonics in the A-C Circuits of Grid-Controlled Rectifiers and Inverters, **R. D. Evans, H. N. Muller, Jr.** *Ibid.*, vol. 58, 1939, pp. 861–70.

10. History and Development of the Electronic Power Converter, **E. F. W. Alexanderson, E. L. Phillipi.** *Ibid.*, vol. 63, Sept. 1944, pp. 654–57.

11. Static Converter with Current and Voltage Smoothers for Flexibly Coupling a Three-Phase 50 Cycle Network with a Single Phase $16^2/_3$ Cycle Network, **C. Ehrensperger.** *Brown Boveri Review*, Baden, Switzerland, June 1934, pp. 96–112.

12. The Flexible Coupling of Independent Three-Phase Networks by Means of a Single Mutator, **E. Kern.** *Ibid.*, Dec. 1934, pp. 214–18.

13. Synchronizing of an Induction Motor, **E. McP Leyton.** *U. S. Patent no. 2,650,335*, Aug. 25, 1953.

14. Electrical Apparatus, **C. I. MacNeil.** *U. S. Patent no. 2,659,044*, Nov. 10, 1953.

15. Constant Frequency Power Supply, **W. E. Sargeant.** *U. S. Patent no. 2,776,379*, Jan. 1, 1957.

16. Frequency Control Apparatus for Alternators, **L. J. Johnson.** *U. S. Patent no. 2,854,617*, Sept. 30, 1958.

Discussion

M. Chirgwin and L. J. Stratton (Jack & intz, Inc., Cleveland, Ohio): It seems us that it is the development of semi- nductor frequency changers that has made f (variable speed constant frequency) erating systems for aircraft feasible at s time. It is appropriate, therefore, that r. Hoard's paper should have been the t to be read at the first Air Transportation ssion on vscf generators, because Mr. oard was one of the pioneers of vscf genera- s which use semiconductor frequency angers.

There are a number of points in the paper ich we would like to discuss. The first concerns Table I wherein the weights of the main rotating machines of four different arrangements are compared. In Table I the speed range is 2:1 for all of the four arrangements but the actual minimum and maximum speeds differ and, as Mr. Hoard points out, at least part of the weight differences shown in the table can be ascribed to these speed differences.

In Fig. 5 we have attempted to present the variables in such a way that these speed differences can be taken into account in making weight comparisons.

In this figure the weight of the generator and the weight of generator and exciter are both plotted as continuous functions of the speed which is selected as the synchronous speed of the generator. Some of the discrete synchronous speeds which can be selected to give 400-cps output frequency from the main generator are shown on the horizontal axis. Curves are shown for the same minimum speeds and for the same 2:1 speed range used by Mr. Hoard in his Table I. The curves are based on the assumptions that the weight of a rotating machine is proportioned to its kva divided by its speed of rotation, and that the exciter rating is the system kva times the maximum per-unit slip, i.e., the losses and magnetizing current of the system are neglected.

With these simplifying assumptions, the weight of the generator is inversely proportional to the synchronous speed selected and is independent of minimum speed and of speed range, as shown by the lower curve

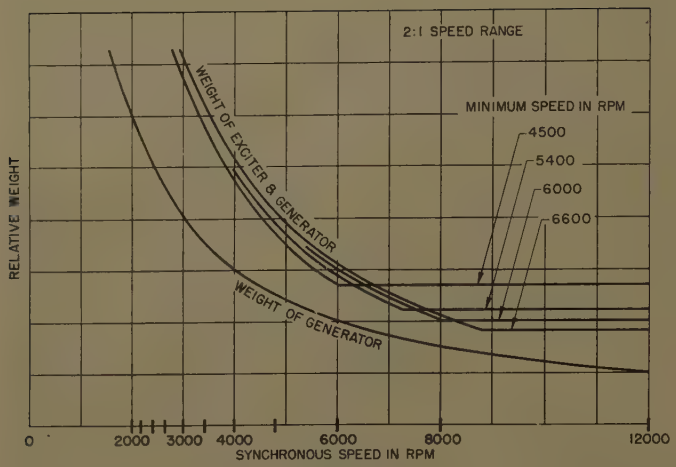

Fig. 5. Rotating machine weights versus the selected synchronous speed of the main generator

of Fig. 5. When the synchronous speed of the generator is selected below the minimum speed or in the lower part of the speed range, then the weight of the exciter is determined by the maximum speed and the slip at maximum speed. This condition gives the curved lines for the combined weight of exciter and generator shown in the left part of Fig. 5. When the synchronous speed of the generator is selected above a certain speed, "corner speed," in the lower part of the speed range, then the exciter weight is determined by the minimum speed and the slip at minimum speed. This condition results in the horizontal straight lines of the combined weight of exciter and generator shown in the right part of Fig. 5. The derivation of these curves is given in more detail in the Appendix.

The significance of these horizontal straight lines is that in this region the combined weight of the two rotating machines is independent of the synchronous speed selected and is inversely proportional to the minimum speed. It is the division of weight between the generator and the exciter which is determined by the synchronous speed selected. It should also be noted that the horizontal line is the lowest combined weight for a given minimum speed.

For an *AA* system the synchronous speed always falls in the curved combined weight region and is therefore always heavier than either a *BTA* or an *AB* system. This confirms Mr. Hoard's findings.

Provided the synchronous speed of the *BTA* system is selected above the "corner speed" then, with the simplifying assumptions, the combined weight is exactly the same as that of the *AB* system no matter what synchronous speed is selected.

Provided the synchronous speed of the *BTA* system can be selected near the middle of the speed range, then the power rating, and the weight and volume of the power handling components of the frequency changer are all about 50% of those of an *AB* system having the same minimum speed. Because of this and because the machine weights are equal, the *BTA* system is the lighter.

Mr. Hoard expects that there will be difficulties in operating the frequency changer with reversed power flow, and in maintaining control while passing through synchronous speed with a *BTA* system. We have found that these difficulties can be overcome with very little addition to the weight and volume of the frequency changer.

When we come to actual systems, generalizations are difficult to make because many other factors such as losses, magnetizing current, power factor, overloads, and fault capability must be included when making weight comparisons. We have found from detailed comparisons of systems for a number of different specifications that with the *BTA* system the volume of the frequency changer permits it to be located inside the shaft and that the *BTA* system has the lowest weight.

Since it is our company which has advocated the use of a floating synchronous machine which we term a Voltage Balancer, we feel it incumbent upon us to say a little about the need for such a machine. If the Voltage Balancer were omitted, then the requirements of the system in respect to reactive kva, waveform, and fault capability could all be met if suitable changes were made in other components of the system. But we believe either this machine or an equal induction machine is presently needed if the usual military specifications on voltage unbalance are to be met. Furthermore, we feel that considerable development must occur before this machine can be replaced by static components or eliminated altogether.

As will appear in the reply to a discussion of our paper[1] by J. T. Duane, the presence of the voltage balancer allows a reduction in the weight of the main generator and exciter, since it supplies reactive kva to the system. We believe Mr. Hoard takes an unduly pessimistic view of the bearing problems of this machine, which will likely be located in a more favorable environment than the main machine.

Appendix. Derivation of the Weight Comparison Curves

This derivation is based on two simplifying assumptions: 1. The weight of a rotating machine is proportional to its kva output divided by its speed of rotation; 2. The rating of the exciter is the system kva multiplied by the per-unit slip.

The main generator is a synchronous flux machine so its weight is proportional to the system kva K divided by the synchronous speed, N_s, selected for this machine.

$$\text{Generator weight} = C \cdot \frac{K}{N_s} \qquad (1)$$

where C is the constant of proportionalit
Plotting this equation on Fig. 5 gives
rectangular hyperbola, which is labell
Generator Weight.

If the variable speed shaft which driv
the rotating machines is rotating at a spe
N then the slip at which the synchron
flux generator is operating is given by

$$\text{Per-unit slip} = \frac{N_s - N}{N_s}$$

This equation results in negative values
slip when the shaft speed is higher than
synchronous speed of the generator.

The kva required of the exciter at t
shaft speed N is

$$\text{Exciter kva} = K \cdot \frac{N_s - N}{N_s}$$

This equation gives negative values for
kva when N is above synchronous spe
the interpretation of this negative sign
that at these speeds the exciter is working
a synchronous motor and returning pow
to the shaft.

At this same shaft speed N the weight
the exciter required is given by

$$\text{Weight of exciter} = C \cdot \frac{K}{N} \cdot \frac{N_s - N}{N_s}$$

In this equation the negative sign th
appears when the speed N is greater th
synchronous speed should be ignored, sin
obviously the weight of the exciter wh
operating as a synchronous motor is
negative.

Adding equations 1 and 4 gives the co
bined weight of exciter and generator nee
for the particular shaft speed N:

$$\text{Combined weight} = C \cdot \frac{K}{N_s} + C \cdot \frac{K}{N} \cdot \frac{N_s - N}{N_s}$$

for speed N when $N < N_s$

$$= C \cdot \frac{K}{N_s} + C \cdot \frac{K}{N} \cdot \frac{N - N_s}{N_s}$$

when $N > N_s$

Collecting like terms in equations 5 gi

$$\text{Combined weight} = C \cdot \frac{K}{N}$$

when $N < N_s$

$$= 2C \cdot \frac{K}{N_s} - C \cdot \frac{K}{N}$$

when $N > N_s$

In the vscf system the shaft speed
will vary over a speed range from $N_{\min}$
$N_{\max}$. and machines of sufficient rating
weight must be provided to enable the s
tem to put out the rated kva, K, at
speeds within this range. If N_s is selec
so that $N_{\max.} < N_s$, AB system, then eq
tion 6(A) applies and the combined wei
of the machines required for the speed ra
is

$$\text{Combined weight for speed range} = C \cdot \frac{K}{N_{\min.}}$$

If N_s is selected so that $N_{\min.} > N_s$,
system, then equation 6(B) applies and

mbined weight of the machines required the speed range is

mbined weight for speed range

$$=2C\cdot\frac{K}{N_s}-C\,\frac{K}{N_{max.}} \quad (8)$$

For the *BTA* system where $N_{min.}<N_s<$ ax. it is not immediately apparent whether uation 6(A) or 6(B) applies. So both ould be tried and the one that leads to the eater weight should be used. Doing this ds to the conclusion that equation 6(A) verns when N_s is in the upper part of the eed range and equation 7 gives the correct mbined weight, that equation 6(B) verns when N_s is in the lower part of the eed range and equation 8 gives the cor- t combined weight, and that the change- er point occurs when the synchronous eed is so selected that the weight given by e two equations is equal; that is, when

$$\frac{K}{N_{min.}}=2C\cdot\frac{K}{N_s}-C\cdot\frac{K}{N_{max.}}$$

when

$$=1/2\cdot\frac{N_{mux.}\cdot N_{min.}}{N_{max.}+N_{min.}} \quad (9)$$

This value of the selected synchronous eed given by equation 9 is called the corner eed. Equation 7 therefore applies at all eeds above the corner speed and equation t all speeds below the corner speed.

In Fig. 5 the weights given by equations and 8 are plotted for the four values of in. that Mr. Hoard uses in his Table I.

EFERENCE

Variable-Speed Constant-Frequency Gen- ator System for Aircraft, **K. M. Chirgwin, L. Stratton.** *AIEE Transactions*, pp. 304–10 of this ue.

S. Toffolo (U. S. Naval Research Labora- ry, Washington, D. C.): The author eaking from experience, cites examples of eas where improvement of present day nstant frequency systems is desired. The ird example is a qualitative statement for, til the author defines poor, fair, good, and cellent quality of frequency supply in antitative terms, his assessment of the uation remains subjective.

His statement concerning the elimination special high quality power supplies needed sensitive loads is somewhat gratuitous. r such sensitive loads are usually equally rmonic conscious if not more so. Yet e author recommends, if all else fails, a evaluation of military specification re- irements.

To the remarks concerning parallel opera- n, the writer notes that this is what esent systems do and in addition to which esent parallel systems have synchronizing rque going for them. The author should alize that his and all other constant locity magnetic field devices where the agnetic field has no fixed space relation to y set of windings in the generator, have synchronizing torque between them. As consequence, there will be serious oscilla- ry load division problems which the author ll dearly wish he had never encountered. ople who wander with frequency-make-up nerators into the parallel system area where numerous are the pitfalls and deep the holes would be exceedingly wise to emulate the angels!

After reading the author's description of the system components and looking at the block diagram shown in Fig. 1, the writer is not convinced that proper real load division will occur simply because the author states that a phase shift in the reference frequency supply to the signal generator or in the signal generator stator windings will do the job. Has the author calculated the magnitude of the phase shifts required and the response times involved and how close to parity of load sharing such a scheme will achieve?

Further, as the writer has pointed out in his comments to another frequency-make-up generator proposal,[1] has the author considered what happens to his parallel system, in fact, to his entire generating capacity if the reference frequency is lost? Does the author not consider that such a failure is of the nature of an unpredictable failure and for him it is not only that but catastrophic as well?

In view of the remarks made by the author concerning re-evaluation of military specifications, the writer regards the weight comparisons developed by the author as irrelevant.

In the paper, the author states under "Test Machine" that limited tests were made to establish "proof of principle." Proof of what principle? Proof that the frequency-make-up principle is a unity power factor principle? Even that he has not proved. For all unity power factor loads are not linear. In fact, for some electronic loads, the flow of armature current is of the fractional cycle type, continuously, and such loads, completely 3-phase balanced, will play havoc with his generator. One could, of course, re-evaluate the military specifications again.

Under "Frequency Control" the author states that when a step load is added, only a decrease in phase angle occurs due to the load addition. The author does not define what this phase angle is. If he means by this the angle between the phasor representing the excitation voltage and the phasor representing the terminal voltage, his statement is incorrect. For a frequency-make-up generator, the power angle (the difference between the two phasors above) increases with load as in conventional generators.

In this writer's opinion, the remarks under "Conclusions" are not conclusions, but speculations. For instance, the circuit shown in Fig. 2 cannot be used for controlled rectifiers if one merely replaces the transistors Q by controlled rectifiers. Since the author does not include any other schematic diagrams, the writer assumes from the author's statements about simplicity et al, that it is his intention to do so. The author should investigate the problem of turning off the controlled rectifier once it has been turned on and tied to a positive d-c bus.

The writer has no quarrel with those who strive to develop constant frequency generators for flight vehicle systems. In fact, he is one of them. He does have a quarrel with those who presume to develop such a machine for flight vehicle conditions and then propose to change the system conditions and/or present their case, based on infinitesimal amounts of experimental data, in a rather speculative manner.

REFERENCE

1. Precision Power Frequency with Variable Speed Generators, S. E. Rauch, L. J. Johnson. *AIEE CP 59-772* (available on request).

Bert V. Hoard: I appreciate the discussion of my paper by Mr. Chirgwin and Mr. Stratton very much. It is stimulating to have honest differences of opinion as to the best way to develop new types of apparatus because it usually results in better equipement. Actually, in this case our opinions are not far apart.

I believe that evaluation of weight and performance of the final hardware and presently unknown developments in the semiconductor field may well be the only means of determining which system will be better or preferable.

I think we can agree that if a rotating machine providing balancing action is necessary, and it could well be under present military specification requirements, that it is preferable to have a synchronous type balancer rather than an induction machine; that considerable reactive kva for the system can be advantageously supplied by this machine using d-c excitation rather than supplying it via the main exciter, the frequency changer, and the main generator; that weight and total generation losses could be saved.

Mr. Toffolo has placed his own interpretations on a number of the statements made in my paper. With most of these interpretations and conclusions I do not agree.

With present efforts to obtain nearly balanced loads on a-c aircraft systems, I believe that a re-evaluation of the minimum unbalanced voltage requirements for unbalanced loads called for in military specifications should be made, and if these requirements can be relaxed, some weight will be saved in any a-c generator with negligible decrease in performance as long as the load is balanced.

As to parallel operation of frequency-make-up generators, I foresee no paralleling problems anywhere near as difficult as those originally overcome before the 400-cycle a-c electrical system was finally successfully paralleled. An advance in the phase angle of the signal generator will gate excitation currents sooner in each cycle into the specific generator rotor and advances its phase angle electrically compared to another paralleled machine, and the machine will pick up a greater percentage of the total load. The machines have synchronizing torque as long as they have correct excitation. If a differential real load loop is used for controlling the relative phase angle of gating excitation currents into the various generator rotors, I am positive we can overcome Mr. Toffolo's suggested pitfalls, holes, and even the oscillations without special help from the angels. The response times for load equalization will be much faster than presently attainable by having to accelerate mechanical inertias to obtain phase angle shifts and provide for frequency recovery.

I do agree with Mr. Toffolo that this system, if it has a single frequency reference, is vulnerable to failure similar to the one he referenced. This does not mean that modifications to a single reference system cannot be made so that its failure will not be catastrophic to the system as a whole.

Regarding my statement "only a decrease in phase angle occurs due to addition of a step load," since the intended conclusions were not obtained by the reader, I should have amplified the statement. When a conventional generator which is driven by a constant speed drive has a large step load added to it, the governor and other controls act relatively slowly, and it is possible to lose more than a complete cycle before the frequency is restored to normal value. If the constant speed drive is badly worn and the load increment is large, more than one cycle may be lost. On the generator with the step load addition, there also occurs a phase angle lag in terminal voltage behind its no load phase angle with respect to air gap flux as a reference, since it is the cutting of air gap flux that produces machines internal voltage.

On the frequency-make-up generator with addition of an equivalent step load a phase angle shift only occurs. This phase angle shift might be assumed to be greater than for the conventional generator especially at low shaft speeds because of the increased lag between the applied excitation voltage and the resultant excitation current. Note that it is excitation current that produces air gap flux in this generator system. Actually with the effect of the relatively slow mechanical control action included, the total phase angle lag will be much greate in the conventional system. With a goo reference system the frequency-make-u system may give integrated frequen accuracy of one part in 10^5 cycles and i stantaneous frequency deviations conside ably less than one cycle. Mechanic frequency controlled systems do not a proach these values.

I feel the weight comparisons for excit and generator, the two heaviest pieces, a decidedly relevant for the comparison pu poses used in the paper. If requirements a placed on one generator which increase weight then a proportional weight increa will occur in the other generator system.

Variable-Speed Constant-Frequency Generator System for Aircraft

K. M. CHIRGWIN
ASSOCIATE MEMBER AIEE

L. J. STRATTON
ASSOCIATE MEMBER AIEE

Synopsis: Variable-speed constant-frequency (vscf) generator systems are studied as an extension of well-known vscf motor technology. The vscf generator systems become practical for aircraft main generating systems when the commutator function is performed by semiconductor devices. It is concluded that the best scheme for this application is one using as the main generator a wound rotor induction machine operated above and below synchronous speed, and a slip channel comprised of a semiconductor frequency changer and a synchronous machine driven by the variable-speed shaft.

This system was built and tested in the laboratory using commercial-type machines. Test results and oscillograms are presented.

EVER SINCE 400-cycle electric systems have been used on aircraft, it has been a goal of the aircraft accessory industry to generate this power from the variable-speed shaft of the prime mover without the need for a constant-speed drive. This is now possible using a vscf generator system.

A vscf generator system is here defined as an assemblage of rotating electric machines and other electric equipment that is capable of taking mechanical energy directly from a shaft which rotates at a variable speed and converting this energy into a-c electric energy at a constant frequency.

The vscf systems will likely have many applications. This paper is confined to the use of such a system as the main electric generating system of an aircraft. Application in this manner sets definite bounds to the system. For example, ratings are probably from 20 to 120 kva, the output is 120/208 volts, 3-phase, 400 cps (cycles per second), to meet specifications indicated in reference 1, or some similar specification. The input shaft rotates at conventional drive-pad speeds; that is, a speed range of between 2:1 and 3:1 with a mid-range speed of approximately 6,000 or 8,000 rpm.

VSCF System Classification

The vscf systems operated as motors[2] have been known for a long while, and a great deal of knowledge has accumulated over the years. In a vscf motor system the frequency is determined by the frequency of the synchronous supply system from which the motor derives its pow In a vscf generator system, however, frequency reference signal must be add to the system in such a way that it det mines the frequency at which the pow is generated. Ways in which the f quency-reference signal may be integrat with the rest of the generating system v not be discussed, since they are outs the scope of this paper.

When the power-handling parts of t system are considered, the vscf motor a the vscf generator systems are essentia the same and can be conveniently clas fied in three groups as shown in Fig. 1 a Table 1. Fig. 1(A) shows a wound-ro induction machine with a variable resi ance connected across the slip rin When operated as a motor on a consta frequency supply, the motor speed c be reduced below synchronous speed an amount which depends upon the lo on the shaft and the amount of resistan in the rotor circuit.[3] When operated a vscf generator, this scheme allows speed of the shaft to be raised above s chronous speed by an amount which determined by the power output of generator and the amount of resistance the rotor circuit. For either the motor the generator, power equal to the times the power output is dissipated in resistances. Slip is defined by equat 1:

$$\text{Slip} = \frac{\text{Synchronous Speed} - \text{Actual Spee}}{\text{Synchronous Speed}}$$

Table I. VSCF Power Circuits

Classification	Power Relations	Commutator Machines
Synchronous flux, wasteful, Fig. 1(A)*	slip power wasted in resistances	none
Synchronous flux, differential, Fig. 1(B)†	slip power returned to or supplied from shaft	handles slip power at slip quency
Full rated, Fig. 1(C)	full power	handles full output power at 4 cps frequency

* Eliminated because losses are large in wide speed range.
† Single or double range. Double range halves slip, slip frequency, and slip power, but passing thro synchronous speed is difficult.

Paper 59-872, recommended by the AIEE Air Transportation Committee and approved by the AIEE Technical Operations Department for presentation at the AIEE Summer and Pacific General Meeting and Air Transportation Conference, Seattle, Wash., June 21–26, 1959. Manuscript submitted March 23, 1959; made available for printing May 4, 1959.

K. M. CHIRGWIN and L. J. STRATTON are with Jack and Heintz, Inc. Cleveland, Ohio.

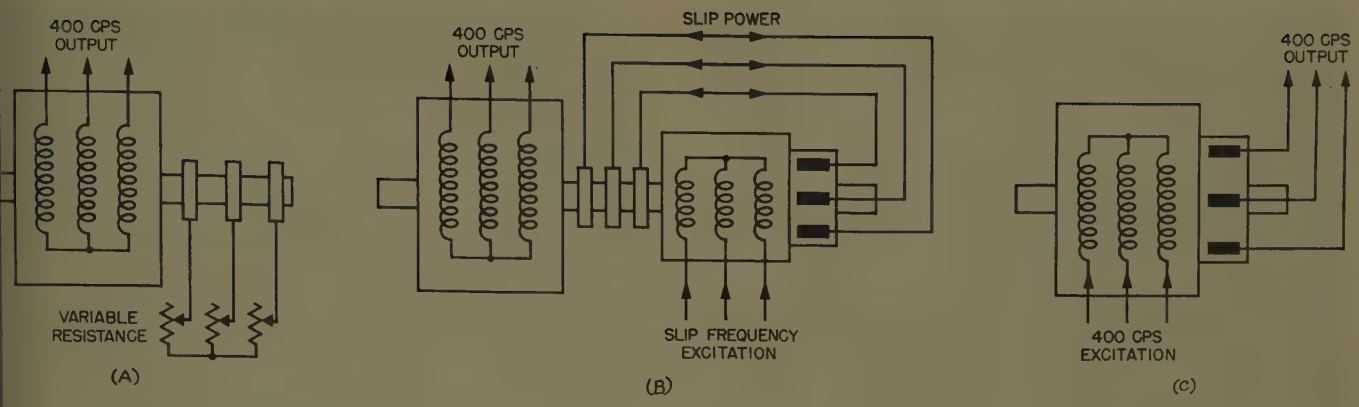

1. Some vscf power circuits. A—Wound-rotor induction machine with resistance in the rotor circuit. B—Wound-rotor induction machine with Scherbius machine handling the slip power. C—Full rated scheme, shunt commutator machine

When the speed range is as wide as 2:1 3:1, the power lost in the resistances is ge, being at least equal to the power put for a 2:1 speed range and at least ce the power output for a 3:1 speed ge. This large amount of power has to dissipated and, in addition, the air- ne has to carry extra fuel in order to erate this additional power. Because the penalties imposed by these two ors, wasteful schemes of this nature not considered for aircraft appli- on. In Table I this scheme is classi- as a synchronous-flux system,[4] since rdless of the speed of rotation of the t, the air-gap flux of the induction hine rotates at synchronous speed.

ig. 1(B), which is also classified as a chronous-flux system, uses the same nd-rotor induction machine, but , instead of slip power being wasted sistances, it is returned to the shaft by ns of an auxiliary commutator ma- e.

the third classification, Fig. 1(C), the iliary commutator machine is in- sed in size to handle the full output er of the system and the induction hine is eliminated. This scheme is a synchronous-flux scheme; how- , schemes derived from this but which other means of commutation do not e a synchronous flux. This scheme, efore, is classified as a full-rated me because the commutator has to dle full output power of the system.

he arrangements shown in Figs. 1(B) 1(C) are representative only. The motor technology includes so many rent arrangements that it is not pos- e to discuss them in detail. It is, ever, possible to draw a number of ral conclusions.

ncluded in the differential synchro- s-flux category shown in Fig. 1(B) are power handling schemes which allow system to operate on one side of chronous speed only, because real power can flow in only one direction through one or more of the slip channel components. Such a slip channel cannot transmit reactive power because reactive power requires reversal of power flow once each cycle, so the system must be magnetized from the stator (high frequency) side of the induction machine.

There are other schemes in this category in which the slip channel can handle power in either direction, so the system can be magnetized from the rotor (low frequency) side of the induction machine, but the system is still confined to operation on one side of synchronous speed because, for one of a number of reasons, the system cannot pass through synchronous speed.

Table II. Commutating Components

	Two-Way Conduction Controllable	Uncontrolled	Rectifier Limited Control	Controllable
Components	rotating machine with commutator; mechanical rectifier; symmetrical transistor	uncontrolled rectifier (diode)	diode with modulator	controlled rectifier
Characteristics	any delay controlled rectification and inversion	no delay natural commutation, d-c only	limited delay controlled rectification	any delay controlled rectification and inversion
Application to vscf systems	eliminated	not possible	single range full rated; no lagging power-factor load	single range double range full rated; any power-factor load

Table III. Comparison of VSCF Systems

Items	Differential Synchronous Flux		Full Rated
	Double Range	Single Range	
Power in commutating components 2:1 speed range	1/3 of output kva	1/2 of output kva	full output kva
Pad speeds	compatible with present pad speeds		smaller ratings could use higher speeds, but gears needed with present engines
Total system weight	lightest	intermediate	heaviest
Efficiency	highest	lower	lower
Voltage balance	rotating voltage balancer		could use individual phase regulation
Parallel operation	no problem		individual phase regulation complicates problem
Wave form	combination of induction generator and rotating voltage balancer give good waveform		wave shaping necessary
Fault capability	inherent overload capabilities of rectifiers and machines are sufficient for usual faults		rectifiers must be increased in size for 5-per-unit faults
Complexity	similar to rotating rectifier machine with control of rectifiers (partly rotating) plus voltage balancer		rotating rectifier or other brushless machine plus stationary frequency changer and wave shaping

Note: Driven machine for each of the three systems will fit in space presently available.

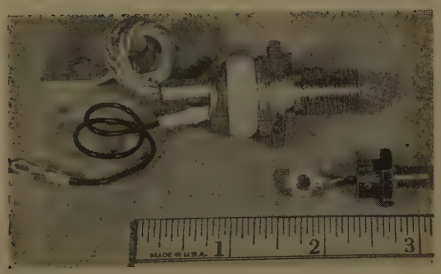

Fig. 2. Silicon p-n-p-n switches: larger one rated 50 amp, 300 volts maximum, smaller one rated 16 amp, 400 volts maximum

There are still other schemes in this category which can successfully pass through synchronous speed and can operate either above or below or at synchronous speed. Such schemes are called double range. The slip channel of these schemes must be able to handle power in either direction, so they are inherently capable of magnetizing the system from the rotor side. The Scherbius system of Fig. 1(B) falls in this group.

In all the nonwasteful synchronous flux schemes there must be at least one commutator-type machine, or its equivalent, which handles power at least as great as the slip times the power output of the system.

When full-rated systems, shown in Fig. 1(C), are considered, there is no question of operation above or below synchronous speed, and usually there will be no need to reverse the direction of power flow in the commutator. However, if the commutator is not capable of 2-way power flow, then it is not possible to supply reactive loads.

Of the schemes so far discussed, the first, Fig. 1(A), has been eliminated because it is wasteful. The two remaining, Figs. 1(B) and 1(C), both use a-c commutators which have to handle a substantial amount of power. Such commutators, as is well known, are not workable in aircraft-type environments; before an aircraft vscf system becomes practical, some other means of performing the commutating function must be used.

Commutating Devices

Table II lists a number of different devices which can be used to perform the commutating function. In the first column, three components are listed as being 2-way conducting and controllable. This means they are capable of carrying current in either direction and that the instant at which they switch or commutate can be controlled. The rotating machine with commutator is, of course, well known. However, it is eliminated from use in vscf systems because even at sea level its output frequency is limited to well below 100 cps. The mechanical rectifier is a mechanically controlled switch which has seen considerable development in the electrochemical industry. This, too, is unsuitable for use in the airplane environments at the frequencies required in vscf systems. The third device included under this listing is a symmetrical transistor. This device is suitable for operation in aircraft environments, but unfortunately its power rating is so small that it, too, is eliminated for use in aircraft vscf systems.

The remaining components listed in Table II are inherently rectifying devices, so some circuit arrangement using two of the components back to back must be used in order to handle current both into and out of the power source or load.

Included under the heading of uncontrolled rectifier (diode) are the mercury-arc rectifier and the semiconductor rectifier. These components have found very large application in conversion a-c into d-c energy. These components suffer from the disadvantage that the instant at which they commutate is controlled entirely by the power circuit voltages. Because of this, the uncontrolled rectifier when used alone cannot produce anything other than d-c energy and because of this cannot result in a vscf system.

Fig. 4. Simulated controlled rectifier ww rack for 18 units and cooling blower

Under the heading of controlled rectifier are included such devices as the gas controlled mercury-arc rectifier, the ignitron, the Thyratron, and such new semiconductor devices as the transistor and the p-n-p-n switch.[5,6] With any of these components, the instant of firing can be delayed by any amount. This means both controlled rectifier operation and inverter operation are possible. That is, power can be handled in either direction by circuits using these components. As has already been seen, capability of handling power in either direction results in a vscf system which can be double ended and which can be magnetized from the low-frequency side.

Intermediate between the uncontrolled and the controlled rectifier is an uncontrolled (diode) rectifier together with some form of modulator. Such a combination is capable of a limited amount of delay. Because of the limit on the amount of delay controlled rectifier operation is possible, but not inverter operation. That is, power can flow in only one direction. This, as we have seen, leads to a vscf system which is single sided and which

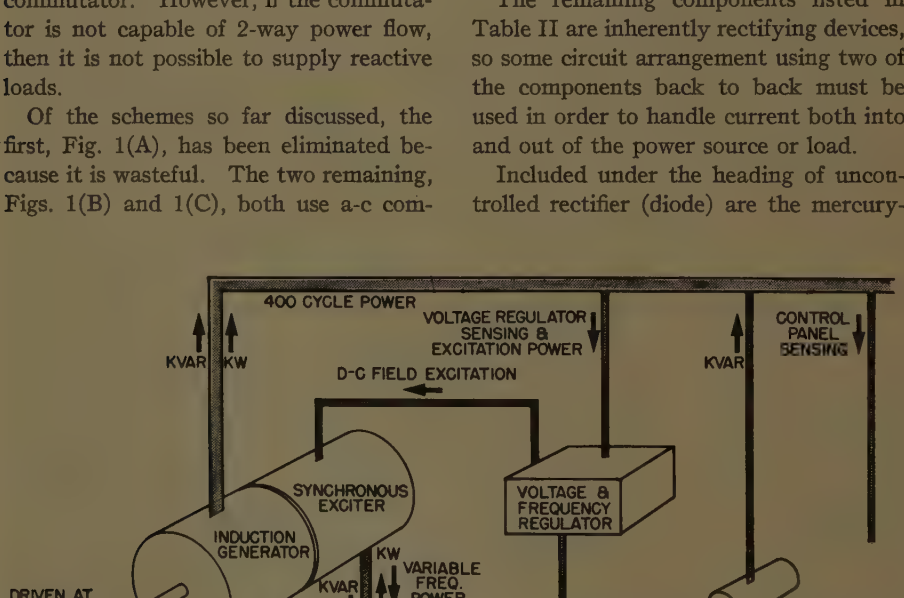

Fig. 3. A vscf system block diagram

. 5. Wound-rotor induction generator and synchronous exciter on the drive stand. Both machines are NEMA 284 frame size

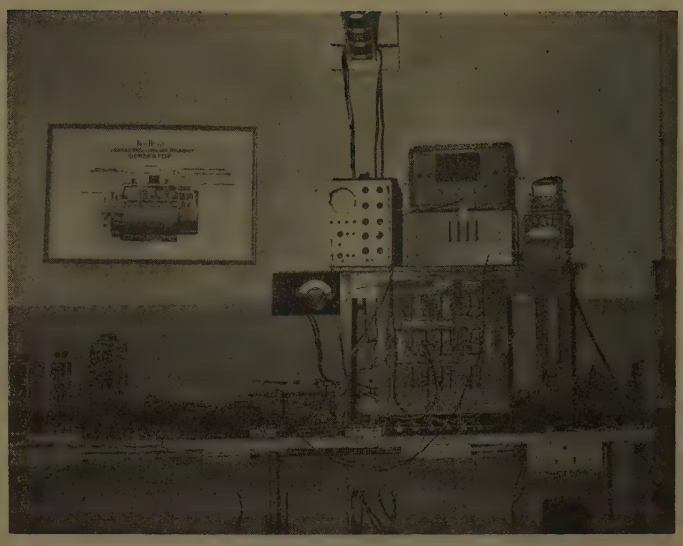

Fig. 6. Frequency changer with control and test instrumentation

magnetized from the high-frequency
0-cycle side.

The foregoing analysis leads to the
nclusions that if there are no commu-
ing devices of any kind in the power
ndling circuits of the system, then the
eme is a wasteful one.[7] If there is a
mmutator machine in the power han-
ng circuits, then either the frequency or
speed range capability of the system
everely limited. If uncontrolled recti-
s together with some kind of modulator
used in the power-handling circuits,
n there must be capacitors to magne-
e the system, and the scheme can be
ner a full-rated or single range synchro-
us-flux system. If controlled rectifiers
used, then the scheme may be a full-
ed system or either single or double
ge synchronous-flux system, and ca-
itors are not needed for magnetiza-
n.

mparison of VSCF Systems

A comparison of nonwasteful vscf sys-
ns is shown in Table III.

Three systems are compared: a full-
ed system; a synchronous-flux system
ich operates above and below synchro-
us speed; and a synchronous-flux sys-
n which is confined to one side of
chronous speed.

From considerations illustrated in
ble III and because of the power
ings of presently available semicon-
tor components, it is concluded that
best system for application as an air-
ft main generator is a double-range
chronous-flux system. As has pre-
usly been pointed out, such a system must use controlled rectifiers, and the only available controlled rectifier which is suitable for aircraft environments is the silicon p-n-p-n switch. This device is now available in ratings large enough to meet most present aircraft requirements as shown in Fig. 2. In fact, it is the advent of this component which has made aircraft vscf systems practical at this time.

Description of the System

A block diagram of the system is shown in Fig. 3.

There are two machines on the variable speed shaft: one the synchronous-flux wound-rotor induction generator; the other, a salient-pole synchronous exciter which in combination with the semiconductor frequency changer handles the slip power. The salient-pole synchronous exciter is an inside-out machine with the d-c field winding on the stator and the a-c output winding on the rotor. The frequency changer is located inside the shaft and rotates with it. This results in a brushless configuration similar to the well-known rotating-rectifier alternator.

A 400-cps reference-frequency signal is provided by a tuning fork or oscillator housed in the same package as the voltage regulator. This signal controls the frequency changer.

The block diagram shows one block called a voltage balancer. This is a free-running synchronous machine floating across the 400-cps bus bars. It is in reality a synchronously rotating amortisseur, whose prime function is to maintain balanced voltages when the load currents are unbalanced. In addition, it supplies some reactive kva to the bus, helps in shaping the 400-cps output voltage wave, and contributes to the fault capability of the system.

Description of the Hardware

Studies along the lines already indicated showed that a vscf aircraft main generator system would be practical and competitive in size and weight, when silicon p-n-p-n switches became available in power ratings of several kw.

Instead of waiting for these components

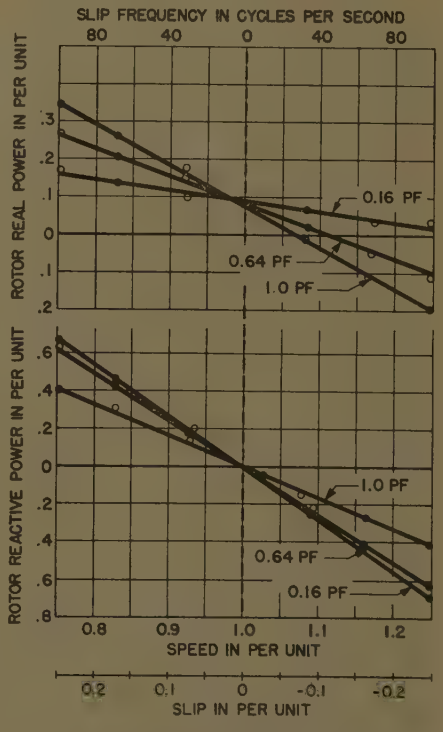

Fig. 7. Frequency changer power output

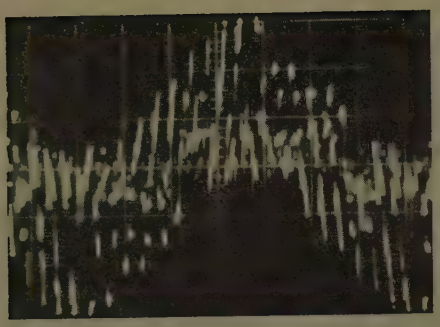

Fig. 8. Oscillogram of the slip frequency voltage fabricated by the frequency changer

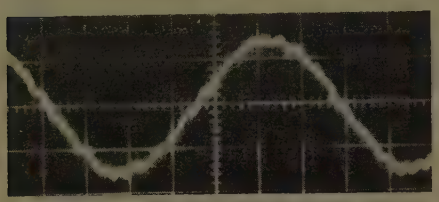

Fig. 9. Oscillogram of the slip frequency current flowing in the frequency changer

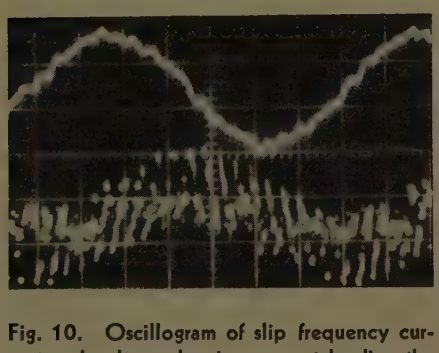

Fig. 10. Oscillogram of slip frequency current and voltage showing current leading the voltage by approximately 100 degrees

to become available, it was decided to build and test hardware using available components, in order to prove the principles and to explore as many of the problems as possible.

The first system was essentially that shown in the block diagram of Fig. 3 except that the frequency changer was stationary and both the rotating machines were provided with slip rings. The controlled rectifiers required for the frequency changer were simulated by using three transistors and approximately 15 other circuit components to represent each controlled rectifier. Fig. 4 shows in the foreground one simulated controlled rectifier mounted on its heat sink. Visible behind this is a rack in which 18 simulated controlled rectifiers are mounted; part of the blower used to cool them is also visible. With this apparatus, a few kva of constant 400-cps frequency power was successfully generated from a variable speed shaft.

As soon as it was determined that the available silicon p-n-p-n switches were sufficiently advanced in their development, a second set of hardware was built, using this component in the frequency changer, and incorporating all the improvements resulting from work with the first set of hardware. Fig. 5 shows the two rotating machines mounted on the drive stand; these are standard commercial machines and are provided with slip rings. Fig. 6 shows the stationary frequency changer together with the control and test instrumentation.

The system shown in these two illustrations, Figs. 5 and 6, is essentially that shown in the system block diagram of Fig. 3, except that voltage regulation is performed manually, the frequency changer is stationary, and the two rotating machines are provided with slip rings.

Test Results

An extensive program of tests was carried out using the hardware shown in Figs. 5 and 6. From these tests the following conclusions can be drawn.

1. A double-range synchronous-flux vscf generator system for a speed range of 2:1 or more is feasible, and in particular that the difficulties of passing through synchronous speed have been overcome.

2. The frequency of the power generated follows that of the frequency-reference signal exactly, no matter what the speed of rotation of the shaft may be, with frequency transients which amount to no more than wave distortion, and phase shift. This means that the integrated frequency error of the system is the same as that of the reference, which can be made very small, and that the frequency transient is so much reduced that a new definition is required.

3. The system behaves substantially

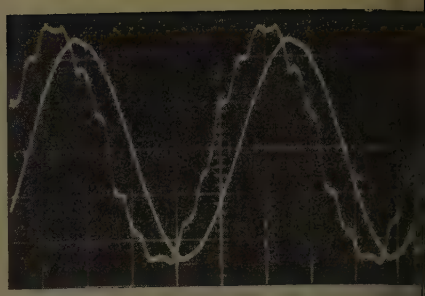

Fig. 11. Oscillogram showing 400-cps o put current and voltage at 0.65 power fac

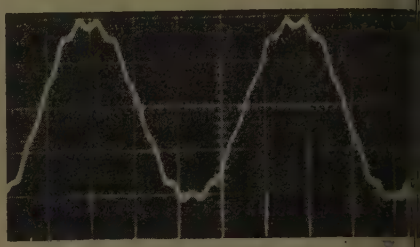

Fig. 12. Oscillogram showing output volt with d-c excitation of induction generator r

in the manner predicted. Fig. 7 i plot of measurements of the real and active power output of the freque changer for various 400-cps loads power factors, over a speed range. T plots agree, within the limits of exp mental error, with theoretical pre tions.[8]

4. The frequency changer fabric the correct slip frequency voltage current and can handle real and reac power flow in either direction. measurements plotted in Fig. 7 show latter. The oscillogram of Fig. 8 sh the slip frequency voltage that is fa cated by the frequency changer, Fi shows the slip frequency current, Fig. 10 shows the current and voltag the same oscillogram with the cor

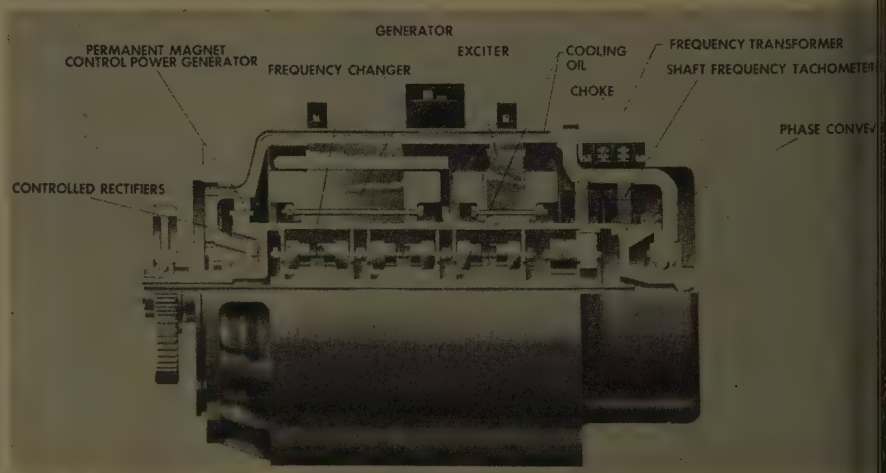

Fig. 13. A 60-kva vscf generator, oil-cooled

ase relationship, the current leading the ltage by about 100 degrees in the case own.

5. Acceptable 400-cps output voltage ve shape results. Fig. 11 is an oscillo- am of the 400-cps output current and ltage with a lagging load of about 0.65 wer factor, taken without the voltage lancer connected to the systems. The rrent wave shape is quite acceptable, e voltage wave shape contains some ple; however, a major part of this ple is due to slot harmonic voltage in e induction generator and could, there- re, be eliminated by proper design of is machine. Fig. 12 is an oscillogram the 400-cps output voltage of the in- ction generator when its rotor is ex- ed with direct current, where the slot rmonic voltage is clearly visible.

tual System Designs

As a result of the extensive test pro- am with the laboratory system, it has en possible to make extrapolations to tual aircraft systems with a fair degree accuracy. A number of complete air- ft systems have been designed. Fig. is a cutaway view of a 60-kva 4,500/ 00-rpm oil-cooled machine.

nclusion

From designs made, it is concluded that actical vscf generator systems of this e can be built using the silicon p-n-p-n itches which are now becoming avail- le. These systems are competitive in e and total weight with present hydro- chanical constant-speed drive and syn- ronous generator combinations, and y have better efficiency, much better quency regulation, and will likely prove be more reliable than the present con- nt-speed drive and generator com- ation.

ferences

GENERAL SPECIFICATION FOR AIR-COOLED , AIRCRAFT GENERATORS AND REGULATORS. *itary Specification, MIL-G-6099A (ASG)*, De- tment of the Air Force and Bureau of Aero- tics, U. S. Navy, Mar. 25, 1957; Amendment pr. 15, 1958.

POLYPHASE COMMUTATOR MACHINES (book), Adkins, W. J. Gibbs. Cambridge University s, Cambridge, England, 1951.

THE NATURE OF POLYPHASE INDUCTION MA- ES (book), P. L. Alger. John Wiley & Sons, , New York, N.Y., 1951.

SYNCHRONOUS-FLUX GENERATOR, O. J. M. th. *Electrical Engineering*, vol. 77, 1958, pp. -10.

A SILICON-CONTROLLED RECTIFIER, D. K. on, R. F. Dyer. *AIEE Transactions*, pt. I *mmunication and Electronics*), vol. 78, May , pp. 102–06.

HIGH-CURRENT TRANISTORS, F. S. Stein, E. W. k. *AIEE CP58-1397* (available on request).

7. THE LIMITATIONS OF INDUCTION GENERATORS IN CONSTANT-FREQUENCY AIRCRAFT SYSTEMS, E. Erdelyi, E. E. Kolatorowicz, W. R. Miller. *AIEE Transactions*, pt. II (*Applications and Industry*), vol. 77, Nov. 1958, pp. 348–52.

8. ENERGY CONVERSION PROPERTIES OF INDUCTION MACHINES IN VARIABLE-SPEED CONSTANT-FREQUENCY GENERATING SYSTEMS, M. Riaz. *Ibid.*, vol. 78, Mar. 1959, pp. 25–30.

Discussion

J. T. Duane (General Electric Company, Erie, Pa.): The authors are to be complimented on an interesting and informative discussion of their approach to the generation of constant frequency power with variable speed machines. Generator configurations of this type are receiving increasing amounts of attention throughout the industry and the experimental results reported here provide a useful supplement to some of the theoretical work already published.

Previously available discussions of vscf systems using induction generators, as mentioned in references 7 and 8 of the paper, have presented careful and complete analyses of power flow and distribution within the induction generator. Unfortunately, equal attention has not been given to the problems associated with the generation and transfer of reactive power. Since the authors are reporting experimental data, their comments on the problems associated with reactive power distribution should be extremely interesting.

It is necessary to supply significant amounts of lagging reactive power to induction generators whenever they are operated at slip other than zero. In typical induction motors this reactive power requirement represents a significant percentage of total rating. Do the authors feel that this is the case in the systems they describe, and can they offer an estimate of the reactive power requirements for the induction generator as a percentage of system output?

All reactive power in the system shown in Fig. 3 must be supplied by either the synchronous exciter or the voltage balancer, at other than zero slip. It would appear desirable to minimize that portion of the reactive power generated by the synchronous exciter, since those kilovars (kvar) must be transferred through the frequency changer and the induction generator thus increasing the size of both of these elements of the system. Have the authors reached any conclusions as to what a desirable balance is for the division of reactive power generating capability between the synchronous exciter and the voltage balancer?

The paper points out that the use of a floating synchronous machine on the line can provide amortisseur action to yield balanced voltages under unbalanced load conditions. This will require that the floating machine have a low value of negative sequence reactance. The authors suggest that this can be obtained with a relatively small machine. Experience in the design of conventional synchronous alternators suggests that ohmic values of negative sequence reactance are closely coupled to machine size. Do the authors feel that special or unusual design techniques will be required to build a voltage balancer with a negative sequence reactance as low as a conventional generator without the device being almost as heavy as the conventional generator, and are such techniques already available?

If the voltage balancing function can be provided by a very small machine, will it have the power-dissipating capability necessary to permit extended periods of operation under conditions of unbalanced system loads?

Bert V. Hoard (Boeing Airplane Company, Seattle, Wash.): The authors have written a very good paper on a complex subject. However, there are some areas on operation and performance of the system which, if amplified, will improve its value. The authors state that the difficulties of passing through synchronous speed have been overcome. Have the tests shown any tendency toward roughness, or harmonics of slip frequency in output voltage, or current at or near synchronous speed, as the generator rotor slips or commutates from one phase to another in a slip cycle?

The oscillogram trace of slip frequency voltage, slip frequency not stated, in Fig. 8, as fabricated by the frequency changer, indicates a considerable amount of certain harmonics although the current flowing (Fig. 9) has a materially lower percentage of harmonics. How do these harmonics affect the weight and efficiency of the frequency changer and the exciter at, say, minimum speed and at synchronous speed?

The frequency changer real and reactive power output curves, Fig. 7, are quite interesting. At minimum speed, 25% slip, and unity power factor load on the generator, it appears that more reactive power must be supplied by the frequency changer to the generator rotor than real power. And when the load power factor is lagging at 64%, the reactive power required is almost 100% greater than the real power requirements at unity power factory. Is it correct to conclude that reactive requirements of the generator rotor have more influence in determining the rating and weight of the exciter and frequency changer than real power requirements of the generator rotor both at the minimum speed?

Normal loading for the semiconductors in the frequency changer that is considerably below their rating, probably has been necessary to prevent failure during abnormal generator loading conditions. These abnormal conditions may be 200% load, or balanced or unbalanced faults, followed by removal of the abnormal load and then transient high over voltage occurs. Have any approximate derating factors been determined for the semiconductors to prevent failure during these abnormal conditions?

What is the expected efficiency of the 60-kva generator, Fig. 13, when operating at rated load and power factor at minimum speed and at synchronous speed?

K. M. Chirgwin and **L. J. Stratton**: Mr. Duane raises the problem of the flow and distribution of reactive power in the induction generator. This problem is analyzed in reference 8 of the paper, but from the questions that have been asked it seems that this problem is not well understood.

The behavior of an induction machine

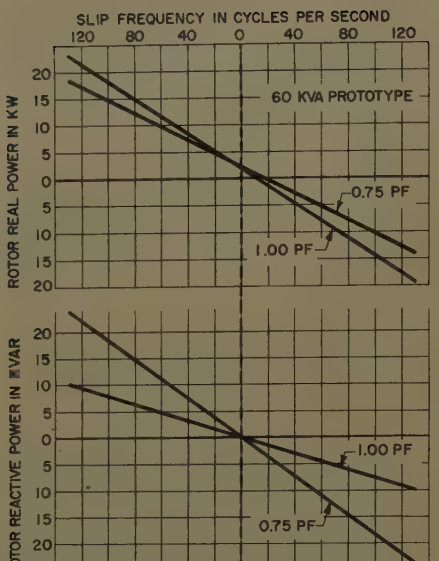

Fig. 14. Rotor power requirements of the induction generator

when its rotor circuits are excited by an external source differs from its behavior when its rotor is short-circuited or closed through resistances. In particular the excited induction machine is capable of generating reactive kva. A fraction s of the kvar generated in the stator must be supplied to the rotor from the external exciting source, but the balance or a fraction $1-s$ times the kvar generated originates inside the induction machine itself, where s is the per-unit slip. Operation at synchronous speed is not an isolated point but merely the point at which s is zero and where all the kvar originates inside the induction machine. Above synchronous speed more kvar than is needed is generated inside the induction machine and the extra kvar is absorbed by the external exciting source.

The curves of Fig. 14 have been prepared to show the real and reactive power requirements of a 60-kva flyable prototype system which our company is presently building.

Mr. Duane asks what is a desirable balance between generating kvar in the voltage balancer on the stator side and generating kvar in the synchronous exciter on the rotor side of the induction generator. The voltage balancer is a constant speed, probably high-speed, machine, probably operating in a favorable environment and so can undoubtedly put out a given kvar for less weight than can the synchronous exciter. On the rotor side of the induction generator, however, only a fraction s of the kvar is needed, so this favors the exciter, but handling these kvar increases the size and weight of the frequency changer and the induction generator. So we prefer to make the trade off between the voltage balancer and the main machine package, which comprises exciter, frequency changer, and induction generator.

In making such a trade off all the following functions of the voltage balancer should be considered, since if they are not performed by the voltage balancer then the weight of the main machine or other components of the system must be increased:

1. Voltage balance
2. Supply of kvar
3. Output wave shaping
4. Fault kva capability

If the trade off is based only on considerations of kvar then it can be said that low synchronous speed of the voltage balancer, now a synchronous condenser, high minimum speed of the main machine, and narrow speed range of the main machine, all tend to reduce the proportion of the kvar that should be supplied by the voltage balancer. In the limit this will lead to a constant speed synchronous alternator where, as is well known, no synchronous condenser is indicated.

In vscf systems designed to meet military specifications the size of the voltage balancer is determined by the voltage unbalance requirements. The data given below refer to the voltage balancer which forms part of the 60-kva flyable prototype system which is presently being built. The nominal rating of the voltage balancer is 15 kvar. On the 15-kvar base, the negative sequence quantities are: reactance 7.45%, resistance 4.15%, impedance 8.45%.

The electromagnetic weight of this machine, while it is greater than that of a conventional 15-kva synchronous condenser, is only about one half the weight of a conventional 60-kva alternator for the same speed and environment. The design to achieve this is unusual because the requirements are unusual, but the design techniques are no different from those used for normal synchronous machines. The thermal capability of the amortisseur of this voltage balancer is such that it can carry continuously a single-phase current equal to one third of the normal full load current of the system.

Mr. Hoard asks if there is any tendency toward roughness in the output voltage when operating very near synchronous speed.

The operation of the frequency changer is the same whether the frequency being fabricated is 100 cps or a fraction of a cps so synchronous speed does not represent a discontinuous point and there is no tendency toward roughness in passing through this speed. During demonstration of our vscf hardware we have shown that, with the drive stand speed set as close as possible to synchronous speed, the output wave form of the frequency changer automatically compensates for speed irregularities caused by the drive stand governor. In fact, the frequency changer fabricates the most precise wave when the ratio of input to output frequencies is the greatest. Therefore, operation near synchronous speed represents the best condition since the ratio is approaching infinity.

As can be seen from Fig. 8, the fabricated slip frequency voltage which is approximately 70 cps, contains harmonics, with 1,400 cps being the largest component. These harmonics result from the fabrication process wherein a low-frequency voltage is fabricated from a high-frequency voltage by switching in pieces of the high-frequency waves.

A choke is included in each phase of the frequency changer to absorb the harmonic in the same way as a choke is used to filter the output of a d-c rectifier power supply. The effectiveness of these chokes is illustrated by the smoothness of the slip frequency current wave. The weight of the chokes is determined by the minimum speed since the harmonic frequencies are the lowest for that condition. From other considerations, the weight of the exciter is also determined by the minimum speed and the additional harmonic power represents only a slight increase in the total exciter kva, and only a slight increase in exciter weight.

The harmonics do not materially affect the frequency changer efficiency since the forward voltage drop of the controlled rectifier is in the order of a volt and the slight increase in current contributed by the harmonics does not represent many watts. Because the controlled rectifiers are either "full-on" and are "naturally commutated" to "full-off," they provide the most efficient switching process. It is important that a semiconductor frequency changer be operated in this manner since if wave shaping is accomplished by absorbing voltage across the switching element, appreciable power is dissipated in the switch with attendant loss in efficiency and with considerable derating of the switching element. Therefore, it is better to allow harmonics to be produced in the conversion or frequency changing process and to filter them out, rather than avoid producing them in the conversion process and causing high power dissipation in the switching elements.

The ratio of real and reactive power values shown in Fig. 7 presents a somewhat distorted picture since the wound rotor induction generator used for the data was a commercial machine having a magnetizing reactive power requirement equal to 1.6 times its output kva rating. More typical requirements for a 60-kva system with a 15 kvar voltage balancer are shown by Fig. 14. The rating and weight of the frequency changer is determined by the maximum kva which occurs at either the minimum or maximum speed.

The amount of derating of the semiconductors in the frequency changer depends not only on meeting overload and fault conditions but also on cooling air velocity and temperature. Presently available controlled rectifiers are rated for a continuous peak inverse voltage of 300 volts and a current of 50 amperes which corresponds to 15 kw. Since 18 controlled rectifiers are used in the frequency changer, and considering approximately 30 kva need be converted in the frequency changer for a 60-kva machine, adequate switching capacity is available in presently available controlled rectifiers.

Calculated efficiencies for a 60-kva vscf cooled machine similar to that shown in Fig. 13 including voltage balancer losses are 82.2% at minimum speed and 81.6% at synchronous speed for rated kva and unity power factor load; and 77.1% at minimum speed and 77.4% at synchronous speed for rated kva and 0.8 power factor load.

A High-Capacity Maintenance-Free Generating System for Motor Coaches

R. L. LARSON
ASSOCIATE MEMBER AIEE

HE TREND of electric loads on mobile equipment has been upward at an r-increasing rate since the first gentors were installed on automobiles in 9.

In the past the load-trend curve has ghly followed that of the electrical ity industry which doubles in load ry 10 years. But the adoption of airditioning equipment in recent years increased the connected load on omotive-type equipment far beyond value which would have been pre- ted by the load-trend curve. The hest electric load on commercial ve- les is encountered on city coaches. e growth of the electric load for coaches h 12-volt systems is shown in Fig. 1. he capacity of the generator used to ply the load increased from 50 amperes 1933 to 120 amperes in 1946. How- r, even this striking increase in output s not indicate the relative capacities he two generators since the 120-ampere t began supplying current to the load 550 rpm, while the 50-ampere unit uired a speed of 900 rpm to produce ful output. The speed at which the erator begins to supply current to the tem became more important with the ption of the hydraulic transmission, as much as the normal pattern of ration in large cities is to operate the ine at full throttle for a period meas- d in seconds, then coast to the next).

Until this year, the standard generating tem for most large city coaches consisted of a 120-ampere d-c generator and double voltage and current regulators of the vibrating contact type. The generator was gear driven at a 1.94 ratio and produced 80 amperes at engine idle speed. The field circuit was split into halves with each half regulated by a separate voltage and current regulator, so that twice the normal field strength could be used without exceeding the maximum current rating of the regulator contacts.

Several things happened that determined that the d-c generator system was headed for obsolescence on large city coaches. In addition to the rising load trend curve heading toward a point where the electric capacity and speed range of the largest conventional d-c generators would be inadequate, the diesel engines were being improved to the extent that engine overhauls were made less and less frequently. No longer would the generator and regulator operate satisfactorily without maintenance over the lengthened engine overhaul periods. In fact, the increased electric loads and the high engine compartment temperatures, which resulted from increased engine loads, contributed to the reduction in life of the brushes, oil seals, bearings, and other components from that which previously had been obtained. Alternating-current generators with selenium rectifiers had been applied on some coaches with higher than normal electric loads. However, although these generators would solve the electric capacity problem for several years, the existing units had the same mechanical construction deficiencies as the d-c generator and, in addition, required the use of a large, expensive, and vulnerable selenium rectifier.

Design Objectives

About 1955, the engineers at General Motors Truck and Coach Division began setting down specifications for the type of generating system which would be needed in the future. Because this generating system was expected to be one which would supply the needs of the coach operators for a number of years without any major revisions, the requirements set down were not met by any generating system in existence. A goal of 1 million miles of maintenance-free operation was set up to correspond to the expected life of the engine. The minimum generator capacity was set at 200 amperes, with 125 amperes output available at engine idle speed with provision to increase this output in the future with only minor revisions in the generator. The generator was to be of the a-c type with built-in silicon rectifiers and, in order to obtain the long life operation desired, would have to be brushless and have permanently lubricated bearings. To prevent failures caused by the entry of dirt, detergents, and other foreign matter into the generator or failures caused by lack of proper maintenance on air filters designed to prevent such damage, the generator was required to be environment free. The regulator was required to be of a completely static design to eliminate all wearing parts and was to have the ability to retain its voltage setting unchanged over a period of years.

In order that maximum performance could be obtained from a given size generator, the regulator was also required to supply much higher field power than had previously been thought practical.

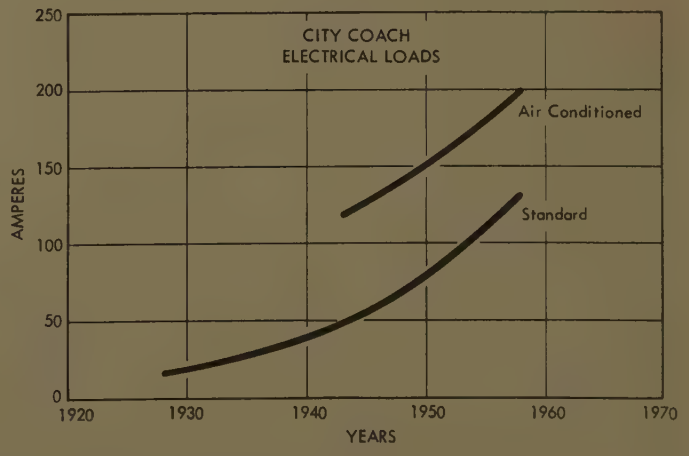

Fig. 1. Load-trend curve of motor coaches

er 59-779, recommended by the AIEE Land nsportation Committee and approved by the E Technical Operations Department for presenon at the AIEE Summer and Pacific General ting and Air Transportation Conference, tle, Wash., June 21–26, 1959. Manuscript nitted March 20, 1959; made available for ting April 10, 1959.

. Larson is with the Delco-Remy Division, eral Motors Corporation, Anderson, Ind.

author wishes to acknowledge the contribution e following people who were instrumental in the lopment of this system: the original concepof such a system and much of the early work on generator was done by R. H. Bertsche, R. O. by, E. E. Gegenheimer, and R. A. Carlson, of General Motors Truck and Coach Division. transistor regulator development was done by R. Hetzler and L. J. Sheldrake and the refineits in design and later development work on the generator and the regulator carried out . J. Raver; all three of these men are with the lo-Remy Division of General Motors.

Fig. 2. Transistor regulator and oil-cooled generator

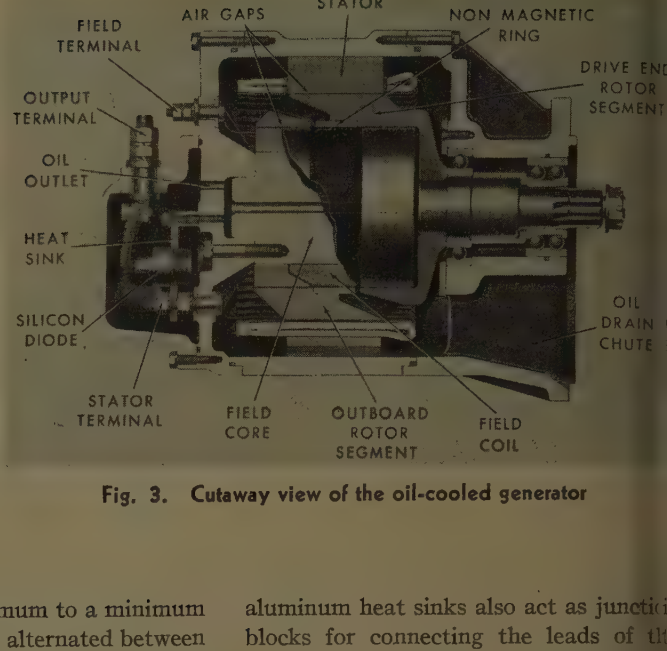

Fig. 3. Cutaway view of the oil-cooled generator

Generator Design

The generator and regulator designed to meet the objectives specified is shown in Fig. 2, and a cutaway view of the generator is shown in Fig. 3. Basically, the machine is a 3-phase alternator with a 12-pole Lundell-type rotor. To obtain the brushless feature, however, several modifications have been made in the normal Lundell rotor construction. Two bearings are used on the drive end so that the entire rotor is supported from that end in an overhung fashion. A nonmagnetic ring has been added between the six poles of the drive-end rotor segment and the six poles of the outboard rotor segment, so that the outboard segment is supported mechanically from the drive-end segment although the two are still isolated magnetically. An interior air gap has been added to separate the field coil and core assembly from the rotor poles, and the field coil and core assembly is supported from the end frame opposite the drive end.

In this manner, a rotating field machine is made in which both the field winding and the output winding are stationary so that no brushes are required. There are several advantages of this type of design as compared with other types of brushless generators that are known. A permanent magnet generator could be used for an application such as this, but it is difficult to regulate the output voltage accurately without a considerable amount of bulky and expensive extra equipment. Also the field strength of such a generator is limited as compared with that obtainable in an excited field machine. An inductor alternator would be another possibility, but this type of machine has an inherent 2-to-1 penalty in size and weight because the flux is pulsated from a maximum to a minimum value instead of being alternated between positive maximum and negative maximum values. A rotating rectifier type of machine could also be used but, in the size of generator considered here, an exciter is not needed to amplify the excitation power available from the regulator to a level sufficient to excite the main field. Consequently, the exciter becomes merely added weight, space, and expense which serves no purpose other than to transfer the excitation power from the stationary member to the rotating member.

An additional advantage of the double air-gap Lundell construction as compared to the normal Lundell construction arises from the separation of the rotating member from the field coil and core assembly. This reduces the moment of inertia of the rotor from 125 pound-inches^2 for a comparable size generator of standard Lundell construction to 96 pound-inches.^{2} This reduction in inertia is important since the generator-to-engine gear ratio is limited to a value which will not cause shaft and gear damage from the torsional vibrations of the diesel engine. Because of this reduction in inertia, it was possible to raise the gear ratio from 1.94 to 2.29. It would have been possible to raise the ratio even further had not the gear center distances available imposed a further restriction.

Rectifier Construction

The 3-phase full-wave bridge rectifier is made up of three silicon diodes mounted in the end frame and three silicon diodes mounted in small aluminum heat sinks, which are themselves supported from, and electrically common with, the three terminals of the stator winding which extend through the end frame. The aluminum heat sinks also act as junctio blocks for connecting the leads of th three end-frame-mounted diodes to th stator terminals. All six of the diod are of the same polarity in this co struction.

Oil Cooling System

Several attempts were made to ma the generator environment free by utili ing totally enclosed or totally enclos fan-cooled construction but it was fou that at the ambient temperatures pr vailing in the engine compartment, su a machine became too large and t heavy for consideration. Water coolil was also considered, but this involv the use of tubes and passages to condu the water to and from the heat sour in the generator and was thought to too expensive and too vulnerable to lea to be considered. The only other cooli medium available on the engine was engine oil. Since the oil is not el trically conductive, it can be thro directly on the windings without fear causing electrical failure, and it has added advantage of furnishing a p manent lubrication supply for the be ings. For these reasons, oil cooling adopted for this generator.

The rectifier cover casting has provis to receive a fitting from an oil line wh is connected to the engine oil galle There is a small orifice drilled in t casting which restricts the flow of oil approximately one gallon per minute the 40 pounds per square inch regula oil pressure which is available when engine is operating in its normal sp range. The orifice also acts to produc high velocity jet of oil down one side the rectifier chamber, which keeps the in the chamber in motion and preve large temperature differences around

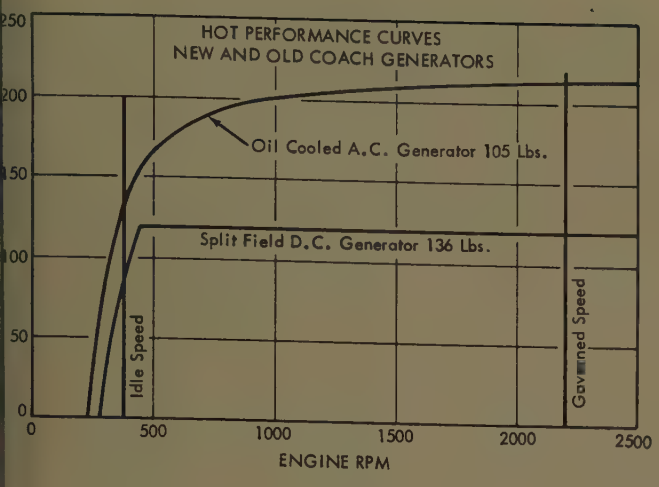

Fig. 4. Comparison of generator output curves

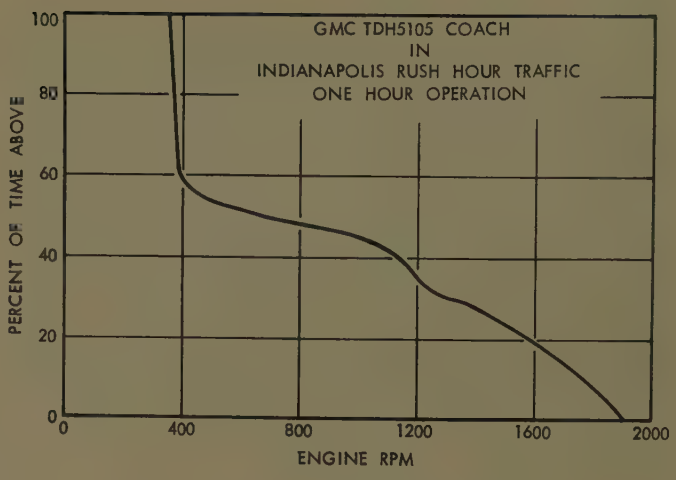

Fig. 5. Engine operating speed characteristic

les. With the diodes entirely sub-ged in oil, excellent heat transfer btained so that large heat sinks are ecessary. The oil fills the rectifier mber to the level of the oil outlet. hen flows through the oil outlet and ugh the hole in the center of the field . At the end of the field core the is discharged against the inner sur- of the rotor and is carried outward by rifugal force to the inner air gap, ugh which it flows toward the rec- r end of the machine. Some of the escapes through slots between the magnetic ring and the drive-end r segment and follows the underside he poles outward until it is thrown he poles onto the inside of the stator ding at the drive end. The rest of oil continues toward the rectifier end he machine until some of it escapes ugh the slots between the nonmag- c ring and the outboard rotor seg- t. The remainder continues through air gap to the end of the rotor where it hrown on the inside of the stator ling at the rectifier end. Thus, the oil s the stator winding by direct con- with the end windings and cools field winding by conduction of heat ugh the core assembly and by direct act with the field winding at the r air gap. It then drains to the bot- of the stator assembly and, in the of the oil at the rectifier end, flows ugh a notch between the stator nations and the stator frame and ns down the chute in the drive-end e to the flywheel housing of the ne. The oil level in the generator ains below the height of the air gap hat the rotor does not pick up the which has drained to the bottom of tator.

he oil is taken from the engine after s passed through the full-flow filter the oil cooler in order that the cleanest and the coolest oil in the system will be used in the generator. Even under these conditions, however, the oil can at times reach an inlet temperature of 240 F (degrees Farenheit), although the most normal operating range is around 200 F. The temperature of the oil increases about 50 F in passing through the generator under full load conditions at high speed. One of the major problems to be solved in the development of the oil cooling system was the selection of insulation which would withstand the high temperature oil bath. The insulation system being used consists of an epoxy coating on the magnet wire with glass tape on the field coil and isocyanate-impregnated glass slot insulation in the stator. All assemblies receive two coats of an oil modified phenolic varnish which was selected after extensive testing of all available varnishes in a 300 F bath of used engine oil. The components used in the insulation system all have successfully withstood more than 12,000 hours in this bath. No difficulty has been experienced in operating units from insulation failures due to deterioration of the insulation.

When the oil cooling system was first proposed, it was thought that the generator would act as a centrifugal and magnetic oil filter and would soon be rendered inoperative by an accommodation of sludge. These fears have proved groundless, even when the experimental generators were operated on old engines with bypass oil filters that permitted quite dirty oil to flow through the generator. The heads of the bolts which extend into the rectifier chamber from the field core are highly magnetized and attract any iron particles which come through the oil system. The only particles discovered on the bolt heads have been particles of approximately 1 micron in diameter which pass freely through the oil filter. Particles of this small size should not cause damage even if they pass completely through the generator.

Performance

A comparison between the performance of the new a-c generator system and the d-c generator system which it replaced is shown in Fig. 4. This illustrates the increase in output of approximately 75% throughout the speed range and the 23% reduction in weight which was obtained. Part of this increase in performance, of course, is the result of the 18% increase in gear ratio on the new system.

The importance of obtaining high generator output at engine idle speed becomes apparent if the curve of engine operating speed versus percentage of time shown in Fig. 5 is examined. This particular engine speed curve was taken on a coach operating in downtown Indianapolis, Ind., during a normal afternoon rush hour, but it is representative of the conditions encountered in most medium size cities. Surveys were made of the operating conditions in metropolitan New York City and New Orleans, La., during the rush hour a few years ago which indicated that the engine operated at idle speed as much as 70% of the time.

The engine operating speed characteristic can be combined with the generator performance curve, the generator drive ratio, and the battery characteristics to determine the amount of load which can be carried by the equipment in question on that particular driving schedule without producing a net charge or discharge of the battery. This value of system load is referred to as the "city load-carrying capacity" (CLCC). In determining the CLCC, an assumption must be made as to the state of charge and the temperature of the battery since this de-

Table I. City Load-Carrying Capacity of Transit Coach Generators with Two 205-Ampere-Hour Batteries on Indianapolis Schedule

Generator	Gear Ratio	Voltage Regulator Setting	Battery		CLCC
			Temperature, F	Per-Cent Charge	
Split Field	1.9375	14.5	−10	60	88.7
Split Field	1.9375	14.5	−10	80	81.1
Split Field	1.9375	14.5	+100	80	98.7
Oil Cooled	2.29	14.0	−10	80	124.1
Oil Cooled	2.29	14.0	+100	80	163.5
Oil Cooled	2.29	14.0	+100	100	137.9
Oil Cooled	1.9375	14.0	+100	80	142.0

termines the rate at which the battery will accept a charge. The battery temperature also determines the efficiency of the battery in ampere-hours of output as compared to the ampere-hours of input. The CLCC rating of a generator gives a much more accurate measure of its load carrying ability under variable-speed driving conditions than does the maximum output rating. A comparison of the CLCC rating of the two coach generator systems with various battery conditions is given in Table I. The split-field generator calculations were made on the basis of a 14.5-volt regulator setting because that is a normal setting. The oil-cooled generator calculations are based upon a 14.0-volt setting because the battery can be kept charged with the lower setting when the higher capacity generator is used. The lower system voltage lengthens the life of lights and other electric equipment and reduces battery maintenance.

Regulator Design

The only regulating unit that is necessary with this oil-cooled generator is a voltage regulator. No current regulator is required since the generator is inherently current limited and no cutout relay is required since the silicon diodes effectively block any reverse current. The elimination of these two components from the regulator eliminates the need for heavy leads and large terminals to handle the output current and consequently reduces the size and weight of the regulator greatly. A comparison of the size and complexity of the transistor regulator used with the oil-cooled generator and the split field regulator used with the d-c generator and the carbon-pile regulator used with the older style a-c generators is shown in Fig. 6. The comparison in size is even more striking when it is considered that the transistor regulator will handle two to three times as much field power and give much closer voltage regulation.

Circuit

The circuit of the transistor regulator is shown in Fig. 7 and the physical arrangement of the components on the printed circuit board is shown in Fig. 8. The voltage divider network at the left side merely provides a means of adjusting the regulator voltage setting and of compensating for variations in the Zener voltage of the voltage reference diode. When the system voltage is higher than the regulator setting, the voltage reference diode will pass current, and this current flows in the emitter-base circuit of the driver transistor, turning it "on." In the "on" condition, the emitter-collector circuit of the driver transistor is essentially a short circuit which is connected across the emitter-base circuit of the two output transistors. This effectively short-circuits any base current which would tend to flow in the output transistors and turns them "off." Since the output transistors are in series with the generator field winding, no field current can flow. With the field current turned off, the system voltage will fall until it reaches a value at which the voltage reference diode will no longer conduct current. Under those conditions the diode blocks any current flow to the emitter-base circuit of the driver transistor and turns it off, thus it removes the short circuit from the emitter-base circuit of the output transistors. Current will then flow through the emitter-base circuit of the output transistors and will turn them on so that field current can flow.

There are a few circuit refinements which aid the basic operation of the regulator as previously described. A silicon diode is connected between the positive line and the emitters of the output transistors so that field current flows through it in the forward direction. This is referred to as the back-bias diode. A high-resistance back-bias bleed resistor is connected from the negative side of the diode to the negative line. The purpose of this combination is to prevent excessive leakage through the output transistors when they are in the "off" condition. The driver transistor is not a perfect short circuit in the "on" condition and would tend to allow a small amount of base current to flow in the output transistors, which would in turn allow a high leakage current to flow through the field. The drop across the driver transistor is approximately 0.7 volt in magnitude. By bleeding a small amount of current through the back-bias diode to develop its threshold voltage of approximately 0.5 volt, the voltage relationship at the output transistors is established with the bases being slightly more positive than the emitters. This biases the emitter junctions in the reverse direction and prevents any base current from flowing, thereby reducing the leakage current to a very low value. A nonlinear forward characteristic of the back-bias diode is used in place of a linear characteristic of a resistor to avoid dissipating a large amount of power in the regulator and reducing the power available for excitation of the field.

The feedback resistor is a low-value resistor which will have a voltage drop of approximately 0.1 volt across it when full field current is flowing. Its function is to cause the switching action of the regulator to occur very rapidly so that the output transistors are either in the full "on" or "full off" condition. It accomplishes this by subtracting a small increment of voltage from the voltage reference diode when the field current is turned on and adding a small increment of voltage to the voltage

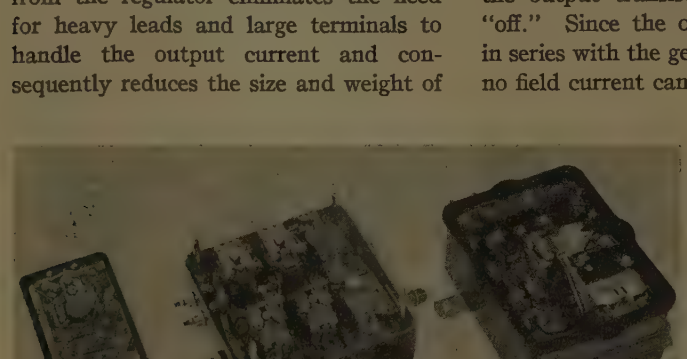

(A) (B) (C)

Fig. 6. Regulators used on motor coaches

A—Transistor voltage regulator
B—Split field voltage and current regulator with cutout relay
C—Carbon pile voltage regulator with cutout relay

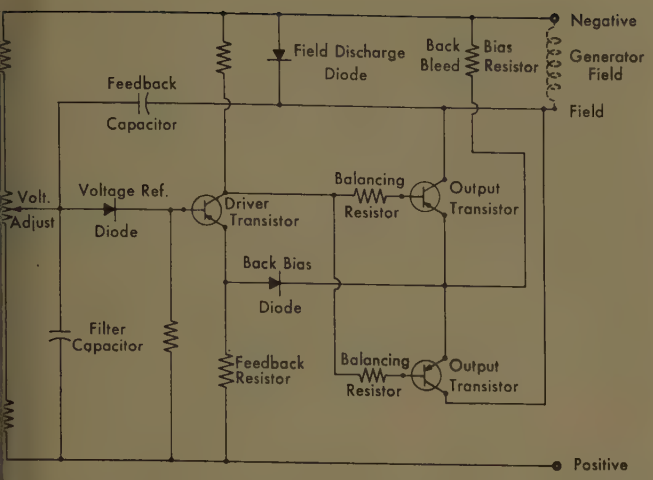

7. Schematic circuit diagram of the transistor voltage regulator

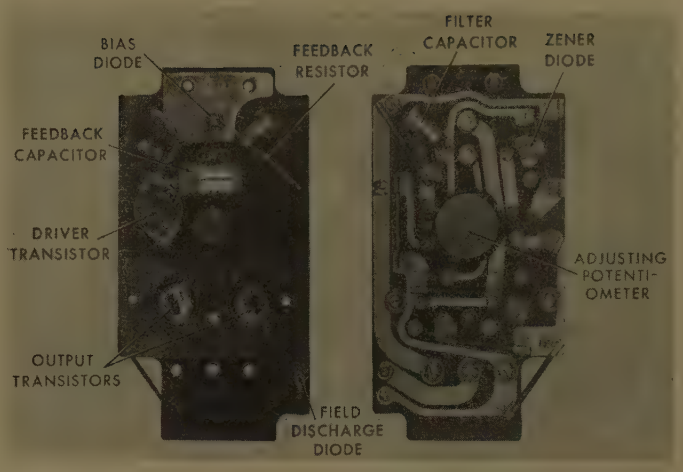

Fig. 8. View of both sides of the printed circuit board assembly from the transistor voltage regulator

ice diode when the field current is ned off. This mode of operation is essary so that the output transistors go rapidly through the "partially condition, which is the condition of ximum heat dissipation. If the transis- were to operate by modulating the d current rather than by switching it, er the heat sinks provided would have be of an excessively large size or the rent rating of the unit would have to be ced drastically. The feedback ca- itor aids in securing this sharp switch- action by transferring a voltage e from the output circuit back to the age sensing circuit.

The field-discharge diode is connected hat it is in parallel with the generator d coil. When the generator field is ned off suddenly, a high voltage will induced in the field winding if no h is provided to dissipate the energy ed in the magnetic field. This high age would puncture the output nsistors. The field discharge diode vides a low impedance path through ch the field current can circulate to harge the stored energy but does not ipate any power when the field cur- is on since its leakage current is e small. The time constant of the d winding with this low external stance in series is high enough that regulator does not switch in an ex- nely rapid manner as would be the if a discharge resistor were used. e the absence of light flicker in the h is obtained with this regulator by very small value of voltage excursion er than by a high rate of switching, low switching rate is desirable to t the transistor heating.

he filter capacitor in the voltage- ing network has the function of ting the ripple which appears at the age reference diode. The action of the regulator is so fast that it would be actuated by each ripple peak on the voltage and would regulate at the peak value of the ripple instead of at the average value. This is not desirable since the magnitude of the ripple changes with load and frequency so that controlling the ripple peaks would result in variations of the average voltage of the system. In automotive application, there is nearly always a battery on the system which acts as an excellent ripple filter, and thus, aids this filter capacitor in performing its function.

The switching action of the regulator is illustrated by the oscillograms of field voltage, field current, and terminal voltage in Fig. 9. It is readily apparent how the relative time duration of the "on" and "off" periods varies with the load on the system. Because of this action, the regulator is referred to as being of the pulse time controlled type. The temperature characteristics of the voltage reference diode and of the driver transistor are approximately equal and opposite so that the regulated voltage does not vary appreciably with changes in ambient temperature. This is a desirable characteristic for a coach regulator. Because the regulator is mounted at a considerable distance from the battery, its temperature does not reflect battery temperature, for which many automotive regulators are compensated.

The ripple which appears on the field voltage and terminal voltage waves is 60 cycles, picked up by the oscillograph. When this ripple is eliminated, the terminal voltage excursions during switching are found to be about ± 0.1 volt and the variation in the average voltage with changes in load and generator speed does not exceed 0.4 volt over a temperature range of -20 F to $+160$ F. This represents much better voltage regulation than has been available on any automotive-type equipment in the past.

Coach Circuit

The generator and regulator described are markedly different from those which have been used in the past and consequently the application of these units to the coach brings up some problems that have not existed previously.

A d-c generator and a cutout relay are normally applied with the shunt field connected to the generator side of the cutout relay. When the engine is started, the generator builds up enough voltage to close the cutout relay and begins to supply current to the system. When the

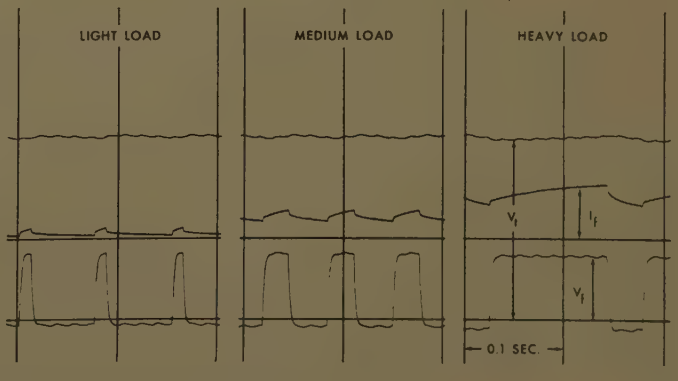

Fig. 9. Oscillograms of field voltage V_f, field current I_f, and terminal voltage V_t of oil-cooled generator with transistor regulator in operation

engine is stopped, current from the battery will flow in a reverse direction through the cutout relay to drive the generator as a motor. This reverse current is used to open the relay and disconnect the generator from the system. With the a-c generator and the silicon rectifier, however, a cutout relay is not used. Since the field must be connected on the d-c side of the rectifier, there is nothing to prevent the battery from furnishing field current even when the engine is not in operation. In order to prevent discharge of the batteries by this field current, a field relay must be provided which disconnects the field from the battery when the engine is shut down. This relay is normally actuated from the ignition switch of a gasoline engine or from the "run" switch of the diesel engine.

The voltage appearing across the cutout relay contacts is frequently used to operate various interlock circuits on the coach, in as much as no voltage can appear at that point when the engine is operating and the generating system is normal because the contacts will be closed. In order that interlock circuits can be actuated, one a-c terminal is brought out of the oil-cooled generator and a relay coil is connected between this terminal and ground. Thus, the relay coil is connected across one of the silicon diodes so that the pulsating reverse voltage appearing across the diode actuates the relay coil when the generator is in operation. When the engine is not in operation, the diodes in the opposite arm of the bridge block the battery voltage so that the relay coil is not energized. This relay in turn operates the interlock circuits through normally open or normally closed contacts as desired. This connection was tried previously with selenium rectifiers and was unsuccessful because the high leakage of the selenium cells would sometimes allow the relay to remain actuated even though the engine was shut down, but the very low leakage of the silicon cells makes this system practical.

Conclusions

The electric system described has been developed primarily for operation on motor coaches, but there are many other types of heavy-duty applications where high electric output and long life without maintenance are required. It is felt that this environment free generator and regulator combination will find application on marine engines, power shovels, and military equipment. The advantage of a generator having no wearing parts other than the continuously lubricated ball bearings and the advantage of a regulator which has no moving parts to wear out or change adjustment have been recognized by all operating personnel having contact with this system. Its reception has been gratifying.

Experimental units have been on test since December 1956 and limited production has been under way since February 1958. The results of these operating units indicate that this approach is basically sound.

Multiple-Unit Operation of Diesel and Electric Locomotives on the Milwaukee Road

LAURENCE WYLIE
FELLOW AIEE

THE USE of a diesel-electric locomotive booster unit in conjunction with one or more straight electric locomotive units was conceived to meet specific requirements of heavy freight train operation on the electrified Rocky Mountain Division of the Milwaukee Road; see track profile, Fig. 1.

Nature of the Problem

Prior to the use of the diesel booster, fast-time freight trains were handled on the Rocky Mountain Division by road locomotives, comprised of two units of the *EF-4* class, which are modern 3,300-volt d-c locomotives with continuous unit rating of 5,110 horsepower, 78,300 lb (pounds) tractive effort, and speed of 25.2 mph (miles per hour). Due to speed–tractive effort characteristics of the original electric freight units, they are not suitable for this service and, even if they were suitable, they could not be operated with more than four units in multiple and could not be operated in conjunction with the modern *EF-4* units due to the differences in control system and speed characteristics.

The problem under discussion is that of synchronizing the operation of one or more diesel-electric units equipped with multiple-unit engine-load-regulator type of control with one or more 3,300-volt d-c electric locomotives equipped with type *P* multiple-unit control, and to have all coupled units respond to the movement of a main controller in the operating cab of an electric unit.

Six years prior to the use of the diesel booster, eastward freight trains with 5,800 tons trailing were handled from Avery, Idaho, to Deer Lodge, Mont., a distance of 211 miles, by road locomotives consisting of two *EF-4* units coupled a the road locomotive. A helper locomotive, consisting of four *EF-1* units was and still is, used on the 1.7% grade between Avery, Idaho, and Haugan, Mont a distance of 38 miles, and over the Continental Divide between Butte Yard and Piedmont, on 1.6 and 2.0% grades, distance of 36 miles. Prior to the use the diesel booster unit, it was necessary to reduce a train of 5,800 tons to a train 4,800 tons at Deer Lodge in order t eliminate the use of a helper locomotive on the long 1.0% grade between Lombard and Loweth, a distance of 48 miles. Th use of the diesel booster eliminated necessity for train reduction at Deer Lodge an improved the running time, even with 5,800 tons, between Deer Lodge an Harlowton.

Due to the demand for increased speed of westward time freight trains with 3,600 tons trailing, it was necessary to increase the tractive effort and horsepower of the road locomotives used on these trains to such an extent that a speed

Paper 59-492, recommended by the AIEE Land Transportation Committee and approved by the AIEE Technical Operations Department for presentation at the AIEE-ASME Railroad Conference, Chicago, Ill., April 7–9, 1959, and presented at the Summer and Pacific General Meeting and Air Transportation Conference, Seattle, Wash., June 21–26, 1959. Manuscript submitted December 15, 1958; made available for printing January 30, 1959.

LAURENCE WYLIE is a Consulting Electrical Engineer, Seattle, Wash.

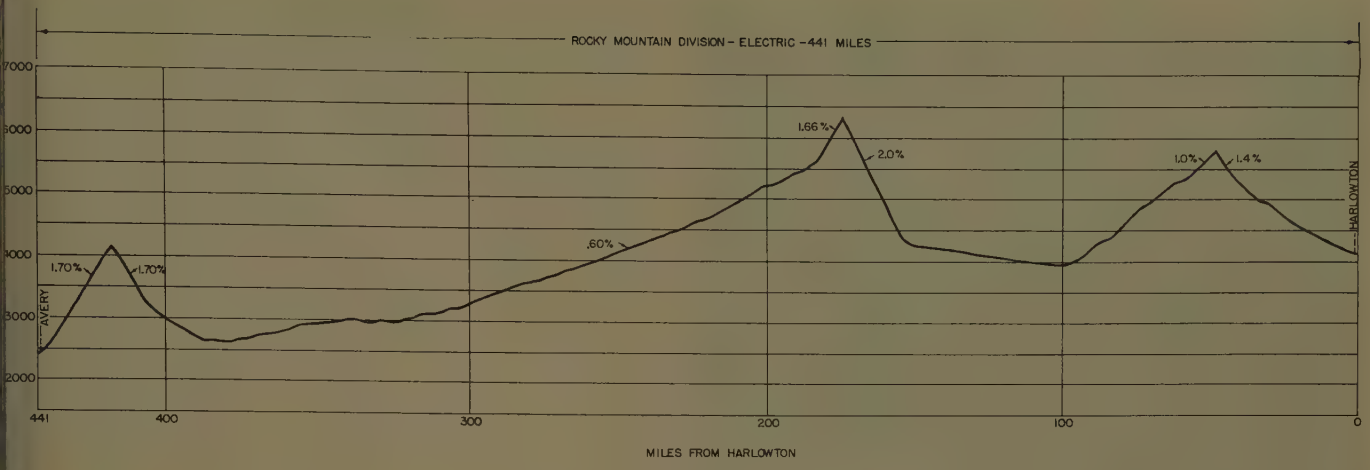

Fig. 1. Profile of Rocky Mountain Division

proximately 25 mph could be made ile ascending the 2.0% grade between dmont and Donald, a distance of 21 les, without the use of a helper loco- tive, and with consequent increase in in speed at other locations where track ndition and curvature would permit. As the principal advantage of the use of e diesel booster occurs between Deer dge and Harlowton, with either east- rd or westward trains, the booster unit occasionally operated only between se two points.

uipment for Control of Booster Unit

The control of the diesel booster unit is complished in the following manner:

A standard 27-wire control cable is talled in each unit of the electric loco- tive and control circuit completed be- en the two electric units and the diesel it by means of standard diesel receptacles d jumper cables.

A miniature diesel controller (hereafter erred to as the diesel synchronizing, or S controller) is mounted on the forward e of each main controller in the operating, uncoupled, ends of the electric units. ese miniature controllers are connected by a rack and pinion to the main controller handle of the electric units in such manner that movement of the electric controller handle will rotate the drum of the DS controller in proper sequence.

3. Microswitches, to control the operation of the reverser on the diesel unit, are mounted inside the case of the main controller on the electric locomotive.

4. A miniature diesel meter and switch panel is installed at the right side of the electric locomotive meter panel. This diesel panel contains the following equipment:

Ammeter, indicating diesel traction motor current.

Switches for control of equipment in diesel unit as follows:

Control and fuel pump
Engine run and controller
Generator field
Headlight
Sanders
Engine stop button
Alarm bell
Wheel slip light

DS Controller Mounting and Mechanical Connection to Main Electric Controller

The DS controller is mounted on a heavy sheet iron bracket which is secured firmly to the main electric controller case by heavy cap screws at the forward end of the controller braking segment; see Fig 2. A composite view of the main electric controller, diesel controller, and meter panels, is shown in Fig. 3.

Rotation for positioning of the DS controller cam shaft is accomplished by means of a gear rack connected to the main electric controller handle by means of a heavy "*Z*" bar bolted to the controller handle and a roller bearing rod end on the rack bar. This rack bar is held in mesh with the small gear on the diesel controller by a spring-mounted roller bearing on top of the diesel controller case. The back of the rack bar is milled to a predetermined profile which is governed by movement of the electric controller handle and eccentric mounting of the gear on the DS controller. The eccentric mounting of the gear and the irregular movement of the rack bar combine to rotate the shaft of the diesel controller through 222 degrees with a corresponding movement of only 42 degrees of the electric controller handle while moving from *OFF* to the 16th notch, or series parallel position, and through only 108 degrees while the electric controller is moved from the 16th

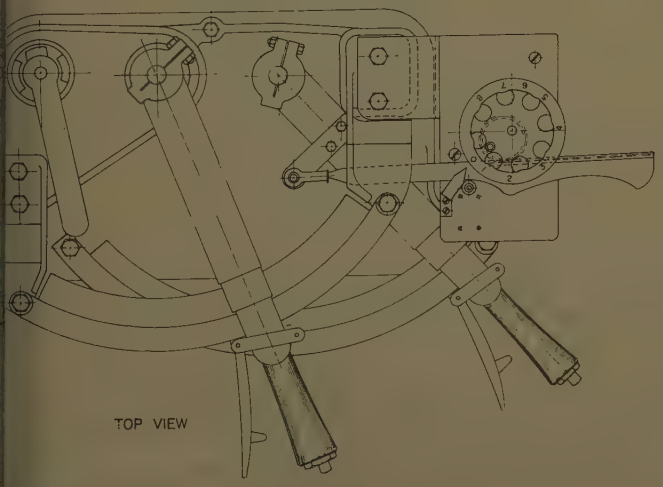

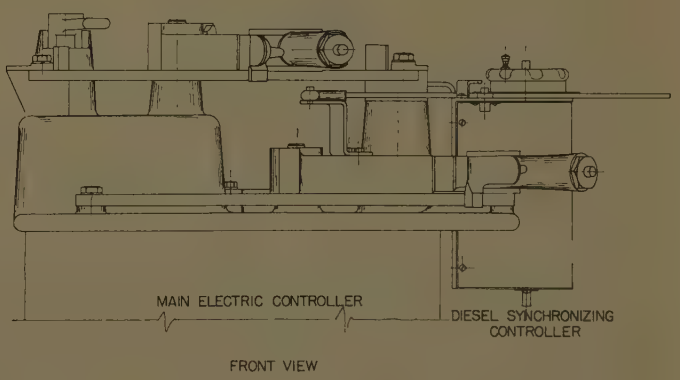

Fig. 2. Main electric and DS controllers

Fig. 3. Meter and switch panel of main and diesel controller

notch to the 37th notch, or an additional 45 degrees, to the full parallel position.

Description of DS Controller

A front and side view drawing of the DS controller, with cover removed, is shown in Fig. 4. The controller consists of a welded-sheet-metal box 6 inches wide, 5 inches deep, and 8 inches high, containing a roller-bearing-mounted shaft on which is mounted six Dilecto fiber disks 1/4 inch thick and $3^1/_2$ inches in diameter. Five of these disks are cam-cut to control the operation of microswitches mounted on a removable rack, and the sixth disk serves as a stop and positioning device to prevent undesired rotation of the cam shaft.

On the protruding upper end of the cam shaft are mounted a small spur toot gear, which is mounted off-center, and heavy Dilecto fiber handle for manu operation of the switch in case of necessit or emergency. This handle is fastene securely to the cam shaft and is fitted wit a manual control locking pin, by means which the spur gear can be locked to tl manual handle and shaft for automat operation of the DS controller by mov ment of the handle of the electric loc motive controller handle.

The bottom of the DS controller ca is fitted with a 6-point receptacle f ease in connecting and disconnecting t 6-wire cable containing the diesel gove nor control wires.

Electrical Characteristics of Diesel Control Circuits and DS Controller

A schematic diagram of the dies synchronizing control circuits is sho in Fig. 5. Control current for operati of the diesel unit is supplied by the ba tery on the diesel unit. The microswit in the circuit controlling the diesel ge erator field contactor must rupture current of 0.80 ampere and, for t

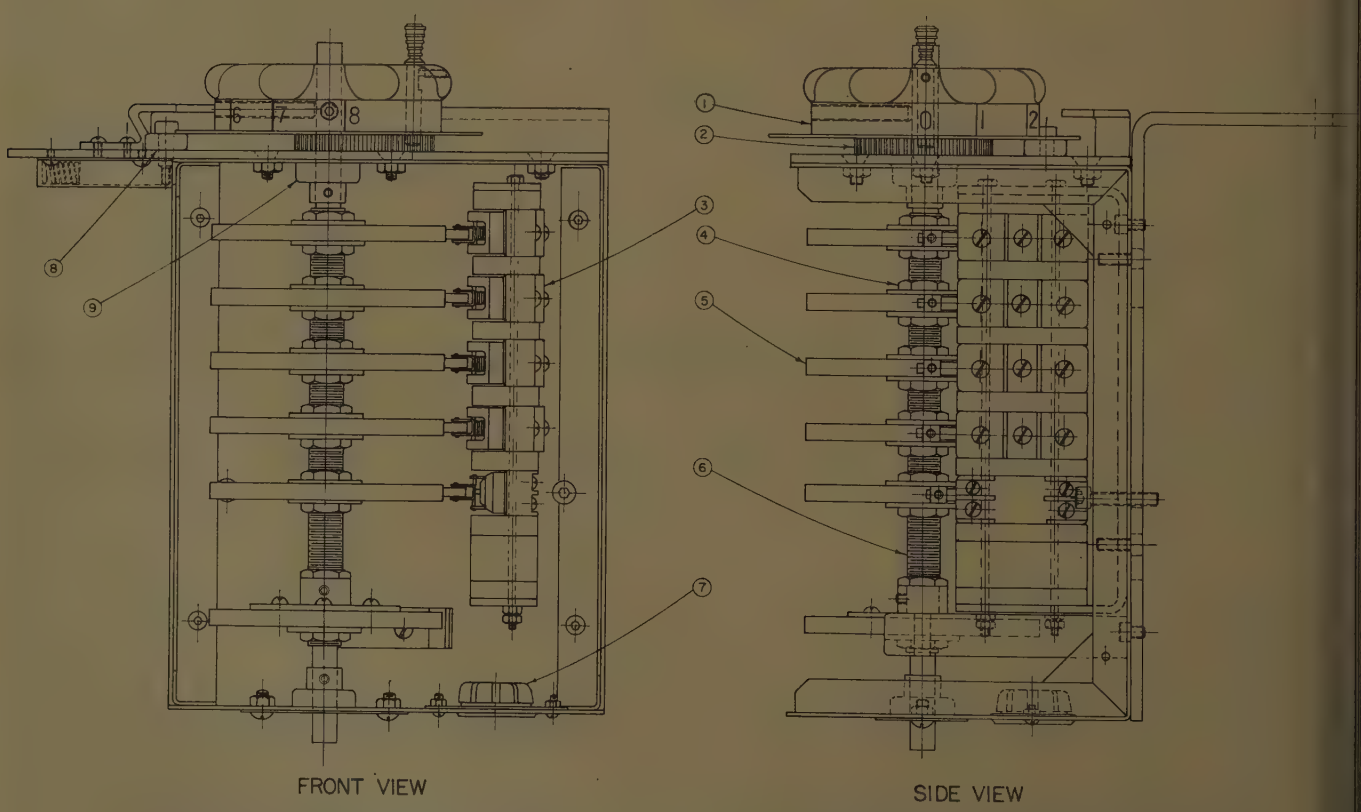

Fig. 4. Drawing of DS controller illustrating the various parts as given below, with the number of each required

1—Manual control knob (1)
2—Spur gear (1)
3—Microswitch (5)
4—Nut and washer for cam adjustment (12)
5—Linen base Dilecto cam 1/4x$3^1/_2$ O. D. (6).
6—Cam shaft ((1)
7—Amphenol socket (1)
8—Bearing (1)
9—Cam shaft bearing (2)

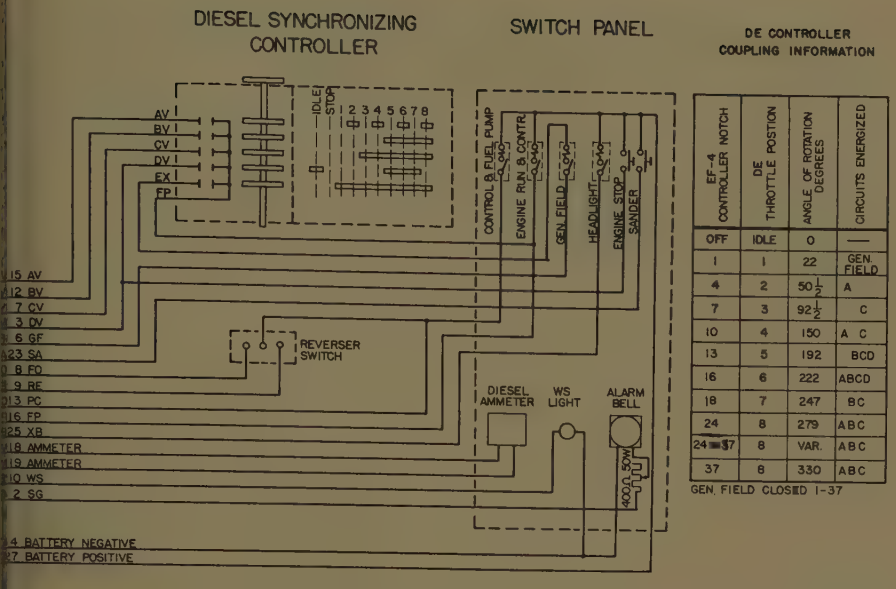

Fig. 5. Schematic diagram of DS control circuits

ason, this switch is provided with a agnetic blowout. The other four icroswitches each carry a current of ly 0.10 ampere and so do not require agnetic blowout protection. All micro-vitches have roller bearings on the oper-ing lever. The outer ends of the operat-g levers require a movement of less an 1/8 inch, and the cams are cut ac-rdingly to a depth of 1/8 inch.

The DS controller is designed to super-de the functions of the controller in e diesel unit when the diesel unit is ing used as a booster with one or more ectric units. The load on the diesel it is regulated by energizing a single il, or various combinations of coils, in e load governor on the diesel unit. In der to avoid overloading the traction otors and wheel slipping on the diesel it, the Run 8 throttle position is not ached until the electric controller ndle has been advanced to the 18th tch, or just beyond the series parallel sition, and corresponding to a speed approximately 15 mph, or well above e point where wheel slipping might rmally occur on the diesel unit. The esel unit then continues to operate in un 8 throttle position at all speeds above 5 mph, or until the diesel unit is cut out, anged to manual control, or the elec-ic controller handle is retarded below e 18th notch.

In starting a heavy train on a grade, or r other reasons, the DS controller can disconnected mechanically from the ectric controller and set manually in y desired position and will remain in at position regardless of the movement the electric controller handle. The erating mechanism of the DS controller can manually be locked to the electric controller mechanism at the will of the operator, and can only be so locked in the proper position.

Regeneration and Dynamic Braking

Extra wires are provided in the 27-wire control cable to provide for control of dynamic braking on the diesel unit if this should be necessary or advisable. At the present time, dynamic braking is not used on the diesel booster unit as the electric road and helper locomotives have sufficient capacity to handle the train while descending the heavy mountain grades and, in this way, secure credit for the electric energy which is returned to the power supply system or absorbed by trains in the vicinity which are using power.

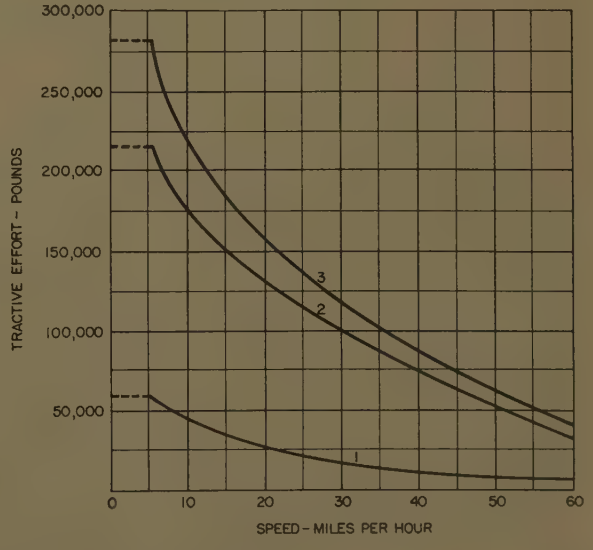

Fig. 6. Speed–tractive effort characteristics of diesel and electric units

1—One EMD 1,750-horsepower diesel unit
2—Two EF-4 electric units
3—One diesel unit and two EF-4 electric units

Preparation and Operation of Multiple-Unit Diesel and Electric Locomotive

The diesel locomotive should be coupled to the back end of a type *EF-4* electric locomotive after which the procedure should be as follows:

Air

Couple brake pipe and signal line hoses and open hose cocks. Couple equalizing pipe hose on diesel to independent application pipe hose on electric locomotive and open hose cocks. Do not couple main reservoir equalizing pipe hose or sanding pipe hose. Condition brake equipment on diesel for "trailing" movement.

Control Jumpers

Install diesel-type control jumper between diesel and electric locomotive, and also between electric locomotives if two electric locomotives are used.

Control Transfer

Proceed as follows:

In electric locomotive operating cab, on diesel control panel in cowl in front of of engineer, close the following switches:

1. Control and fuel pump.
2. Engine run.

In diesel locomotive operating cab, on engineer's panel, open all switches except automatic sander. In diesel control cabinet, all switches must be in ON position and isolation switch in RUN. Headlight controller switch, located below window in front of engineer, must be placed in 9 o'clock position, marked "Controlled from another unit coupled at either end." Control of diesel locomotive is now transferred to operating cab of electric locomotive.

Cutting in Diesel Locomotive

Close engine run and generator field switches, located in diesel control panel in cowl in front of engineer in electric locomotive operating cab. Diesel locomotive will then follow the operation of the electric locomotive controller and provide tractive effort according to position of the controller.

Cutting out Diesel Locomotive

Open engine run and generator field switches, located in diesel control panel in cowl in front of engineer in electric locomotive operating cab.

Normal Operation: Motoring

Throw the reverser on *EF-4* controller for desired direction of movement and then advance the controller handle in the usual manner, allowing sufficient time for slack action in the train and for throttle governor control in the diesel unit. The diesel throttle controller will follow the movement of the *EF-4* controller so that the diesel locomotive will be in no. 8 throttle, or full run position, when the *EF-4* controller is partially out. During further advance of the *EF-4* controller, the diesel locomotive continues in no. 8 throttle position. Any running position on the *EF-4* controller is a running position on the diesel locomotive.

If the diesel locomotive begins slipping for any reason, it will automatically sand and ultimately unload itself. Before this condition develops, action should be taken to correct by partially unloading the diesel locomotive.

Regeneration

Before commencing regeneration, the *EF-4* controller handle must be moved to the OFF position and engine run and generator field switches on diesel panel in the *EF-4* cab must be thrown to the OFF position and left in that position until regeneration is discontinued.

General

The diesel booster should only be cut in when there is actual need for additional tractive effort to handle a train on an ascending grade.

When an electric locomotive is used without a diesel booster, the locking pin in top of diesel throttle controller should be raised.

Effect of High Tractive Effort on Draft Gear

Approximate tractive effort–speed curves for one diesel unit, two *EF-4* electric units, and for three units combined, are shown in Fig. 6. Starting tractive effort at 25% coefficient of adhesion for the three units is 277,000 pounds. At 25 mph, the combined output at the rail is 11,500 horsepower.

Mechanical characteristics of couplers applied to locomotives and freight cars are as follows:

1. Older type *E* couplers with *E 50* knuckles, grade *B* steel normalized average 225,000 lb:
   Yield point, 560,000 lb.
   Ultimate strength, 600,000 lb.
   Safe load, 200,000 lb.

2. New type *E* couplers with *E 50* knuckles, normalized and tempered:
   Yield point, 300,000 lb.
   Ultimate strength, 535,000 to 630,000 lb.
   Safe load, 250,000 lb.

3. Type *E* couplers for diesel or electric locomotives with type *E* quenched and tempered high-tensile-strength knuckles:
   Yield point, 700,000 to 750,000 lb.
   Safe load, 350,000 lb.

The use of the two *EF-4* units with the diesel booster has not caused failures of draft gear on locomotives or cars. Ou observations on the performance of thi combination of locomotive units an other locomotives with high tracti effort and horsepower, indicates that t locomotive which can exert a gradu and sustained increase in tractive effo in starting a train is less severe on dra equipment than the undersized locom tive which must start a train by fir bunching the slack to make use of th energy thus stored in the draft ge springs and cushions.

Conclusions

Due to the nature of the profile an the traffic to be handled, the princip advantages of the diesel booster a realized between Deer Lodge and Harlo ton, on both eastward and westwa trains. On this subdivision, the increa in gross ton-miles per train-hour whi can be attributed to the use of the die booster with full-tonnage trains is 13,7 for eastward trains and 25,700 for we ward trains. The more favorable showi on westward trains is due to the fact th on these trains there is a much great percentage in the increase in train to nage, with the prevailing grade descen ing, as compared to ascending for ea ward trains.

The performance of the auxiliary die control equipment has been satisfacto The use of a single diesel booster un with two electric units comprising a ro locomotive for through service, wi helper locomotives on heavy grades required, has improved freight train pe formance by combining the charact istics of the two different types of moti power, and by providing additional tra tive effort where required for heavy gra operation.

Discussion

W. S. H. Hamilton (New York Central Railroad (retired); now Larchmont, N. Y.): I read Mr. Wylie's paper with a great deal of interest, especially in view of our long association. It shows great ingenuity in solving a difficult if somewhat special problem and Mr. Wylie is to be highly commended for the solution at which he arrived. It can well be used as a guide in solving other special problems that arise which are not provided for by the standardized locomotives of today.

In view of the problems which were overcome, it would not surprise me if Mr. Wylie in the near future came up with an arrangement for operating locomotives in two different locations in the train using wireless for control.

As one of the original instructors of enginemen at the time of the electrification of the Milwaukee Road in 1915, I used to know nearly every foot of the right-of-way of the section shown in Fig. 1. The weight of train handled as given in the paper has greatly increased since those days, the original trailing tonnage being 2,500, as I remember it. Also, train speeds have just about doubled, which is to be expected in order to keep up with modern-day progress.

I was glad to note that the freight car couplers have also kept up with progress to a degree that permits concentrating the amount of drawbar pull, that the locomotives described can exert, at the head end of the train. In my day helper locomotives had to be cut into the middle of the tra and even then one had to be careful starting lest some drawbar, or "lung" the trainmen called them, came out by "roots."

Laurence Wylie: Mr. Hamilton's co ments are appreciated greatly, especially view of his long and varied experience w electrical problems associated with railro transportation. It is regretted that m written discussion of this paper was submitted by others.

The matter of remote control of electric diesel locomotives placed at various lo tions throughout long trains is receiv attention by this author, as well as by oth now interested in such proposed operati

Variable-Speed Constant-Frequency Devices: A Survey of the Methods in Use and Proposed

T. B. OWEN
MEMBER AIEE

VER since the advent of a-c systems in aircraft, designers have been creasingly led to consider methods of taining constant frequency from vari-le-speed sources, as the aircraft engine usually at least two to one in speed nge. The first device to obtain con-nt speed from a variable-speed source s under development for many years, d it is only recently that it has been nsidered reliable enough for general e. Fortunately, the timing has been od, since the very large increase in rcraft electrical loads has coincided nost exactly with the availability of is device. Of course, the large increase electrical loads has led to the proposal many devices either to provide con-nt speed to drive a generator, or to tain constant frequency directly from generator driven at a variable speed.

ne Mechanical Differential

Before surveying the methods pro-sed, the mechanical differential will be amined in some detail. It will become parent as this discussion progresses at the differential method outlined is nployed, in one form or another, in ost of the proposed devices. If, for ample, a constant output shaft speed 6,000 rpm is required, and a variable put speed of from 4,000 to 5,000 rpm available, it is clear that some type of riable-ratio gearing must be interposed tween the input and output shafts. ne possible means of doing this is shown Fig. 1, where the speed ratio between e input and output shafts depends on the position of the roller upon the ne. This is a very common method, d is frequently seen in applications such the step pulley on lathes.

Another possibility is that shown in Fig. 2, the planetary gear system. Here, where there are two input shafts, the speed of the output shaft depends upon the direction of rotation and the speed of the two input shafts. The differential shaft may, of course, be turned by any of several methods. One method is to run a variable-displacement hydraulic pump from the input shaft. A fixed displacement hydraulic motor then drives the differential shaft at the speed fixed by the setting of the variable-displacement pump. The output shaft speed will be the sum of the input speeds. On the other hand, if the input shaft speed is above the desired output shaft speed, the motor and pump exchange functions. The output shaft speed is now the difference between the two input shaft speeds. It is important to see here that in the first instance the differential shaft *adds* power as well as rpm, while in the second case, the differential shaft *subtracts* power as well as rpm. An electric generator-motor combination, of course, may be used in lieu of the hydraulic-pump–motor combination.

A third possibility is shown in Fig. 3. Here, the variable-speed input shaft drives a variable-displacement hydraulic pump to which is fixed the body of a fixed-displacement hydraulic motor. The motor output drives the output shaft directly. The output shaft speed is the sum of the input speed and the speed of the motor relative to that of the pump. This is, of course, fixed by the wobble-plate setting of the pump. Again, where the input speed is higher than the output shaft speed, the functions of pump and motor are reversed, and the output shaft speed is the difference between the input speed and the motor-pump speed relative to the input. The hydraulic-pump–motor combination could have been replaced here also by an electric generator-motor combination.

Mathematical Relations

It is now necessary to set up the mathematical relationship which relate the input, output, and differential torques, powers, and speeds. For this, the following nomenclature will be used:

w_i = angular input speed
w_o = angular output speed
w_{dir} = angular component of speed transmitted directly, as that of the input shaft of the planetary gear arrangement of Fig. 2
w_{dif} = angular component of speed transmitted through the differential, as in Fig. 2
T_i, T_o, T_{dir}, T_{dif} apply similarly to torque
P_i, P_o, P_{dir}, P_{dif} apply similarly to power
f_i, f_o, f_{dir}, f_{dif} apply similarly to frequency

From an examination of Fig. 2, the planetary gear arrangement, it is apparent that between the input and output there are two speed-torque combinations that add or subtract to equal the output.

1. An input torque T_{dir} which is transmitted at the input speed, or w_{dir}.

2. A differential torque T_{dif} which is transmitted at the differential speed w_{dif}.

Now neglecting efficiencies, and considering only where the input speed is below the output:

$$w_{dir}+w_{dif}=w_o \quad (1)$$

$$w_{dir}T_{dir}+w_{dif}T_{dif}=w_oT_o \quad (2)$$

$$P_{dir}+P_{dif}=P_o \quad (3)$$

Equation 3 is simply another way of

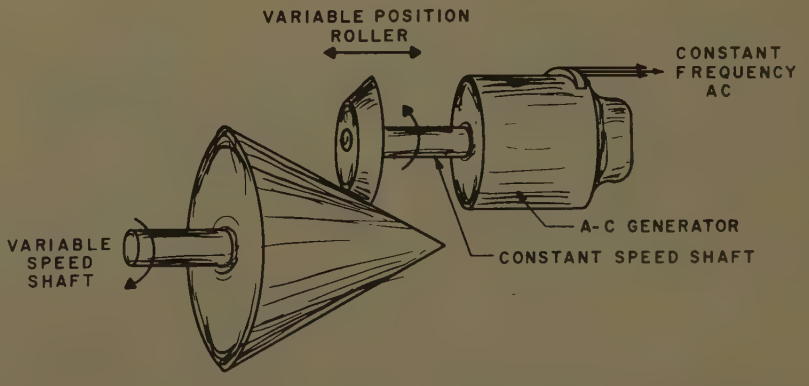

Fig. 1. Variable-ratio gears to provide constant speed from variable speed

per 59-780, recommended by the AIEE Air ansportation Committee and approved by the EE Technical Operations Department for sentation at the AIEE Summer and Pacific neral Meeting and Air Transportation Confer-ce, Seattle, Wash., June 21–26, 1959. Manu-ipt submitted March 16, 1959; made available printing April 10, 1959.

B. OWEN is with the Douglas Aircraft Com-ny, Santa Monica, Calif.

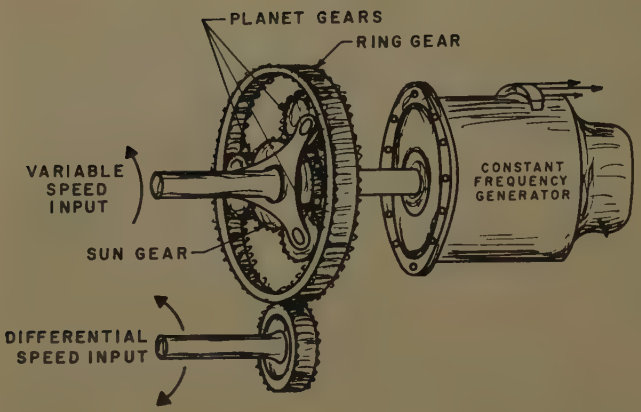

Fig. 2. Planetary gear arrangement for differential speed

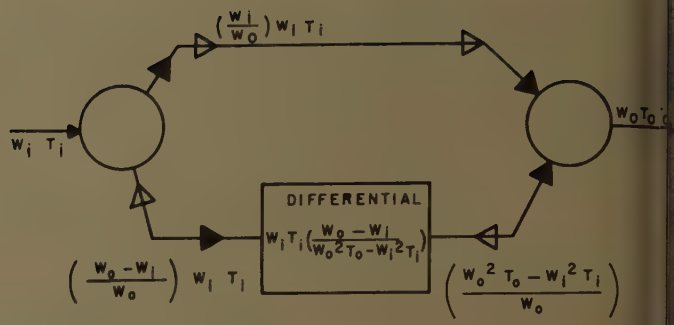

Fig. 4. Schematic diagram of power flow

Black arrow: below synchronous speed
Light arrow: above synchronous speed

stating equation 2, as power is the product of torque and speed.

Further consideration will also show that the direct, differential, and output powers are proportional to the speeds. That is, if $w_{dir}=3{,}000$, $w_{dif}=3{,}000$, and $w_o=6{,}000$, one half the output power is supplied by the differential and one half by the direct path. This relationship may be summarized as follows:

$$w_{dir}:w_{dif}:w_o=P_{dir}:P_{dif}:P_o \qquad (4)$$

Now if the case where the input speed is above the output is considered, the following is obvious:

$$w_{dir}-w_{dif}=w_o \qquad (1A)$$

Then, further consideration will show that the power equation becomes:

$$P_{dir}-P_{dif}=P_o \qquad (2A)$$

That is, both power and speed are subtracted. If the differential speed and power are considered negative where $w_i>w_o$, equations 1 and 2 stand as they are.

To see what the foregoing equations actually mean, consider a case where $w_o=6{,}000$ and $P_o=100$. In one case, let the input $w_i=3{,}000$; in the other, $w_i=9{,}000$. Since $w_i=w_{dir}$, in each case $w_{dif}=3{,}000$. Then, making the proper substitutions in equation 4:

Case I
3,000: 3,000: 6,000 = P_{dir}: P_{dif}: 100
$P_{dir}=50$
$P_{dif}=50$

Case II
9,000: 3,000: 6,000 = P_{dir}: P_{dif}: 100
$P_{dir}=150$
$P_{dif}=50$

The significance of this is that where the input speed is below output speed, the output power is the sum of the direct and differential powers; where the input speed is above the output speed, the output power is the difference between the direct and differential powers. The differential power is thus returned to the shaft. This is why the pump-motor or generator-motor combinations reverse their roles. This must be accomplished or the efficiency would be very low indeed, for otherwise this power is dissipated in the machine.

The two cases illustrated, where the input speed is either below or above the output speed, have been reduced to a single servo-type diagram which is shown in Fig. 4. All quantities are in terms of the input and output speeds and torques and the direct and differential paths are shown and are labeled as such. T direction and quantity of the power fl are shown by the arrows and labels. T quantity in the differential box is the or multiplication factor necessary transform the power in the differen loop to that required.

Classification of Methods of Obtaining Constant Frequency from Variable-Speed Sources

In general, three methods are current in use to obtain constant frequen First, using some mechanical device, c tain a constant speed and drive a co ventional generator. Second, drive t generator at the variable speed and special methods obtain constant-frequen output. Last, use one of the frequen changers. As will be shown, the first tw methods are differential, while the third nondifferential. For the sake of co venience, the following classification presented:

Differential

A. Constant-speed output devices:

1. Differential action by means of variab roller dimensions or by variable roller po tion.

2. Differential action by means of a h draulic-pump–motor combination.

3. Differential action by means of an el tric generator-motor combination.

B. Constant-frequency output devices

1. Differential action by supplying generator field with slip-frequency powe
   (*a*) Exciter-frequency changer.
   (*b*) Exciter-rotary amplifier.

Nondifferential Methods

A. Frequency changers:
1. Rotary motor generators.
2. Static frequency changers.

CONSTANT-SPEED DEVICES

1. The first class listed includes the r chanical speed changers, several of which being actively promoted at this time. Th

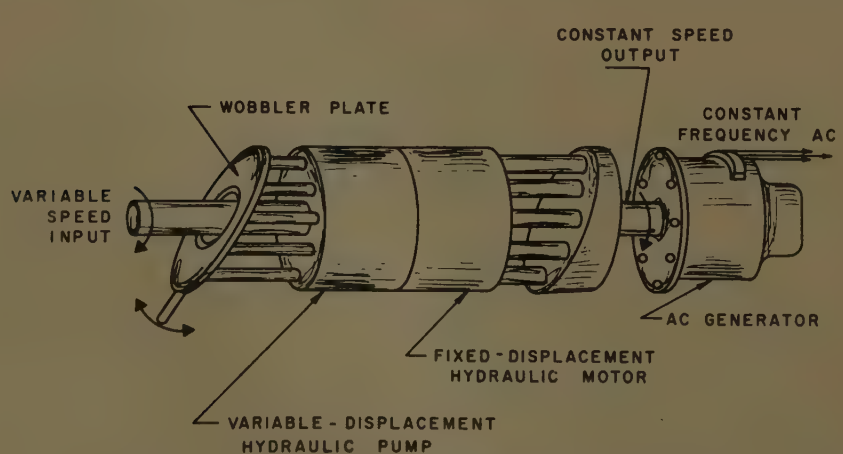

Fig. 3. Hydraulic-motor–pump differential for constant speed

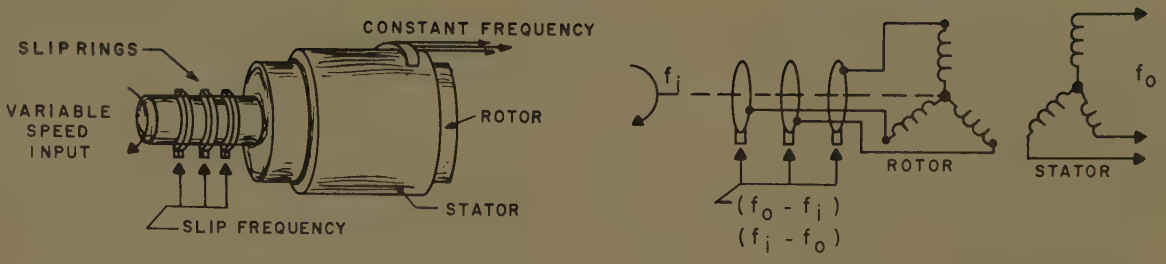

g. 5. Constant quency from iable speed by o-frequency exci- tation of rotor

e adequately represented by the device ctured in Fig. 1.

The second class listed includes the dromechanical devices in rather common e today, and is represented in Figs. 2 and Some devices of this type use piston-type draulic pumps and motors; others use lls, pistons, or a combination of the two.

The main difference in the third type of nstant speed device is the substitution of electric generator-motor combination in ace of the hydraulic-pump–motor com- nation. With this in mind, Figs. 2 and 3 e adequate.

ONSTANT-FREQUENCY DEVICES

In contrast with the constant-speed vices, these devices use no mechanical xiliaries. A variable-speed shaft drives e a-c generator, and constant frequency taken from the generator output. The inciple is illustrated in Fig. 5. Here the put shaft speed is w_i generating the equency f_i. A frequency $(f_o - f_i)$ is fed to the rotor and the output frequency ill be the sum, f_o. By proper choice of e frequency fed into the rotor, the de- ed frequency will appear at the stator tput.

It must be appreciated that exactly the me rules apply here as to the mechanical fferential. Differential power supplied extracted is always proportional to the fferential speed or frequency which is lled the "slip speed" or "slip fre- ency." The servo-type diagram of Fig. is applicable here as in the case of the echanical differential. Neglect of this s led many would-be inventors astray.

The exciter-frequency changer is shown Fig. 6. The exciter and generator tors are on the same shaft. The exciter equency is changed from f_i to $(f_o - f_i)$ by e frequency changer and this is fed to e rotor. The output frequency is $+(f_o - f_i) = f_o$. This applies to the case below synchronism. For above syn- ronism, f_i is changed to $(f_i - f_o)$ and is btracted from f_i, $f_i - (f_i - f_o) = f_o$. The equency changer is not necessarily exter- l to the machine, but may be on the aft.

The exciter-rotary amplifier is shown in g. 7. Here, no frequency changer as ch is employed. The field excitation of e exciter is at the differential frequency that it acts as a rotary amplifier.

NONDIFFERENTIAL METHODS

Frequency changers of various types are well known and need no explanation. Several new approaches which utilize solid-state devices seem to show considerable promise. The scheme is either to rectify the variable-frequency alternating current and then produce alternating current of the desired frequency by some variation of the oscillator–power-amplifier principles, or to generate at much higher frequencies than the final desired frequency and then, by switching accurately, to produce the lower frequency.

Development of Efficiency Equations

The first part of this paper encompassed only physical methods of conversion to a constant frequency. In all of the cases noted, no account was taken of the efficiencies, nor was the problem of obtaining excitation power considered. In this section, the efficiencies will be noted and describing equations developed, but no numerical comparisons will be made. The excitation problem will not be dealt with, except superficially. Further, the losses occasioned by auxiliary devices such as pumps or fans for coolant distribution, and friction and windage losses will be neglected entirely. For practical use, therefore, the expressions developed will have to be modified to take excitation, friction, windage, and auxiliary devices into account. Also, electrical and/or mechanical difficulties that would be encountered in making a device operable will not be considered.

CONSTANT-SPEED DEVICES DRIVING A GENERATOR (FIGS. 1–3)

There are two possible modes of operation, below synchronism and above syn-

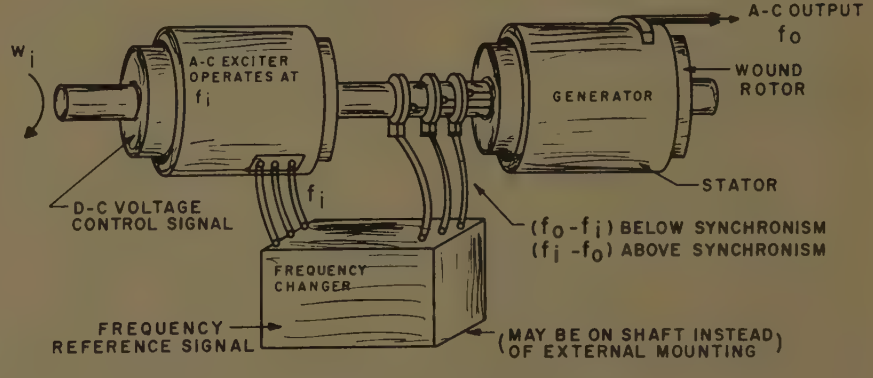

Fig. 6. Differential by frequency changer

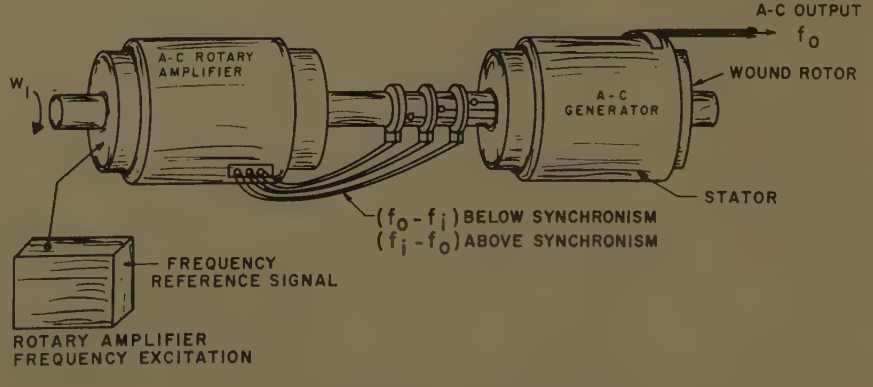

Fig. 7. Differential by rotary amplifier

chronism. For the development of this discussion, the following nomenclature will be used:

K_g = mechanical to electrical efficiency to the generator
K_{dir} = efficiency of transmission of power at shaft rpm
K_{dif} = efficiency of the pump-motor and motor-pump

Input Speed Below Synchronism

If the power out of the drive is P_{do}, the power contributed by the direct and differential portions is as follows:

$$P_{dir} = \frac{w_i}{w_o} P_{do} \tag{5}$$

$$P_{dif} = \frac{(w_o - w_i)}{w_o} P_{do} \tag{6}$$

These two components, with the appropriate efficiencies applied, and with $R = w_i/w_o$, $(1-R) = (w_o - w_i)/w_o$

$$P_{dir}\text{ input} = \frac{RP_{do}}{K_{dir}} \tag{5A}$$

$$P_{dif}\text{ input} = \frac{(1-R)P_{do}}{K_{dif}} \tag{6A}$$

The total drive input is equation 5(A) plus equation 6(A). Then, since the drive output P_{do} is the generator output at the efficiency K_g, the over-all efficiency of this system becomes:

$$\text{Efficiency} = \frac{K_g K_{dir} K_{dif}}{RK_{dif} + (1-R)K_{dir}} \tag{7}$$

Input Speed Above Synchronism

The direct and differential powers are the same as in equations 5 and 6. However, the differential portion of equation 6 is put back into the shaft at the efficiency K_{dif}. Further, since w_i is now greater than w_o, then $(w_i - w_o = (R-1)$ and equation 6(A) becomes:

$$P_{dif}\text{ return} = (R-1)P_{do}K_{dif} \tag{6B}$$

The shaft input is then equation 5(A) minus equation 6(B) with the proper substitution made for P_{do}. The efficiency of the system now becomes:

$$\text{Efficiency} = \frac{K_g K_{dir}}{R + (R-1)K_{dif}K_{dir}} \tag{8}$$

DIFFERENTIAL DEVICES: CONSTANT-FREQUENCY GENERATOR (FIG. 6)

The approach here must be different, as other efficiencies are involved, and the generator is not in series with the constant speed drive. The nomenclature will be

K_g = mechanical to electrical efficiency of the generator
K_{eg} = mechanical to electrical efficiency of the exciter acting as a generator
K_{em} = electrical to mechanical efficiency of the exciter acting as a motor
K_f = conversion efficiency of the frequency converter in either direction
K_t = transformation efficiency of differential power from the rotor to the stator, or vice versa

$w_i/w_o = R$
$\frac{w_o - w_i}{w_i} = (1-R)$ below synchronism
$(R-1)$ above synchronism

Input Speed Below Synchronism

If the output power of the generator is P_o, the power transmitted across the air gap (*ag*) (direct) and from the rotor to the stator by transformer action (*dif*) is as follows:

$$P_{ag} = RP_o \tag{9C}$$

$$P_{dif} = (1-R)P_o \tag{10C}$$

At the efficiencies involved in each path these become:

$$P_{ag}\text{ input} = \frac{RP_o}{K_g} \tag{9A}$$

$$P_{dif}\text{ input} = \frac{(1-R)P_o}{K_t K_f K_{eg}} \tag{10A}$$

The total power input is equation 9(A) plus equation 10(A). Adding, and then taking the efficiency:

$$\text{Efficiency} = \frac{K_g K_t K_f K_{eg}}{RK_t K_f K_{eg} + (1-R)K_g} \tag{11}$$

Input Speed Above Synchronism

In this case the differential power subtracted from the armature, $(R-1)P_o$, is put back into the shaft at the efficiencies K_t, K_f, and K_{em}. Equation 10(A) must now be revised as follows:

$$P_{dif}\text{ return} = (R-1)P_o K_t K_f K_{em} \tag{10B}$$

The shaft power input is now equation 9(A) minus 10(B). Making the subtraction, and finding the efficiency:

$$\text{Efficiency} = \frac{K_g}{R + (R-1)K_t K_f K_{em} K_g} \tag{12}$$

DIFFERENTIAL DEVICES: CONSTANT-FREQUENCY GENERATOR (FIG. 7)

If this figure is examined closely, it will be seen that the circuit is very much the same as that of Fig. 6, with the exception that K_f, the frequency converter efficiency, is not present. Thus, if K_f in equations 11 and 12 is taken as unity

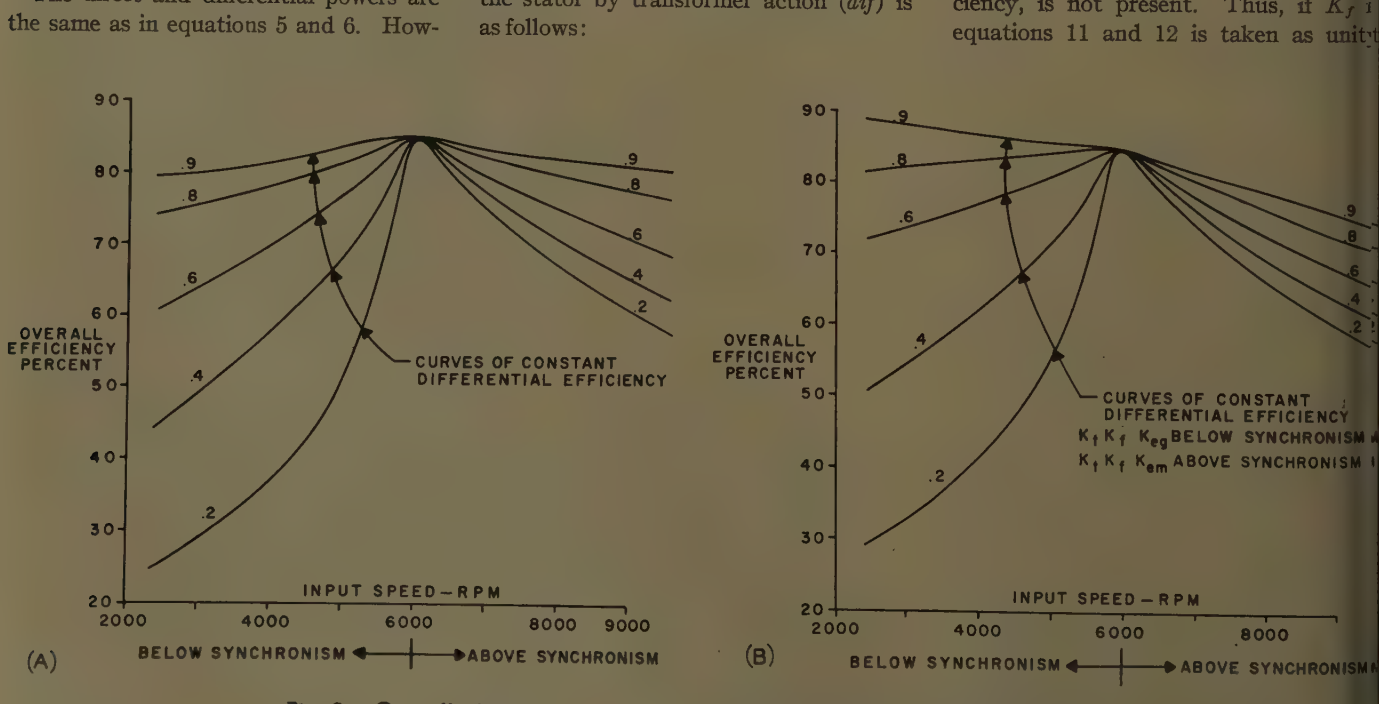

Fig. 8. Over-all efficiency as a function of differential efficiency and input speed

A—Constant-speed device plus generator
B—Variable-speed constant-frequency generator

se equations will serve equally well for case of Fig. 7. (The fact that K_f is present in the equations for this sys- does not necessarily mean that the r-all efficiency will be better. K_{eg} and are different for the two systems, without direct knowledge of the ues in each case, it cannot be said t one would be more efficient than the er on the basis of the equations de- oped.)

iciency Evaluation

With the development of the basic ciency equations, it is now possible to ke an assessment of over-all efficiency a function of input speed, with certain tors being held constant. These con- nts will be defined for each of the two es considered.

NSTANT-SPEED SYSTEM

Here, constant speed is obtained by a chanical device and used to turn the nerator. Typically, the generator may assigned an efficiency of 85%. The ciency K_{dif} may be considered as being ity as it is essentially a gearing effi- ncy, and is quite high in any event. $_{if}$ may be subject to wide variations. th these assumptions, over-all effi- ncy is plotted in Fig. 8(A) as a function input rpm for values of K_{dif} from to 0.9.

NSTANT-FREQUENCY SYSTEM

In this case, no constant-speed device interposed between the variable-speed rce and the generator. Again, genera- efficiency is held at 85% over the ire speed range, although it is probable that there would be some variation both above and below this figure. If one examines equations 11 and 12, it is seen that the efficiencies associated with the differential system occur as a group, and if the differential efficiency is held constant, Fig. 8(B) is the result. Over-all efficiency is plotted as a function of input rpm for values of the "differential efficiency" ($K_tK_fK_{eg}$) and ($K_tK_fK_{em}$) held constant at values from 0.2 to 0.9. Where systems are studied in which K_f does not appear, it may again be treated as being unity, and the curves are still valid.

COMPARATIVE DISCUSSION

The notable fact about Figs. 8(A) and 8(B) is that there is such great similarity. However, no account is taken of the actual efficiencies to be expected in the various systems. Therefore, a very brief note of the probable range of each is given in the following.

K_{dif}. This is probably quite high, in the range of 0.8 or above.

K_{em} *and* K_{eg}. On the usual synchronous machine with a rotary exciter, the exciter efficiency is commonly in the order of 70% or less because the exciter of such a machine must have a high forcing action to supply the needed excitation for load changes, faults, etc., at the speeds necessary in the modern electric system. A high-efficiency machine does not have the reserve capacity necessary to accomplish this function. Since the exciter in the cases presented here is more than an ordinary exciter, in that it supplies power as well as excitation, it is not clear whether its efficiency will be as low as in the case of the d-c exciter. In any event, it certainly cannot exceed the usual generator efficiency of 85%, and is more likely less than 80% efficient.

K_f. Reliable sources have stated that the efficiency of this device will be 90% or above, which seems reasonable.

K_t. This is essentially a high-reactance transformer efficiency since there is an air-gap between the rotor and the stator. It is difficult to see how its efficiency can exceed 80%.

Conclusions

No definite conclusions can be drawn from the preceding development, and none were intended. The intention was merely to point out that all of the proposed "new" systems are basically very similar to the old ones, and a preference for one over the other will mainly depend upon availability and the state of development. Certainly there is nothing here to indicate radical superiority in any case.

The efficiencies cited here may, in fact, not be realizable on a practical system, as other considerations must be entertained. Further, the most efficient system may be such that it cannot be built to operate both above and below the synchronous speed, and though many such disabilities may occur, it is not the function of this paper to point these out.

References

1. THEORY AND CALCULATIONS OF ELECTRICAL APPARATUS (book), **Charles Proteus Steinmetz.** McGraw-Hill Book Company, Inc., New York, N. Y., 1917, chaps. 12 and 13.

2. THEORY AND CALCULATION OF ALTERNATING CURRENT PHENOMENA (book), **Charles Proteus Steinmetz.** McGraw-Hill Book Company, Inc., 1916, chap. 19.

3. THE LIMITATIONS OF INDUCTION GENERATORS IN CONSTANT-FREQUENCY AIRCRAFT SYSTEMS, **E. Erdelyi, E. E. Kolatorowicz, W. R. Miller.** *AIEE Transactions*, pt. II (*Applications and Industry*), vol. 77, Nov. 1958, pp. 348–51.

4. ENERGY-CONVERSION PROPERTIES OF INDUCTION MACHINES IN VARIABLE-SPEED CONSTANT-FREQUENCY GENERATING SYSTEMS, **M. Riaz.** *Ibid.*, vol. 78, Mar. 1959, pp. 25–30.

Discussion

rt V. Hoard (Boeing Airplane Company, ttle, Wash.): The results given in Mr. ven's paper are quite interesting. Fre- ency make-up systems or differential stems, as a class, certainly are not new. e use of low-loss semiconductors with se systems is new and will provide better stems than were previously available in ost every respect. That factor with pect to aircraft electric systems is very irable.

I have some questions and comments ich, I hope, will elicit a clearer definition the limits of application of the paper and usefulness to the industry.

The efficiencies shown in Fig. 8(B) are what percentage load and power fac- on the generator over the speed ranges wn?

Were the exciter efficiencies K_{eg} and K_{em} assumed constant or variable for the curves of Fig. 8(B)? This is a very important factor since, for some systems of this type, the exciter physical size may equal or exceed that of the generator. However, for rated generator load at minimum speed, the exciter voltage output and its required excitation are high, hence there are high losses; while at generator synchronous speed the exciter output and losses may both be low. Reasonably correct efficiency values may be hard to estimate for this important machine over the speed range. For the system indicated in Fig. 7, the statements are made in the paper that, "Here no frequency changer as such is employed. The field excitation of the exciter is at the differential frequency, so that it acts as a rotary amplifier." I cannot agree with this relatively simple conclusion since the exciter rotor or armature is rotating at an equivalent shaft frequency and under some conditions there may be present in the exciter output, the shaft frequency, the excitation or slip frequency, and their sum and difference. Some frequency-changing device is needed to obtain only the amplified slip frequence W_o-W_i for use of the generator rotor.

T. B. Owen: I believe the two questions asked by Mr. Hoard can be answered by one statement. The over-all efficiency curves of both Figs. 8(A) and (B) are based on three simple assumptions:

1. The generator efficiency K_g is 85% for any load put on it, at any input speed. Obviously, this can only be true for a limited area of loads, speeds, and power factors, but any other approach leads to utter confusion.

2. The differential loop efficiencies, K_t, K_f,K_{em}, K_{eg}, are not individually segregated. That is, for a constant differential efficiency curve of 0.9, say, the product $K_t \times K_f \times K_{em}$ or $K_t \times K_f \times K_{eg}$ is 0.9. The in-

dividual efficiencies can be anything, as long as the product is 0.9.

3. No account is taken of excitation. This is a loss which must be factored in, as well as windage, copper, iron, etc.

In order to define the limits of this paper, as requested by Mr. Hoard, I would like to note that all I have done is to present a method of analysis, and to show that all methods come down to the same thing, whether they function hydraulically or electrically. The way the curves of Figs. 8(A) and (B) should be used is to assume some speed range, and from Fig. 8(A), find the over-all efficiency of the constant-speed drive plus generator, assuming that the differential loop efficiency of the pump-motor combination is known. Then, for the same speed range, Fig. 8(B) will give the required differential loop efficiency for the systems of Figs. 6 and 7.

If the efficiency of the latter is appreciably less than that of the former, and shows the possibility of less complication, then it will be worth further investigation. I think that if Mr. Hoard uses my paper in this manner, he will not find very significant differences between the over-all efficiencies between the constant-speed and the constant-frequency systems.

I do not quite understand Mr. Hoard's statement regarding Fig. 7. If he will refer to Fig. 6, he will note that there is a physical, discrete, frequency changer between the exciter and the generator. In Fig. 7, a frequency changer, as such, certainly is not present. Further, any generator may be considered as a rotary amplifier; the output voltage, frequency, and power are functions of shaft speed, load, and field excitation. I believe my statement will stand as written.

I have serious doubts that the development of low-loss semiconductors will do much toward making the "differential" or "frequency make-up" systems practical. This, I will admit, is an unpopular opinion, since almost everybody is going in the oth direction, but if the frequency converter Fig. 6 and the rotary amplifier of Fig. are practical for the applications show they should be even more practical wh used directly as generators. For examp a 60-kva "frequency make-up" system w require at least a 20-kva, and possibly 30-kva, frequency changer, and there a a number of generators of this capacity use today. To my mind, this is a mu more practical application than in the sy tems shown, and would be a major st toward simplifying systems now in use.

My thanks go to Mr. Hoard and to tho who made oral comments on my pap I trust that the paper will be helpful evaluating the problems we have in th area. Also, I am very much indebted Mr. Johnson of Hallamore and Mr. Chi win of Jack & Heintz for valuable disc sions prior to writing this paper. Witho their comments, I could not have prepar it.

Practical Considerations of an Ion Propulsion System

A. E. LENNERT
NONMEMBER AIEE

IT CAN logically be assumed that within 5 years it will be possible to project into orbit a 20,000-lb (pound) vehicle, five times as heavy as the largest satellite now in orbit. This payload capability is a necessary intermediate step in the long-range program leading to manned space flight.

Today's space vehicles cannot maneuver nor, until the recently announced SNAP III device, could they carry on uninterrupted communications for a great length of time. Control and communication then are the main obstacles blocking the way to space travel for other than exploratory and academic purposes.

The ion rocket is a reasonable system which has the inherent growth potential to power a space vehicle on extended journeys. In various forms, it has been the subject of several papers. This paper presents a parameter study of the ion propulsion system in terms of driving a 20,000-lb vehicle into space where the power source stems from the direct conversion of nuclear to electric energy.

Comparison of Space Propulsion Systems

An ion system may be justified mainly by the requirements of future space vehicles, requirements such as extreme reliability, development time cost, power source, specific power generation, specific impulse, payload capability, and many others too numerous to mention. Table I briefly outlines the characteristics of a number of propulsion systems that have been mentioned for use in space flig

The ion system is among those th meet the major requirement for spa propulsion: high I_{sp} and hence low Other systems with this quality prese their own problems (see the Append which compares all the systems on a ba of thrust-to-weight ratio, $T/W=5\times10$ while carrying a payload of appro mately 3,000 lb).

Ion Rocket Description

A conceptual design of a preliminary i rocket system, which can be called a te bed, is shown schematically in Figs. 1 an 2. It functions in this manner. The c sium tank and associated pressurizati and control equipment are in a compar ment between the direct conversion n clear-electric power supply and the d-c d-c inversion-transforming housing. either side of the cesium tank are th sheets of highly reflecting material whi prevent a large temperature rise within t tank and accelerating equipment compar ments. With the aid of proper contro the cesium flows into the ion-forming gion and is sprayed through carefully c

Table I. Principal Propulsion Parameters

	Chemical	Plasma	Solar	Radio-isotope	Photon	Ion
Specific impulse, seconds (I_{sp})	400*	900−2×10⁴	high	high	high	2×10⁴
Thrust to weight, acceleration in g's (T/W)	2†	8×10^{-5}	low	low	extremely low	$10^{-4}\rightarrow5\times10$
Electric power thrust, kw/lb (P_e/T)	25	30→300	zero‡	low	low	286→500

* Considered an upper limit of the chemical system.

† Considered minimum at take-off, increases with altitude in view of the decrease in gravitational fie and atmospheric pressure.

‡ Depends upon the microscopic viewpoint that the sun's energy is being absorbed and then reradiate for which $w_p\neq0$, or macroscopically reflected for which $w=0$.

Paper 59-833, recommended by the AIEE Air Transportation Committee and approved by the AIEE Technical Operations Department for presentation at the AIEE Summer and Pacific General Meeting and Air Transportation Conference, Seattle, Wash., June 21–26, 1959. Manuscript submitted March 20, 1959; made available for printing April 17, 1959.

A. E. LENNERT is with the Martin Company, Baltimore, Md.

The author wishes to express his appreciation to S. Taborsky for his suggestions and circuit design for the d-c to d-c conversion system and to L. D. Hassell for his assistance with the design of the cesium flow system.

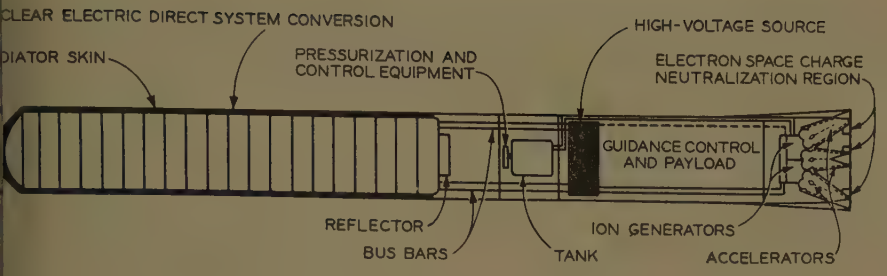

Fig. 1. Ion test bed layout

ned nozzles against a tungsten spray n, see Fig. 2. When an atom of an al-li metal strikes a hot tungsten surface electron is given up by the neutral om and then rebounds in the form of a sitive ion.

If the ionization potential, E_i, of the utral impinging atom is lower than the rk function, $e\phi$, of the material being uck, then there is a certain probability the impinging atom to lose its valence ctron. The ratio of the number of sitive ions, n^+, evaporating from the rface of the tungsten spray pan to the mber of neutral atoms, n, may be deter-ned from the following relationship.[1]

$$n^+/n = e^{\frac{e\phi - E_i}{kT}}$$

ere

=8.5×10⁻⁴ev/K (electron-volts per degree Kelvin)
=degrees K
and $e\phi$ are measured in ev

As a typical example, consider the case cesium being sprayed upon a hot tung-n surface maintained at a temperature 1,200 K. $kT = 0.1$ ev; $e\phi - E_i = 4.52 - 3.87 = 0.65$. Thus, the ratio $n^+/n = e^{6.5}$, or approximately 400, re-lts, which for all practical purposes indi-tes 100% positive ion formation. Ex-rimental data verifying the analytical lution may be found in reference 2. he positive ions thus created are ex-acted from the ion-forming region by eans of suitably designed electrostatic lds which control the drift of positive ns into an accelerator region. There, itable potentials are applied to accelera-e the positive ions to a predetermined locity, yielding the thrust component r which the system is designed.

A separate, but similar, system is re-ired for the removal, focussing, and ac-leration of electrons; however, the ac-lerating voltage in this instance is ex-emely small compared with that re-ired for the positive ions. This is due the difference in masses of the electrons d the positive ions, clearly shown by uation 5. Instead of using a complete stem to accelerate electrons, it is possi-ble to bleed the excess electrons from the tungsten spray pan and, with sufficient potential, boil them off at the same velocity and direction as the positive ion stream thus neutralizing the positive ion space charge. This design feature is necessary in order to overcome the deleterious effect of space caused by the positive ion beam. In addition, it tends to keep the vehicle electrically neutral thereby preventing additional problems due to a highly charged vehicle.

Velocity components of the electrons should be comparable to the positive ion velocities so that the electrons will remain in the close proximity of the positive ions, hence increasing the probability for charge neutralization.

Mathematical Analysis

The equations for analysis of an ion propulsion system are interrelated in graphical form at the end of this section.

The space-charge-limited current density within a constant accelerating field of voltage, E_b, for the case of parallel plate geometry is described by reference 3.

$$j = \frac{i}{S^2} = \frac{\epsilon_0}{2.25}\sqrt{\frac{2eQ}{m_p M}}\,E_b\,\frac{E_b}{d^2}\ \frac{\text{amp}}{m^2} \qquad (1)$$

where

i = ion beam current, amperes (amp)
ϵ_0 = permittivity in free space, meter-kilogram-second system
e = charge on the electron, coulombs
m_p = mass of the proton, kilograms
Q = degree of ionization (in this report singly only)
M = atomic weight of the ion (cesium 132.91)
E_b = accelerating voltage
d = plate spacing, meters
S^2 = area of the plates, meters²

To obtain an expression for electric power P_e that is applied to the ion accelerator, as a function of vehicle thrust (T), it is noted that

$$P_e = E_b i \qquad (2)$$

and from fundamental considerations

$$i = 0.45\dot{w}\,\frac{eQ}{m_p M}\ \text{amp} \qquad (3)$$

where $\dot{w}$ is the propellant flow rate in lb/-sec (second). The thrust is obtained from Newton's second law:

$$T = d/dt\left(\frac{w}{g}v_e\right) = \frac{\dot{w}v_e}{g}\ \text{lb} \qquad (4)$$

In this equation the exhaust velocity of the ions is assumed to be constant, which is quite valid so long as the accelerator plate potential is constant.

g = acceleration due to gravity, meters/sec²
v_e = exhaust velocity of the accelerated ions

Exhaust velocity is described by the following equation:

$$v_e = \sqrt{\frac{2eQ}{m_p M}\,E_b}\ \text{meters/sec} \qquad (5)$$

Combining equations 2–5 gives the power required per unit thrust

$$\frac{P_e}{T} = 30.8\sqrt{\frac{QE_b}{M}}\ \text{kw/lb} \qquad (6)$$

(Equation 6 leads to a conservative estimate of the thrust for given electric power because, in equations 4 and 6, acceleration due to gravity (g) is assumed constant. Actually, in a 2-body problem, it decreases with altitude as $g = g_o(r_o/r)^2$, g_o being the value at the earth's surface, 9.8 meters/sec,² and r_o being the radius of the earth and $r = r + h$ where h is the height above the earth's surface.)

Another useful expression, relating the thrust and the propellant flow rate, from equations 4 and 5

$$T = \frac{1}{g}\sqrt{\frac{2eQ}{m_p M}}\,E_b\,\dot{w}\ \text{lb} \qquad (7)$$

The design of the ion accelerator portion itself requires a knowledge of the voltage gradient, area of the plates, and the thrust demanded by the system.

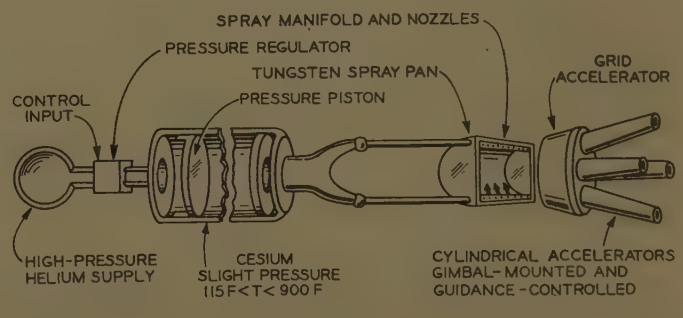

Fig. 2. Cesium system layout

These are obtained from equations 1, 2, 4, and 5 in the form. From equation 8, given a value of the voltage gradient E_b/d in volts/meter, the area of the accelerator plates required for each pound of thrust may be obtained.

$$\frac{S^2}{T} = \frac{6.03 \times 10''}{(E_b/d)^2} \text{ ft}^2 \text{ (square feet)/lb} \qquad (8)$$

Equations 1 through 7 consider the major parameters required for the study of the ion system itself, with no regard for the vehicle trajectory in space. However, such quantities as thrust, T, and over-all weight, W, do influence the vehicle trajectory and are particularly important for any contemplated mission. Indeed, the ratio of thrust to weight is extremely important for this is the g acceleration the vehicle is constantly experiencing, the key factor in determining the time required to complete any mission.

Graphical Interrelationship of Parameters

The ion system parameters just described in equation form are presented graphically in Figs. 3–8. From these curves a conceptual design of the ion vehicle can be projected, based upon the following assumptions:

1. The vehicle is initially in the earth's orbit, projected there by a booster mechanism comparable to the advanced Titan system.

2. Minimum perigee is approximately 300 miles. (This condition is imposed because drag forces are extremely low at this altitude with negligible effect on the applied thrust. Reference 5 reports that a vehicle, with area dimensions somewhat greater than the current design, experienced a drag force of approximately 10^{-5} lb at 300-mile altitude.)

3. Controlled flight time is arbitrarily selected as 500 days.

4. Total vehicle weight (booster payload) is selected as 20,000 lb, apportioned as follows:

(*a*). Direct nuclear-electric reactor and associated control equipment	8,000
(*b*). Electric transformation equipment	2,000
(*c*). Tankage and allied equipment	1,000
(*d*). Ion fuel (based on cesium which imposes the greatest weight penalty)	3,000
(*e*). Accelerator and allied equipment	1,000
(*f*). Structure	1,000
(*g*). Payload (guidance and control equipment, cameras, transmitters, receivers, scientific instruments, etc.)	3,000
Subtotal	19,000
Contingencies	1,000
Total	20,000 lb

5. Power at the bus bar is 400 kw.

Fig. 3 shows the variation of thrust with electric power, using the accelerator plate voltage and the ion propellant as parameters. It is readily seen that for a given power setting thrust varies inversely with plate voltage and directly with the atomic weight of the propellant. It appears, at the outset, that if power is the overriding concern, the accelerator plate voltage should be as low as possible and materials having the greatest atomic weight should be selected.

Fig. 4 is a plot of thrust versus propellant flow rate, with the parameters again being the accelerator plate voltage and the atomic weight of the propellant. If propellant weight is the dictating parameter, then it appears that the propellant should be of the lowest atomic weight.

Fig. 5 indicates thrust versus ion current, with the accelerator plate voltage and the propellant as additional parameters. For a given thrust and plate voltage, it is seen that the ion current varies inversely as the atomic weight of the propellant. For a given plate voltage, the exhaust velocity of the ion beam increases inversely as the square root of the atomic weight of the material as described by equation 5.

Fig. 6 (obtained from equation 3) describes the variation of propellant flow rate with ion current for the two materials being considered, cesium and potassium

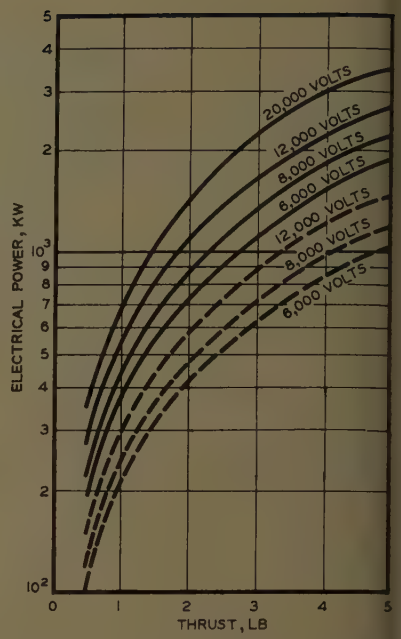

Fig. 3. Electric power versus thrust

----Cesium
——Potassium
Voltage parameter is the accelerator plate voltage

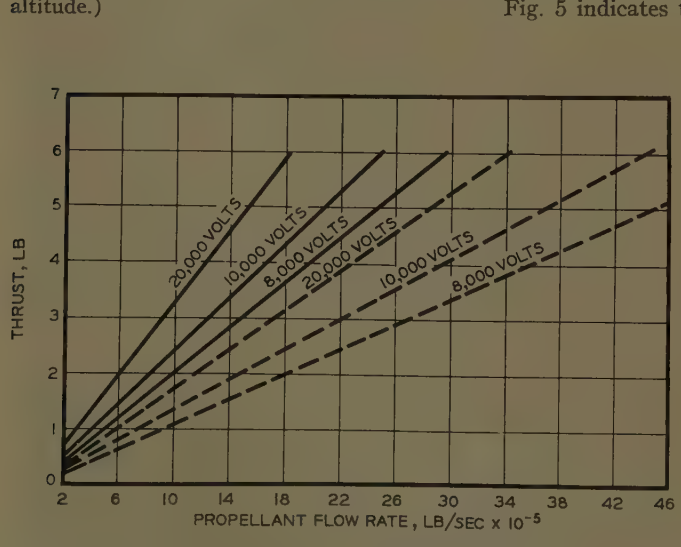

Fig. 4. Thrust versus propellant flow rate

----Cesium
——Potassium
Voltages are the accelerator plate voltage

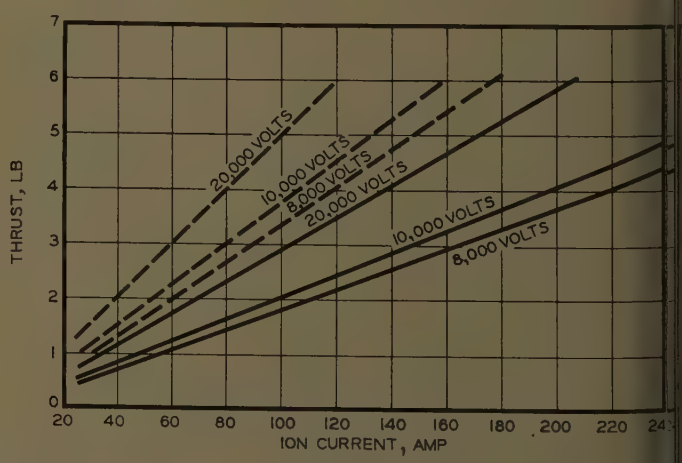

Fig. 5. Thrust versus ion current

----Cesium
——Potassium
Voltages are the accelerator plate voltage

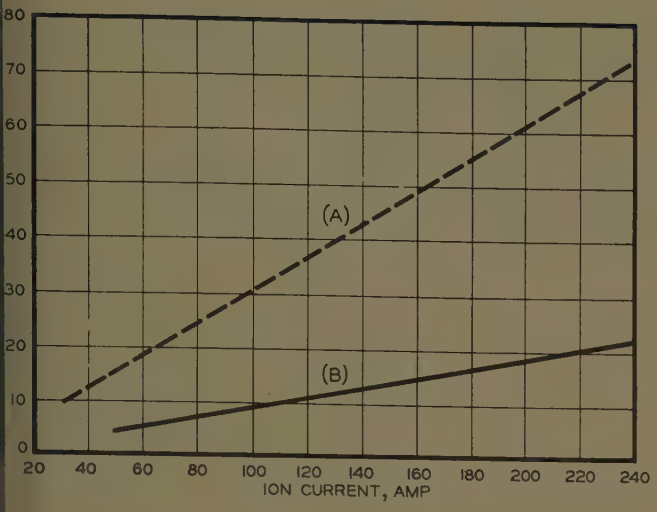

Fig. 6. Propellant flow rate versus ion current

----Cesium
——Potassium

e curves show that the ion current re-red for a given flow rate decreases as atomic weight of the propellant in-ases. Again, if propellant weight is a erion, then the highest weight should sought, consistent with the dictating uirement of producing positive ions ciently.

Fig. 7 summarizes a number of accel-tor characteristics. Plate spacing be-een the accelerator plates is plotted inst accelerator voltage. Parameters the field strength (volts/meter) and surface area required per unit thrust /lb). For a field strength of 10^5 volts/-ter, accelerator spacing is in the order 0 cm (centimeters) for 12,000 volts on accelerator plates. Although this de-n feature is quite practical, the ac-erator surface area required, because rent density is limited by the effects

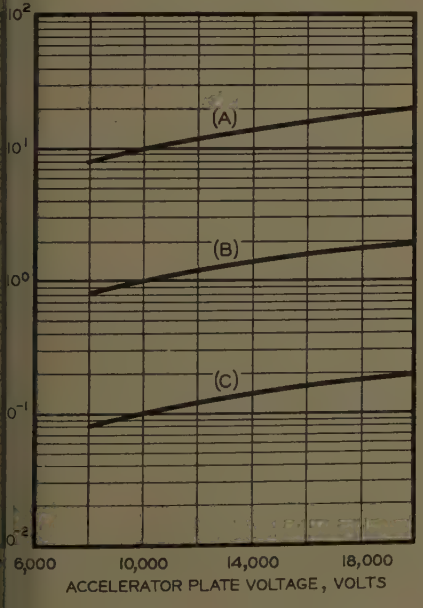

7. Plate spacing versus plate voltage

$E_b/d=10^5$ volts/meter; $S^2/T=603$ ft²/lb
$E_bd=10^6$ volts/meter; $S^2/T=6.03$ ft²/lb
$E_bd=10^7$ volts/meter; $S^2/T=0.06$ ft²/lb

of space charge, is approximately 600 ft²/lb thrust. This is rather an impractical value for the present system design. Increasing the field strength by an order of magnitude to 10^6 volts/meter indicates that the plate spacing would be in the order of 1 cm while the required plate area is reduced by approximately 6 ft²/lb of thrust. As these values are reasonable and practical to attain, they merit further consideration in the system design.

Upon increasing the field strength still further, it is seen that the accelerator plate spacing is in the order of 0.1 cm and the accelerator plate area in the order of 0.06 ft²/lb of thrust. Although the latter value is quite attractive and appears practical, the small plate spacing poses a number of problems. In this region, the field is strong enough to create disturbances within the ion beam. Electrical breakdown may result, thereby destroying the entire accelerator system. Therefore, the field strength should be considered initially in the order of 10^6 volts/-meter with a minimum of 12,000 volts on the accelerator plates. The other values should be adjusted accordingly.

The reason for selecting 12,000 volts as the minimum plate voltage is clearly shown in Fig. 8, a plot of ion beam and accelerator plate currents as a function of accelerator plate voltage. With relatively low voltages applied to the accelerator plates, the plates tend to draw at least an equal, if not greater, amount of current than that of the ion beam. This phenomenon occurs because, when the accelerator voltage is relatively low, a considerable portion of the ion beam current is attracted to the accelerator plates. Fig. 8 indicates that the accelerator current reaches its maximum at 5-kv plate potential and then decreases markedly as voltage is increased. The accelerator beam current becomes asymptotic in the neighborhood of 12 to 14 kv. It is believed this large value for the accelerating potential could be decreased by designing guard rings properly and by cooling the acceleration plates.

Electrical System

The electrical system functions in the following manner. The output from the nuclear reactor is in the form of high-current–low-voltage direct current. By means of properly designed busbars the current flows to the inversion-transforming region. The output from the nuclear power plant is in the order of 500 kw. With approximately 80% over-all efficiency, the power to the accelerator is approximately 400 kw.

The inversion process may be effected with the use of "gated" silicon rectifier cells in a manner similar to the ignitron conversion, with the gate serving as a commutation device used in conjunction with a sequence timer. Conventional silicon cells currently in operation may carry peak currents of 1,000 amp with the gated version available to carry approximately 25 amp. With several years of further developmental effort, larger ratings for this application may be anticipated in a low-duty-cycle arrangement as shown in Fig. 9. Frequency of operation would be limited by the permissible duty cycle.

The voltage drop across the silicon cells is approximately 1 volt with a resultant efficiency of approximately 98% for this application. The rectifier requirement is a half-wave 6-phase circuit with a number of silicon rectifiers in each phase depending upon the ratings of the rectifiers. The over-all efficiency from the reactor output to the bus bars is about 80%.

Conclusions

As in many other types of propulsion, there are a number of unsolved problems

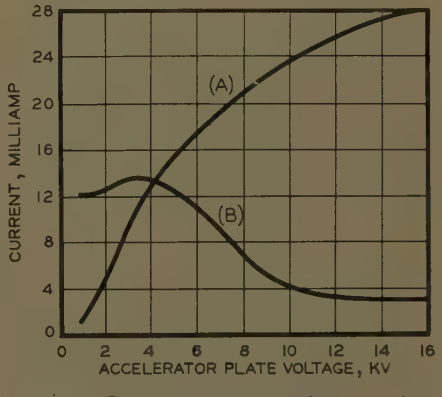

Fig. 8. Current versus accelerator plate voltage

A—Ion beam current
B—Accelerator electrode current

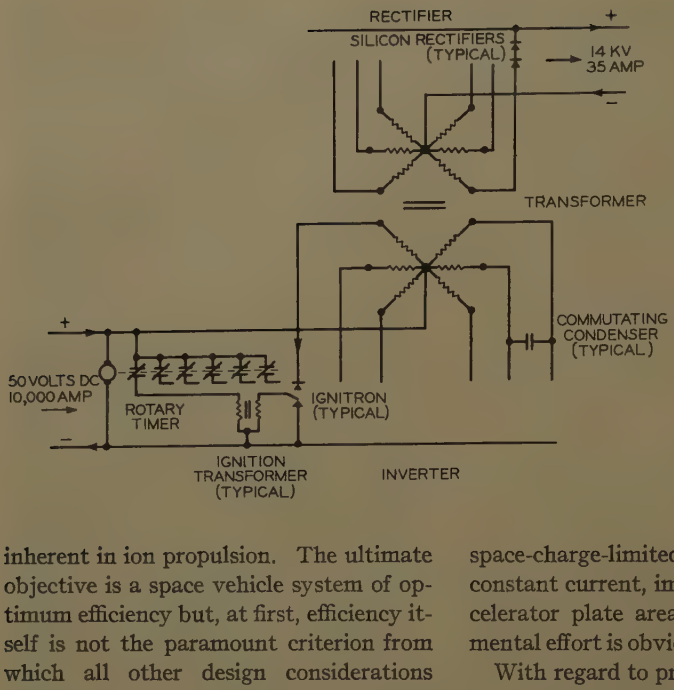

Fig. 9. Ignitron inverter - transformer - rectifier circuit (elementary diagram)

inherent in ion propulsion. The ultimate objective is a space vehicle system of optimum efficiency but, at first, efficiency itself is not the paramount criterion from which all other design considerations must originate. It is of more immediate importance to design, construct, and ground-test an operational vehicle and then optimize the system for the greatest over-all efficiency. This is particularly true of the ion system where a strong interrelationship exists among parameters. Individual parameters might be superficially optimized only to find that the process upsets some other paramerer.

As an example, it is sometimes stated that the greater the plate voltage, the greater the exhaust velocity, and hence the more efficiency the system. That this is not necessarily true can be seen from equations 3, 4, and 5, which indicate that an increase in accelerator plate voltage E_b increases the exhaust velocity v_e of the positive ions. For constant power, an increase in plate voltage E_b corresponds to a decrease in the current i. However, the thrust T depends more strongly upon the current than upon the voltage. In fact, an increase in accelerator voltage E_b actually decreases the thrust under constant power operation.

With these considerations in mind, a number of problems associated with anion propulsion system may be considered under three main categories: (1) ion thrust chambers, (2) propellants, and (3) high specific power generation.

Problems associated with the ion thrust chamber are related to such items as the ion source, electron source (necessary for space charge neutralization), and the ion accelerator system. In each case, although design feasibility may be established by means of the equations, further theoretical and experimental work, in the tens of ampere range, is essential. Increasing the voltage gradients raises the space-charge-limited currents which, for constant current, implies reducing the accelerator plate areas. Detailed experimental effort is obviously in order.

With regard to propellants, the over-all propellant weight for an alkali ion system appears to vary between limits that are not too great, whether cesium or sodium is used. That is, alkali metals have atomic weights between 23 and 133, so that at constant current the propellant flow rate, and hence total propellant weight W_p, may vary by a factor of 6 (equation 3). It may be possible to utilize heavy molecules for the propellant, such as SbI_5 which has a molecular weight of approximately 757, the provision being that it would be possible to remove an electron. This would bring about a new positive charge on the molecule and enhance the system's characteristics. This area merits more detailed effort.

The third category, high specific power generation, also requires considerable experimental effort in building a direct nuclear-electric conversion system as outlined in Fig. 1. At present the fuel loading appears enormous (approximately 20 lb per linear ft of reactor) and the power density is on the order to 35 kw per cubic ft. In addition, further work is needed on semiconductor rectifiers to handle extremely high currents and voltages.

There is no doubt that the problems inherent in the ion system design challenge the engineering mind. However, it is strongly believed that if the requirement for such a system were generated these major problems would be resolved.

Appendix. Comparison of Space Propulsion Systems[6]

Chemical Rocket

Even though the chemical rocket exhibits high thrust and a high thrust to weight ratio, it offers little promise for space propulsion in view of its high propellant consumption characteristics. Its I_{sp} is limited to values below 400 sec.

Photon Rocket

Equations describing the energy and momentum of photons may be written:

$$E = h\nu = \frac{hc}{\lambda} \quad (9$$

$$p = h/\lambda \quad (10$$

where

h = Planck's constant
ν = photon radiation frequency
c = velocity of light 3×10^{10} cm/sec
λ = photon radiation wavelength
p = momentum

Since the thrust

$$T = d/dt(P) \quad (11$$

by combining equations 9–11 the following is obtained:

$$T = d/dt(E/c) = \frac{1}{c}\frac{dE}{dt} \quad (12$$

A photon rocket, depending upon a nuclear reactor for its source of photons, will be assumed to weigh approximately 20,0 lb with a 3,000-lb payload. For T/W 5×10^{-6}, the thrust would be approximately 1 lb. For 1 lb of thrust equals 4.45×1 dynes, the fuel burn-up required per u time is obtained by the use of equation 12

$$\Delta E = \int \frac{dE}{dt}\,dt = \int cT\,dt = cT\Delta T$$
$$= 3\times10^{10}\times4.45\times10^{5}$$
$$= 8.34\times10^{21} \text{ mev/sec} \quad (13$$

Consider the use of fissionable materi (U-235) for the creation of photons an assume that the efficiency of production 10%. The energy that can be supplied

$$E_s = (0.10)200\ \frac{\text{mev}}{\text{fission}} \times 6.02\times10^{23}\ \frac{\text{atoms}}{\text{gm(gram)-atom}} \times \frac{1}{235}\ \frac{\text{gm-atoms}}{\text{gm}} \times$$
$$454\ \frac{\text{gm}}{\text{lb}}$$
$$= 2.33\times10^{25}\ \frac{\text{mev}}{\text{lb U-235}} \quad (1$$

Dividing equation 13 by 14, it is seen tha

$$\frac{8.35\times10^{21} \text{ mev/sec}}{2.33\times10^{25} \text{ mev/lb of U}} = 3.57\times10^{-4}$$
$$\text{lb/sec} = 1.63 \text{ gm/sec} \quad (1$$

For one day of operation approximate 1.41 kilograms of U-235 would be require for burn-up, which would cost approx mately $21,125. This does not take into a count the nonfission absorptions which i creases the fuel investment by approx mately 10%, nor is the normal fuel loadi required for criticality considered. The fu required for burn-up due to all processes f long-term operation is only about 20 of the total fuel investment. Fuel co

ne makes the photon rocket unattractive
v.

lar Rocket

A solar rocket derives its component of
ust from a sail that reflects solar energy
notons). The sail must have considerable
face area in order to reflect a sufficient
ount of energy to give it the desried
ust. The intensity of solar radiation
ut the earth is approximately 1 kw/
ter[2,6] and on reflection from the sail (say,
minum-coated), the intensity is doubled
2 kw/meter². If it is assumed that the
ght of the sail and the structure is ap-
ximately half the vehicle weight, then a
al weight $W=6{,}000$ lb and the sail
ght is approximately 3,000 lb. For the
ust to weight ratio T/W of 5×10^{-5} the
ust is found to be 0.3 lb. Using equation
$dE/dt=4\times10^{5}$ kw, the sail area re-
red for this thrust is

$$\frac{\times10^{5}\text{ kw}}{\text{kw/meter}^2}=2\times10^{5}\text{ meter}^2$$

This is an area, if taken as a square, with
side of approximately 480 yards. Also,
view of its extremely small skin thickness,
solar sail is subject to rupture by pene-
tion of meteorite particles and does not
bear practical for long range space flight,
does it have a promising growth poten-
l for increase in power density.

dioisotope Rocket

Space propulsion may be accomplished
means of a polonium sail[7] which utilizes
natural radioactive decay particles of
isotope Po-210. Po-210 decays by
ha-particle emission, and a sail coated
h a thin layer of the material could pro-
e trouble-free operation. Other alpha-
rticle emitters are also possible, although
-210 seems to strike a good compromise
ween alpha-particle decay energy and
atively long half-life.
Three parameters of interest for this
-210 sail system are (1) dynes thrust/gm
Po-210, (2) areal density (gm/cm²), and
cost. To obtain parameter 1, note that
thrust/gm of Po-210 is

$$\frac{d}{dt}(mv)\doteq v\frac{dm}{dt}=v\frac{dN}{dt}(m_\alpha) \qquad (16)$$

ere

=total mass ejected from rocket
=mass of alpha-particle
velocity of alpha-particle
$/dt$=number of Po-210 atoms disinte-
grating/sec/gm of Po-210 with emis-
sion of an alpha-particle, i.e, number
of alpha-particles/sec/gm of Po-210
-210 emits an alpha-particle of average
rgy $\bar{E}=5.3$ mev, so that

$$v=\sqrt{\frac{2\bar{E}}{m_\alpha}}=\sqrt{\frac{2(5.3)1.602\times10^{-6}}{(4)\,1.66\times10^{-24}}}$$
$$=1.6\times10^{9}\text{ cm/sec} \qquad (17)$$

Recent information from an Atomic Energy Commission representative at Mound Laboratory indicates Po-210 with a source strength of 1.4 micrograms/millicurie may be obtained at a cost of $0.10 per millicurie in large lots. Therefore, for 1 gm of Po-210

$$\frac{dN}{dt}=\frac{1}{1.4\text{ microgram/millicurie}}=(715)\,3.7\times10^{10}\text{ alpha-particles/sec/gm Po-210} \qquad (18)$$

Combining equations 16–18

$$T=1.6\times10^{9}(715)\,3.7\times10^{10}(4)\,1.66\times10^{-24}$$
$$=0.28\text{ dyne/gm Po-210}$$
$$=6.3\times10^{-7}\text{ lb thrust/gm Po-210} \qquad (19)$$

The areal density (gm/cm²) of the Po-210 coating on the sail can be conservatively estimated by choosing a thickness of Po-210 equal to the range of 5.3 mev alpha-particles in polonium itself. Since this range turns out to be about 10^{-3} cm, and the volume density of polonium $\rho=9.4$ gm/cm³, the areal density becomes 9.4×10^{-3} gm/cm².

To determine the third item (cost), it is necessary to know the sail area required. Here again a conservative guess of sail weight equal to half the total vehicle weight implies, for a 3,000-lb payload, a sail of about 3,000 lb, and total vehicle weight of about 6,000 lb. But, with $T/W\sim5\times10^{-5}$ and $W=6{,}000$ lb, $T=0.30$ lb$=1.3\times10^{5}$ dynes. This, coupled with equation 19, indicates that the amount of polonium needed is

$$(1.3\times10^{5}\text{ dynes})/(2.8\times10^{-1}\text{ dynes/gm Po-210})=4.65\times10^{5}\text{ gm Po-210} \qquad (20)$$

From equation 18, 715×10^{3} millicuries/gm Po-210 is the available source strength, which results in a total strength of

$$(4.65\times10^{5}\text{ gm Po-210})(7.15\times10^{5}\text{ millicuries/gm Po-210})=3.32\times10^{11}\text{ millicuries} \qquad (21)$$

At a cost of $0.10 per millicuries this means that the necessary sail would cost about 33 billion dollars, which is, of course, the most significant deterrent to the whole concept.

The actual sail size, which depends on the areal density and the mass of Po-210, is then

$$(4.65\times10^{5}\text{ gm})/(9.4\times10^{-3}\text{ gm/cm}^2)\rightarrow 2{,}420\text{ yards}^2 \qquad (22)$$

An equivalent square would thus have a length of 49.3 yard on each side.

Finally, it must be borne in mind that although the 33.2 billion dollar cost is prohibitive, it is based on a 3,000-lb payload with $T/W\sim5\times10^{-5}$. For smaller payloads, it may well be that the radioisotope sail is more attractive. However, one drawback is the difficulty of both obtaining the needed Po-210 and coating the sail.

Plasma Rocket

W. Bostick states that his plasma gun fires about 10^{-7} gms of plasma per pulse, and that velocities of the order of 10^{7} cm/sec can be obtained for these plasmas. Since Bostick visualizes the need for a primary electric power source for his plasma gun rocket, as, for example a nuclear reactor system, it is reasonable to assume, as for the ion system, a total vehicle weight $W=$ 20,000 lb. Maintaining the T/W ratio at 5×10^{-5} implies a thrust of $T=$[1.0 lb]$=4.45\times10^{5}$ dynes. In general though, $T=(4.45\times10^{5})/10^{7}=4.45\times10^{-2}$ gm/sec. Each gun is capable of 10^{-7} gm plasma/pulse, yielding 0.45×10^{6} pulses/sec, or about 2 microsec/pulse.

If this can be accomplished by one gun, or perhaps several guns operating together, then the plasma system is a promising one.

An inherent advantage of plasma propulsion over ion propulsion is the essentially neutral character of the plasma. That is, while space charge neutralization is necessary for the ion system, no such provision must be made for the plasma system. However one disadvantage lies in the electrode erosion[2] during continuous operation which tends to limit the use of plasma systems.

In conclusion, Bostick indicates that current work on plasma acceleration by so-called rails, etc., may soon allow plasma velocities to become as high as 10^{8} cm/sec. This is a significant advance, at least as regards propulsion possibilities.

References

1. Electronic and Ionic Impact Phenomena, H. S. W. Massey, E. H. C. Burhop. Clarendon Press, Oxford, England; also Oxford University Press, New York, N. Y., 1952.

2. Ionization on Platinum and Tungsten Surfaces, I—The Alkali Metals, Sheldon Datz, E. H. Taylor. *Journal of Chemical Physics* New York, N. Y., vol. 25, no. 3, Sept. 1956.

3. Electronics, J. Millman, S. Seely. McGraw-Hill Book Company, Inc., New York, N. Y., 1941, p. 211.

4. Ion Source for the Production of Multiply Charged Heavy Ions, C. F. Anderson, K. W. Ehlers. *Review of Scientific Instruments*, American Institute of Physics, New York, N. Y., vol. 27, no. 10, Oct. 1956, pp. 809–15.

5. American Physical Society, New York, N. Y. May 1958.

6. Ion Rocket Test Bed, P. E. Grant, A. E. Lennert. *Engineering Report 9963*, Martin Company, Baltimore, Md., June 1958.

7. R. W. Bussard. *Jet Propulsion*, New York, N. Y., vol. 28, 1958, p. 223.

Discussion

W. Stineman (Boeing Airplane Company, Seattle, Wash.): The author's
lation 5 results in an overly optimistic
ue for the exhaust velocity to be ex-
ted from an ion accelerator, because the equation implicitly assumes that all of the electric energy being supplied to the accelerator is converted to ordered kinetic energy of the exhaust stream. This may be a reasonable assumption for a few widely separated ions. However, in the relatively dense ion streams envisaged for propulsion apparatus, interaction between ions will partially disorder the motion of the ions, thus converting some of the energy into heat. Another factor is that an ion cannot fall through the full potential difference between electrodes, E_b, unless it actually strikes the attracting electrode. Ions which are discharged into space can be accelerated by only a fraction of the total voltage. Good

design can make this fraction large, but not unity. In general then, a factor should be included under the radical in equation 5 to represent the efficiency of converting electric energy to ordered kinetic energy. The determination and optimization of this efficiency is one of the problems to be solved.

Exception is taken to the author's contention that equation 6 is conservative. There appears to be a misinterpretation of the meaning of g in equation 4. Equation 4 is simply a statement of Newton's second law of motion. However, with force expressed in pounds, mass in pounds, and velocity in meters per second, a unit conversion factor is required. The fact that this constant unit conversion factor happens to be equal to the sea-level acceleration of gravity is coincidental. Note that the author's reasoning would lead to the untenable conclusion that in interstellar space, where local gravity is virtually zero, an infinite amount of thrust could be attained from a minute amount of power. In addition, the preceding discussion of equation 5 is equally applicable to the equations which are derived from it.

Figs. 3 and 4 present useful design information, but do not support the author's comments regarding selection of propellant. Any desired ratio of power to thrust or thrust to flow rate can be attained for any propellant material by selecting the accelerating voltage accordingly. The reason for selecting a heavy ion is best illustrated by Fig. 6, which shows that less current is required for a given flow rate with heavy ions, thus minimizing space charge problems.

Very general analyses of propulsion mechanics made by D. B. Langmuir and J. H. Irving of Ramo-Wooldridge have shown that minimization of initial gross mass depends only upon proper choice of exhaust velocity and ratio of power plant mass to propellant mass. Since the optimum exhaust velocity can be attained with any propellant material by proper selection of accelerating voltage, it is not clear why the author's weight analysis table implies a weight penalty for the use of cesium, especially when cesium tends to have fewer problems with space charge. It might also be pointed out that the afore-mentioned analyses show that when a 20,000-lb vehicle has a payload of 3,000 lb, then the optimum allocation of the remaining weight is about 12,500 lb of propellant and 4,500 lb for the power plant. The author's choice of 3,000 lb of propellant thus appears to be somewhat removed from optimum.

The source and derivation of Fig. 8 are not clear. It seems likely that the specific values shown are for some specific configuration, rather than having general applicability. Consequently, it does not appear that 12,000 volts is necessarily the minimum practical voltage, irrespective of electrode shape or spacing. Clarification of this point by the author would be appreciated. Also, it would be of value to have a further discussion of what is meant by electrical breakdown of the ion stream in a strong field, since it is not clear how already ionized gas would break down.

A. E. Lennert: Mr. Stineman raises some noteworthy points. Certainly the electrical-mechanical efficiency conversions would have to be considered as he suggests. They were not specifically mentioned in the paper because they are strongly dependent on the specific mission, which was not treated. Even so, the efficiency of conversion was taken into account in the analysis. It was taken to be approximately 80% with an additional 5% loss due to other items such as line losses, etc.

My usage of g should have been more correctly identified as the gravitational constant which, as Mr. Stineman states, happens to be the sea-level acceleration of gravity.

I must take exception to the remarks on the allocation of weights. Granting that propulsion mechanics may dictate optimum performance, one must nevertheless consider the practical aspects of the system design. Since the aggregate weight of the nucle power plant plus controls, instrumentati associated transformation equipment, ski structure, and a host of other items amoun to 14,000 lb, 50% of the remaining weig (6,000 lbs) was reserved for payload. instead of 20,000 lbs, the boost capabili within the time limit was increased 100,000 lbs, then one could reasonably i crease the propellant fraction to the amou dictated by theoretical propulsion mechani Here again optimum performance must related to a specific mission. Since no m sion was specified, we may consider that vehicle is designed for rocket test purpos

Anderson and Ehlers[1] have conduct experiments whereby one may establ preliminary estimates of the minimum vo age required for accelerating heavy io In the paper the ion beam passed through electrode with a slotted aperture which designed to satisfy Pierce's conditio Phenomenologically the events were brie summarized in my paper, however, furth details may be obtained from reference and 2.

Finally, singly ionized cesium atoms m be ionized doubly, triply, and so on, un eventually all of the orbital electrons removed from the atom. However, term "breakdown of the field" implies som thing else, namely: as the field strengt continously increased, electrons are dra from the loosely bound conduction electr of the accelerator; also, other mechanis such as secondary electron emission, ther ionic emission, etc., may cause electr to enter the ion stream, thereby creatin conduction path resulting in flashover breakdown, of the accelerating field. F ther details may be found in reference 3.

REFERENCES

1. See reference 4 of the paper.

2. RECTILINEAR ELECTRON FLOW IN BE J. R. Pierce. *Journal of Applied Physics*, York, N. Y., vol. 11, Aug. 1940, pp. 548–54.

3. HANDBUCH DER PHYSIK, VOL. 22, GAS CHARGES (book). Springer-Verlag, Berlin, many, 1956.

Optimum Reflector-Absorber Geometry for a Solar Generator

R. W. STINEMAN
ASSOCIATE MEMBER AIEE

AS AN initial step toward the eventual realization of a completely static system for converting solar radiation to electric power, the analysis and testing of a laboratory thermoelectric generator has been undertaken. A description of the over-all project is given in reference 1. An essential part of the over-all system is the combination of reflector and absorber used to collect and concentrate the solar radiation. This paper deals with the geometrical optimization of the reflector and absorber.

The elements of a power-conversion system must be treated somewhat differently from the analogous parts of a solar furnace. These differences arise from the following considerations:

1. The reflector and absorber in a power-conversion system must collect and transmit solar energy to the generating elements with an acceptable efficiency. Any reflected energy which does not impinge the absorber, or which is reflected or radiated from the absorber, must be c sidered as loss in the determination efficiency. In contrast, a solar furn operates (in the foregoing sense) at z efficiency, with maximum absorber te perature being the prime objective.

2. Since the study of a power-conver system is directed toward an ultim installation on a space vehicle, it is reas able to assume that irregularities in reflector surface and misalignment of reflector (with respect to the sun) m cause the reflected rays to deviate from ideal. On the other hand, most s

Paper 59-869, recommended by the AIEE Transportation Committee and approved by AIEE Technical Operations Department presentation at the AIEE Summer and Pa General Meeting and Air Transportation C ference, Seattle, Wash., June 21–26, 1959. Ma script submitted March 20, 1959; made avail for printing April 28, 1959.

R. W. STINEMAN is with the Boeing Airp Company, Seattle, Wash.

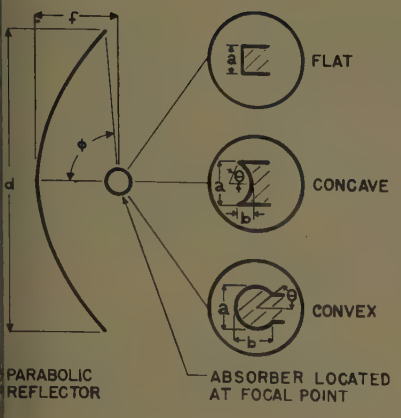

. 1. **Basic reflector and absorber geometry**

rnace analyses have assumed a me-anically perfect reflector.[2–5]

efinition of the Problem

Briefly stated, the problem under con-leration is to find the geometrical prop-ies of the reflector and absorber which sult in the most efficient collection of lar radiation for any given set of condi-ns. Collection efficiency is defined as fined as follows:

$$\text{ficiency} = \frac{\text{Net power absorbed}}{\text{Solar power intercepted}}$$

Net absorption" refers to the power ailable for useful purposes after ac-unting for all losses, such as reradiation m the absorber surface. "Solar power tercepted" refers to all solar radiation rected toward the area enclosed by the rimeter of the reflector, regardless of ether such radiation actually reaches e reflector or is intercepted by an struction. The variables which enter o the determination of efficiency are w discussed.

Shape. At present, analysis has been nfined to the cylindrical shapes shown cross section in Fig. 1. The reflector is parabolic cylinder. Three different sorber shapes are considered. The t absorber has the advantage of mini-m reradiating area for a given width. e circular cylindrical absorbers (espe-lly the convex type) are more suited an the flat absorber for receiving radia-n from a wide-angle reflector; i.e., when e angle ϕ shown in Fig. 1 is large.

Reflector diameter, d. With increas-reflector diameter, more radiation is lected but the reflected rays approach e absorber from a wider angle.

Tolerance on reflected rays, δ. As the ult of manufacturing irregularities in e slope of a reflector and misalignment of the reflector-absorber assembly with respect to the sun, any given reflected ray may deviate from its ideal direction by an angular tolerance equal to $\pm\delta$. It may be noted that a manufacturing irregularity which produces a given angular perturbation of the reflector surface will cause the reflected ray to deviate by twice as great an angle. On the other hand, misalignment of the assembly by a given angle will cause a reflected ray to deviate by an equal angle (relative to the absorber), since any misalignment results in a partially compensating relative rotation of the reflector and absorber. Linear (as opposed to angular) manufacturing irregularities are disregarded, since their effects would be negligible compared with angular irregularities.

Maximum allowable angle of incidence at absorber, γ. Certain selective absorbing surfaces, to be discussed later in more detail, require for efficient performance that radiation be incident somewhere near perpendicular to the surface. The angle γ is the maximum allowable deviation from perpendicular.

Absorber width, a. The minimum absorber width which will intercept all of the reflected radiation with an acceptable angle of incidence depends on all of the previously discussed variables; i.e., absorber shape, d, δ, and γ. If all variables but d remain fixed, then as d increases, a must also increase. The increase in d increases the amount of solar radiation being collected, but the corresponding increase in a results in increasing losses. If a point is reached where the losses increase proportionately faster than the radiation collected, then an optimum condition will be reached. Subsequent analysis will show that such an optimum does exist at which efficiency is maximized.

Absorber depth, b. The shape of a circular cylindrical absorber may be quantitatively specified by means of the distance b, shown in Fig. 1. Large values of b are most suitable for wide-angle reflectors. Subsequent analyses employ the ratio b/a, rather than b alone.

Reflector focal length, f. By expressing the other lengths shown in Fig. 1 in terms of a ratio of f, the focal length is eliminated as an explicit variable. This is essentially the same as fixing f at a value of 1 unit. If the other lengths remain at fixed proportions of f and f varies, then both the net power absorbed and solar power intercepted will vary proportionately, and efficiency will be unchanged. Thus, the efficiency obtained is valid for any value of f.

Corrected solar radiation intensity, I. The intensity of solar radiation is the power-per-unit area normal to the sun's rays. The intensity after reflection is somewhat reduced since no reflector is perfect. However, for purposes of analysis, it is acceptable to assume a perfect reflector and to reduce the value of the intensity to account for the actual reflectivity. Thus, corrected intensity, I, represents the actual solar intensity multiplied by the specular reflectivity of the reflector. Since the corrected intensity is used in the determination of solar power intercepted, the calculated efficiencies do not include any effect due to losses at the reflector.

Absorber temperature, T. The analysis is performed in terms of a specified absorber temperature, rather than finding the temperature for a specified configuration, both for ease of analysis and because the requirements of the generating elements will usually require a specified input temperature. Since reradiation losses from the absorber depend on its temperature, it may turn out for a given set of conditions that the net power absorption is negative. This would simply mean that the specified absorber temperature is not realizable with the other given conditions, even at zero efficiency. It is apparent that the absorber temperature is not entirely arbitrary, but must be kept within reasonable bounds in order to obtain realistic results.

Selectively absorbing surfaces. Several publications have described developments of surfaces which are good absorbers of wavelengths in the high-energy part of the solar spectrum, but are poor emitters in the high-energy part of the infrared radiation spectrum characteristic of bodies at moderately elevated temperatures.[6–9] For such surfaces, the over-all effective absorptivity for solar radiation is denoted α, while the over-all effective emissivity at the specified absorber temperature is denoted ϵ.

Analysis and Results

Details of the method of analysis are given in the Appendix. The required calculations are not complex. However, the number of variables is such that several dozen cases must be considered to even roughly determine the effects of all variations. Consequently, it was economical to execute the calculations on an IBM (International Business Machines Corporation) *704* digital computer. Details of the computer program are not given, but should be obvious to any reader with computer experience. The

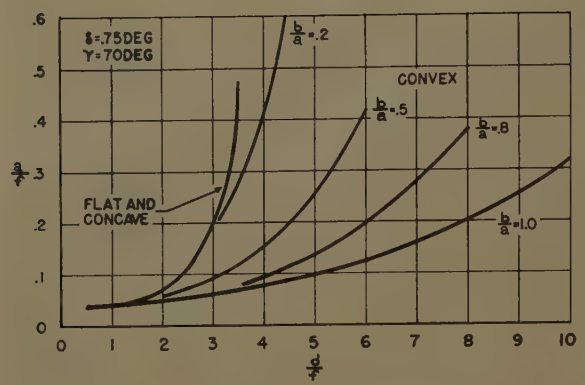

Fig. 2 (left). Typical variation of absorber width versus reflector diameter

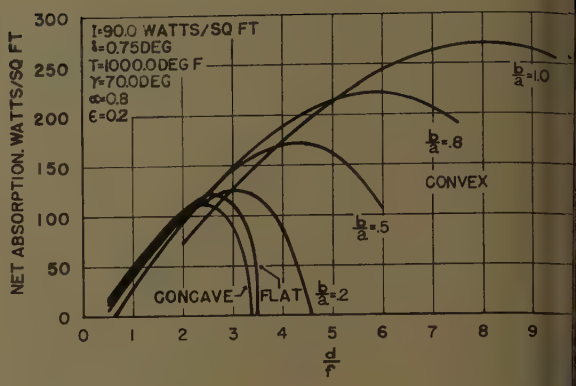

Fig. 3 (right). Typical variation of net power absorption versus reflector diameter

essential nature of the analysis is outlined as:

1. The radiation reflected from an element of the cylindrical reflector falls within a wedge having an angular width which exceeds the angular diameter of the sun by 2δ, where δ is the angular tolerance of reflected rays. Assuming the radiation to be uniformly distributed within the described wedge, it can readily be shown that collection efficiency is maximum if the absorber is just large enough to intercept all of the reflected radiation. The ratio a to f (see Fig. 1) can then be determined as a function of d/f if the absorber shape and the angles δ and γ (see preceding section) are specified. Curves of a/f versus d/f are shown in Fig. 2 for typical values of δ and γ.

2. The solar power intercepted for unit length (1 foot) perpendicular to the plane of Fig. 1, is the product of I and d, which, when expressed per unit (pu) focal length, becomes Id/f. The solar power reaching the reflector and subsequently impinging upon the absorber is somewhat less because some of the radiation is blocked by the power-conversion equipment installed adjacent to the absorber. The width so blocked is assumed to be equal to the absorber width.

3. After obtaining the radiation impinging upon the absorber, multiplying by the absorptivity, α, and subtracting the reradiation loss yields the net power absorption. Then dividing by the solar power intercepted gives the collection efficiency. Curves of net power absorbed versus d/f for a typical condition are shown in Fig. 3. Fig. 4 shows curves of collection efficiency versus d/f for the same condition as Fig. 3. The efficiency is independent of the focal length, f, and the distance perpendicular to the plane of Fig. 1.

Selective Surfaces

In all cases investigated, the use of a selectively absorbing surface resulted in higher efficiency than with a black surface. For example, with all conditions the same as in Fig. 4 except for changing the absorber surface to black (i.e., $\alpha=\epsilon=1.0$), the maximum efficiency is only 0.07 pu. (As is shown in the Appendix, a black absorber is superior to any other surface with constant emissivity.) The superiority of selective surfaces undoubtedly stems from the use of a cylindrical configuration, which results in a larger absorber area and hence larger reradiation loss, than the more common paraboloidal or spherical reflectors. Setting $\alpha=0.8$ and $\epsilon=0.2$ provides a slightly conservative representation of the best selective surfaces, and these values are used throughout this paper except where stated otherwise.[8-9] It may be noted that for the values chosen, collection efficiency can not exceed 0.8 pu, except possibly with a concave absorber where the cavity effect produces a slight increase in equivalent absorptivity. Evaluation of any geometry should compare actual efficiency with this 0.8 pu limit.

Absorber Shape

Other conditions being equal, the collection efficiency attainable with a flat or concave absorber is generally greater than the efficiency for a convex absorber. However, for conditions which result in high efficiency, the difference in maximum efficiency for the several shapes becomes very small. Since most practical applications would, by necessity, operate at high efficiency, the choice of absorber shape may be based on practical factors rather than efficiency. Fig. 5 shows the variation in efficiency with shape, for the same conditions as in Figs. 3 and 4.

The efficiency of a concave absorber may be either greater or less than a flat absorber depending on the relative importance of reflection loss and reradiation loss. The cavity effect for a concave absorber increases the effective values of both α and ϵ. If reflection loss is predominate, then the increased absorption results in higher efficiency for the concave absorber. If reradiation loss is predominate, then the increased emission results in lower efficiency for the concave absorber. This is illustrated by the curves in Fig. 6, where as temperature increases, the reradiation loss tends to predominate. However, it is evident that the difference in efficiency between flat and concave absorbers is small at the high efficiencies.

Reflector Diameter

The reflector diameter which results in maximum efficiency depends on the absorber shape. Typical values of the optimum ratio of diameter to focal length are shown in Fig. 5. It turned out for a wide variety of cases investigated that the optimum value of d/f for flat or near-flat absorbers is very nearly equal to 5. For absorbers with relatively large values of b/a, there is more variation in the optimum value of d/f, but in no case does the optimum differ from the curve in Fig. 5 by more than 50%. Furthermore, the value of d/f becomes less critical as b/a increases, as is shown by the broad maxima of the curves in Fig. 4 for large b/a.

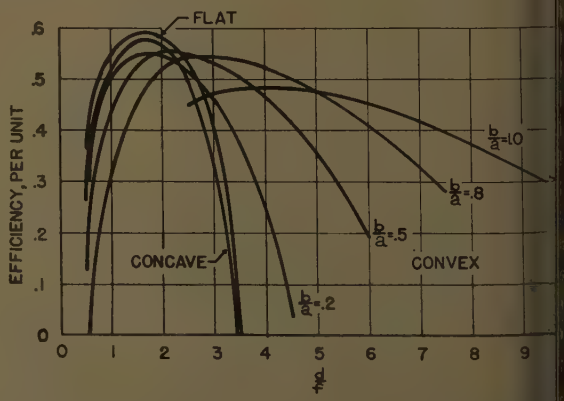

Fig. 4. Typical variation of collection efficiency versus reflector diameter

I=90 watts/sq ft
δ=0.75 degree
T=1,000 F
γ=70 degrees
α=0.8
ε=0.2

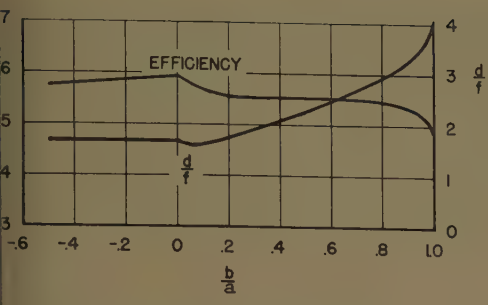

5. Maximum collection efficiency and ector diameter at which maximum efficiency urs versus absorber shape ratio. See Fig. 4 for specified conditions

b/a>0, convex absorber
b/a=0, flat absorber
b/a<0, concave absorber

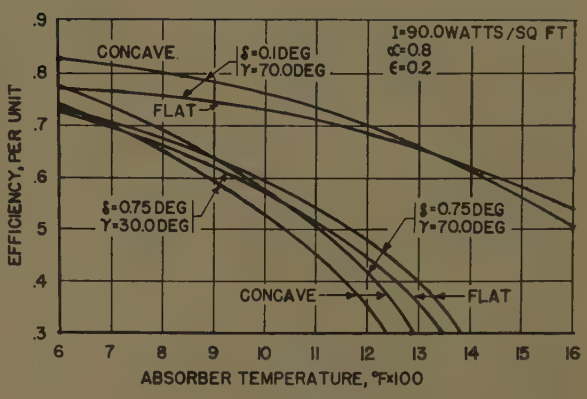

Fig. 6. Maximum collection efficiency versus absorber temperature for flat and concave absorbers

δ=tolerance on reflected rays
γ=maximum allowable angle of incidence at absorber

SORBER TEMPERATURE

ince radiation from a surface is pro-tional to the fourth power of tempera-e, the reradiation losses increase as orber temperature increases. The re-ing drop in efficiency is shown in Fig.

ERANCE ON REFLECTED RAYS

he larger the tolerance, δ, the larger st be the absorber to intercept all ected rays. Since reradiation losses proportional to absorber area, a er value of δ results in a smaller collec-efficiency. Stated another way, maximum absorber temperature that be attained without dropping below minimum acceptable efficiency de-ds upon the value of δ. For the ditions in Fig. 6, an efficiency of pu can be realized at a temperature 1,450 F if $\delta=0.1$ degree, while a perature of only 980 F can be realized the same conditions if $\delta=0.75$ degree.

XIMUM ALLOWABLE ANGLE OF NCIDENCE AT ABSORBER

or cylindrical absorbers, either con-or concave, a small value of the angle as the result that only the central ion of the absorber visible from any icular direction is effective for ab-tion. Thus for small values of γ, total absorber area increases, and the lting increase in reradiation losses ds lower collection efficiency. This t is illustrated in Fig. 6 for a concave rber.

or a flat absorber, the value of γ has direct effect on the absorber width a. vever, the reflector diameter is limited value such that the angle ϕ in Fig. 1 not exceed γ. For a flat absorber, optimum value of ϕ is very nearly l to 45 degrees. Thus, if γ is less than 45 degrees, the reflector diameter must be less than what would otherwise be optimum. However, as shown in Fig. 6, the decrease in efficiency is small even for γ as low as 30 degrees.

CORRECTED SOLAR RADIATION INTENSITY

Any variation in solar intensity results in a corresponding variation in the power impinging upon the absorber, yet reradiation losses remain the same. Consequently, a reduction in solar intensity causes a drop in collection efficiency. The solar intensity outside the earth's atmosphere is 126 watts/sq ft, while the intensity at the earth's surface at noon on a bright clear summer day in the United States is about 85 watts/sq ft.[10] Since the corrected value used in the analysis includes the effect of imperfect reflection, it is apparent that the value of 90 watts/sq ft used for Figs. 3 through 6 is a little low for space applications and is a little high for surface installations. However, at high efficiencies, where absorber reflection losses exceed reradiation losses, only small changes in efficiency result from moderate variations in solar intensity. For example, for the same condition as in Figs. 3 through 5, except using corrected intensities of 70 and 115 watts/sq ft, the maximum efficiencies are 0.54 and 0.64 pu, respectively.

FUTURE ANALYSIS

All of the foregoing results are, of course, applicable to the cylindrical configuration of Fig. 1 only. It is expected that future requirements will result in extending the analysis to other configurations, such as a paraboloidal (cup-shaped) reflector with a circular or spherical absorber. The general method of analysis will be the same as described in this paper. However, the results for other configurations may be quite different. It is hoped that the results of subsequent analyses can be published in the not too distant future.

Conclusions

The important conclusions that can be drawn for the cylindrical configuration of Fig. 1 are as follows:

1. An absorber surface having high absorptivity for solar radiation and low emissivity in the infrared region results in significantly higher collection efficiency than with a nonselective surface.

2. In most cases of practical significance, collection efficiency does not depend to any great significance upon absorber shape. However, for each absorber shape there is an optimum ratio of reflector diameter to focal length which results in maximum efficiency. For flat or nearly flat absorbers, the optimum ratio of diameter to focal length is close to 5 to 3. For the more nearly circular absorbers, the optimum ratio is generally greater than 5 to 3, is more variable with changes in other conditions, but is less critical because of a broad maximum.

3. The absorber temperature range that can be attained with reasonably high collection efficiency depends on the accuracy of manufacture and alignment of the reflector. Relatively high precision is required for absorber temperatures in the range of 1,200 to 1,500 F, while moderate errors can be tolerated below 1,000 F.

4. Moderate variations in solar intensity and in the maximum allowable angle of incidence at the absorber have relatively minor effects upon maximum attainable collection efficiencies.

Appendix. Methods of Calculation

Calculations are based on the geometry of Fig. 1, and, where applicable, assume unit length perpendicular to the plane of Fig. 1. All angles are expressed in degrees. Symbols used are those discussed under "Definition of the Problem" plus the following:

ϕ and θ=angles shown in Fig. 1
β=angular diameter of the sun, approximately 32 minutes
r=distance from an edge of the reflector to the focal point
c=projection, normal to the length r, of that portion of the absorber width which is effective in absorbing rays parallel to r

σ = Stefan-Boltzmann constant
P = net power absorbed per-unit length perpendicular to the plane of Fig. 1
x and y = rectangular co-ordinates with origin at the center of the reflector and the y-axis passing through the focal point

The reflected rays from each element of the reflector fall within a wedge depending on the angular diameter of the sun and the tolerance δ. If radiation is assumed to be uniformly distributed within each wedge, and if absorber losses are less than the power incident upon the absorber, then if any reflected radiation misses the absorber the escaping radiation will exceed the losses which would be incurred by increasing the size of the absorber. On the other hand, if the absorber is larger than necessary for the interception of all reflected rays, then the absorber losses will be larger than necessary. In either case, the collection efficiency will suffer. The optimum size absorber is just big enough to intercept all reflected rays. The critical condition which establishes the size of the absorber is the wedge of reflected rays from the edge of the reflector. This particular wedge travels farthest to reach the absorber, thus spreading out the most, and strikes the absorber at least as obliquely as any other wedge.

The equation of the parabolic section is

$$y=\frac{x^2}{4f}$$

The distance from the focal point to a point on the reflector is given by:

$$\sqrt{x^2+(f-y)^2}=f+y$$

from which

$$r=f+\frac{d^2}{16f}$$

Dividing by f to convert to dimensionless ratios yields

$$\frac{r}{f}=1+\frac{1}{16}\left(\frac{d}{f}\right)^2$$

An expression for ϕ which is convenient for execution on a digital computer is

$$\phi=90^\circ-\tan^{-1}\frac{f-\frac{d^2}{16f}}{\frac{d}{2}}$$

$$=90^\circ-\tan^{-1}\left(\frac{2f}{d}-\frac{d}{8f}\right)$$

The remaining calculations depend on the shape of the absorber.

Flat Absorber

The ratio of d to f is limited by the restriction that $\phi \leq \gamma \leq 90$ degrees. This restriction assures that the maximum angle of incidence at the absorber does not exceed γ. Next, $c=a\cos\phi$, or $c/f=a/f\cos\phi$. Since β and δ are both very small,

$$\beta+2\delta=\frac{c}{r}\text{ radians}\quad\frac{180\text{ degrees}}{\pi\text{ radians}}=\frac{180}{\pi}\frac{c}{r}$$

Solving for the ratio of absorber width to focal length:

$$\frac{a}{f}=\frac{c}{f\cos\phi}=\frac{\pi}{180}\frac{r}{f}\frac{\beta+2\delta}{\cos\phi}$$

Solar power intercepter pu focal length is Id/f. The unobstructed portion which reaches the reflector and is then reflected to the absorber is given by

$$I\frac{d-a}{f}=I\left(\frac{d}{f}-\frac{a}{f}\right)$$

The net absorted power pu focal length is then

$$\frac{P}{f}=\alpha I\left(\frac{d}{f}-\frac{a}{f}\right)-\epsilon\sigma T^4\frac{a}{f}$$

Finally,

$$\text{Efficiency}=\frac{P/f}{Id/f}=\alpha\left(1-\frac{a}{d}\right)-\frac{\epsilon\sigma T^4}{I}\frac{a}{d}$$

Concave Absorber

The best match between absorber and reflector is obtained with $\theta=\phi+\gamma$ with the restriction that $\theta\leq 90$ degrees. Then:

$$\frac{b}{a}=\frac{1}{2}\tan\frac{\theta}{2}$$

Now

$$\beta+2\delta=\frac{180}{\pi}\frac{c}{r}$$

or

$$\frac{c}{f}=\frac{\pi}{180}\frac{r}{f}(\beta+2\delta)$$

If $\phi+\gamma\leq 90$ degrees, then

$$\frac{a}{f}=\frac{c}{f\sin\gamma}=\frac{\pi}{180}\frac{r}{f}\frac{\beta+2\delta}{\sin\gamma}$$

If $\phi+\gamma>90$ degrees, but with $\phi<90$ degrees, then

$$\frac{a}{f}=\frac{c}{f\cos\phi}=\frac{\pi}{180}\frac{r}{f}\frac{\beta+2\delta}{\cos\phi}$$

ϕ can not exceed 90 degrees. If it did, rays from the edge of the mirror could not reach the absorbing surface.

The cavity effect for the concave absorber causes the effective values of absorptivity and emissivity to increase. The following expressions are readily derived, where the effective values are denoted by primes:

$$\alpha'=\alpha\frac{\frac{\pi}{180}\frac{\theta}{\sin\theta}+\frac{90-\gamma}{90+\gamma}}{\frac{\pi}{180}\frac{\theta}{\sin\theta}\alpha+\frac{180}{90+\gamma}-\alpha}$$

$$\epsilon'=\frac{\epsilon}{\epsilon+\frac{180}{\pi}\frac{\sin\theta}{\theta}(1-\epsilon)}$$

Then

$$\frac{P}{f}=\alpha' I\left(\frac{d}{f}-\frac{a}{f}\right)-\epsilon'\sigma T^4\frac{a}{f}$$

and

$$\text{Efficiency}=\frac{P/f}{Id/f}=\alpha'\left(1-\frac{a}{d}\right)-\frac{\epsilon'\sigma T^4}{I}\frac{a}{d}$$

For any selected value of b/a,

$$\theta=90+\tan^{-1}\frac{\frac{1}{2}-\frac{b}{a}}{\sqrt{\frac{b}{a}\left(1-\frac{b}{a}\right)}}$$

where this expression is well adapted execution on a digital computer.

As before:

$$\frac{c}{f}=\frac{\pi}{180}\frac{r}{f}(\beta+2\delta)$$

If 180 degrees $-\theta-\phi>\gamma$,

$$\frac{a}{f}=\frac{c}{f\sin\gamma}=\frac{\pi}{180}\frac{r}{f}\frac{\beta+2\delta}{\sin\gamma}$$

If 180 degrees $-\theta+\phi>\gamma>180$ degrees $-\theta-\phi$,

$$\frac{a}{f}=\frac{c}{f}\frac{2}{\sin\gamma+\sin(180^\circ-\theta-\phi)}$$

$$-\frac{\pi}{90}\frac{r}{f}\frac{\beta+2\delta}{\sin\gamma+\sin(180^\circ-\theta-$$

If 180 degrees $-\theta+\phi<\gamma$ and $\phi+\theta-1$ degrees $<\gamma$,

$$\frac{a}{f}=\frac{c}{f}\frac{2}{\sin(180^\circ-\theta+\phi)+\sin(180^\circ-\theta-\phi)}$$

The angular sum, $\phi+\theta-180$ degrees, c not exceed γ; if it did, rays from the ed of the reflector could not reach the absorb surface at an angle of incidence less than If $\theta\leq 90$ degrees,

$$\frac{P}{f}=\alpha I\left(\frac{d}{f}-\frac{a}{f}\right)-\epsilon\sigma T^4\pi\left(1-\frac{\theta}{180}\right)\frac{a}{f}$$

If $\theta>90$ degrees,

$$\frac{P}{f}=\alpha I\left(\frac{d}{f}-\frac{a}{f}\sin\theta\right)-\epsilon\sigma T^4\pi\left(1-\frac{\theta}{180}\right)\frac{a}{f}$$

Finally,

$$\text{Efficiency}=\frac{P/f}{Id/f}=\frac{P}{Id}$$

Nonselective Absorber Surface

For the special case where $\alpha=\epsilon$, it apparent for all absorber shapes that various expressions for net absorbed pow all reduce to the form $P/f=\epsilon K$, where is independent of ϵ. It is thus obvio that the greatest net absorption will occ if $\alpha=\epsilon=1.0$; i.e., a black absorbing surf is better than any other nonselect surface.

References

1. Solar-Powered Thermoelectric Genera Design Considerations, N. F. Schuh, R. Tallent. *AIEE Transactions*, see pp. 345–52 this issue.

2. Notes on Optical Design Principl Concentration Ratios, and Maximum T perature of Parabolic Solar Furnaces, R. Bliss, Jr. *Technical Memorandum HDW-T 56-1*, Holloman Air Development Center, Mex., July 1956.

3. The Flux Through the Focal Spot o Solar Furnace, P. D. Jose. *Technical Memo dum HDRRM-TM-57-3*, Holloman Air Deve ment center, Apr. 1957.

CALCULATION OF THE CONCENTRATION OF THE AR RADIATION THROUGH THE FOCAL SPOT OF PARABOLIC MIRROR, A. W. Simon. *Technical morandum HDGR-57-10*, Holloman Air De- opment Center, Aug. 1957.

UTILIZATION OF SOLAR FURNACES IN HIGH MPERATURE RESEARCH, P. Duwez. *Transactions*, erican Society of Mechanical Engineers, New rk, July 1957.

6. SELECTIVE RADIATION, H. Tabor. *Bulletin*, Research Council of Israel, Jerusalem, Israel, vol. 5, sect. A, 1955.

7. SOLAR ENERGY DESIGN, H. Tabor. *Ibid.*, vol. 5, sect. C, 1955.

8. THE PREPARATION OF A SELECTIVELY BLACK SURFACE FOR USE IN COLLECTING SOLAR ENERGY, T. A. Unger. *Doctoral Thesis*, Department of Chemical Engineering, Massachusetts Institute of Technology, Cambridge, Mass., 1955.

9. FILMED SURFACES FOR REFLECTING OPTICS, G. Hass. *Journal*, Optical Society of America, New York, N. Y., Nov. 1955.

10. HANDBOOK OF GEOPHYSICS FOR AIR FORCE DESIGNERS (book). Air Force Cambridge Research Center, Cambridge, Mass., 1957, chap. 16.

A Practical Standard Transistorized Optimum Response Controller

KAN CHEN
ASSOCIATE MEMBER AIEE

D. R. LITTLE
ASSOCIATE MEMBER AIEE

nopsis: The principle of nonlinear op- num response control has found a new d unique application in the develop- nt of a standard controller. The transis- ized controller can work in a great iety of feedback systems because it has gligible time delay. Optimum response a specified step input can be obtained very ily by experiment because linear switch- is used. The response is still nearly imum when the input is not of the cified form and magnitude, or when system parameters change with environ- ntal variations. Solution of practical blems in the development are discussed the paper. A mathematical proof is en to show that optimum response to a cified step input, for the systems under sideration, can always be obtained with ar switching.

THE PRESENT METHODS of de- signing practical control systems leave ch to be desired insofar as engineering e is concerned. In most cases, the npensation networks and at least one the control amplifiers are custom-made meet individual system specifications. hough systems designed in this manner e fairly satisfactory results, two stions are ever present:

Is this the best system which can be duced for the material cost involved, i.e., here maximum utilization of all com- ents?

Is there a possibility of producing one troller, amplifier and compensation in- ded in one package, which will be applicable in a wide range of systems instead of designing a special controller for each system?

Hitherto, no controller appears to have been designed which will answer both questions. It has been proved analytically that for second order systems, i.e., systems of two time constants, the best transient response for a given available forcing can be obtained by using an ideal on-off amplifier with a nonlinear function generator, the so-called bang-bang control.[1–4] In other words, this leads to minimization of necessary forcing to meet certain specifications on recovery time, and, in general, minimum forcing means minimum material cost for the controller. Thus, this would seem to be an answer to the first question above. However, the use of a nonlinear function generator is objectionable. Moreover, an ideal on-off amplifier remains to be developed. As to the second question, a number of attempts have been made to develop some form of a standard controller which is more than just a standard amplifier, to be used in a great variety of control systems. Of these, most, if not all, have been designed from the standpoint of linear theory and, although some have succeeded in insuring adequate control under small disturbances,[5,6] none have yet been developed which can provide nearly optimum control under large disturbances. Furthermore, the adjustments of compensation networks in these controllers are complicated and require the engineering judgment or calculation of experienced personnel.

The new controller described in this paper is the result of an attempt to realize a practical controller which would answer both of the questions mentioned above. Since the on-off type of operation produces the best transient response, it was decided to devise a practical on-off type of standard controller without resorting to complicated circuitry. This then would guarantee the realization of maximum utilization of components, at least under the condition of worst system disturbance when maximum utilization of components is most desired. It was also determined that the controller should be able to control many different systems with relatively few adjustments. The controller was to be a standard controller in the strictest sense; that is, even an inexperienced technician can obtain the best system performance with the few adjustments provided by the controller. Naturally, such a controller has many advantages. Not only is the mass production of such controllers and the maximum utilization of components feasible, but the design engineering and construction time can be reduced to a bare minimum.

Optimum Response

Let us review briefly the idea of nonlinear optimum response control before we extend it to the development of a standard controller. Fig. 1 shows a nonlinear optimum response system with a second-order overdamped controlled element, the type most commonly encountered in industrial applications. The positive and negative forcings of the

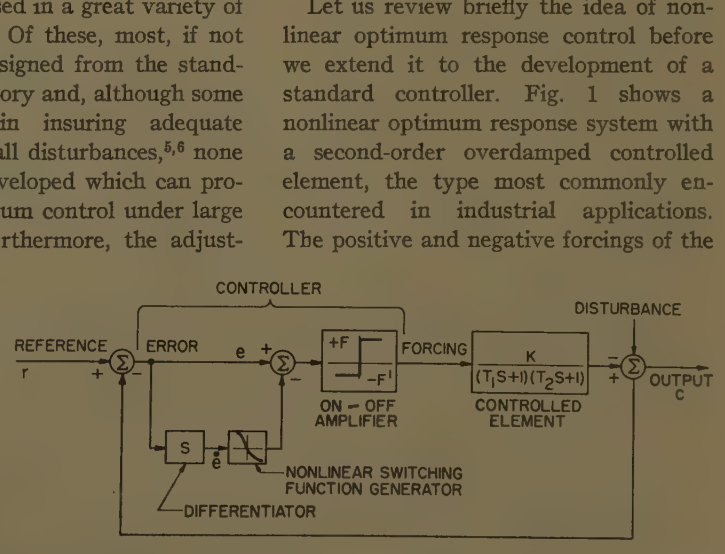

Fig. 1. On-off control system

er 59-838, recommended by the AIEE Feedback trol Systems Committee and approved by the E Technical Operations Department for entation at the AIEE Summer and Pacific eral Meeting and Air Transportation Confer-, Seattle, Wash., June 21–26, 1959. Manu- pt submitted March 16, 1959; made available printing May 13, 1959.

CHEN is with the Westinghouse Electric poration, East Pittsburgh, Pa., and D. R. LITTLE ith the Curtiss-Wright Corporation, Quehanna,

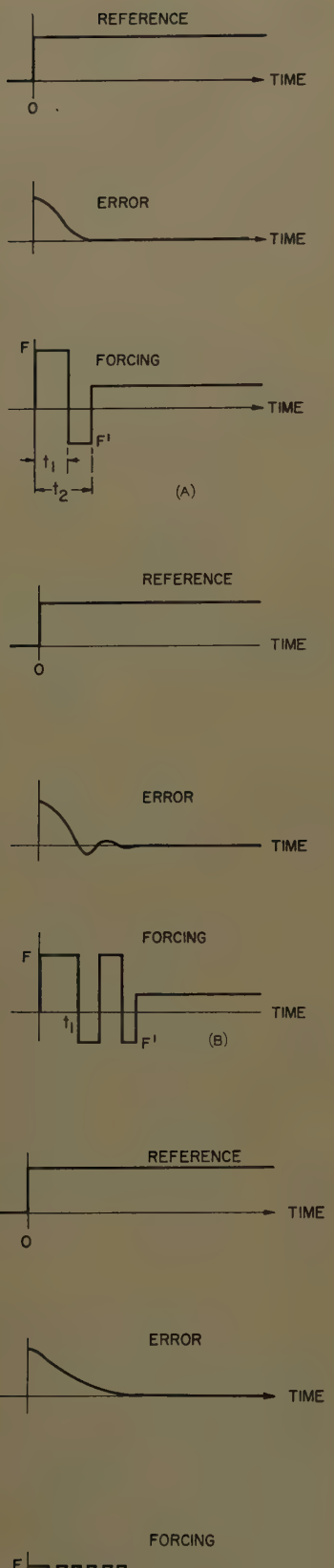

Fig. 2. Transients

A—Under ideal switching
B—When first switching is too late
C—When first switching is too early

on-off amplifier are unsymmetrical in the general case. Thus, the case of a single-ended amplifier is definitely included. In this control system, if a proper nonlinear switching curve is used to determine when to switch from positive to negative forcing, then the graph of the reference step input, the error, and the forcing with respect to time is shown in Fig. 2(A). These curves will then describe the so-called "optimum" case where t_1 denotes the time at which forcing was switched from full positive to full negative and t_2 when forcing is switched to a value just sufficient to maintain the desired output. In the controller scheme shown, the actual system will jitter at a very high frequency under steady state, and the durations of positive and negative controller output are so proportioned that zero error is maintained. It has been shown mathematically that the optimum case described corresponds indeed to minimum time for the system error to reach and remain zero subject to the constraint of the given maximum available forcing of the controller.[3] If the switching time, t_1, is too late, then the curves of Fig. 2(B) describe the behavior of the system. When the switching time, t_1, is too early the curves of Fig. 2(C) characterize the system behavior. In either case, the response time is longer than that in the optimum case shown in Fig. 2(A).

A frequently used example to illustrate the optimum response principle is that the quickest way to race an automobile from one stop light to another is to press down the accelerator to the floor and hold it there for a critical period of time and then to apply full braking. In this manner, an automobile can beat another with a more powerful engine but not using full power and braking during the race.

Mathematical Description

The performance of the optimum system in Fig. 1 can be described quantitatively in a phase plane plot of the first derivate of the error $\dot{e}$ versus the error e. From Fig. 1 we can derive the following expression:

$$T_1T_2\,\dddot{c}+(T_1+T_2)\,\ddot{c}+\dot{c}=Kf$$

where T_1 and T_2=time constants of the controlled element, assumed to be positive real numbers, or overdamped, and $T_1<T_2$.

K=gain of the controlled element
c=system output
$f\begin{cases}=F>0 \text{ for positive forcing}\\=F'<0 \text{ for negative forcing}\end{cases}$

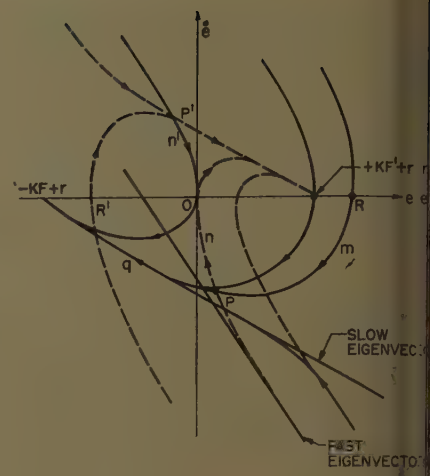

Fig. 3. Phase-plane trajectories of the id on-off system

Referring again to the closed loop syst of Fig. 1 and assuming that the refere input r is a step function (i.e., r is constant during the system transie then

$$e=r-c$$
$$\dot{e}=-\dot{c}$$
$$\ddot{e}=-\ddot{c}$$

so that

$$T_1T_2\dddot{e}+(T_1+T_2)\ddot{e}+\dot{e}=K_1$$

where

$$K_1=-Kf+\dot{r}$$

The general solution of equation 1 is

$$e=A\epsilon^{-t/T_1}+B\epsilon^{-t/T_2}+K_1$$

where the constants A and B depend the initial conditions and ϵ is base natural logarithms.

We then find the derivative of error to be

$$\dot{e}=\frac{A}{T_1}\epsilon^{-t/T_1}-\frac{B}{T_2}\epsilon^{-t/T_2}$$

Eliminating t from equations 2 an yields

$$T_1\ln\frac{(e-K_1)+T_2\dot{e}}{A(1-T_2/T_1)}=T_2\ln\frac{(e-K_1)+T_1\dot{e}}{B(1-T_1/T_2)}$$

which describes the trajectories in phase plane. A few trajectories, corresponding to a different set of va of A and B are shown in Fig. 3. solid curves are indicative of posi forcing and the dash curves of nega forcing. The arrows indicate the di tion taken by the operating point increasing time.

It is important to point out that trajectories near the nodes (K_1, 0) proach asymptotically to the slow ei vector with an absolute slope equa

$_2$, and those far away from the nodes
rge asymptotically from the fast
nvector with an absolute slope equal
$/T_1$.

TCHING CURVE

uppose a step input R is initiated in
reference r such that $e=R$ and $\dot{e}=0$
ially. If, as the result of this condi-
, positive forcing is initiated, the
rating point will move along curve m
, unless switching occurs at point P,
operating point will move towards and
ntually reach the point $(-KF+r, 0)$
g path q. However, if at point P
system switches from full positive
ing to full negative forcing, the
rating point will follow path n into the
in. The system will come to rest at
origin; that is, the error and the
vative of error are zero simultaneously
om this time on, the average output
he controller is just enough to main-
the output at its desired level. If
system is switched at any point other
point P, the operating point will not
able to reach the origin without
ching at least once more since the
e n is the only negative forcing curve
ing through the origin. If the initial
is negative and places the operating
t at R', then a similar case exists
re P' is the switching point and n' is
curve passing through the origin.
e the negative forcing period precedes
positive forcing period.
nce a wide range of positive step
rbances are possible and since it is
rable to come into the origin via the
e n, it is apparent that the switching
positive to negative forcing must
r when the path of the operating
t intersects curve n. Similarly, for
case of a negative step the curve n'
e path that should be followed into
origin. Hence, the combined curves
should be the so-called "switching
e." This means that when the
ating point is to the right of the
ching curve, positive forcing should
employed, and to the left negative

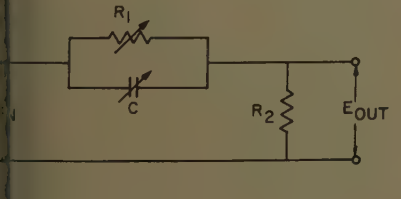

$$\frac{E_{OUT}(S)}{E_{IN}(S)} = \frac{R_2}{R_1+R_2} \cdot \frac{1+R_1CS}{1+\frac{R_1R_2}{R_1+R_2}CS}$$

Fig. 4. Derivative network

forcing should be employed in order to accomplish optimum response in all cases. One way to achieve the switching curve is indicated in Fig. 1 by the blocks between the error and the ideal on-off amplifier.

Solving the Practical Difficulties

The optimum response system described has attracted the interest of many engineers and scientists in the field of advanced control development, as is evidenced by the large number of recent technical papers on this subject. However, the system has not been used extensively in practice so far. One may summarize the doubts about the practicalities of such a system as follows:

1. The system response is optimum for only step and ramp inputs or disturbances.

2. The controlled element may not be linear, second order, and overdamped, as assumed in the foregoing analysis.

3. Pure differentiation of error assumed in the analysis is difficult to achieve and tends to accentuate noise.

4. The high-frequency jittering of the on-off amplifier may cause intolerable ripple in the output signal.

5. The ideal on-off amplifier may be difficult to approach with practical circuits.

6. The nonlinear function generator, shown in Fig. 1, used in such a system is objectionable from the standpoints of cost and adjustability.

7. The optimum response may be critically affected by changes of system parameters due to load or environmental variations.

These doubts are quite reasonable for one who has had extensive practical experience in developing control systems. The remaining part of this report will explain how the practical difficulties are overcome or circumvented. Here are the point-to-point answers to the objections listed above:

1. The worst input and disturbance to many control systems are actually in the form of a step or ramp. In fact, most industrial control systems are specified in terms of such inputs.

2. Most industrial control systems are higher than second order mainly because of the appreciable time delay attributed to the power amplifiers and the compensation networks. If the ideal on-off amplifier can provide sufficient control power for the output element without any significant time delay and no compensation other than that in the standard configuration given in Fig. 1 is used, most system controlled elements are essentially second order and overdamped. For example, the time constants of the exciter and of the generator are the essential delays in a voltage regulating system, and the time constants of the generator and of the motor are the essential delays in a speed control system. As to the effects of slight nonlinearities in the controlled elements, they are best determined by an analog computer.

3. Of course, pure differentiation is not feasible to achieve in practice. However, it can certainly be approximated by a simple resistance-capacitance (RC) network, such as given in Fig. 4. The small time lag in this derivative network as well as the large time delays in the controlled element should tend to alleviate the problem of high-frequency noise.

4. The output elements, because of their inherent time delays, should serve as low-pass filters to attenuate the jittering in the on-off amplifier output under steady state. As long as the jittering frequency is high enough, the ripple in the system output signal should not be discernible. This is true in the same sense that periodic output waveforms of such devices as magnetic amplifiers and thyratrons do not cause discernible ripple in the system output. Furthermore, the jittering of the on-off amplifier can be avoided if the on-off amplifier is allowed to have a narrow linear range and provided that the system is stable within this linear range.

5. Most on-off amplifiers which have been considered in the literature to achieve optimum system response are electromechanical relays. Their wear and tear, appreciable switching time, and hysteresis characteristics make their use in control systems very undesirable. The problem can be circumvented if transistors are used as the basic components of the amplifier. The requirements of the on-off amplifier will be discussed later in a separate section.

6, 7. These problems are dealt with in the next section.

Linear Switching

To avoid the cost and the inflexibility of a nonlinear function generator, we shall consider replacing the nonlinear curve in Figs. 1 and 3 by a straight line. If the curve nn' in Fig. 3 is substituted by a straight line AA' going through the points O and P as shown in Fig. 5, the

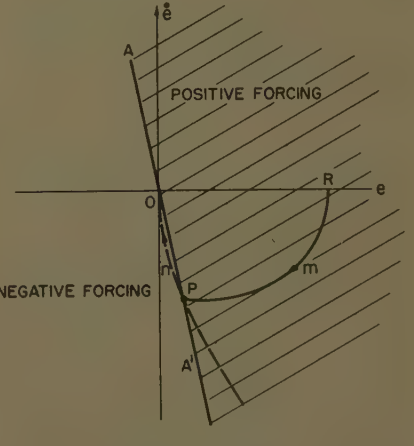

Fig. 5. Phase-plane trajectories of the linear on-off system

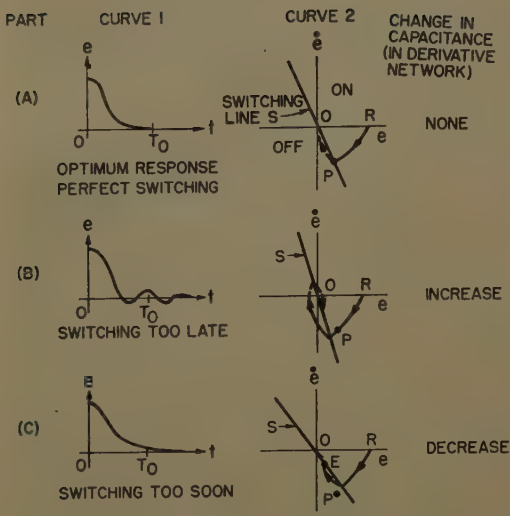

Fig. 6. Optimum response adjustments

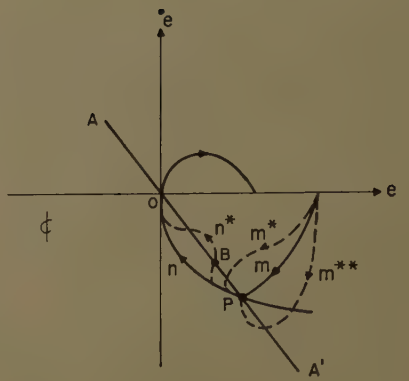

Fig. 7. Apparently possible trajectories crossing the optimum switching line

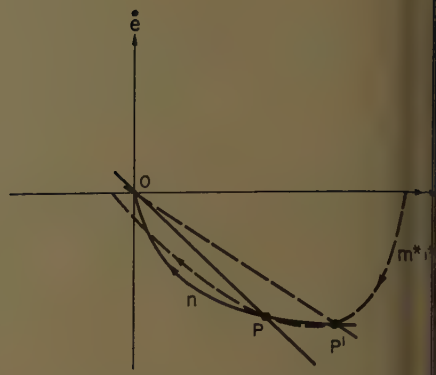

Fig. 8. More than one intersections of m and n trajectories in the fourth quadrant

curve m still lies completely in the positive forcing region and the curve n still lies completely in the negative forcing region, as they did in Fig. 3. Hence, the system still responds in an optimum manner to an input step change exactly equal to R. Suppose R is the worst step input or disturbance for which the system specification is written, then to a less severe input or disturbance the response will not be optimum but is likely to be within the specified recovery time for the worst case. The observation that the ideal switching curve n approaches the fast eigenvector, a straight line, in the region remote from the origin of the phase plane leads one to suspect that replacement of n by an appropriate straight line would result in nearly optimum or quasi-optimum response for all step inputs. Furthermore, with system parameters changing with load and environmental conditions, it is senseless to attempt achieving exact optimum response under all conditions in a practical application. How much the system transient response departs from optimum, because of parameter variations and input magnitude variations will be discussed in the section on computer study.

Experimental Adjustment

Substituting a straight line for the nonlinear curve in Fig. 1 means that the block between the error signal and the on-off amplifier can be physically realized by the RC derivative network shown in Fig. 4. The slope of the switching line in the phase plane can therefore be simply adjusted by changing either the resistance R_1 or the capacitance C of the lead network. However, changing R_1 will change the ratio of the lead and lag time constants as well as the gain of the derivative network. Therefore, it is advisable to adjust the slope of the linear switching line by changing the capacitance alone.

If the controlled element is second-order and overdamped, the only parameter on the controller to be adjusted is the capacitance alone as far as adjustment for optimum transient response is concerned. Of course, the position of this "simple knob" on the controller can be determined by calculation based on the gain and time constants of the controlled element and the positive and negative forcing of the controller. However, a more practical way of adjusting this single knob is by experiment. The procedure consists of feeding the largest expected, or specified, step input or disturbance to the system and examining the time response. If there is an overshoot, the time of the first switching should be made earlier by increasing the capacitor C. If the response has a long tail, the time of the first switching should be made later by decreasing the capacitor C. The optimum response corresponds to no overshoot nor tail, that is, dead-beat response. The transient responses of these 3 cases are illustrated in Fig. 6, together with their corresponding phase-plane trajectories. The procedure is so simple that even an inexperienced technician can determine the correct setting of the capacitor to obtain optimum response. Another experimental method of determining the correct setting of the capacitor is to see that one and only one switching of the controller output occurs between the beginning and the end of the transient.

Part C of Fig. 6 shows that the "end-point" phenomenon[7] occurs when the capacitance of the derivative network is too large. After the end-point E is reached the controller output oscillates at a very high frequency and with such an on-off time ratio that the operating points proceeds along the switching line S to t origin of the phase plane. The respon for this part of the transient is an exp nential function of time with a time co stant equal to R_1C of the derivative ne work. Although it takes theoretica infinite time to reach steady state, t time it takes to reach and remain with specified band around the final value finite.

A similar statement may be made regard to part B of Fig. 6, the oversho case.

Mathematical Proof

Consider an on-off system with second-order, overdamped controlled e ment. Although linear switching w not result in optimum response for magnitudes of step inputs, it can proved mathematically that for a giv step input, an on-off controller employi a proper linear switching function c always achieve optimum response. T previous discussion, based on the pha plane trajectory in Fig. 5, has illustrat the possibility of obtaining optimum sponse with a linear switching li However, this is possible only if straight line AA' linking the origin, and the optimum switching point, (Fig. 5), puts the trajectories m and entirely in the two separate half-pla divided by AA'. For example, if trajectory corresponding to negat forcing were like n^* instead of n, depic in Fig. 7, the use of AA' as the switch

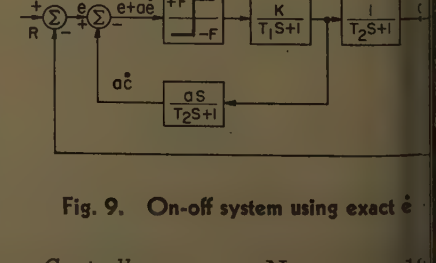

Fig. 9. On-off system using exact ė

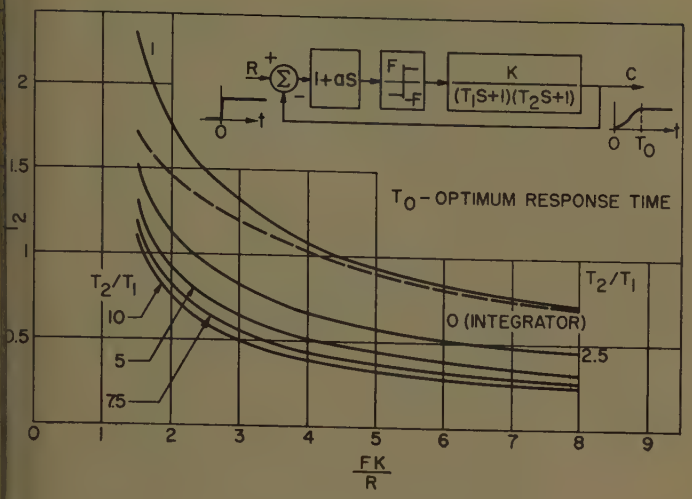

Fig. 10 (left). Optimum response time

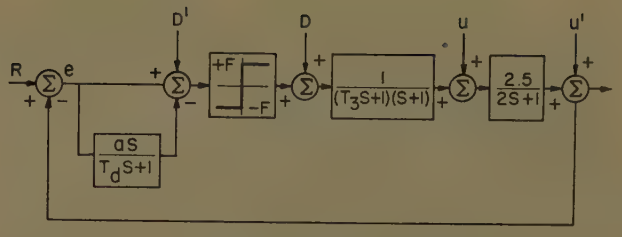

Fig. 11 (above). On-off system using approximate $\dot{e}$

would cause the on-off controller to tch back to positive forcing at B, reas negative forcing is required to e optimum response. For the same son, if the trajectory corresponding to itive forcing were like m^* or m^{**} in- d of m, as depicted in Fig. 7, it would be possible with linear switching to ain optimum response to a given step ut. The purpose of the following hematical proof is to show that none he trajectories m^*, m^{**}, and n^* can ur.

If the trajectory n^* occurred, the of change of the slope $d\dot{e}/de$ with ect to time t would have to change From equations 2 and 3,

$$\frac{d\dot{e}}{dt}\Big/\frac{de}{dt}=\frac{d\dot{e}}{dt}\Big/\dot{e}$$

$$=\left(\frac{A}{T_1^2}\epsilon^{-t/T_1}+\frac{B}{T_2^2}\epsilon^{-t/T_2}\right)\Big/\left(-\frac{A}{T_1}\epsilon^{-t/T_1}-\frac{B}{T_2}\epsilon^{-t/T_2}\right) \quad (5)$$

refore,

$$\left(\frac{\dot{e}}{e}\right)\Big/dt=\frac{AB(T_1+T_2)^2}{T_1^3T_2^3\left(\frac{A}{T_1}\epsilon^{-t/T_1}+\frac{B}{T_2}\epsilon^{-t/T_2}\right)}\times\epsilon^{-\left(\frac{t}{T_1}+\frac{t}{T_2}\right)} \quad (6)$$

s expression does not change sign as a ction of t; and hence the trajectory n^* not occur.

It is obvious that the trajectory cannot occur: for the approach of m^* from the left implies the impossible irement of e increasing with time for ing negative.

The occurrence of m^{**} would imply lative configuration of m^{**} and n as wn in Fig. 8. This seems possible be- se both m^{**} and n are concave upward intersect the e-axis at the right points. se trajectories now have three intersections in the fourth quadrant of the phase plane. If this should occur, P would still be the optimum switching point and the switching line OP would still put m^{**} and n in two separate half planes. However, the use of another switching line OP' would result in a dead-beat response with one switching during the transient. This would mean that the dead-beat transient response would not correspond uniquely to the optimum response.

It is recalled that the phase-plane trajectories for the second-order systems under consideration always diverge asymptotically from the fast eigenvector and approach asymptotically to the slow eigenvector. Therefore, in the fourth quadrant of the phase plane, the m trajectories should have a slope between $+\infty$ and $-1/T_2$ and the n trajectories should have a slope between $-1/T_1$ and $-\infty$. Since $-1/T_2$ is larger than $-1/T_1$ algebraically, the slope of m should always be larger than that of n in the fourth quadrant. This condition is violated at the intersection point P in Fig. 8 where the slope of m^{**} is less than that of n. Therefore m^{**} cannot occur. The same reason rules out all possibilities but that of only one intersection of the m and n trajectories in the fourth quadrant.

Thus, it has been shown mathematically that optimum response can always be achieved by using proper linear switching and that optimum response corresponds uniquely to dead-beat response for the systems under consideration.

Computer Study

The objective of the computer study was twofold: 1. To determine the optimum system response time as a function of the available forcing and of the parameters of the controlled element when a system exactly like that in Fig. 1 is obtainable; 2. To determine the effects upon the optimum response time in a typical case when the exact control system of Fig. 1 has to be modified for various practical reasons given in the previous sections. The analog computer was used because analytical methods were time-consuming and the 1 to 2% error in the computer results is considered within reasonable tolerance for practical purposes.

It has been pointed out in the previous section that the optimum response provided by the system in Fig. 1 can be exactly reproduced through proper linear switching if the input step is fixed. Hence, the first objective of the computer study was attained by conducting computer experiments on the system shown in Fig. 9. Here the error derivative $\dot{e}$ $(=-\dot{c})$ is exact since no disturbance is introduced into the output element. The system is optimized by adjusting a, which controls the slope of the switching line, until the system error comes to rest after exactly one switching of the on-off amplifier. The realization of optimum response can be checked further by seeing that the output transient has neither overshoot nor a tail. The information on the exact optimum response time is presented in the form of a family of curves in Fig. 10. The parameters are normalized in order to maximize the range of application of the curves. Symmetrical forcing is assumed for these results.

The second objective of the computer study was attained by performing computer experiments on a typical system with ± 50 volts of available forcing and controlled element with the following nominal parameter values:

Gain $K=2.5$
Time constants $T_1=1$ second
$T_2=2$ seconds

The results are tabulated in the Appendix.

Part I of the Appendix shows the response time of the optimized system for

various step inputs. The results differ from those in Fig. 10 because of different definitions of response time. In Fig. 10, the response time is defined as the time required for the system error to return with $\pm 1\%$ of 50 volts, or $\pm 1/2$ volt, after the application of a step input. The values in Part I serve as a standard of comparison for the following results.

Part II shows the effect of variation of step inputs when the linear switching line is adjusted only for optimum response following a step input of 50 volts and is held fixed thereafter for any other inputs. The responses of the system to step inputs other than 50 volts are therefore non-optimum. However, there is little difference between the response times of Part I and their corresponding ones in Part II. This confirms the belief that the exact switching curve nn' of Fig. 3 is nearly linear for a second-order, overdamped, controlled element, and hence nn' can be approximated quite satisfactorily by a straight line. The results in Part II are significant in that they justify the use of linear switching. Note that the method of obtaining the exact $\dot{e}$ in Fig. 9 is good only when there is no load disturbance on the controlled element. Therefore, this method cannot be used in practice. Fig. 11 shows the basic system simulated on the computer for all of the remaining parts of the computer study. This system uses an approximation to the $\dot{e}$ signal and is constructed in such a manner that disturbances can be injected in any one of four locations.

Part III shows the effect of using approximate instead of exact $\dot{e}$ in addition to linear switching. The time lag T_d of the derivative network is 0.01 second. The results of this part indicate that the increases of response time, compared with Part I, are well within 10%. The lag effect due to T_d helps to reduce the effect of high-frequency pickup or noises. Fig. 12 shows the transients resulting from a 10-volt step, using approximate $\dot{e}$ in the system, while the linear switching line has been adjusted to give optimum response for a 50-volt step input.

Parts IV and V show the effect of an appreciable third time constant T_3. In Part IV, $T_3=0.1$ second and in Part V, $T_3=0.5$ second. Results again appear in the Appendix. These results indicate that a third time constant (T_3) of 1/10 the smaller time constant, $1/10T_1$, does not appreciably affect the system response; however, for $T_3=1/2T_1$, the system is adversely affected. In such cases, the system should be treated as essentially third order. Systems higher than the second order can be optimized by measuring the second and higher derivatives of the error. However, they will not be considered in this paper.

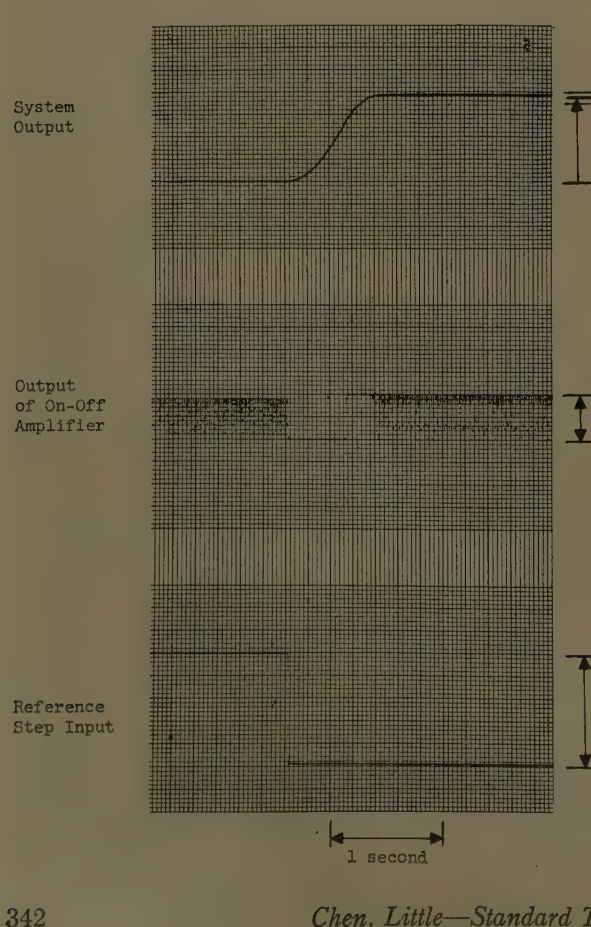

Fig. 12. Computer result, 10-volt step input with approximate $\dot{e}$; system optimized for 50-volt step input

In order more fully to justify the sys tem described, the following study of tl effects of drift and disturbances are mad The system was adjusted for optimu response to a 50-volt step change reference. The reference was then plac at 50 volts and T_3, U, U', D, and D' we set to zero unless otherwise indicated l the following description.

1. The effects of disturbances are shown Parts VI through IX of the Appendi Some response times are zero because t disturbances are so small that the err never exceeds ± 1 volt during the transien These results indicate that the system o timized for 50-volt step input can regula satisfactorily under various load distur ances.

2. The effects of drift and 60-cycle pick upon the steady-state error are shown Parts X through XIII. Note that th experiment involved adding a d-c level points indicated in Fig. 11. This did n involve step or ramp disturbances.

These results indicate that the optimu system has good accuracy, as may expected due to the extremely high ga of the on-off amplifier. The drift at t input end of the controller is equivalent error in the system measurement devi and is therefore directly reflected in t system error. The ability of the syste to regulate satisfactorily under a lar amount of 60-cps (cycles per secon pickup is of interest. It shows that t lead network does not accentuate hig frequency noises to an unacceptable e tent.

The last portion of the computer stud Part XIV, consisted of varying the valu of T_1, T_2, and K and recording the syste response to a 50-volt step change in ref ence. In this part, as in the parts i mediately preceding, the system was for optimum response following a 50-v step change in reference with $T_1=$ second, $T_2=2$ seconds, and $K=2.5$. T response time for each condition, i.e., various values of T_1, T_2, and K, is in cated in Part XIV of the Appendix. T actual curves for cases 9 and 10 in t part are shown in Figs. 13(A) a (B), respectively. These correspond t change in both time constants of 30% a a change in K by 69%, representing t variation in these parameters due to t change in the resistance of copper w in a 2-stage electrical amplifier (magne amplifiers or rotating machines) when t temperature is varied from -60 F (grees Fahrenheit) to 180 F (-50 C [grees centigrade] to 75 C). Note th although the responses in the last part the computer study were not optimu the response time was still well wit 10% of the optimum values, which w

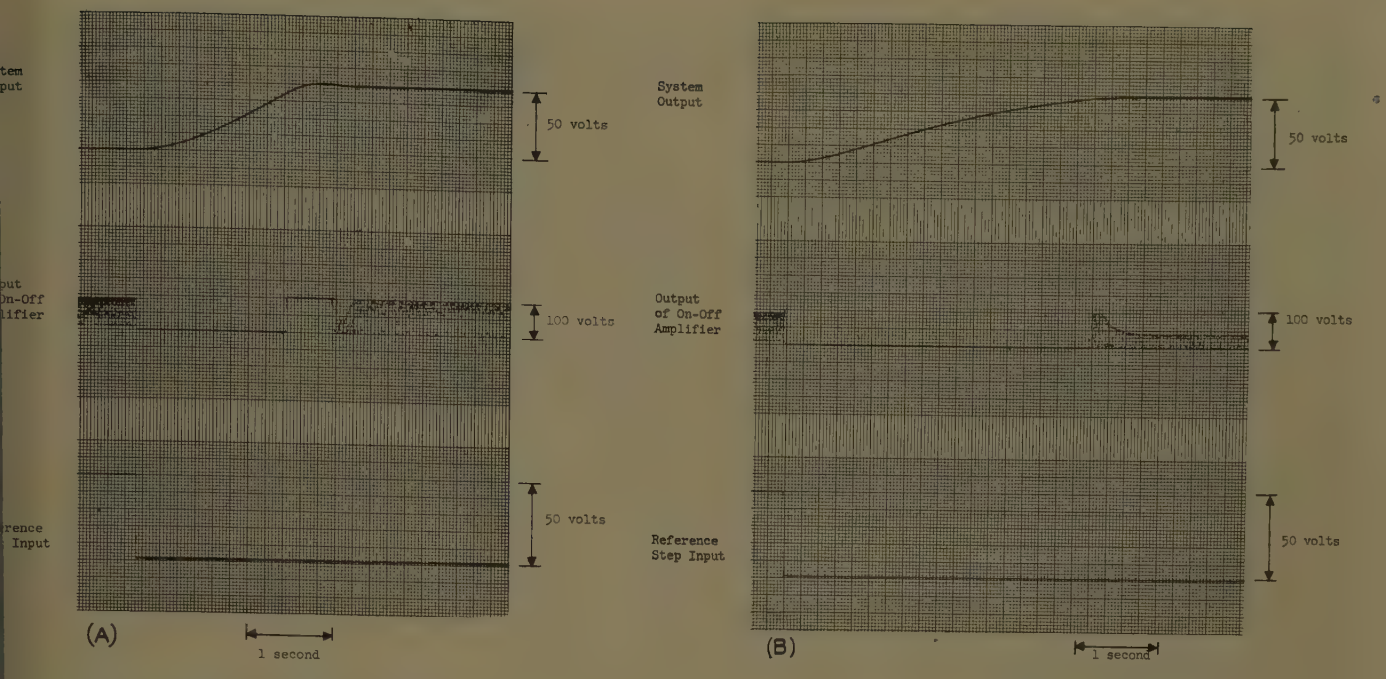

Fig. 13. Computer result, 50-volt step input, approximate ė; system optimized for 50-volt step input under normal temperature

A—System under simulated high temperature
B—System under simulated low temperature

ained by readjusting the switching . This shows that the practical tems under study have "flat" optimum ponses; that is, their optimum re- nses are not critical to parameter iations.

A brief study has also been made on the nputer as to the effect of slight non- arities, especially the saturation type, the controlled elements. The con- sion is that the switching line can ays be readjusted to give optimum response. No special adverse effects have been observed that can be ascribed to the presence of slight nonlinearities in the output elements.

In summary, the results of the computer study are quite encouraging, as evidenced by the values in the Appendix. The experience gained during the computer study confirmed the earlier prediction that the optimization of system response can be quickly achieved by simple adjustments of the switching line.

Practical Circuits

Because of its simplicity and flexibility, the lead network shown in Fig. 4 will be used as the inherent compensation of the controller. The main problem is then the physical realization of the on-off amplifier. Ideally the amplifier should have the following characteristics: 1. No delay in responding to command; 2. No delay in switching from one state of output to the other; 3.

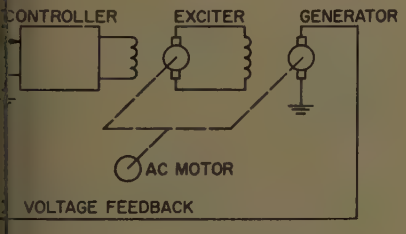

Fig. 14. Voltage regulator

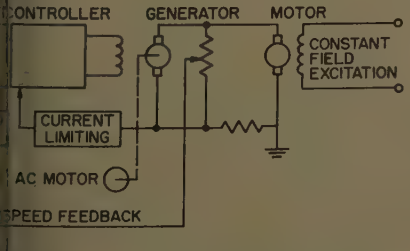

g. 15. Ward Leonard speed regulator

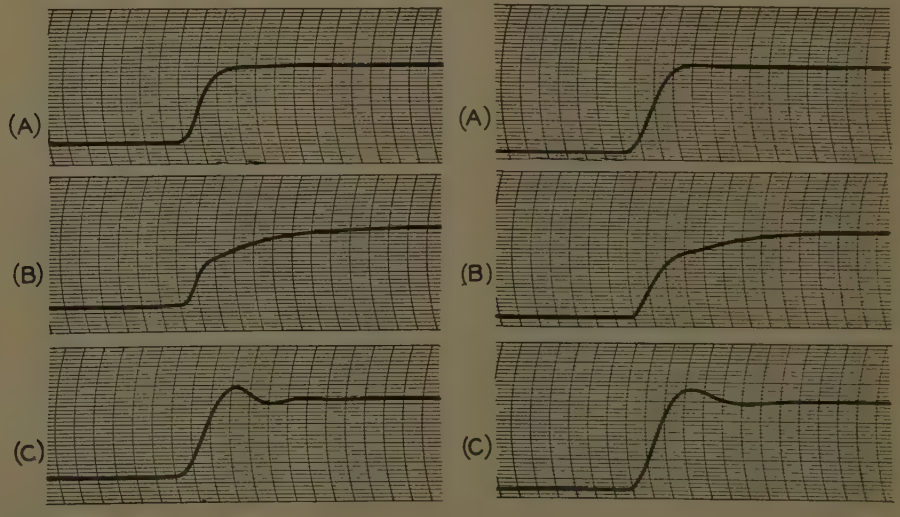

Fig. 16. Demonstration unit

Rugged; no wear and tear; 4. Long life; 5. Wide range of input and output power levels; 6. No zero drift; 7. No hysteresis or dead zone; 8. Minimum cost.

To satisfy the first three requirements, transistors were chosen as the basic components, although high-frequency magnetic amplifiers can provide similar characteristics. The fourth and fifth requirements are achieved by operating transistors as switches with appropriate derating. The last three conditions are, in general, not compatible. How good a compromise can be reached depends on engineering judgment and ingenuity of circuit design.

Several practical circuits have proved to give similar gross characteristics approximating those listed in the foregoing for an ideal on-off amplifier. A variety of circuits are used to satisfy different needs of output forms, e.g., single-ended and push-pull, d-c and a-c, single-phase and multiphase. The details and analyses of these circuits will be reported elsewhere. However, it is of interest to point out that all these circuits are functionally represented by the single block for the on-off amplifier in Fig. 1. Therefore, the approach is that of forcing a physical system to take the desirable functional form depicted by Fig. 1, with the exception of using linear switching. The difficulty in analyzing an on-off system with dead time delay and/or hysteresis is thus avoided.

Practical Demonstration

The new controller has been employed in a variety of control systems. While its industrial application will be reported elsewhere, we shall describe its application in a demonstration unit, which can be either a voltage regulator or a Ward-Leonard speed control system, depending on the mechanical and electrical arrangement. The unit is composed of an a-c motor and two d-c machines. Diagrams of the two possible configurations are shown in Figs. 14 and 15, respectively. Parts A, B, and C of Fig. 16 show the output responses of the two systems when switching occurs properly, too early, and too late. Notice that optimum response in part A gives minimum response time. Each of these systems are essentially second order. The voltage regulator time constants are the fields of the exciter and generator. The generator field time constant and the mechanical time constant of the motor produce second order system for the speed control. In both cases the system response is made optimum by simply adjusting one knob which controls the capacitance of the derivative network.

Conclusions

The standard transistorized optimum response controller gives nearly optimum response to a great variety of feedback control systems under a wide range of input conditions. Its proper application should not only save materials cost but, more important for system engineering, reduce development cost.

The results of using linear switching function to obtain nearly optimum response are quite encouraging. Its extension to higher order systems would lead to the division by the phase space into two halves by a hyperplane, which could be generated without a multivariable function generator though higher derivatives would still have to be measured.

The successful development of the standard transistorized optimum response controller has proven that it is more rewarding practically to force a physical system to take a desirable functional form by hardware synthesis rather than to analyze an on-off servomechanism including all the imperfections of the on-off device.

Appendix. Results of the Computer Study

Step Change in Reference, Volts	Seconds				
	Part I	Part II	Part III	Part IV	Part V
50	2.0	2.0	2.04	2.04	8
100	4.44	4.44	4.54	4.6	8.06
10	0.66	0.66	0.7	0.82	4.02
1	0.13	0.14	0.15	0.28	0.44

PART VI

Step Change in U, Volts	Response Time, Seconds
5	0
10	0.76
30	3.04
1	0

PART VII

Step Change in U′, Volts	Response Time, Seconds
12.5	1.02
25	1.4
75	2.5
1	0.1

PART VIII

Ramp Change in U	Response Time, Seconds
50 t	0
10 t	0
30 t	5.04
t	0

PART IX

Ramp Change in U′	Response Time, Seconds
12.5 t	0
25 t	0.78
75 t	3.36
t	0

PART X

Signal on D	Change in Error, (Δe), V
10	0.15
1	0.02

In Parts X through XIII, 0.5 $V = 1\%$

PART XI

Signal on D′, Volts	Change in Error, (Δe), V
10	10
1	1

PART XII

60-CPS RMS, Volts	Error, Volts
0.15	−0.0
0.3	0
0.4	+0.
0.45	+0.
0.52	+0.

PART XIII

60-CPS RMS, Volts	Error, Volts
7	+0.
4	+0.
3	+0.

PART XIV

T_1	T_2	K	Actual Response Time, Seconds	Ideal Response Time, Sec
1	2.4	2.5	2.35	2.25
1	1.6	2.5	2.0	1.85
1.2	2	2.5	2.25	2.25
0.8	2	2.5	2.0	1.82
1	2	3	1.9	1.8
1	2	2	2.6	2.6
1.2	2.4	3.6	2.1	2.0
1.2	2.4	1.6	3.8	3.8
0.7	1.4	1.225	3.3	3.3
1.3	2.6	4.125	2.3	2.1

References

Nonlinear Techniques for Improving o Performance, D. C. McDonald. *Proceed-* National Electronics Conference, Chicago, ol. 6, 1950, pp. 400–21.

A Phase-Plane Approach to the Compensa- of Saturating Servomechanisms, A. M. Hopkin. *AIEE Transactions*, vol. 70, pt. I, 1951, pp. 631–39.

3. On the Bang-Bang Control Problem, R. Bellman, I. Glicksberg, O. Gross. *Quarterly of Applied Mathematics*, Providence, R. I., vol. 14, 1956, pp. 11–18.

4. Differential Equations with a Discontinuous Forcing Term, D. W. Bushaw. *Report no. 469*, "Experimental Towing Tank," Stevens Institute of Technology, Hoboken, N. J., 1953.

5. Process Instruments and Controls Handbook (book), D. M. Considine. McGraw-Hill Book Company, Inc., New York, N. Y., 1957, section 5.

6. On the Synthesis of Optimalized Control Loops, C. Kessler. *Regelungstechnik*, Dec. 1954–Feb. 1955.

7. Discontinuous Automatic Control, I. Flugge-Lotz. Princeton University Press, Princeton, N. J., 1953.

Discussion

old Chestnut (General Electric Com- y, Schenectady, N. Y.): The authors to be complimented on a most interest- and valuable paper, in which the prac- aspects of performance that can be ob- able with standardized controller equip- t are emphasized. In stressing the im- ance of cost and reliability as factors to iven proper consideration by the con- er system designers, the authors have erly placed the attention on those por- s of the controller system design which he past have not received proper atten- namely, reliability and cost. Through se of standardized components in con- ers, it is to be hoped that improvements oth reliability and cost can be made h far outweigh the minor degradation rformance of the order of 10% which ars to have been obtained in the results d for this paper.

their paper, the authors have answered y questions concerning the control of second order systems. The writer would appreciate hearing from the authors what approach is suggested when higher order systems are employed and in systems in which the parameters of the system may change of the order of plus or minus 20%. Have the authors been able to develop criteria for obtaining an equivalent second order system, for systems actually having higher orders up into the fourth and fifth order category which equivalent second-order systems prove to have the satisfactory characteristics for describing the actual system performance?

Kan Chen and **D. R. Little**: The authors wish to thank Mr. Chestnut for his comments on the paper. It is heartening to hear an experienced control expert agreeing with the authors on the theme of this paper, which stresses the practical aspects of nonlinear control systems.

Part XIV of the Appendix gives the effects of parameter changes in the order of plus and minus 30% for a second order system controlled by the standard transitorized optimum response controller. For higher order systems, the extension of the linear switching approach means to divide the phase space into two halves by a hyperplane. The authors have studied the case of an essentially third order system on an analog computer. It was not difficult to obtain the exact $\dot{e}$ and $\ddot{e}$ (first and second derivatives of the error signal) on a computer.

A converging experimental procedure was developed to determine the proper linear combination of e, $\dot{e}$ and $\ddot{e}$ in the compensation network in order to achieve optimum response to a step input. This means the determination of the proper switching plane in the three dimensional phase space by experiment. However, in a practical circuit, it was difficult to obtain both $\dot{e}$ and $\ddot{e}$. It was even more difficult to obtain independent adjustments of the multiplying factors for $\dot{e}$ and $\ddot{e}$. Therefore, no practical results can be reported at this time in regard to high-order optimum response systems using linear switching.

olar-Powered Thermoelectric Generator Design Considerations

N. F. SCHUH
MEMBER AIEE

R. J. TALLENT
ASSOCIATE MEMBER AIEE

psis: With the coming space age, derable attention is being focused the problem of supplying secondary r to the vehicles of the future. It is ipated that future space vehicles perform missions which will require hs and perhaps years to complete. irements for the secondary power e serving these vehicles will be very ent. Weight will be at a premium, fore, the unit must have a high power- ight ratio. Reliability must be high ust be accomplished with little or no enance and without excessive re- ancy. The life expectancy must be

sent-day systems possess a number rtcomings which may preclude their n extended mission vehicles. There ne doubt that these systems can be sfully modified to overcome these comings. Accordingly, much effort g expended to explore new types of systems which will be able to meet eds of this new age.

One system that appears to show considerable merit is a solar-powered thermoelectric generator. Solar power is fairly abundant in space, and the solar-powered system would have an advantage in that it would require no fuel or shielding. The thermoelectric generator is a static conversion device and should have a fairly long life with good reliability. This paper presents, in a brief manner, some of the principles and problems which may be expected in applying solar energy to a thermoelectric generator serving a space vehicle and also describes a small solar-powered thermoelectric generator which was constructed to study these problems.

A THERMOELECTRIC generator operates as a heat engine to statically convert heat into electricity. As such, heat must flow through the thermoelectric material. Some of this heat is converted into electricity and the remaining unavailable energy must be dissipated. A solar system will thus consist of:

1. A means for collecting and concentrating the solar energy.
2. A means for converting the radiant energy into heat.
3. A thermoelectric generator.
4. A means for dissipating the waste heat.

Basic Elements

Collector–Concentrator

The solar-energy density at various points in the solar system is shown in

Paper 59-847, recommended by the AIEE Air Transportation Committee and approved by the AIEE Technical Operations Department for presentation at the AIEE Summer and Pacific General Meeting and Air Transportation Conference, Seattle, Wash., June 21–26, 1959. Manuscript submitted March 23, 1959; made available for printing April 23, 1959.

N. F. Schuh is with Westinghouse Electric Corporation, Lima, Ohio, and R. J. Tallent is with the Boeing Airplane Company, Seattle, Wash.

The authors wish to acknowledge the valuable guidance of S. J. Angello and others, Westinghouse Research Laboratory, in the field of thermoelectricity; and the contributions made by the members of the Materials and Processes Staff and Systems Management Office, Boeing Airplane Company, in the field of solar energy.

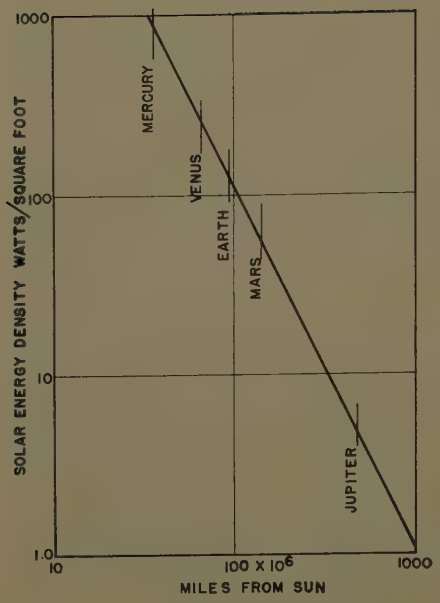

Fig. 1. Solar energy density at various points in solar system

Fig. 1. This plot shows that the power densities in the areas of space in which man may be interested will be too low to efficiently operate a heat engine so some means must be provided for increasing the energy density to workable levels.

The energy density can be increased by collection and concentration with some type of a reflective concentrator or mirror. The optical design and construction of a large-scale reflective concentrator for a power system will be similar to that of a solar furnace. However, concentration requirements will be much less. The term "concentration ratio" as used hereafter is defined as the ratio of the image-energy density with concentration to the energy density without concentration assuming a perfect concentrator with a reflectance of unity. Table I shows the input heat density of some present-day thermoelectric materials and the concentration ratio necessary to provide these densities in space. Note that only fairly modest ratios will be required, whereas solar furnaces usually require concentration ratios in the order of 10,000–30,000. A review of the published papers[1–14] covering the theory and design of solar furnaces indicates that with the low concentrations required, the optical design of a power-system concentrator should not be a major problem.

Table I. Input Heat Density of Some Present-Day Thermoelectric Materials

Thermoelectric Materials	Heat-Input Density, Watts/Sq Ft	Concentration Ratio Required to Supply Heat Input Plus Radiation Loss
Lead–telluride—P Lead–telluride—N	1,400	26
Zinc–antimonide—P Indium–antimonide—N	5,000	61
Lead–telluride—P Indium–antimonide—N	4,000	51

Solar constant = 130 watts/sq ft
Hot junction temperature = 450 C (723 K)
Cold junction temperature = 270 C (543 K)
Length of element = 0.5 inch
$\alpha = \epsilon = 1.0$
Furnace factor = 0.8
Solar-image area equal to load area

In space applications the major concentrator problem is one of a mechanical nature. Because of the large area which will be required, the collector must be in a collapsed form during the ascent through the dense air and must then be extended or erected upon reaching space altitudes. The extension system must be capable of forming a large complex surface with good accuracy. Considerable work is being done by the National Aeronautics and Space Administration and others on the problem of developing suitable extension systems.

Some shapes may be more easily formed by an extension system than others. Some reflective systems which have been considered for terrestrial applications are shown in Fig. 2 and may be worth considering from the standpoint of reducing the extension problem. Fig. 3 compares the concentration ratio of some of the more basic designs. Note that for the small concentration ratios, the simple shapes perform nearly as well as a parabola.

In a practical system, the concentrator will not deliver all of the intercepted energy to the solar image. Losses will occur due to the absorption at the reflective surface, scattering as caused by diffuse reflection, and imperfections in the basic shape. The total intercepted energy must be increased by some factor to account for these losses. In solar furnace work this factor is commonly called the "Furnace Factor" and was found to vary from about 0.3 to 0.7. Because of the low concentration ratio required in a thermoelectric system, it is expected that somewhat higher factors may be attained.

Absorber

The absorber has the function of converting the collected radiant energy into heat and conducting this heat to the generator. The conversion efficiency will depend upon the shape, surface materials, area, and temperature. The effect of the absorber shape on performance will be discussed in a companion paper.[4]

The incident energy which strikes the absorber will be either reflected or

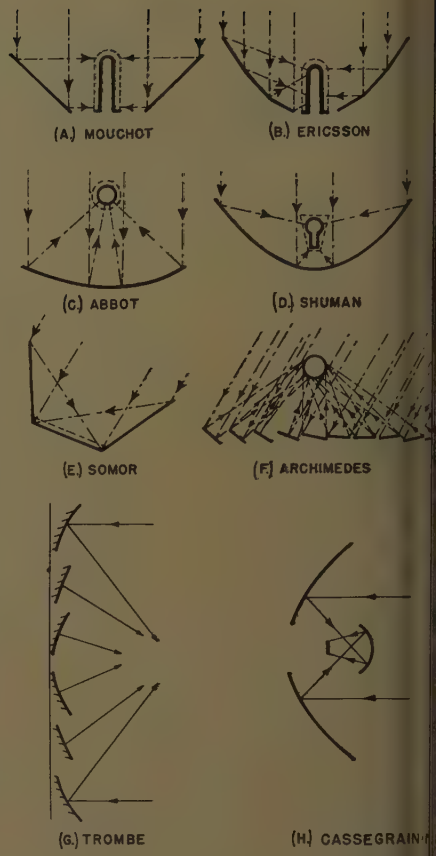

Fig. 2. Solar energy concentration syste from references 1–3

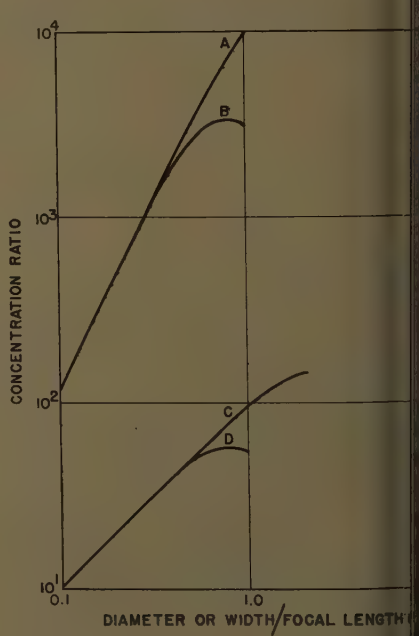

Fig. 3. Concentration ratios for va concentrator designs

A—Paraboloid or circular Archimedes
B—Semisphere
C—Parabolic cylinder or rectangular A medes array
D—Semicircular cylinder

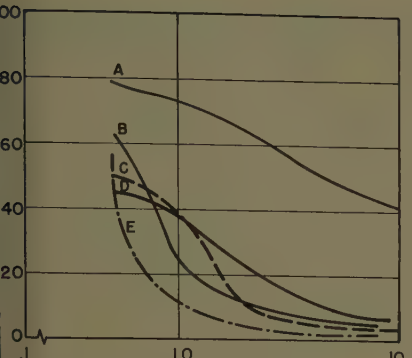

4. Spectral emissivity of some elemental urfaces; data taken from reference 5

A—Graphite
B—Tantalum
C—Tungsten
D—Iron
E—Copper

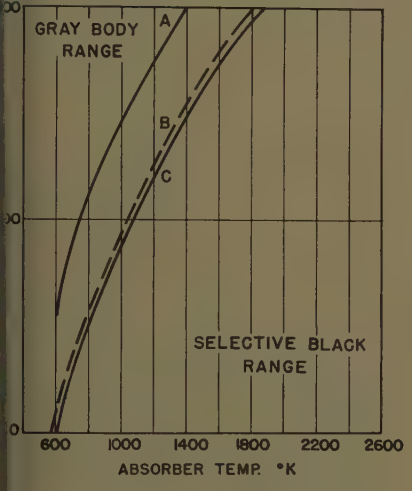

5. Dividing lines determining applica-n areas for absorber surface coatings

A—$\alpha=0.8$, $\epsilon=0.1$
B—$\alpha=0.7$, $\epsilon=0.5$
C—$\alpha=0.4$, $\epsilon=0.07$
Solar constant = 130 watts/ft²
Furnace factor = 0.8
Reference gray body = $\alpha=\epsilon=0.95$

rbed. The ratio between the ab-ed energy and total-incident energy es the absorptivity coefficient of the ce. The absorbed heat will thus be l to

$SA_cF\alpha$

e

bsorptivity coefficient to solar energy olar energy density, watts/sq ft (watts per square foot)
area of the concentrator, sq ft
urnace factor

me of the absorbed heat will be lost infrared radiation from the hot absorber surface. This loss can be expressed by the following equation:

$$Q_r=\epsilon\sigma A_a(T_a^4-T_o^4)$$

where

ϵ = emissivity coefficient at the temperature of the absorber
σ = Stefan-Boltzman constant = 5.267×10^{-9} watts/sq ft/degree⁴
A_a = area of the absorber, sq ft
T_a = temperature of the absorber, degrees Kelvin (K)
T_o = effective sink temperature, K

The heat available to the generator will thus be the difference between the absorbed power and the radiated heat. The heat-balance equation of the absorber can be written as follows:

$$Q_a=Q_g+Q_r$$

or

$$\alpha SA_cF=Q_g+\epsilon\sigma A_a(T^4-T_o^4)$$

where

Q_g = heat delivered to the thermoelectric generator

From this equation, it is evident that the heat delivered to the thermoelectric generator will be increased when either the absorptivity is increased, the emissivity decreased, or the absorber area decreased by increasing the concentration ratio. By maximizing the power delivered, the area of the concentrator can be reduced and a saving in weight realized.

If the absorber area is made small in an effort to reduce the radiation loss and the input heat density becomes much larger than the generator density, much of the heat must then be conducted over a fairly long path. The weight of the heat transfer system may offset the weight saving in the concentrator. Additional study will be required to optimize the absorber area with respect to the other elements of the solar system.

It is obvious that for a given absorber area, concentrator, and solar constant, the heat delivered will be a maximum when the solar absorptivity is equal to unity and the low-temperature emissivity is equal to zero. Unfortunately, materials with such properties are not available. However, in many materials the emissivity-absorptivity coefficient is not a constant but changes with temperature and wavelength. It may be possible to select materials which have the property of efficiently absorbing solar energy but inefficiently radiating infrared thus approaching the ideal material. Such materials are called selective blacks. Fig. 4 shows the spectral emissivity characteristics for some materials.

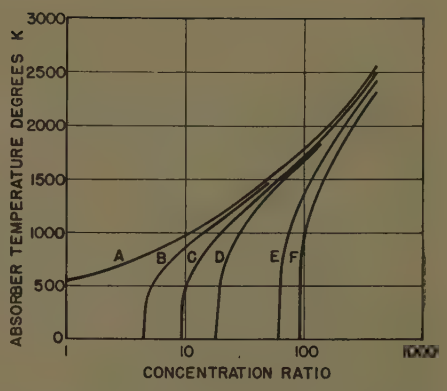

Fig. 6. Absorber temperature and concentration ratio relations at various input heat densities to thermoelements

A—0 watts/ft²
B—250 watts/ft²
C—500 watts/ft²
D—1,000 watts/ft²
E—2,000 watts/ft²
F—5,000 watts/ft²
Solar constant = 130 watts/ft²
Furnace factor = 0.7
$\alpha=0.6$, $\epsilon=0.1$

From the absorber heat-balance equation, it can be shown that under certain conditions, selective black materials with less than ideal characteristics will be superior to highly absorptive gray-body materials ($\alpha=\epsilon=$constant). Fig. 5 compares three selective blacks with a highly absorptive gray body. These curves show the concentration ratios and temperatures at which a selective black is equal to the gray body. The selective black will be superior at all points falling to the right of the appropriate curve and the gray body superior for all points to the left side of the curve. In general, for a given concentration ratio, the selective blacks will be superior at the higher temperatures and the gray body at the lower temperatures.

The absorber heat-balance equation also provides a means for calculating the temperature of the absorber. The temperature of the absorber is jointly fixed by the heat loss from the absorber surface and the heat flow through the thermoelectric generator to the radiator and thence to space. The expression defining the absorber temperature in these terms is quite complex and awkward. The calculation can be simplified by assuming the power flow through the thermoelectric generator to be a constant. Based on this simplifying assumption, Fig. 6 shows the absorber temperature as a function of concentration ratio with input heat density as a parameter.

Thermoelectric Generator

A brief review of thermoelectric theory may be helpful in understanding the

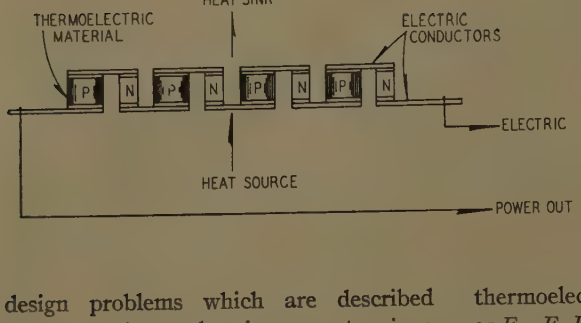

Fig. 7. Basic thermoelectric generator arrangement

design problems which are described later. A thermoelectric generator is a heat engine and therefore the maximum available fraction of the total energy is given by the Carnot cycle efficiency. This cycle efficiency, E_c is expressed as the difference in the heat-in and heat-out temperatures divided by the heat-in temperature in absolute degrees.

$$E_c = \frac{T_a - T_r}{T_a}$$

The portion of this available energy which can be converted by a thermocouple (called the thermocouple efficiency, E_{tc}) is a function of the thermoelectric material properties and the temperature. The basic material properties are the Seebeck coefficient S (in volts-per-degree-centigrade temperature difference between junctions), thermal conductivity, k, and electrical resistivity, ρ. A figure of merit Z, relating these materials properties is expressed as $Z = S^2/\rho k$.

By considering the effects of Peltier heat, Thomson heat, and Seebeck voltage it can be shown that the thermocouple efficiency is

$$E_{tc} = \frac{\sqrt{1+TZ}-1}{\sqrt{1+TZ}+T_a/T_r}$$

Now the over-all efficiency E of a thermoelectric generator can be expressed as $E = E_c E_{tc}$ and the electric power output available is $P = Q_g E_c E_{tc}$, where Q_g = the heat flow into the thermoelectric material.

It is important to note that the material properties appear only as S^2 divided by ρk in the expression for efficiency. This indicates that the material properties are not independently important but only in respect to one another.

Metals are not good materials for thermoelectric power generators because of their low thermocouple efficiency. By plotting the figure of merit with respect to the current-carrier density or resistivity it can be shown that the best thermoelectric materials apparently lie in the semiconductor or semimetal range. Indeed, most of the material development today is directed at thermoelements in this range. Unfortunately, semiconductors are not high-temperature materials, being limited to 500–700 C (degrees centigrade) as far as we know today. This means that the heat energy available in the form of burning fuels, concentrated sunlight, and nuclear reactors cannot be used at its maximum temperature and therefore maximum energy conversion cannot be obtained. It would be very desirable then to increase the efficiency by increasing the operating temperature of the thermoelement materials. A large effort is underway to convert insulator class materials into good thermoelectric materials by increasing their electrical conductivity without appreciably increasing their thermal conductivity or decreasing their Seebeck voltage. Mixed valence materials such as lithium nickel oxide appear very promising in the 700–1,500 C range.

The major electrical characteristics of a thermoelectric generator can be defined by the power output, the open-circuit voltage, and the internal resistance. The power output at matched load has previously been given approximately as the product of the heat flow into the material and the over-all efficiency. The open circuit voltage (V_o) is calculated from

$$V_o = NS\Delta T$$

where

N = number of thermoelements
S = Seebeck voltage
$\Delta T = T_a - T_r$

The internal resistance of the genera (R_g) is calculated from

$$R_g = N\rho l/A$$

where

ρ = electrical resistivity
l/A = dimensions of the thermoelements

Maximum load power occurs when load resistance is equal to R_g. The l voltage then is equal to 1/2 V_o. In practical case voltage drops will also oc at the contacts and in the conduct These drops are generally assumed to no greater than 5% of the total voltag

The design of a thermoelectric gen tor will vary greatly with energy sou application, environment, and mate state-of-the-art. Whatever the detai appearance, however, a heat path mus provided from the heat source, thro the thermoelements, and into the sink as shown in Fig. 7. Generally sp ing, the elements are thermally in par and electrically in series which indic one of the problem areas in any prac design. Thermal contact areas mus good heat conductors and at the same must be good insulating electrical faces.

Another problem area results from relatively high operating temperature countered. High-temperature the elements must be connected together high-temperature conductors, held gether with high-temperature struc materials, and protected by high-temp ture finishes. These requirements re the number of available materials w

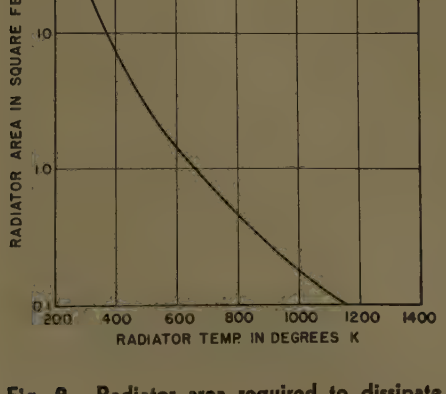

Fig. 8. Radiator area required to dissipate 1 kw of heat

$\epsilon = 1.0$
Sink temperature = 0 K

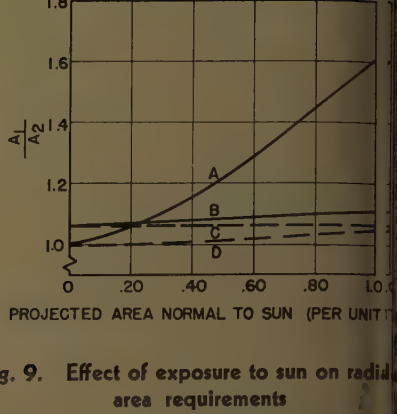

Fig. 9. Effect of exposure to sun on radia area requirements

A—$\epsilon = \alpha = 0.95$, $T_r = 500$ K
B—$\epsilon = 0.9$, $\alpha = 0.1$, $T_r = 500$ K
C—$\epsilon = 0.9$, $\alpha = 0.1$, $T_r = 1{,}000$ K
D—$\epsilon = \alpha = 0.95$, $T_r = 1{,}000$ K
A_1 = area required with various exposures to sun
A_2 = gray-body area required with no exposure to sun

g. 10. Solar-powered thermoelectric generator test model; vacuum enclosure not shown

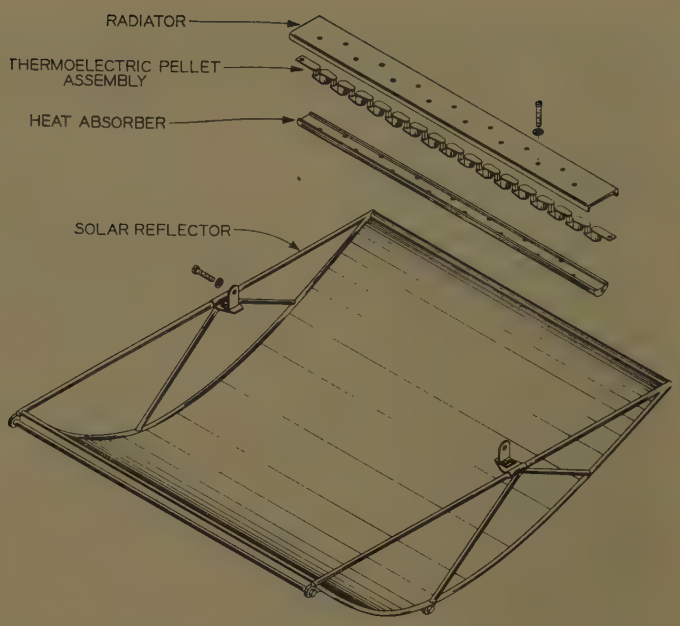

Fig. 11. Exploded view of principal elements of solar-powered thermoelectric generator test model

n be used even at nominal thermo-ctric temperatures like 400–500 C.

A thermoelectric generator is essentially low-voltage high-current device with a latively high internal impedance. This eans that the output voltage will change nsiderably with load. The change in ad voltage with load current will not be actly linear because of the Peltier effect. he Peltier effect is in such a direction as tend to cool the hot junction and heat e cold junction. As the current is re-ced by increasing the load resistance, e hot and cold junction temperatures nd to increase. These increases tend to approximately the same so that ΔT is most constant. Deviations from linear ltage regulation are due to changes in T and the resultant changes in material aracteristics with temperature change. Because of the inherently slow response ne of such a thermally operated device, od voltage regulation under load anges would be difficult to obtain by ying to control the heat flow. In most plications it is anticipated that some rm of power-conversion equipment will used either to raise the direct voltage vel or to convert the direct current to ternating current. Voltage regulation n be very nicely accomplished in this nversion equipment.

ADIATOR

The function of the radiator is to dissi-te the waste heat from the generator it and to control the temperature of the ld junction. At the present, the radiator appears to be one of the larger problem areas in a solar-powered thermoelectric system.

In space, the only mode for heat removal is by radiation. Fig. 8 shows the familiar relation between the radiator area and temperature required to dissipate 1 kw of heat. To attain a high Carnot efficiency, the radiator temperature should be as low as practicable, however, low temperatures can only be attained with large radiator areas. With a large radiator and concentrated input, a major portion of the waste heat will be dissipated at areas somewhat removed from the source, and some means must be provided for conveying the heat to these areas.

If a solid-material heat-conduction system is used, the flow of heat by conduction to the dissipative areas will cause a temperature drop. If the drops are large, extra area must be added to compensate for the reduced performance. Since this area will be added at an even greater distance from the source, the dissipative capabilities will be quite low and a point of diminishing returns is rapidly reached.

The flow of heat in a radiator is a complex problem of two-dimensional heat flow. This problem is currently being studied with the aid of a computer. At the time of writing, detailed results have not been obtained. Approximate results indicate that if the power inputs are high and radiation temperatures low, fairly large thermal-conductor cross sections will be required with attendant larger weights.

In a space solar-powered system, the efficiency of the conversion device may not be as significant as in the more familiar terrestrial applications. Solar energy is abundant and free. The main consequence of reduced efficiency will be to increase the size of the concentrator and the conversion device. Since the goal in space applications is to obtain a large power-to-weight ratio, it may be desirable to sacrifice efficiency by using higher radiator temperatures, thereby reducing the radiator weight. Optimization studies will be required to determine the best radiator temperature.

Another factor which will influence the radiator area is the orientation of the emissive surfaces. In some solar systems, the radiator will be exposed to the sun. If the radiator area is to be kept to a minimum, the heat input from the sun must be kept small. This can be done by keeping the area facing the sun small and by using suitable selective black material for the radiator surface. Fig. 9 shows the effect of selective blacks on the total area required with various percentages of the area normal to the sun. Note that if good selective blacks are available or if the temperature is high the solar energy does not significantly increase the radiator area.

In other solar systems, the radiator will be shaded from the sun but exposed to the earth (for earth-orbiting vehicles) during certain portions of the orbit. The earth may be considered as a black body radiating at the average temperature of the earth and reflecting a certain percentage of the solar radiation. Calculations indicate that the effect on radiator require-

ments is insignificant at the higher temperatures. From this work, it appears that radiator orientation need not significantly affect radiator design.

Description of Test Model

A review of the considerations covered in the foregoing indicated that certain problem areas will exist which are not amenable to analytical solution. To better define and evaluate these problems, a solar-powered thermoelectric model was constructed. Temperatures and outputs were established by material and size limitations. No attempt was made to optimize any part of the system or to make the model flyable. The primary objective was to construct a workable model which could be easily instrumented.

The power output was arbitrarily set at 2.5 watts. It was estimated that a minimum thermocouple efficiency of 7.7% could be achieved with today's material and that a Carnot cycle efficiency of 25% was reasonable. This gives an over-all efficiency of 1.92%. Based on this figure a heat input to the thermoelements of 130 watts is required.

The complete model is shown in Fig. 10 and as an exploded view in Fig. 11. It consists of a concentrator, a sidereal drive, an evacuate enclosure, a water-cooled sink and the thermoelectric assembly.

Concentrator

Preliminary investigation on the problem of model concentrator construction and orientation indicated that a cylindrical type mirror would have some advantage over the other types. Such a mirror could be constructed by metal-forming techniques rather than grinding and would require accurate orientation in only one plane. It was thus decided to construct a nonflyable parabolic mirror of this type. The dimensions were arbitrarily set at a width of 20 inches and an aperture of 50 inches by the requirement that the mirror or concentrator be large enough to collect a demonstrational quantity of energy yet small enough to be transportable. The proposed mirror intercepts 6.93 sq ft of solar energy. With a solar constant of 75 watts/sq ft, this is equal to 520 watts.

The focal length was arbitrarily set at 12.5 inches to make the system compact. With this focal length and neglecting aberrations, the concentrator should focus the solar image in the form of a rectangle with a width of 0.116 inch and a length of 20 inches. The aberrations associated with a concentrator of such high aperture diameter to focal length increases the width beyond the theoretical 0.116 inch.

According to catalog information highly reflective aluminum sheets were available which had a solar radiation reflectivity of about 0.83. This material appeared to be equal to, or better than, other finishes with the exception of silver and would not be subject to discoloration from atmospheric corrosion. This material was thus selected as the reflective surface.

The mirror was constructed by mounting the highly polished aluminum sheet in a welded tubular frame. The parabolic surface was generated by preforming the aluminum sheet and inserting it into two slots that were accurately milled in the frame. The mirror and frame assembly was then mounted upon a sidereal drive.

Thermoelectric Calculations

A hot junction temperature of 450 C was selected based on considerations of material availability and long life. With a Carnot efficiency of 25% the cold junction would then be 270 C. Thermoelectric materials such as p-type zinc antimonide and n-type indium antimonide were available and have useful values of efficiency over this temperature range.

The decisions of electric power output, thermoelectric material, and operating temperatures having been made, the component parts could now be designed. The amount of thermoelectric material required is calculated by considering the thermal conductivity and electrical resistivity of the materials and the heat flux desired. The ratio of area to length of the p-type material is calculated using the optimum relationship of the material characteristics.

$$Q_g=\left[1+\frac{\sqrt{\bar{\rho}_n\bar{K}_n}}{\sqrt{\bar{\rho}_p\bar{K}_p}}\right]K_p\frac{A_p}{l_p}(T_a-T_r)$$

$$130=\left[1+\frac{\sqrt{(5.7)(10^{-4})(9.2)(10^{-2})}}{\sqrt{(2.0)(10^{-3})(2.5)(10^{-2})}}\right]\times(2.5)(10^{-2})\frac{A_p}{l_p}(450-270)$$

$$\frac{A_p}{l_p}=14.9 \text{ cm (centimeters) or } 5.9 \text{ inches}$$

In a similar manner, the n-type material is found to require an A/l of 4.1 cm or 1.6 inches. Heat flow being dependent on the ratio of area to length, theoretically the dimensions could be reduced to near zero and the same heat flow obtained as long as the ratio is maintained. In practice the minimum length is limited by mechanical considerations such as thermal stress and heat loss around the elements.

An arbitrary length of 1/2 inch wa chosen for both types of material to sim plify construction. This is not nece sarily the optimum length but rather convenient one. Setting the lengt makes it possible to calculate the tot areas as:

$A_p=3.0$ inches^2

$A_n=0.8$ inch^2

The selection of diameters for the i dividual thermoelements is determined b mechanical considerations and the outpu voltage required. It is generally desirab to break up the total area of thermoele tric material required into as man separate junctions as possible to increa the voltage output.

In this case the p-type material wa readily available in 0.5-inch-diamet pellets. The number of p-type pelle then is:

$$N_p=\frac{3.0}{\pi 0.25^2}=15.5$$

or

$N_p=$ approximately 16

To obtain the same number of matchin n-type pellets:

$$r_n^2\pi=\frac{0.8}{16}$$

and

$r_n=0.13$ inch

Therefore the n-type pellets are approx mately 0.25 inch in diameter.

The open-circuit voltage then is V_o (16) (158+160) (10^{-6}) (180) = 0.92 volt and the internal resistance is $R_g=0.$ ohms. The power output at match load then is $P=3$ watts. The calculat 3-watt output indicates that the over- efficiency is slightly higher than that a sumed originally. In practice, howeve contact drops, conductor resistance, an mechanical deviations will tend to redu the output below this calculated value.

Nickel-plated silver was chosen f conductor material because of its hi electrical and thermal conductivity an its corrosion resistance. The radiat was made of aluminum because of i light weight and high thermal condu tivity.

An aluminum oxide coating was add to provide electrical insulation betwe radiator and thermoelement conducto The radiating surface was coated with black paint to provide maximum radiati of the waste heat.

The absorber was made from a lo carbon steel. This material has an a

table thermal conductivity but more portant it has a matching coefficient of ar expansion. The expansion of the l absorber at its higher temperature tches very closely the expansion of the minum radiator at its lower tempera-e. This arrangement minimizes the eral stresses on the thermoelements. e round side of the semicylindrical orber was coated with tantalum so that bsorbs a majority of the concentrated light and radiates very little heat. e flat side was coated with aluminum de to provide electrical insulation and rmal conduction to the thermoelement ductors. Stainless-steel hardware was cted to hold the structure together. inless steel is corrosion free and has a thermal conductivity thus minimizing loss of heat through the hardware. ing washers were used to take up ensional changes caused by thermal ansion.

SORBER

t was shown that 130 watts at a tem-ature of 450 C must be supplied to the rmoelectric elements to produce an tric power output of 2.5 watts. In ition, mounting and hardware con-tion losses will exist. The total net ver which must be supplied to the gen-or is calculated to be 140 watts.

s described in a foregoing section, the t available to the generator is deter-ed by the absorber heat-balance ation.

$$=Q_g+Q_r\alpha A_c SF=Q_g+A_a\epsilon\sigma(T_a^4-T_0^4)$$

his case, the term Q_g is equal to the t input into the thermoelements plus nting and hardware losses which is al to 140 watts. The intercepted rgy $A_c S$ has already been established he dimensions of the concentrator and found to be 520 watts with a r constant of 75 watts/sq ft. An orber area must now be found which balance the equation with the ab-er at the desired temperature of C.

he absorptivity–emissivity coefficients a function of the surface coating. liminary work indicated that a selec-black material may be superior to a ly absorptive gray-body material in application. A brief search of the rature revealed tantalum to be one of better blacks and it was selected as the face material. The solar absorptivity calculated to be about 0.5 and the ssivity to be about 0.11.

furnace factor of 0.83 appeared sonable in view of the high reflectivity of the concentrator surface. The assembly will be mounted in an evacuated enclosure and some of the concentrated energy will be reflected and absorbed in passing through the glass walls. A transmission factor should thus be added to the left term in the heat-balance equation. Calculations and tables indicate that the transmission factor should be about 0.9.

The required absorber area of 31.7 square inches is now calculated by substituting these values into the heat-balance equation and letting $T_0=323$ K (50 C). Since the radiation losses from the back side of the absorber will be reduced to a small value with insulation, all radiation losses must occur on the front surface. With the length of the absorber fixed at 20 inches by the concentration dimensions, the required width is now found to be 1.59 inches. This width is larger than the theoretical 0.116-inch image that will be cast by the concentrator. However, certain inaccuracies in construction are expected and it is felt that a sizable target will be desirable to effectively collect the concentrated energy. The dimension was thus left as calculated.

From preliminary work, it appears that a plane surface will not efficiently collect energy from the outer surfaces of the concentrator. This is due to the large incident angle of these rays. A cylinder will present a surface area that will be approximately normal to all the rays and should be superior. The absorber was thus constructed as a semicylinder with a diameter of 1 inch.

Evacuated Enclosure

A vacuum enclosure was considered necessary to eliminate convection heat loss and to protect the materials from possible oxidation damage. The envelope consists of a 4-inch Pyrex tube with mechanically sealed end caps. Electrical connections to the thermoelectric generator, voltage probes, and temperature sensing thermocouples were brought out through hermetically sealed connectors mounted in the end caps. The end caps also contain connections for the water supply to the heat sink and the vacuum system. The enclosure is attached to the concentrator frame with an adjustable type of clamp to permit positioning at the point of maximum heat input.

Sink

The Pyrex walls of the enclosure are opaque to the wavelengths emitted by the radiator. The enclosure would thus absorb all of the waste heat and reach an objectionably high temperature. It was considered simpler to absorb the waste energy in an internally mounted water-cooled sink rather than to attempt to cool the glass tube. The sink consists of a semicircular section formed from thin-gage copper which was blackened on the concave side and aluminized on the convex side. Copper tubes for the coolant were soldered to the copper sheet at approximately 2-inch intervals.

Radiator

The heat which must be dissipated by the radiator is equal to the heat conducted into the thermoelectric elements and generator hardware less the electrical output. In this case, the heat input to the radiator is 127.5 watts from the thermoelectric generator plus 10 watts hardware conduction loss for a total of 137.5 watts.

The familiar Stefan-Boltzman radiation law provides the basis for sizing the radiator.

$$Q_w=A_r\epsilon\sigma(T_r^4-T_s^4)$$

where

Q_w = waste heat to be dissipated = 137.5 watts
A_r = area of radiator in sq ft
ϵ = effective emissivity $=(1/\epsilon_r+1/\epsilon_s-1)^{-1}$
ϵ_r = emissivity coefficient of radiator surface
ϵ_s = emissivity coefficient of sink surface
T_r = radiator temperature = 543 K
T_s = sink temperature = 288 K

Since the radiator is shaded from the sun by the sink, minimum area will be obtained with highly emissive surfaces. Emsisivity tables show that surfaces with emissivities in the order of 0.9 can be obtained with lampblack carbon.

The required area of the radiator was calculated to be 56.7 square inches. The radiator was made as a plate 2.8 inches wide and 20 inches long. For structural reasons, the thickness of the radiator could not be made less than 1/8 inch. With power inputs of approximately 70 watts/ft and material thickness of 1/8 inch, the conductor temperature drop should be small, and no allowance is considered necessary to account for varying radiator temperatures.

Test Program

The test model will be subjected to a series of tests designed to determine the performance of the system and to investigate the optical, thermal, and electrical problems. Theoretical considerations will be proved or disproved or otherwise evaluated by comparing calculated results with experimental data. The experience gained in designing, constructing, and testing this small model will be

of considerable benefit in future solar-thermoelectric work.

Conclusions

This paper discusses some design considerations and problems that will be encountered in designing a solar-powered space thermoelectric generator. Results of some studies are presented and a test model of a solar-powered thermoelectric generator is described.

It appears that a solar-powered thermoelectric generator is feasible and may have considerable potential as a secondary power source for future space vehicles. There are many problems which must be explored but these problems appear to be solvable with further engineering effort.

References

1. Power from Solar Energy, J. I. Yellott. *Transactions*, American Society of Mechanical Engineers, New York, N. Y., vol. 79, no. 6, Aug. 1957, pp. 1349–59.

2. High Temperature Furnaces, Felix Trombe. *Proceedings*, Phoenix Symposium on Applied Solar Energy, Phoenix, Ariz., 1955, pp. 63–72.

3. Recent Progress in Solar Furnaces for High Temperature Research and Development Work, W. M. Conn. *Journal*, Franklin Institute, Philadelphia, Pa., vol. 257, no. 1, Jan. 1954, pp. 1–11.

4. Optimum Reflector–Absorber Geometry for a Solar Generator, R. W. Stineman. *AIEE Transactions*, see pp. 332–37 of this issue.

5. American Institute of Physics Handbook (book), D. E. Gray. McGraw-Hill Book Company, Inc., New York, N. Y., 1957.

6. Analysis of Large Aperture Parabolic Mirrors for Solar Furnaces, J. Farber, B. I. Davis. *Journal*, Optical Society of America, New York, N. Y., vol. 47, no. 3, Mar. 1957, pp. 216–20.

7. A Segmented-Mirror Solar Furnace for High Intensity Thermal Radiation Studies, R. Gardon. *Review of Scientific Instruments*, New York, N. Y., vol. 25, no. 5, May 1954, pp. 459–63.

8. Fuel for Solar Furnaces, A. R. Kassander. *The Journal of Solar Energy Science and Engineering*, Phoenix, Ariz., vol. 1, no. 2–3, Apr.-Jul. 1957, pp. 44–47.

9. Designing Solar Furnaces for Specified Performance, Raymond Bliss. *Ibid.*, pp. 55–62.

10. Solar Energy Furnaces, Guy Benvenists. Stanford Research Institute, Menlo Park, Calif. 1955.

11. Semi Conductor Thermoelements and Thermoelectric Cooling (book), A. F. Ioffe. Infosearch, Ltd., London, England, 1957.

12. Climatological Data. Weather Bureau, U. S. Department of Commerce, Washington, D. C., vol. 8, no. 1–12, Jan. to Dec. 1957.

13. Process Heat Transfer (book), Donald Q. Kern. McGraw-Hill Book Company, Inc., 1950.

14. Heat Transmission (book), William H. McAdams. McGraw-Hill Book Company, Inc., 1942.

Some Effects of Hypersonic Ionization on the Design of Electrical and Electronic Components

W. B. SISCO
NONMEMBER AIEE

J. M. FISKIN
NONMEMBER AIEE

VEHICLES traveling at hypersonic velocities in a gaseous atmosphere will be surrounded by a shock-induced high-temperature sheath. As a result of the high temperature, the gaseous sheath has an electron density greater than that of the ambient atmosphere. Since the craft will be immersed in a high-temperature envelope, both it and its components will be subjected to unusual temperatures. Fig. 1 indicates the way in which the air temperature and density varies from the shock front to vehicle surface for a given velocity and altitude.

Currently designed aircraft have temperatures up to 1,000 K (degrees Kelvin) over a majority of the surface. This raises the temperature of interior components to 1,000 K unless a special design is used. As a consequence, emphasis is being placed upon the design of high-temperature electrical and electronic components or on means to protect these components from the hot environment.

In addition to the high-temperature effects, ionization itself directly affects systems on the vehicle, on other vehicles, and on the surface of the earth.

On the aircraft the ionized sheath surrounding the vehicle may cause the following results:

1. Malfunction or inefficient operation of electronic equipment due to the deviation of the radiation resistance from free-space values.

2. Increase in the open-circuit noise in receiver systems.

3. Change in the voltage breakdown properties from ambient properties.

4. Modification of propagation characteristics of the media.

At locations distant from the vehicle two changes will occur. These are:

1. A variation in the radar cross section of the craft.

2. Enhanced response to passive detection devices due to radiation from the hot gases.

Temperature Effects on Equipment

Initially, the design of high-temperature electrical and electronic systems will be based on the prevention of the hot environment from reaching the components. One approach to this is to place the equipment in cooled compartments with only the components able to function at high temperatures external to the compartments.

The design of the compartment so that it will perform its protective function becomes important. One such arrangement is shown in Fig. 2. Essentially the result of such a configuration to make it necessary to remove only the heat rejected by the operating equipment and the heat transferred from 373 [212 F (degrees Fahrenheit)] to 310 (100 F) through the insulation. This can be done by refrigeration or by blowing cool gases over the equipment.

Many electrical components such as isolation transformers, wiring, coaxial cables, waveguides, etc., will probably be located at points in the vehicle that are inaccessible to practical cooling. As a result, they will have to function at temperatures up to 1,000 K. The design of these components will have to rely on materials having the required electrical properties such as dielectric constant, dielectric strengths, conductivities, etc., at these high temperatures. Present indications are that this has been accomplished in many cases. The liberal use of ceramics as dielectric and structural material has increased the high-temperature capability of many passive components. The white noise in the system will increase with the temperature, how-

Paper 59-885, recommended by the AIEE Transportation Committee and approved by the AIEE Technical Operations Department for presentation at the AIEE Summer and Pacific General Meeting and Air Transportation Conference, Seattle, Wash., June 21–26, 1959. Manuscript submitted March 20, 1959; made available for printing April 22, 1959.

W. B. Sisco and J. M. Fiskin are with Douglas Aircraft Company, Inc., Long Beach, Calif.

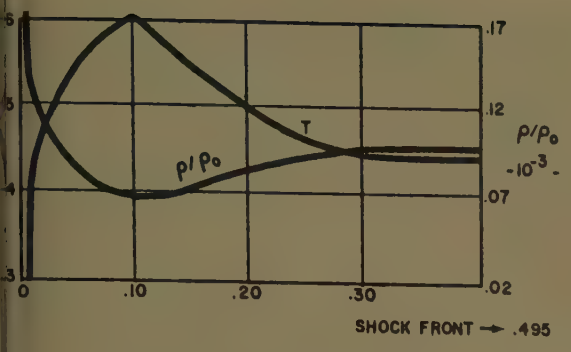

. 1. Temperature and density ratio at various distance from surface

Altitude = 260,000 feet
ρ_0 = density at standard pressure and temperature
U_1 = 25,000 fps
X = 9 feet aft of L.E.

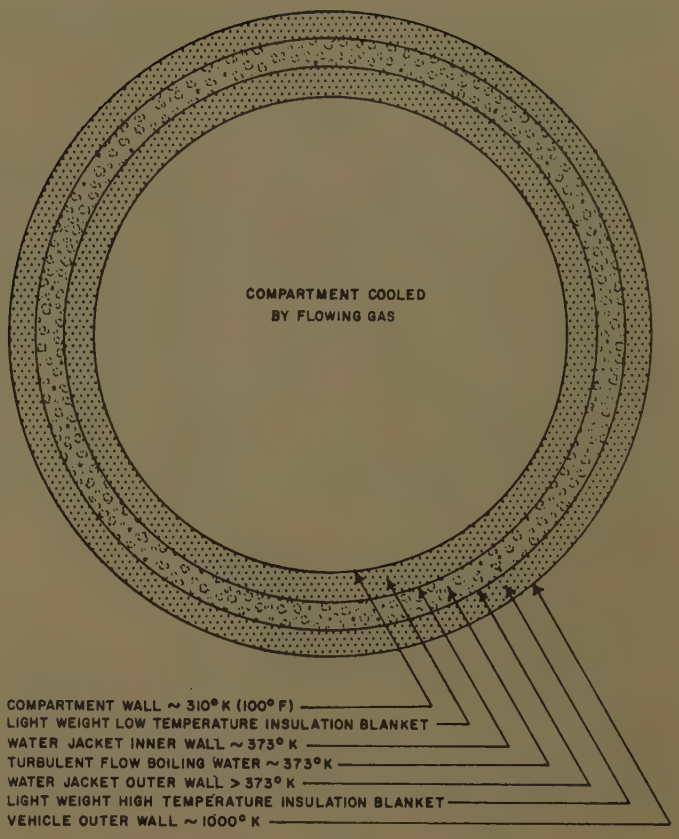

Fig 2 (right). Example of a protected compartment

er, and the high-temperature system's nal-to-noise ratio will decrease.

nization Effects on Equipment

diation Impedance

Because the dielectric constant of the dium surrounding the vehicle is not ual to that of free space, the radiation istance of antennas attached to the face of the vehicle can differ signifintly from their free-space values. ese variations will not necessarily nain constant with time. Unless this liation-resistance variation is compened, it could result in the malfuncn or inefficient operation of electronic uipment. These impedance changes n be obtained approximately by classi- EM (electromagnetic) theory proed the geometry of the sheath is own.

ise Impedance

All of the vehicular antennas are surnded by a conductive medium at atively high temperatures. The real pedance, as differentiated from the liation impedance, appearing across antenna terminals will depend on the metry of the antenna feed points, the pe of the shock-wave sheath and the nductivity and dielectric constant of plasma. The resistive part of this pedance, which can be considered in rallel with the modified radiation reance previously discussed, will gener- an open-circuit noise voltage over a le-frequency spectrum. If there are relatively strong EM fields present within the medium, the noise power will be proportional to the electron temperature, i.e., the temperature of the shocked air. Strong EM fields, for instance, those produced by high-power radar systems, yield effective electron temperatures significantly above the thermal values resulting in even larger noise-power outputs.[1] Generally, the noise in the receiver systems will be increased as a result of the hot gases surrounding the vehicle.

Voltage Breakdown

High-temperature air is basically different from air at standard pressure and density. The extent of the difference depends on the temperature which determines the quantitative amounts of dissociation, ionization, and formation of new products taking place. It is to be expected then that the voltage breakdown properties would differ from ambient air. Theoretically, the breakdown properties could be obtained since the composition of the air is known. Practically, the calculation of ionization and excitation rates is difficult and experimental methods are usually employed.[2] The problem is thus one of maintaining the air at the desired temperature and density for the experiment.

Radar Cross Section

Air and ground detection and tracking systems will also be affected by the ionization present in the sheath surrounding the vehicle. Fig. 3 is a plot of the electron density and plasma-resonance frequency as a function of temperature for various ratios of shocked-air density to standard temperature and pressure-air density. Fig. 4 is a combination of Figs. 1 and 3 showing the way that the plasma-resonance frequency, which is proportional to the square root of the electron density, varies across the sheath.

The shock-ionized layer may be considered as an extension of the vehicle for incoming EM radiation at frequencies in the neighborhood or lower than the critical frequency of the plasma. Additionally, if recombination times are long, an ionized wake may also be present. This, in effect, changes the shape and the radar cross section of the vehicle for some frequencies. Again, this variation can be approximated if the shape of the sheath and wake are known.

Radiation from the ionized sheath may be roughly classified as classical and quantal. Accelerations and deaccelerations of the electrons within the gas will yield radiation similar to that produced in antennas. Rotation, vibration, electronic excitation, and recombination of electrons with positive ions will produce quantal radiation in the microwave, millimeter, infrared, visible and ultraviolet ranges. Thus, the tracking of the vehicle by passive detection systems will be enhanced.

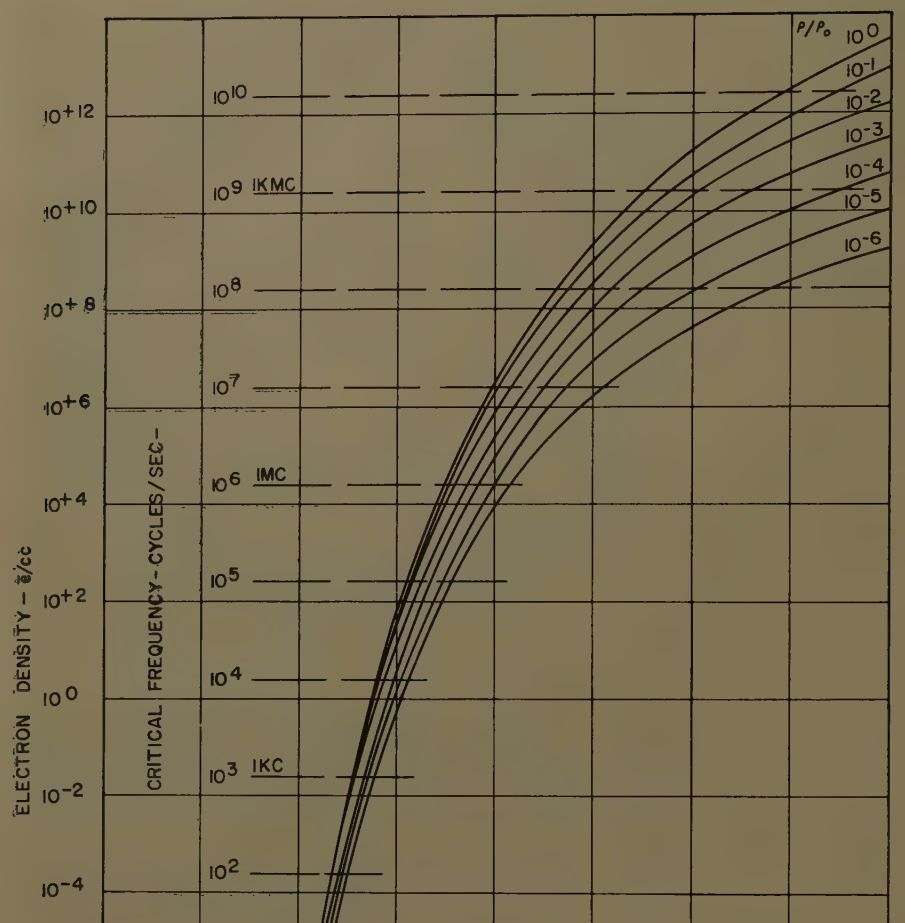

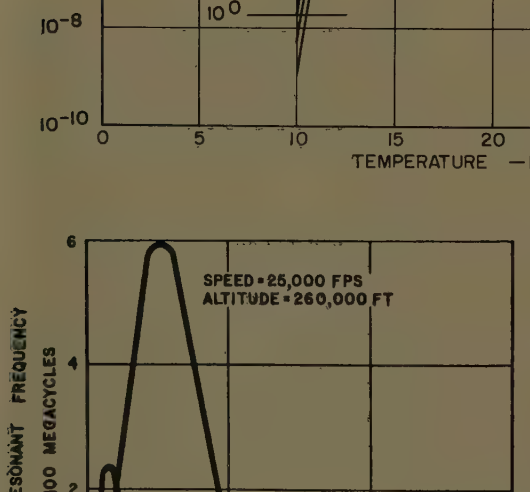

Fig. 3 (above). Critical frequencies for high-temperature air

Fig. 4 (left). Plasma resonant frequency at various distances from surface, 9 feet aft

Basic Design Parameters

Treating the ionized sheath as an ionosphere surrounding the vehicle, the propagation and reflection characteristics of the medium can be determined by employing classical EM theory.[3-4]

Some of the terms used previously are not generally thought of as design terms to be applied to electrical and electronic systems. Since many of the effects mentioned before are dependent on the electron density, heavy-particle density, and temperature, it will be necessary to know these values. It would be desirable to be able to obtain those values from aerodynamicists or some other group associated with the over-all hypersonic vehicle design. However, at temperatures below 5,000 K the electron density, which is very important to the electrical and electronic systems, is generally a negligible factor in their design considerations. Therefore, the electrical engineer is faced with learning a new field in order to obtain design requirements. It is desirable to review briefly the principal theory by which the high temperature and electron density are determined.

Composition and Energy of Gas Behind a Shock Wave

For most aerodynamic shapes the equilibrium composition of the gas and the temperature from the shock front up to the boundary layer (a narrow layer adjacent to the skin of the vehicle) can be obtained. Under some conditions, the boundary-layer composition can also be calculated. The necessary fundamental concepts and equations will be briefly outlined in the following. A more detailed account can be found in reference 5.

From an aerothermodynamic standpoint the problem is essentially one of conserving mass, momentum, and energy flow across the shock front. Expressed mathematically, conservation of mass flow is:

$$\rho_0 U_0 = \rho_1 U_1 \tag{1}$$

conservation of momentum flow is:

$$P_1 - P_0 = \rho_0 U_0 (U_0 - U_1) \tag{2}$$

and conservation of energy flow is:

$$E_1 + P_1\tau_1 + \frac{1}{2}U_1^2 = E_0 + P_0\tau_0 + \frac{1}{2}U_0^2 \tag{3}$$

and

$$h_1 - h_0 = \frac{1}{2}(P_1 - P_0)(\tau_1 + \tau_0)$$

where

ρ = density (mass/unit volume) and $1/\rho$ (specific volume) = τ_0
U = streamwise flow velocity normal to shock front
P = pressure
E = internal energy/unit mass (function of T, temperature)

Zero subscripts indicate the unshocked or ambient gas; a one signifies the shocked gas.

The shock front, which separates the ambient air from the shocked air, can

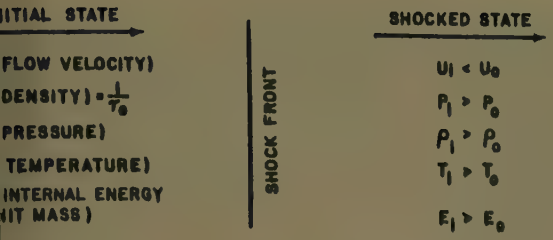

Fig. 5. Flow equations in a normal shock wave

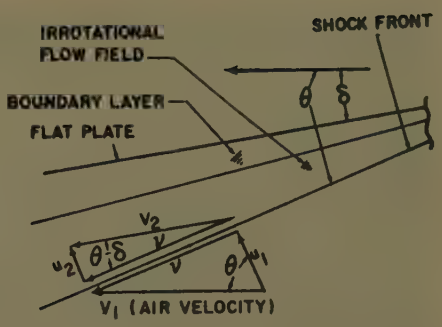

Fig. 7. Flat plate aerodynamic conditions

considered as a transformer in that changes the temperature, density, ssure, internal energy, and streamwise ocity to different values. These trans- mations are conveniently shown in . 5. It is noted that all the values, with exception of the streamwise velocity, rease as the gas flows through the shock nt. This, in effect, means that energy the streamwise flow is converted into ernal energy and compression of the . An idealized picture of how this eamwise flow energy is converted o the various modes of internal energy hown in Fig. 6. In Fig. 7 the geom- y of a shock wave surrounding a surface is shown.

Equations 1, 2, and 3, in conjunction h the perfect gas law,

$$_1 = \Sigma n_j k T_1 \quad (4)$$

ere

= number in volume τ of species j
Boltzmann's constant

n can be solved for a vehicle traveling a specified altitude and velocity pro- ed the composition and the number of rgy modes present remain the same both sides of the shock front. In the th's atmosphere, for air, this would an that dissociation and ionization not occur and vibrational and elec- nic states are not excited. For even tively low hypersonic velocities, how- r, the temperature T_1 of the shocked is sufficient to dissociate, ionize, and ite the particles in the gas. To satisfy the conservation equations under these conditions, the composition of the gas behind the shock must be known.

The composition (number density) of a gas at a specified temperature and density or pressure can be determined employing the principles of physical chemistry and statistical quantum mechanics. The first step in the numerical calculation of the concentration is to postulate the chemical reactions taking place within the hot shocked air. As a simple example, if air were considered to be at 3,000 K or below, the following group of equilibrium relations would generally be valid.

$$N_2 \rightleftarrows N+N \quad (5)$$

$$O_2 \rightleftarrows O+O \quad (6)$$

$$NO \rightleftarrows N+O \quad (7)$$

$$NO \rightleftarrows NO^+ + e^- \quad (8)$$

Equations 5 and 6 are usually sufficient to determine the aerothermodynamic properties of the gas. However, since the electron density is the primary requirement, equations 7 and 8 must also be included. The inclusion or exclusion of an equation depends on whether or not it will significantly affect the aerothermodynamic properties or the number density of the particular species required.

Associated with each chemical equation is an equilibrium constant, K, which can be related to the concentrations and partition functions of each particular species by the law of mass action. Thus,

$$K_1 = \frac{[N][N]}{[N_2]} = \frac{(PF)_N (PF)_N}{(PF)_{N_2}} \left(\frac{1}{\rho_{dr} L}\right) \epsilon^{-\frac{Q_1}{kT}} \quad (9)$$

$$K_2 = \frac{[O][O]}{[O_2]} = \frac{(PF)_O (PF)_O}{(PF)_{O_2}} \left(\frac{1}{\rho_{dr} L}\right) \epsilon^{-\frac{Q_2}{kT}} \quad (10)$$

$$K_3 = \frac{[N][O]}{[NO]} = \frac{(PF)_N (PF)_O}{(PF)_{NO}} \left(\frac{1}{\rho_{dr} L}\right) \epsilon^{-\frac{Q_3}{kT}} \quad (11)$$

$$K_4 = \frac{[NO^+][e]}{[NO]} = \frac{(PF)_{NO} + (PF)_{e^-}}{(PF)_{NO}} \times \left(\frac{1}{\rho_{dr} L}\right) \epsilon^{-\frac{Q_4}{kT}} \quad (12)$$

where

K = equilibrium constant
ρ_{dr} = ratio of actual density to standard density
L = number of air atoms at standard density
k = Boltzmann's constant
Q = energy of dissociation, formation, and ionization
[ ] = concentration (ratio of number of atoms of a particular species, such as N, to total number of atoms present)

The total partition function (PF) is a function of T and can be written very generally as:

$$(PF) = (PF)_{\text{translational}} \times (PF)_{\text{rotational}} \times (PF)_{\text{vibrational}} \times (PF)_{\text{electronic}} \quad (13)$$

where the partition functions for the various energy modes can be obtained from statistical quantum mechanics[6] and

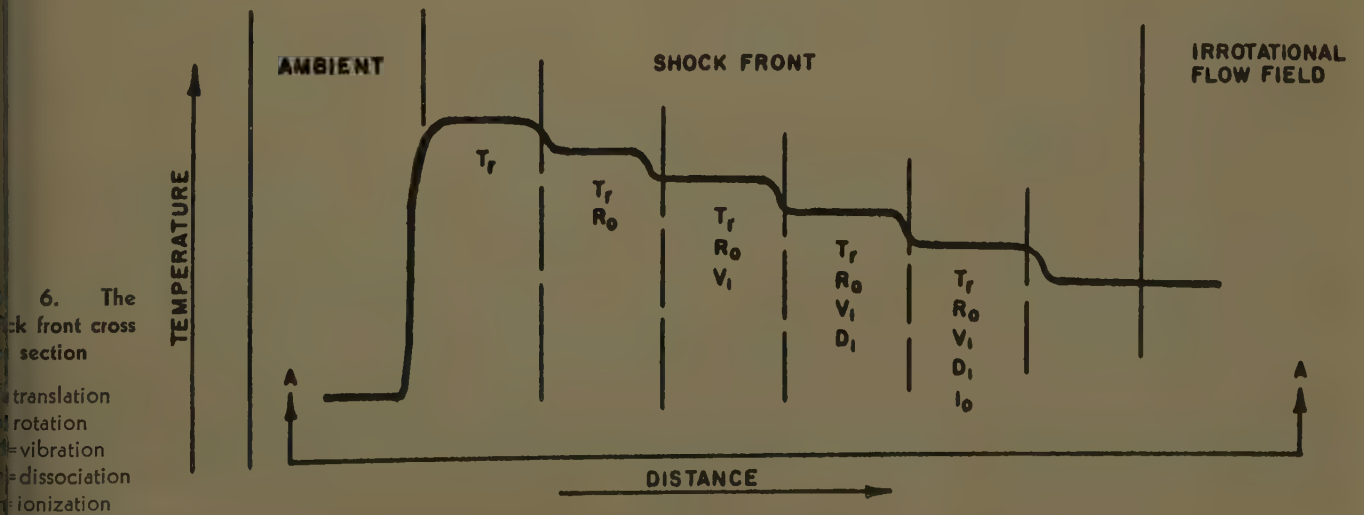

6. The
k front cross
section

translation
rotation
=vibration
=dissociation
=ionization

experimental spectroscopic data.[7–11] The (PF), when calculated, and the energy of reaction, Q, yield the equilibrium constants in equations 9, 10, 11, and 12.

Three additional equations involving the concentrations are also required.

$$2[N_2]+2[O_2]+2[NO]+2[NO^+]+[N]+[O]+[e^-]=1.000$$
mass conservation (14)

$$\frac{2[N_2]+[NO]+[NO^+]+[N]}{2[O_2]+[NO]+[NO^+]+[O]}=4.0$$
material balance conservation–ratio of nitrogen to oxygen atoms (15)

$$[NO^+]=[e^-]$$ charge conservation (16)

The seven equations 9, 10, 11, 12, 14, 15, and 16 form a set containing seven unknowns, the concentrations, []. The simultaneous solution of this set yields the desired concentrations and hence the composition of the gas.

The total energy of the shocked gas including the amount necessary to dissociate, form, and ionize can be obtained once the composition and (PF)s are known. Thus,

$$E=E_{\text{part}}+(E_{\text{diss}}-E_{\text{form}})+E_{\text{ion}} \quad (17)$$

Here E_{part} is the total internal energy of the particles and includes translational, vibrational, rotational, and electronic modes and is given by:

$$E_{\text{part}}=\sum_{ji} n_{ji}\frac{\partial}{\partial T}\ln (PF)_j \quad (18)$$

where j identifies the species of the particle (i.e., N, O_2 . . .) and i the electronic energy level of the species. The dissociation energy is simply the number of particles that dissociate times the dissociation energy Q. Identical procedures are used for the ionization and formation energies.

In obtaining the composition the shocked-air temperature and density were assumed to be known. Actually, they can only be obtained by satisfying the flow conservation relations, (equations 2, 3, and 4). The flow-conservation equations can only be satisfied if the composition is known. To resolve this problem, some type of an iterative procedure is usually adopted. Probably the easiest method in most cases is to compute the composition over a wide range of shocked-air temperatures and densities and then use an iterative procedure to satisfy the conservation equations for a range of ambient velocities and altitudes (densities). The composition tables of Gilmore[10, 12] have been recently extended to include electron densities down to 1,000 K.

Conclusions

Some effects of temperature on equipment and the equipment's environment have been presented. Special emphasis has been placed on a new field of knowledge required by the electrical engineer in the design of systems for hypersonic aircraft.

References

1. Air Composition Below 3000 Degr... Kelvin, **C. A. Roberts, W. B. Sisco.** "Resea... and Development Handbook," *Space/Aeronaut...* New York, N. Y., 1959–60, p. D-19.

2. **R. F. Breakdown in Air as a Function... Altitude, A. D. MacDonald.** *Technical Re... no. MPL-2,* Microwave Physics Laborato... Sylvania Electric Products, Inc., Mountain Vi... Calif.

3. Electromagnetic Waves and Radiati... Systems (book), **E. C. Jordan.** Prentice-H... Inc., Englewood Cliffs, N. J., 1950, pp. 660–62.

4. Electromagnetic Wave Propagation ... Shock-Ionized Media, **W. B. Sisco, J. M. Fisk...** *Engineering Paper no. 633,* Douglas Aircraft C... pany, Inc., Santa Monica, Calif., Apr. 1958.

5. Theory of Equilibrium Electron ... Particle Densities Behind Normal and Obli... Shock Waves in Air, **C. A. Roberts, W. B. Sis... J. M. Fiskin.** *Transactions,* Professional Group... Antennas and Propagation, Institute of Radio ... gineers, New York, N. Y. (To be published.)

6. Statistical Mechanics (book), **G. S. Ru... brook.** Oxford University Press, London, E... land, 1949, chaps. IV, XI, XII.

7. Spectra of Diatomic Molecules (boo... **Gerhard Herzberg.** D. Van Nostrand Compa... Inc., Princeton, N. J., second edition, 1950.

8. Atomic Spectra and Atomic Struct... (book), **Gerhard Herzberg.** Dover Publicati... Inc., New York, N. Y., second edition, 1944.

9. Atomic Energy Levels. *Circular no. ...* National Bureau of Standards, Washington, D.... vols. 1 and 2, 1949, 1952.

10. Equilibrium Composition and Ther... dynamic Properties of Air to 24,000° K (U... Project Rand), **F. R. Gilmore.** *Report RM-1...* The Rand Corporation, Santa Monica, Calif., A... 1955.

11. Photodetachment Cross Section and ... Electron Affinity of Atomic Oxygen, **Lewis ... Branscomb, et al.** *Physical Review,* New Y... N. Y., vol. 111, no. 2, July 15, 1958, pp. 504–13.

12. Effects of Relatively Strong Fields ... the Propagation of EM Waves Through... Hypersonically Produced Plasma, **W. B. Sis... J. M. Fiskin.** *Transactions,* Professional Group... Antennas and Propagation, Institute of Radio ... gineers, July 1959, pp. 240–44.

Functional Cycling to Assure Reliability of Aircraft Control Equipment

R. E. HULSEY
ASSOCIATE MEMBER AIEE

L. L. KESSLER
AFFILIATE AIEE

THE COMPLEXITY of present-day high-performance aircraft and missiles is demanding better reliability of its various subsystems. A considerable amount of the equipment, such as guidance and flight control equipment, depends entirely upon the electric power system. Therefore, the electric power system is of primary importance in the over-all reliability of the aircraft.

The reliability of the electric power system may be increased by paralleling more than one source of power. When two or more generators are operated in parallel, a method must be provided to control these generators and their associated circuit breakers. This is a function of the control panel. A dependable electrical system therefore demands a control panel with a very high degree of reliability.

To obtain the high degree of reliability required, reliability must be designed into the control unit. This necessitates that reliability be considered in component design, circuit design, mechanical design, and manufacture. Even when the best efforts of component design engineers, manufacturers, and quality ... surance personnel are used, studies sh... that early component failures cannot ... eliminated. An effective method has be... developed for eliminating these premat... failures from static control and protect... panels by functional cycling at the e... of the manufacturing process. This n... technique has increased the mean-ti... between failure of static control and p... tective devices by 5,000 per cent.

Paper 59-912, recommended by the AIEE ... Transportation Committee and approved by ... AIEE Technical Operations Department for p... entation at the AIEE Summer and Pacific Gen... Meeting and Air Transportation Conferen... Seattle, Wash., June 21–26, 1959. Manusc... submitted March 20, 1959; made available ... printing April 28, 1959.

R. E. Hulsey and L. L. Kessler are with W... inghouse Electric Corporation, Lima, Ohio.

The authors wish to acknowledge the work ... formed by Mr. R. G. Lee and Mr. D. A. Voge... the development and design of the functi... cycling equipment described herein.

The authors wish to thank the aircraft manu... turers and operators for their co-operation in ... viding information on equipment in the field.

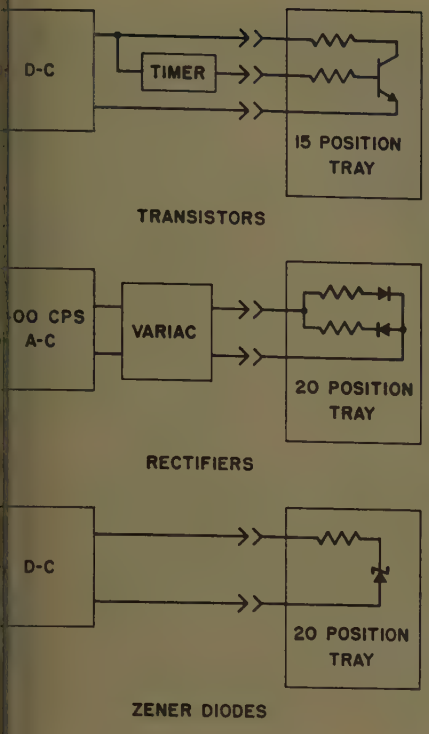

g. 1. Block diagram of functional cycling equipment for semiconductors

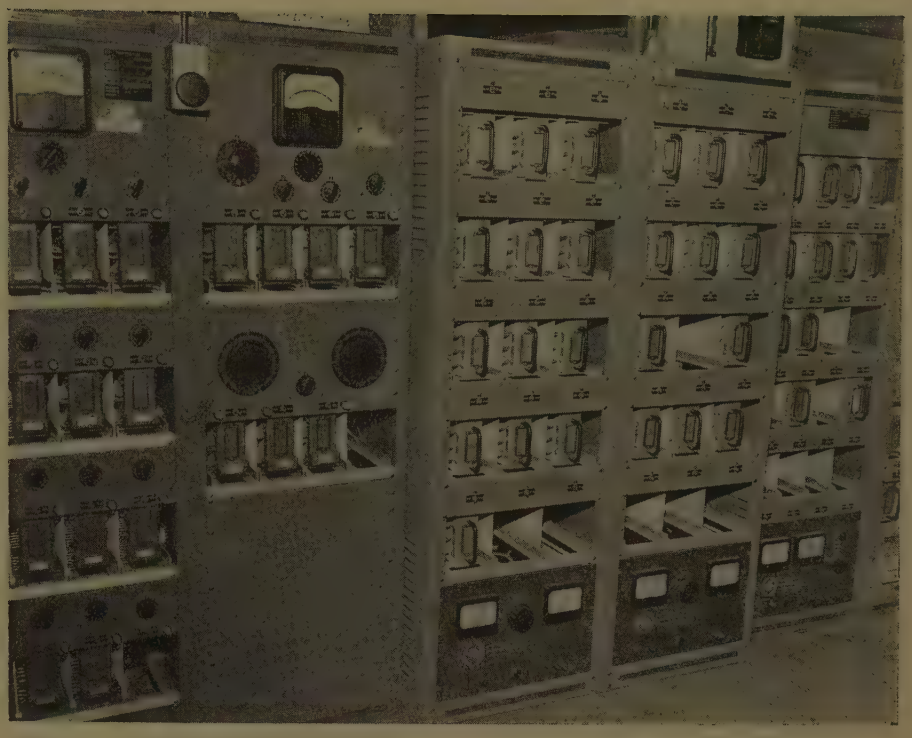

Fig. 2. Functional cycling equipment for semiconductors as described in Fig. 1

ypical Control Panel

The basic functions of a control and otective panel are those of opening and osing the field of the generator and pervising the opening and closing of e generator circuit breaker. In a parlel generator system, supervising the ening and closing of the bus tie circuit eaker is another basic function. In der to perform these control functions a logical manner, a control and proction panel must sense voltages and rrents throughout the electrical system. hese various voltages and currents are easured, compared with standards, me delayed if necessary, mixed in logic rcuits, amplified, and finally used to erform the necessary control functions. he panel protective functions may inude such circuits as overvoltage protecon, undervoltage protection, overcitation protection, underexcitation otection, underspeed protection, underequency protection, stability protecon, negative sequence protection, and fferential current protection. The panel ntrol functions may include lockout rcuits to prevent cycling of circuit eakers and a circuit for automatic aralleling of generators. To meet the ze, weight, environmental and reability requirements of present-day gh-performance aircraft, circuits utilizg static components, such as transistors, ntrol rectifiers, and diodes are used in ace of electromechanical devices.

Verifying the Need for Functional Cycling

It is well known that electronic components exhibit the characteristic of a high initial failure rate. In connection with the development of new products utilizing semiconductors, extensive studies were conducted on semiconductors to determine their initial failure rate characteristics. As a part of these studies, extensive life tests of semiconductors were conducted. In order to predict the reliability of production control equipment with some degree of accuracy, life tests on representative quantities of semiconductors were necessary. Reliability studies on pilot production components and equipment were inconclusive and could not be used as a basis for predicting the reliability of later production equipment.

To study the early failure rate of semiconductors, tests were conducted on representative quantities of each type, rating, and manufacturer used in the equipment. Each diode was operated as a half-wave rectifier on a 400-cps (cycles per second) alternating current source at its rated average forward current and maximum peak inverse voltage. The average forward voltage drop and average reverse leakage was measured periodically and all diodes were monitored to detect catastrophic failures. Each transistor was operated as a switch with rated collector voltage when not conducting, and rated collector current while conducting. During the tests each transistor was operated conducting half, and not conducting half, of each hour. The leakage, direct current gain, and saturation resistance were measured periodically and all transistors were monitored to detect catastrophic failures. Each semiconductor was operated for a minimum of 200 hours.

The results of the studies showed the characteristic of a high initial failure rate. The majority of early catastrophic failures occurred during the first 100 hours of operation. These results were presented to semiconductor manufacturers and arrangements were made to age all semiconductors prior to delivery. It is impractical to age all semiconductors electrically, therefore, extreme temperature aging and cycling is being used by semiconductor manufacturers. To assure proper aging, samples of each semiconductor shipment are electrically aged (functional cycled) as described elsewhere in this paper.

The first pilot production equipment had a mean-time between failure of 80 hours. Since this equipment did not have aged semiconductors, a low mean-time between failure in early life would be expected. To eliminate these early random failures, each piece of pilot production equipment was functional cycled for a minimum of 200 hours.

Production equipment with aged semiconductors was functionally cycled for

Fig. 3 (left). Punch card controlled component tester. Zener diodes are being tested

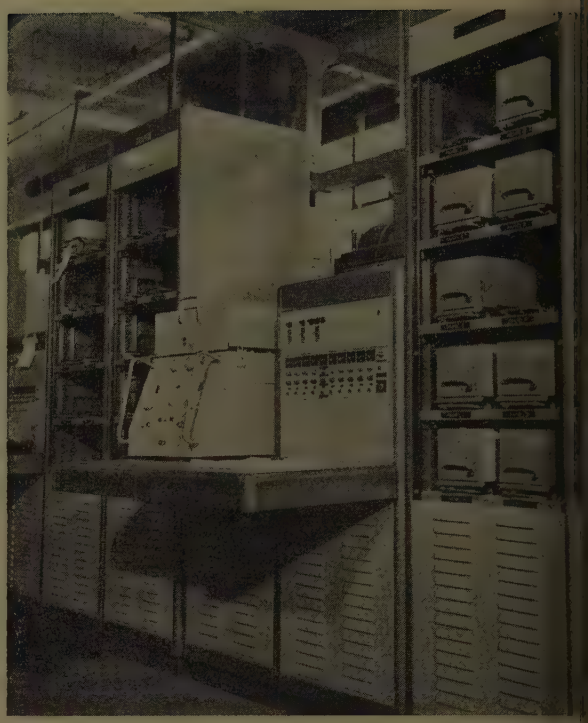

Fig. 5 (right). Functional cycling equipment for control panels as described in Fig. 4

comparison with pilot production equipment. This comparison showed a considerable reduction in failures but random failures still occurred. Further investigation showed that some early failures are inevitable as a result of manufacturing processing even when extreme care is exercised. The failures are of the nature that cannot be detected visually or by short time functional tests. Therefore, the only satisfactory means for eliminating these random failures is to functional cycle each unit for a minimum of 100 hours. Data from the functional cycling test are continually surveyed to establish improved procedures.

Functional Cycling Equipment

Many factors must be considered in the design of functional cycling equipment. The design of the equipment must be flexible, in that it can be readily adapted to new types of control equipment. It is desirable that it be built in module form so that it may be easily maintained. The equipment should be as automatic as is economically possible, providing unattended operation and including self-checking features. Due to the great number of operations that this equipment must perform, it must be designed with the greatest reliability attainable. Because of the differences between semiconductor component and control equipment cycling, two basic types of functional cycling equipment were required.

The functional cycling equipment for semiconductor components is shown in Figs. 1, 2, and 3. It was found convenient to divide the semiconducto components into three categories for th cycling equipment. These categories ar transistors, rectifiers, and zener diodes All components are mounted in plug-in trays for cycling. These trays can b removed from the cycling racks and in serted into automatic test equipmen which tests all components on the tra automatically.

Transistor cycling is accomplishe by applying a constant direct-curren voltage supply through a resistor to th collector continuously. The transisto is conducting half of each hour and i controlled by a timer operated relay through a base-drive limiting resistor Rectifier cycling is accomplished by ap plying a 400-cycle alternating-curren

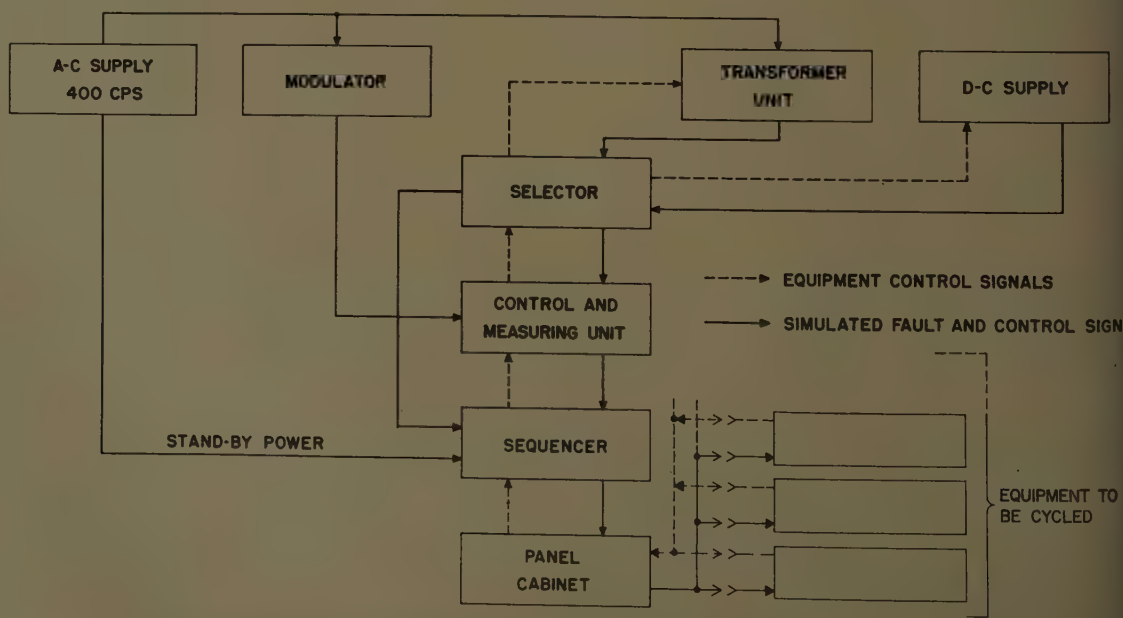

Fig. 4. Block diagram of functional cycling equipment for control panels

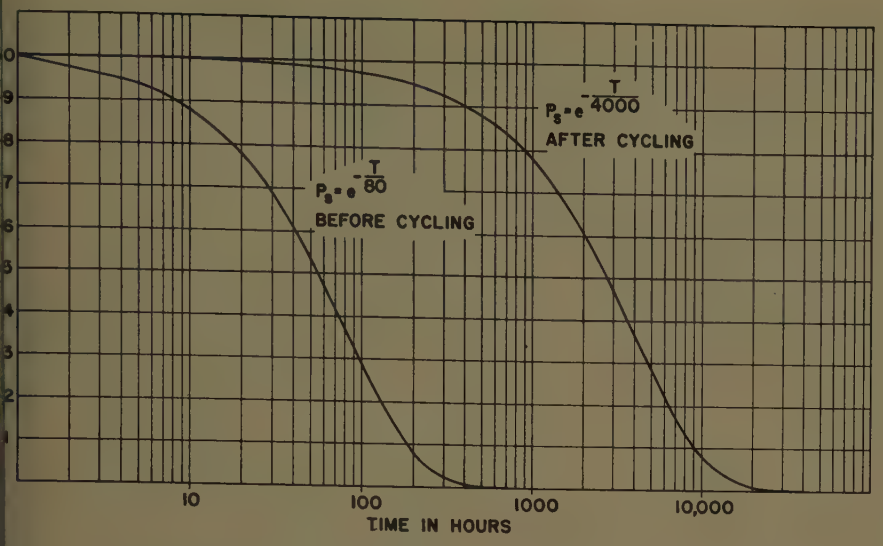

6. This curve demonstrates the improvement in control panel reliability as a result of functional cycling

pply through a load resistor to each de. Each plug-in tray has a variac adjusting peak inverse voltage and is nected so half of the diodes conduct each half-cycle. Zener diode cycling accomplished by applying a constant ct-current voltage supply through a d resistor to each zener diode, the el depending upon the zener voltage. ese trays are very flexible since all rent limiting resistors are mounted the plug-in trays.

Each tray of semiconductors is checked automatic testing equipment at the l of each 24 hours of cycling. The test- procedure for the automatic equip- nt is controlled by punched cards. is equipment scans each position within plug-in tray. If a bad component is nd, the scanner stops and indicates position of the bad component. This ipment checks a plug-in tray of 20 nponents in less than 1 minute.

The functional cycling equipment for complete control panel is more com- x since many control and protective ctions must be cycled. A block dia- m of the functional cycling test set is wn in Fig. 4. For purposes of dis- sion, the functional cycling equipment l be divided into four categories. ese categories are power supplies, con- l and measuring devices, sequencer, d control panel mounting.

At the present time there are three es of power supplies required for cyling tic control panels. A direct-current nstant-voltage power supply, a 3-phase 0-cps constant frequency and voltage pply, and a 3-phase modulated supply tained by modulating the 3-phase nstant-frequency power supply. This dulating device can be controlled to vide amplitude modulation between zero and 40%. The various 3-phase alternating-current voltages required are obtained by using two transformers and an auto transformer for each phase. The secondaries of these transformers are tapped in such a manner that any voltage between zero and 199.5 volts line-to-neutral can be selected in half-volt steps.

The control and measuring device is the heart of the functional cycling equipment. This device controls the operation of the other units in the test set. A typical control panel requires approximately 120 individual steps for cycling. This control and measuring device will perform the 120 individual steps in less than $2^1/_2$ minutes. This control and measuring device is composed of a master control unit and a selector programmed for each particular control panel. The master control contains the basic bridges, the time delays and the means for stepping the selector. The selector is programmed to choose the basic bridge, complete this bridge, select the proper terminals of the control panel, and select the proper power supply. Different programmed selectors may be easily connected to the master control unit.

The sequencer is used to connect the control and measuring device to a particular panel. The sequencer records each complete cycle on a counter, transfers the panel to stand-by power until the next cycle and steps the control and measuring device to the next panel. The panels which fail on any individual step during the cycle are completely disconnected from the two power sources and the failure is indicated by means of a lamp on the sequencer. The sequencer is timed in such a manner that each panel is functionally cycled once each half hour regardless of the number of positions used. If desired, a panel may be selected and cycled manually. Associated with each sequencer is a cabinet containing a quick-eject rack with the proper connector for the panel to be cycled. One complete cycling unit is shown in Fig. 5.

Results of Functional Cycling

Functional cycling is provided today's aircraft and missiles with the most advanced and reliable control and protective panels ever used. Users of a typical control and protective panel have accumulated 16,632 panel-hours to date. Failures have occurred, but the mean-time between failures is over 4,000 hours compared to 80 hours prior to functional cycling (see Fig. 6). The functional cycling equipment is presently providing reliability data at a rate of 650,000 semiconductor hours per month. These data are being accumulated and compiled on a computer. Continued study of the results of functional cycling is providing information for improving component and control panel design and manufacture. These improvements will continue to increase the mean-time between failures of control and protective panels. There is a 10,000-hour life test program in progress on a particular 2-generator parallel system to further study the increased reliability resulting from functional cycling. Table I is a tabulation of data from a

Table I. Mean-Time Between Failures for Different Cycling Periods

Period (Hours)	Cumulative Hours Per Panel	No. of Panels Involved	Cumulative Panel Hours	Period MTBF (Hours)	Remarks
0 to 25	25	83	2,075	520	First 25-hour cycling period (panels had cycled components)
26 to 50	50	83	4,150	415	Second 25-hour cycling period (panels had cycled components)
51 to 75	75	83	6,225	415	Third 25-hour cycling period (panels had cycled components)
76 to 100	100	83	8,300	2,075	Fourth 25-hour cycling period (panels had cycled components)

representative sample of one type of control panel. These data on 83 panels were accumulated during the 100-hour cycling period. The table shows a significant increase in the mean-time between failure during the fourth 25-hour period as compared to any previous 25-hour period. A 100-hour cycling period is adequate for this panel. Another panel, depending on its complexity and on the reliability of the components, may require a cycling period of a longer or a shorter duration.

Conclusions

The advantages of functional cycling as described in this paper are as follows:

1. Increased reliability of semiconductor components.
2. Increased reliability of equipment utilizing semiconductor components.
3. Increased reliability of the over-all aircraft electric power system.
4. A method is provided for continually improving reliability by the study of data from functional cycling.

Functional cycling is a means by which equipment utilizing semiconductors will be manufactured to meet today's reliability requirements.

Reference

1. Static Control and Protection of Aircraft Electric Power Systems, R. E. Hulsey, N. F. Schuh. *AIEE Transactions*, pt. II (*Applications and Industry*), vol. 76, Sept. 1957, pp. 209–13.

High-Speed Restarting and Protection of Large Synchronous Motors

C. L. PHILLIPS
MEMBER AIEE

M. H. YUEN
ASSOCIATE MEMBER AIEE

A WESTERN refinery was adding a new catalytic reformer unit to existing facilities. The chemical process involved, which had a platinum catalyst worth $250,000 in suspension, was dependent upon mechanical power to a compressor. This was a vital drive where loss of mechanical power for a short time meant loss of the catalyst as well as loss of production.

The use of a steam-driven compressor backed up by a steam or electric motor driven stand-by unit is a well-tried solution to such a situation. However, adequate capacity was not available from the existing facilities, and the addition of the necessary boiler capacity meant a capital expenditure of about $300,000.

Hence, the question was asked: Could power continuity be achieved electrically? Two separate reclosing sources of power were to be supplied by the utility and the user assumed the risk of an extended simultaneous loss of power on both utility feeders. After a cost study of the various combinations of electrical drives, three synchronous motors were selected. All three were needed for peak production, but only one was necessary to preserve the catalyst; this represented a double stand-by at the drives. The question now became: What would be the additional cost to achieve short-time continuity of the distribution system between the two power sources and the three drives? Cost estimates indicated that this could be done for between 10% and 20% of the steam stand-by, and the decision was made to go ahead.

The decision to use synchronous motor drivers with a goal of short-time continuity brought with it a series of considerations involving motor protection. Considerable concern has been centered about possible physical damage to large motors where a substantial residual voltage and high-speed restarting and/or a reclosing source are coincident. (See the references.)

Hence, two programs exist: First, high-speed restarting to achieve process continuity and, second, adequate motor protection. This paper demonstrates, with an oscillographic record of successful operation, an electrical solution of these two coincident problems.

System Layout and Equipment

Fig. 1 is the refinery electrical 1-line diagram. Two separate source feeders with reclosers are both energized but only one source energizes the main refinery bus. If the normal utility source fails entirely, a 1.3-sec (second) throw-over to the other source is actuated, re-energizing the main refinery bus. Note that both feeders to the catalytic reformer are normally closed, and that, hence, a utility power discontinuity appears as a momentary complete loss of power to the catalytic reformer. This refinery substation is modern drawout switchgear and is rated AM-13.8-250 megavolt-amperes.

Fig. 2 shows the catalytic reformer 1-line diagram. Here the intent was to provide functional duplication of all equipment, such as equipment which would automatically insure mechanical power to the compressors even though a failure of any piece of equipment or cable were to occur. Second-order failures were considered but not provided for in all cases.

The new 4.16-kv drawout switchgear is rated AM-4.16-150 megavolt-amperes. It is fed by two 1,500-kva transformers rated 12-kv delta to 4.16-kv Y, in one line-up. A 4.16-kv bus is connected overhead to a Limitamp starter line-up of conventional design. The synchronous motors all are rated 600-horsepower, 1.0 power factor, 400-rpm, 4,000-volt, 69.3-ampere full load, 50-degree-centigrade temperature rise, force-ventilated, with separate motor-generator set excitation and 8,500 lb-ft² (pound-feet²) inertia. The compressor is a positive-displacement horizontal opposed-compression frame with 1,000 lb-ft² inertia. The 480-volt auxiliaries are fed by a conventional double-ended load center with each end rated 750-kva, 12-kv delta to 480-volt delta. Conventional magnetic drawout air circuit breakers were used at the 480-volt level with a 1-sec time delay throw-over between the main secondary breakers and the bus tie breaker. This throw-over combined with a lack of under voltage protection for the individual exciter motor-generator sets assures excitation power if there is voltage from either 480-volt switchgear bus. Conventional motor control centers were used. Without exception, all equipment was of outdoor weatherproof construction.

Figs. 3 and 4 respectively illustrate the

Paper 59-822, recommended by the AIEE Chemical Industry Committee and approved by the AIEE Technical Operations Department for presentation at the AIEE Summer and Pacific General Meeting and Air Transportation Conference, Seattle, Wash., June 21–26, 1959. Manuscript submitted March 23, 1959; made available for printing May 4, 1959.

C. L. Phillips is with the General Electric Company, San Francisco, Calif., and M. H. Yuen is with the Bechtel Corporation, San Francisco, Calif.

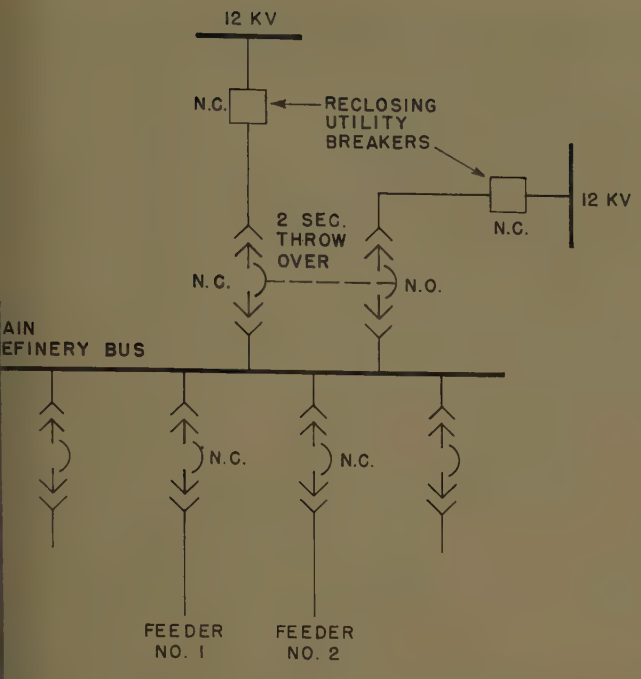

Fig. 1 (above). Over-all refinery 1-line diagram

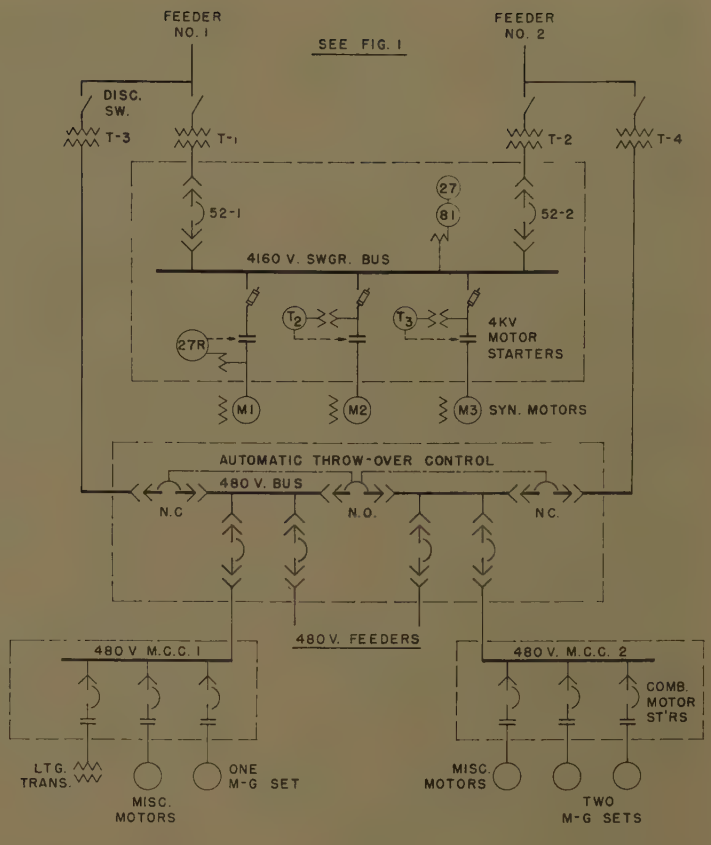

Fig. 2 (right). Catalytic reformer 1-line diagram

p-and-close circuits of *52-1* and *52-2*, d the simplified plant shutdown circuit. ie philosophy of this relaying is based power continuity being maintained these synchronous motors at any cost ort of destroying the motors.

An important risk to the running motor m a high-speed reclosure of a source is isting a shaft or distorting a winding. ie best assurance against such a failure, this writing, is to remove, somehow, e motors from the bus before a reclosure n re-energize the motors. This was ne with a relay tripping *52-1* and *52-2* er the initial opening of the source eaker. The relay chosen here was a neral Electric Company type *CFF13A* h-speed underfrequency (*81*) relay. was originally set at 58 cps (cycles per ond).

Once *52-1* and *52-2* are open, conditions on both sides of these circuit breakers must be returned to normal as rapidly as possible in order to initiate restarting. The reclosure and/or throw-over upstream will restore system voltage to normal anywhere within 20 cycles to 5 sec after the initiating disturbance.

After an open circuit between the source and the motors is established, the motors act as synchronous generators; therefore the same auxiliary relay *86-1*, which is initiated by the *81* that trips the *52-1* and *52-2*, also de-energizes the motor fields. This action is quite essential. With field applied, the motor voltage will vary almost directly as the motor speed, which will show little variation over the short time involved. Without field excitation, the motor voltage decay is primarily a function of the motor time constant, which will usually result in acceptable voltages within a time measured in cycles. By measurement from the oscillographs of Figs. 5 through 11, the time constant, represented by the time required for the armature voltage to decay from very nearly full voltage to 36.8% or $1/e$ pu (per unit) when the field is removed, is in this case 0.153 sec. In order to check this action, a 3-phase residual relay on the first motor to restart acts as a lockout of the starter until this motor's residual voltage decays to 25% of normal. The other two motors are restarted upon a signal from timing relays set much longer than the time required for the residual voltage to reach 25% of normal.

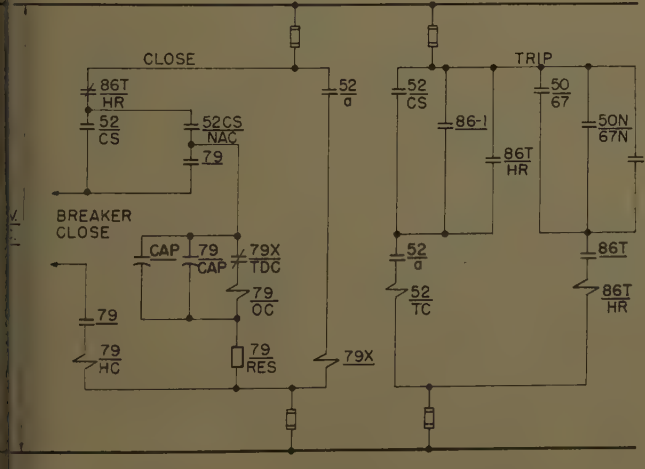

Fig. 3. Simplified breaker trip-and-close circuits of 52-1 and 52-2

52 = air circuit breaker
52/a = air circuit-breaker auxiliary contact
52/cs = air circuit-breaker control switch
52/TC = air circuit-breaker trip coil
50/67 = phase directional overcurrent relay, instantaneous and inverse time
50N/67N = phase directional overcurrent relay, instantaneous and inverse time
51 = phase overcurrent relay inverse time
86T/HR = lockout relay, hand reset
86-1 = plant shutdown auxiliary relay
79 = single-shot reclosing relay
79X = reclosing auxiliary relay

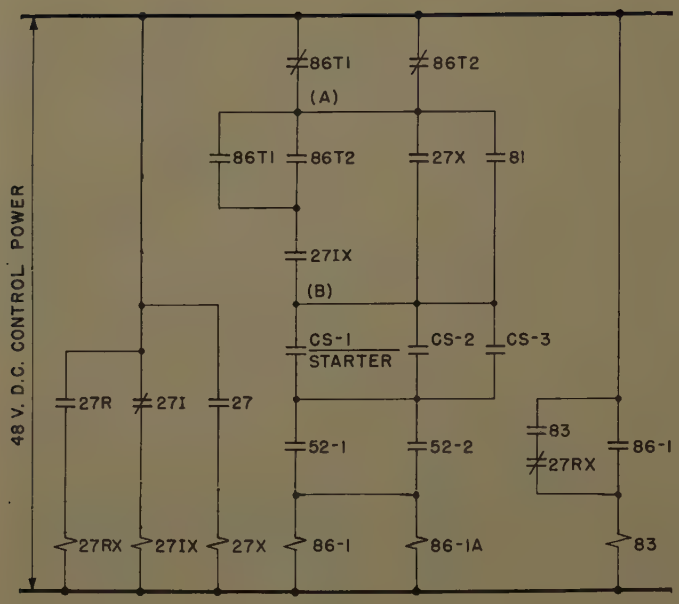

Fig. 4. Plant shutdown circuitry

86T1 = lockout relay for 52-1
86T2 = lockout relay for 52-2
81 = underfrequency relay
27X = inverse time undervoltage auxiliary relay
27IX = instantaneous undervoltage auxiliary relay
86-1 = plant shutdown auxiliary relay for 52-1
86-1A = plant shutdown auxiliary relay for 52-2
27 = inverse time undervoltage relay
27I = instantaneous undervoltage relay
27R = three-phase residual undervoltage relay
27RX = three-phase residual undervoltage auxiliary relay
83 = unloading auxiliary relay

Since the starter's drop-out time after de-energizing its control circuit is in the order of 3 to 5 cycles plus a possible 10-cycle arcing time, *52-1* and *52-2* could have a single 15-cycle time delay reclosure to ready the motor bus for restarting. In designing the relaying it appeared at first as though the tripping and reclosing of the 4.16-kv breakers could be omitted in favor of simply opening the starter contactor. However, the uncertainties of contactor opening time plus a desire for positive operation resulted in the decision to use the deliberate and predictable action of the breakers. The problem can then be demonstrated with:

1. A system layout with adequate standby capability such as that illustrated in Figs. 1 and 2.

2. Breaker trip and close circuits such as that in Fig. 3, illustrating necessary manual controls, conventional overcurrent and short-circuit protection, and special tripping and closing functions.

3. A shutdown circuit such as illustrated in Fig. 4, capable of sensing those conditions which would necessitate a deliberate yet high-speed shutdown and restart.

4. A modified starter control circuit to insure necessary interlocking, early field removal, lockout against excessive residual voltage, provisions for a loaded stop and an unloaded start, and necessary manual controls.

In connection with the designing of the special shutdown circuitry, some uncertainty existed as to whether all the functions and circuits that the actual installation might require could be anticipated. Consequently, if the need for a function was in doubt, it was included. Ample auxiliary relays and contacts were included in anticipation of field modifications. This approach turned out happily as several field changes were easily and quickly made with minimum loss in expense and time. Care was necessary to avoid contact races, and decisions were made concerning the sequence of relay events for each of the multiplicity of conditions that might occur. Those who may toy with the idea of trying this should realize that it takes a great deal of thought and care; simplicity should not be anticipated on the first attempt.

The principal shutdown functions discussed in this paper are found between points *A* and *B* in Fig. 4, and are here limited to:

1. High-speed underfrequency (*81*).
2. Inverse time undervoltage (*27X*).
3. High-speed undervoltage due to upstream fault (*86T* plus *27IX*).

Other, less important, functions were included, though not shown in Fig. 4, and those attempting this work may find other functions special to their condition. Note that in the case of a shutdown because of a fault upstream from the 4.16-kv bus, the 4.16-kv circuit breaker near the fault is locked out but the alternate breaker is permitted to reclose to effect rapid restart.

Regarding the Limitamp starters, care is taken to insure high-speed field removal and to insure that unloading valves have time to operate before a restart. The three starters make an independent try at restarting in time sequence to relieve the strain on a possibly faltering source.

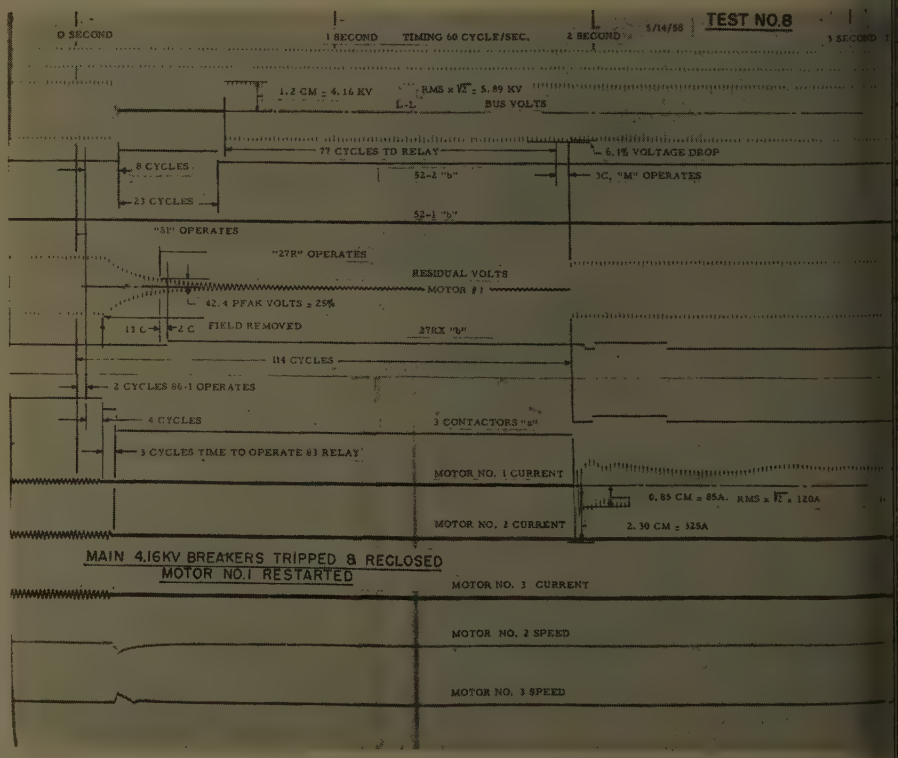

Fig. 5. Oscillographic test 8, manually initiated emergency, first 3 seconds

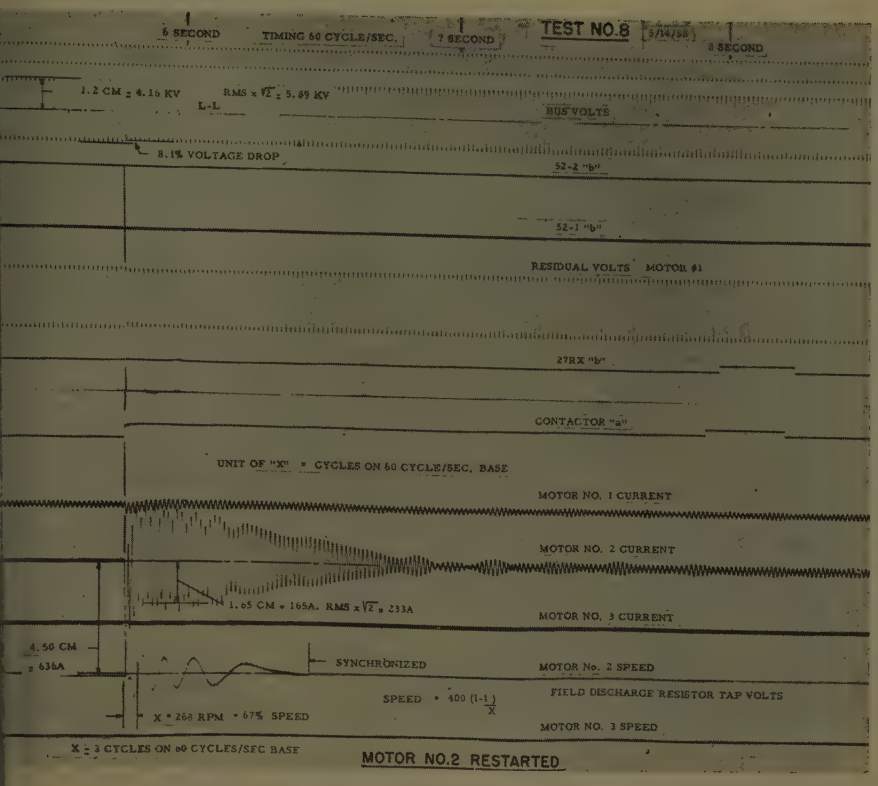

Fig. 6. Oscillographic test 8, motor 2 restarted

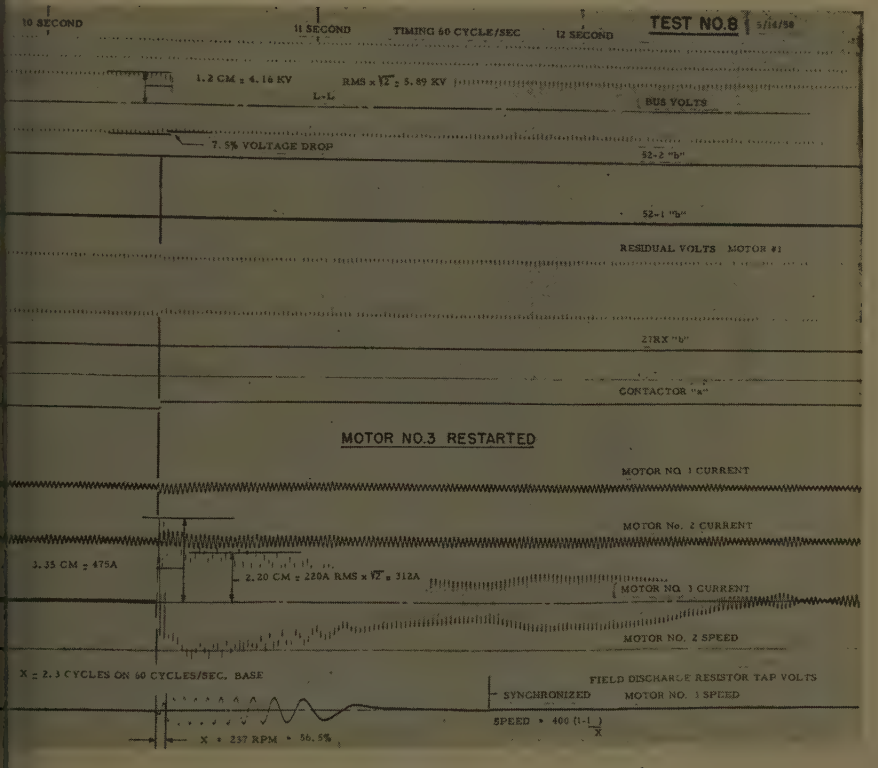

Fig. 7. Oscillographic test 8, motor 3 restarted

her source on another system might it simultaneous restarting with re- al voltage permissive relays on all ers.

he requirements of the process are nent to the question of sequential ing. The subject equipment re- s all three motors to synchronism within 15 sec from the moment of system disturbance. Further, this equipment could accomplish complete sequential starting within 10 sec by simple timer adjustment without stress and without compromise. This was well within the process requirement.

The equipment performance is demonstrated in the oscillograms of Figs. 5 through 7, which illustrate a manually initiated emergency. Here the *81* device was manually closed and the equipment made the record shown. It was demonstrated that the equipment, when experiencing a frequency disturbance, reacted safely and in accordance with its design. The last motor was energized and synchronized within 15 sec.

It remained to simulate an unpredicted emergency; this was done as demonstrated in test 9. Figs. 8 through 11 illustrate test 9, wherein a 12-kv circuit breaker acting as a source breaker was manually tripped and reclosed some 150 cycles later. The delay of 150 cycles was simply to insure clearing the *81* operation. Nothing was touched at the catalytic reformer and the equipment made the record shown. Note the 22-cycle reclosing time of the local breaker *52-2*. Also note the difference in character in the residual voltage and how important it is to remove the field. The fact that the motor contactor opened before the breaker may be significant in future work. If power had returned while *52-2* was open, as is possible, the *27R* would have postponed the first motor restart. The motor-starting traces on the single long oscillograph (Figs. 8 through 11) are conventional, and the voltage drops are all less than 10%. Note the over-all time of less than 15 sec and the space in the time sequence which would permit an over-all time of less than 10 sec. Motor speeds were arrived at by recording a voltage drop on a portion of the motor discharge resistor. This would show the slip frequency in the rotating field while the motor was accelerating. One slip cycle measured in X cycles on a 60-cps base gives the per-cent speed at the time of re-energizing the motor by the equation: per-cent speed $= 100\ (1 - 1/X)$.

Figs. 8 through 11 show that it took circuit breaker *52-2* a total of 40 cycles, on a 60-cps basis, to separate the motors from the failing source. This amount of time could be divided into 30 cycles for the *81* (set to operate at 58 cps) to operate, 2 cycles to operate the *86-1* device, and 8 cycles more to open the breaker. During this time the motors were acting as synchronous generators. Had the initial disturbance resulted in a 30-cycle reclosure, it seems clear that these motors in this system would have been exposed to the risk of shaft damage or winding distortion. The test is a good illustration of the conditions creating the possible hazards of inadequate motor protection. It is these hazards which indicated the need for an oscillographic record in the work. One

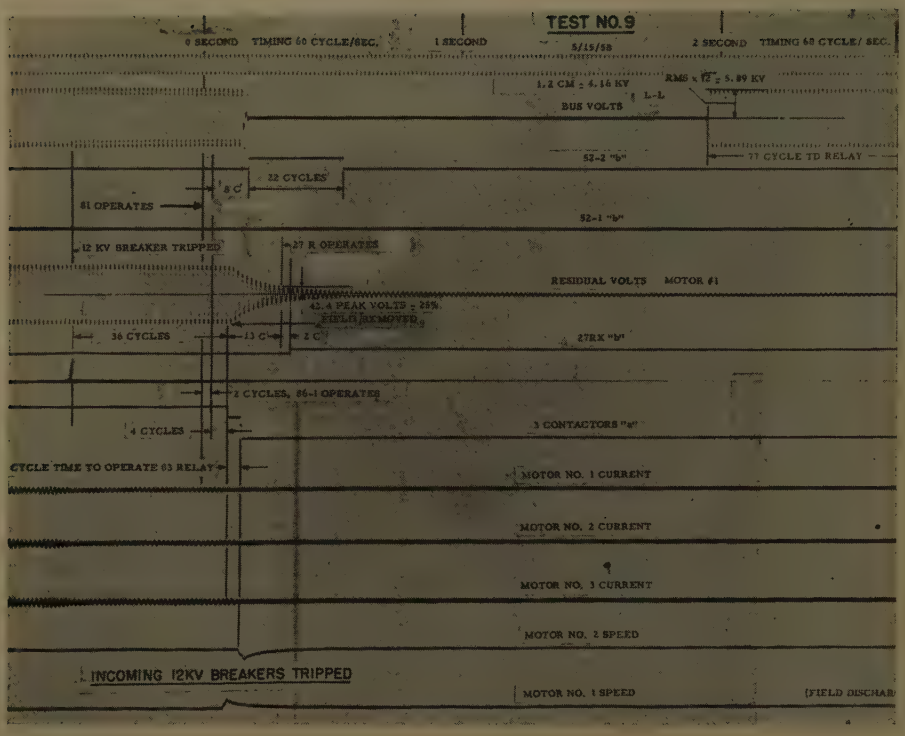

Fig. 8. Oscillographic test 9, automatically initiated emergency, first 3 seconds

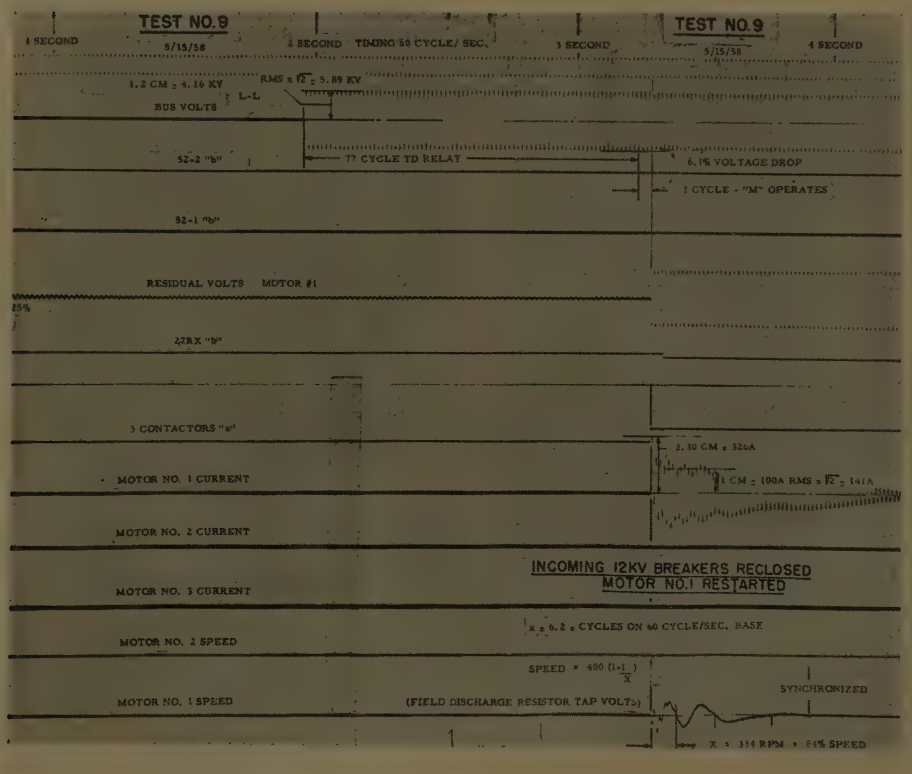

Fig. 9. Oscillographic test 9, motors 1 restarted

of the objectives of the work is an evaluation of the hazards and a reasonable assurance that they have been overcome. The authors believe that this objective was obtained in this case, as will be illustrated later in the paper.

Test 9 was initiated with no electric load in the catalytic unit other than the three synchronous motors, their exciter motor generator sets, and their cooling fans. The mechanical load on the motors was approximately 10%, consisting largely of mechanical and electrical losses in the motors and compressor. It was felt that these conditions would result in the minimum rate of deceleration that could be reasonably expected of the system. the motors could be protected during t conditions of minimum rate of decele tion, it was believed that the system a relay characteristics would surely pr tect the motors during higher rates deceleration.

For those particularly interested in t operation of the *81* device and the ele trical degrees' separation of the sy chronous motors and source immediate after the source breakers opened, Fig. is offered. It is an enlargement of a po tion of Fig. 8.

Fig. 13 depicts the electrical separati of all three motors as a group from t source after the disturbance was initiate Common polar co-ordinates were used a the data were carefully measured fro the oscillograph of test 9. Of perha more value are the same data plotted log-log co-ordinates as shown in Fig. From these curves 4 cps/sec is about t minimum rate of change of frequency be expected from this system.

Note in Fig. 14 that the rate of chan of frequency is shown to be consta following the first 20 cycles after initiati the disturbance. Particularly mysterio is the nonlinear rate of deceleration duri the first 20 cycles. Since this was n anticipated, it received a good deal attention. Past practice has usually bee to assume a constant rate of deceleratio until conditions arise where connecte mechanical and electric loads vary no linearly at reduced frequency and spee The authors would welcome a clarifyi explanation. The significance may that it is possible for some types of electr and mechanical systems to reduce the mi mum rate of deceleration during the cri ical time before 20 cycles after a distur ance is initiated; if so, the difficulties designing adequate protection for t motors are compounded. More oscill graphic data are needed.

Assuming a constant rate of change frequency throughout at 4 cps/sec, Tab I indicates theoretical anticipated clea ing times of the *52-2* circuit breaker f various settings of the *81* relay. Al shown is the relation of the clearing ti experienced in Fig. 8 and suggested mi mum source reclosing times. It is inte esting to note that Fig. 15 shows a prof able gain in the *81* relay operating ti up to about 10 cps/sec; this is a gain 5 cycles. Hence, optimistic estimates the rate of change of frequency of a pa ticular system produce only minor redu tions in total clearing times and minimu reclosing times. It can be stated, thoug that a rate of change of frequency abo the minimum will widen the margin

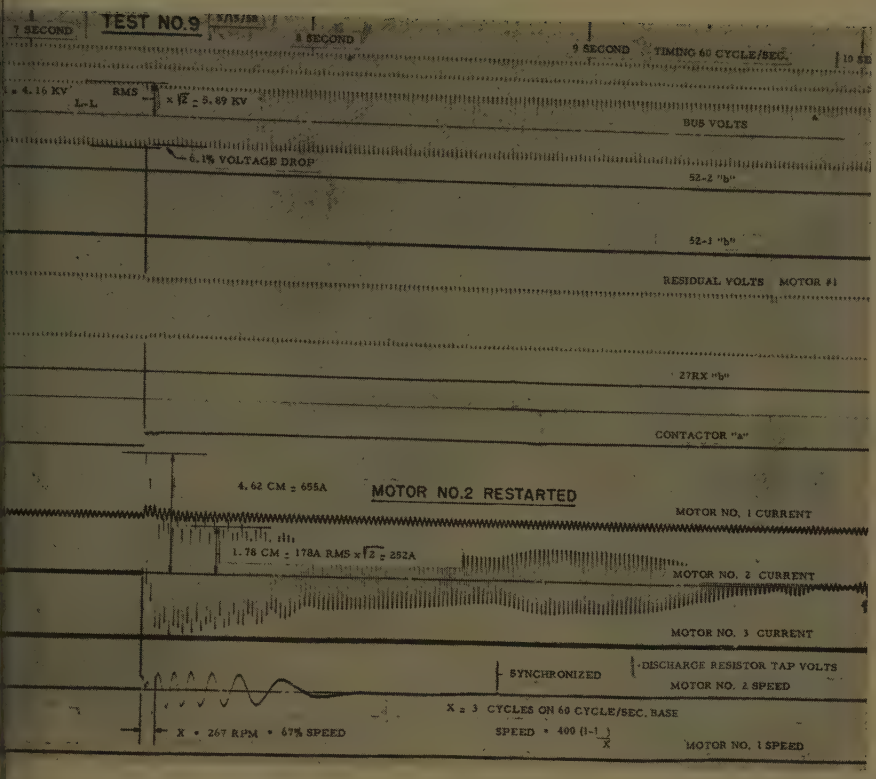

Fig. 10. Oscillographic test 9, motor 2 restarted

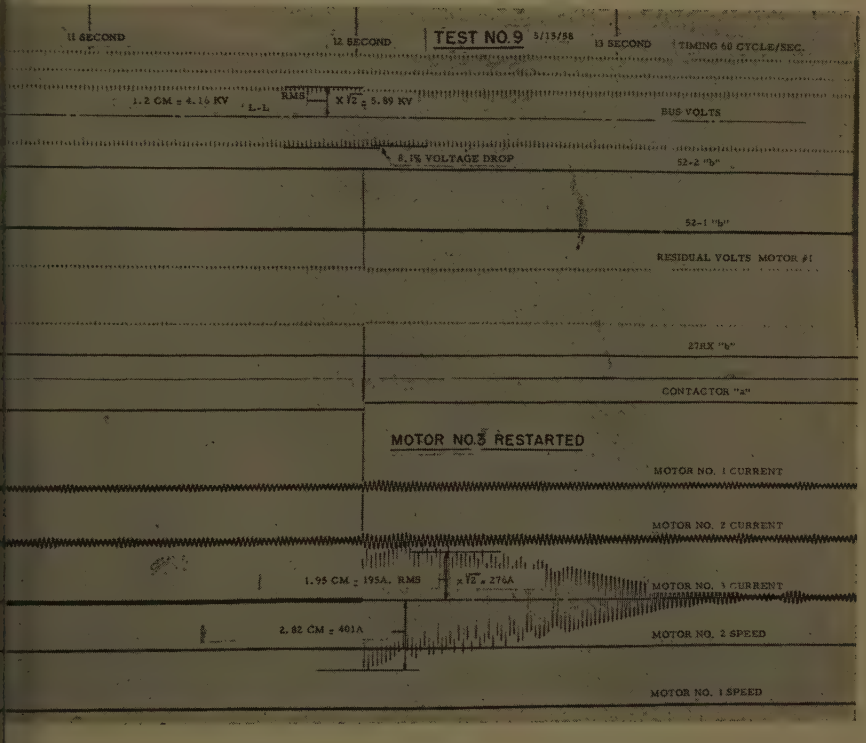

Fig. 11. Oscillographic test 9, motor 3 restarted

between the maximum breaker clear-
ime and the minimum upstream re-
ng time.

ne oscillograph of Figs. 8 through 11
ated a clearing time longer than was
d for. Consequently, thought was
to setting the *81* relay up to 59.5 cps.
ty frequency recordings over the past year indicated that such a setting would not result in excessive nuisance tripping due to utility short-time frequency excursions. The relay was recalibrated to 59.5 cps, where it remained during a winter of many severe electrical storms. Experience thus gained indicated that winter disturbances to the utility system shut

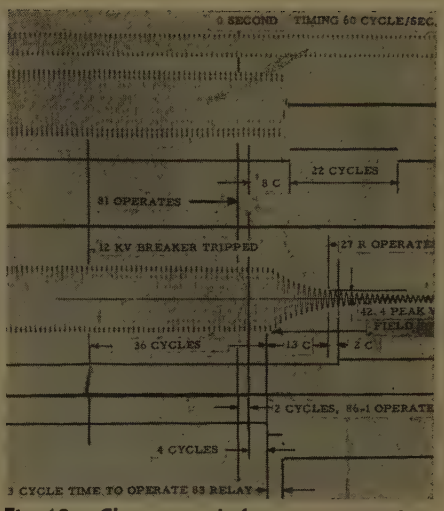

Fig. 12. Close-up underfrequency operation, oscillographic test 9

the catalytic reformer down due to frequency excursions often enough to warrant setting the *81* relay back down to a lower value. The new set point after review of the utility frequency recordings over the winter was determined as 585 cps. Thus, such frequency excursions and how often they occur are an important factor in determining the minimum source reclosing time; for this system it is 45 cycles.

Parenthetically, experience has shown that the equipment has repeatedly protected the process. The operators have related that on one black and stormy night filled with lightning the equipment went through the sequence of events pictured in Figs. 8 through 11 thirteen times, keeping the catalytic reformer on stream.

This experience in gaining confidence in the adequacy of the underfrequency relay in properly protecting these motors was time-consuming and expensive. Since the data presented cannot be extrapolated to other systems, but is applicable only to this system, a need is felt for an analytical technique permitting the confident prediction of a system minimum rate of change of frequency. Subsequent to the taking of these data, this need was answered by a confirming analytical technique presented by Morton and Shepherd.

The equation found in this paper for the rate of change of frequency is

$$\Delta f = \frac{0.972HP}{WK^2N^2}\,10^8 = \text{rate of change of frequency}$$

where HP approximated 60 to 75 (essentially losses); $WK^2 = 9{,}500$ lb-ft^2 $N = 400$ rpm.

These values placed in Morton's equation resulted in a calculated rate of change of frequency between 4 and 5; this, while approximate, lends confidence

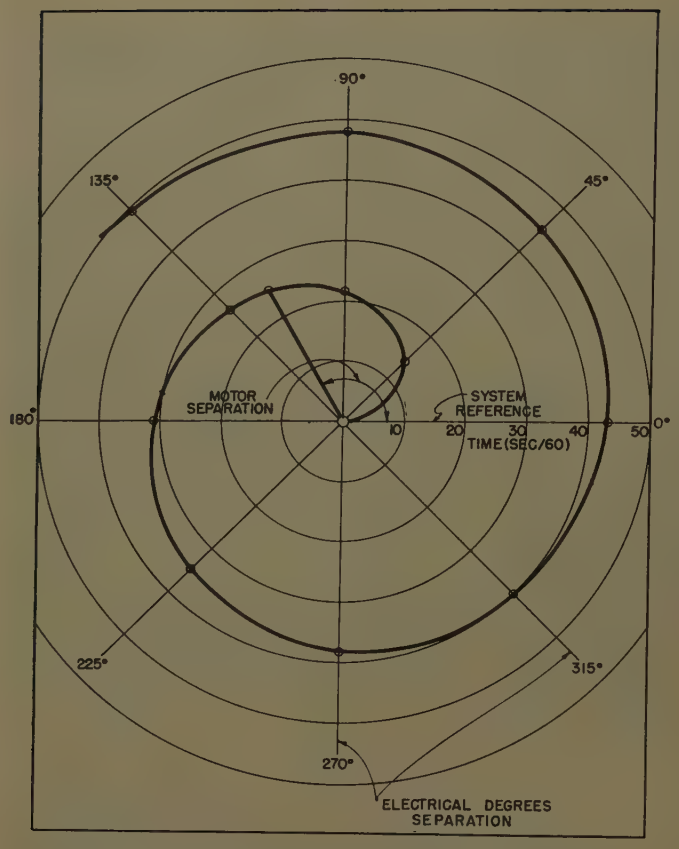

Fig. 13. Electrical separation curve, polar co-ordinates

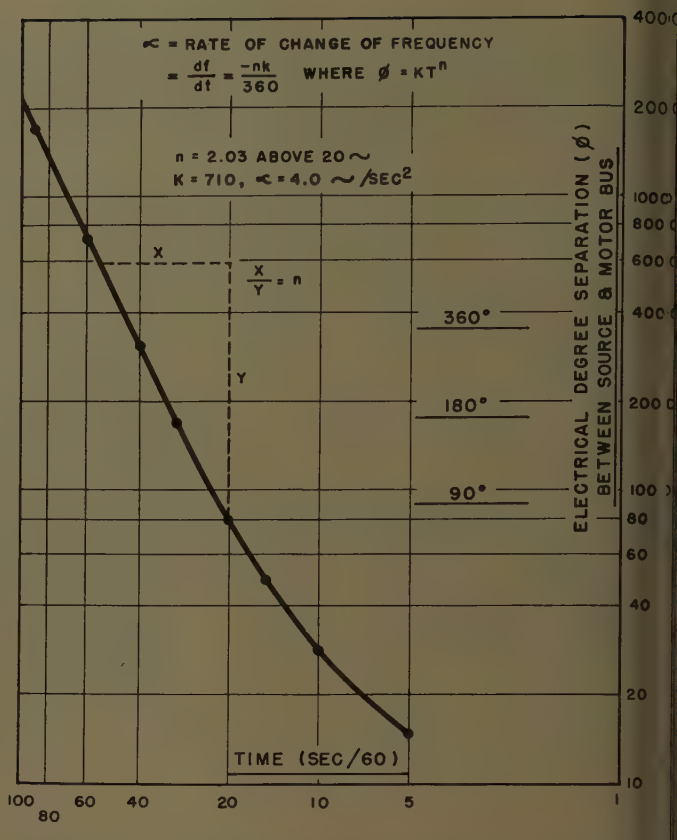

Fig. 14. Electrical separation curve, log-log co-ordinates

to Figs. 8 through 11. The analytical technique and/or oscillograms such as those presented in this paper are the two presently known methods of adequately judging such underfrequency motor protection.

Conclusions

1. High-speed field removal is essential to early residual voltage reduction of a synchronous motor momentarily separated from its power source.

2. The sequence of relaying under the influence of a multiplicity of conditions is complex. It should be approached with respect and deliberate thought should be devoted to insuring performance. Simplicity, always desirable, should be anticipated only after several attempts. In designing the relaying, generosity proves worth while. The inclusion at the beginning of doubtful functions, ample auxiliar relays, and contacts immensely simplifi the metamorphosis of the system ar does so at relatively unimportant cost.

3. Liaison with process people is mo important; they must establish the dollal versus-time evaluation. It would unwise to put time, money, and effo into a system embodying continuity of order unwarranted by the process. Co versely, to economize on the relaying, ar

Table I. Theoretical Clearing Times*

Times	Cycles			
81 relay setting, cps	58.0	58.5	59.0	59.5
81 relay operating time, at 4 cps/sec	11.5	11.5	11.5	11.5
86-1 relay operating time, cycles	2.0	2.0	2.0	2.0
52-2 circuit-breaker operating time, cycles	6.0	6.0	6.0	6.0
Test equipment operating time, cycles	19.5	19.5	19.5	19.5
Motor system deceleration time to *81* relay setting at 4 cps/sec	30.0	22.5	15.0	7.5
Total clearing time, theoretical, cycles	49.5	42.0	34.5	27.0
Total clearing time, Fig. 8, cycles	41.0			
Suggested minimum source reclosing time, cycles	55	45	40	35

* Estimations except for Fig. 8.

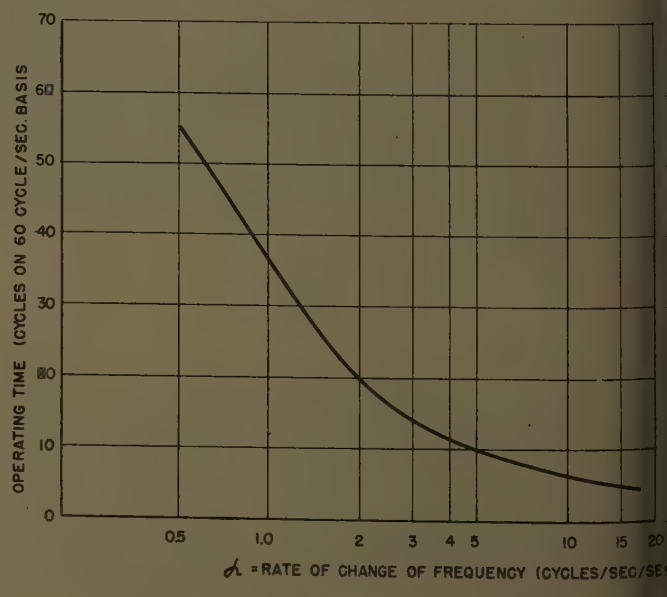

Fig. 15. Operating time of underfrequency relay type CFF13A after system frequency reaches relay setting

so doing fail to protect the process, uld be even more unwise. The ogey" in connection with the equip- nt was based on permitting loss of drogen pressure supplied by any of the ee compressors to a common hydrogen eiver for no more than 10 seconds.

. Oscillographic records clearly in- ate that the equipment meets the cess bogey. An even better indication hat the equipment has already faced re- ted emergencies and performed far ad of an operator to save the catalyst.

. Above a rate of change of frequency about 10 cps/sec, circuit-breaker clear- time is composed primarily of equip- nt operating time. Hence, in the de- n of the system advantage should be en of every opportunity to reduce the r-all equipment operating time. The t and fastest available devices should selected and a minimum number of ices used sequentially in time. Over- imistic estimates should be avoided.

. However, anything other than the ual minimum rate of change of fre- ncy is of little value in evaluating the its of the high-speed underfre- quency relay and in determining the appropriate minimum time for reclosing the upsteam circuit breakers. By oscillographs, the subject motors and their driven equipment produced a practical minimum rate of change of frequency of 4 cps/sec; this in turn ultimately resulted in a suggested minimum 12-kv circuit-breaker reclosure time of 45 cycles, applicable to this system only.

7. An analytical technique permitting a confident prediction of a system minimum rate of deceleration is helpful in judging the adequacy of underfrequency relaying as synchronous motors protection. This, coupled with oscillographic confirmation, should result in a satisfactory extension of such underfrequency protection to other systems.

8. In arriving at the highest practical underfrequency setting of the underfrequency relay there should be careful consultation with utility records and personnel, with the aim of avoiding operation during short-time underfrequency excursions of the utility. Such excursions do occur but for reasons outside the scope of this paper.

References

1. Transfer of Steam-Electric Generating-Station Auxiliary Buses, D. G. Lewis, W. D. March. *AIEE Transactions*, pt. III (*Power Apparatus and Systems*), vol. 74, June 1955, pp. 322–34.

2. Transient Protection Conditions in Pipe-Line Stations, E. B. Turner. *Ibid.*, pt. II (*Applications and Industry*), vol. 77, May 1958, pp. 85–90.

3. The Concept of "In Phase" Transfer Applied to Industrial Systems, Serving Essential Service Motors, C. C. Young, J. Dunki-Jacobs. *AIEE CP 58-1064* (*5033*), (available on request).

4. Transfer Tests on Station Auxiliary Buses, L. E. Backer, Paul Barth, R. A. Huse, D. W. Taylor. *AIEE Transactions*, pt. III (*Power Apparatus and Systems*), vol. 74, 1955 (Feb. 1956 section), pp. 1441–49.

5. Switchgear with Stored-Energy Mechanism Applied to Steam-Station Auxiliary Transfer Arrangements, P. G. Brown, J. J. Heagerty, D. G. Lewis, E. M. Smith. *Ibid.*, vol. 77, June 1958, pp. 310–18.

6. High Speed Reclosing of Circuit Breakers on Systems Utilizing Synchronous Motor, W. R. Morton, R. V. Shepherd. *AIEE CP 59-891* (available on request).

7. A Transient Stability and Voltage Study for a Modern Oil Refinery Distributions System, C. W. Boice, S. R. Durand, D. Dalasta. *AIEE CP 56-76* (available on request).

8. High Speed Breaker Reclosing Can Put Abnormal Stresses on Your Motors, D. Dalasta, S. Durand. *Power*, New York, N. Y., Design and Equipment Application Section, Feb. 1958, pp. 90–93.

Discussion

P. Brightman (General Electric Com- y, Schenectady, N. Y.): The authors to be commended for their useful er. Documented test data is valuable ause it confirms the expected behavior protected and protecting equipment ed on calculations, and because it may eal unsuspected performance charac- stics which add to our store of wledge.

he latter seems to apply here. The hors report that the tests revealed an r-all operating time better than expected, ch was an entirely satisfactory con- ion to the tests as far as the particular allation was concerned. However, the that the performance was better than ld be accounted for by known charac- stics of the motors and relays suggests possibility that some hitherto unknown unappreciated factors were involved. purpose of this discussion is to present results of my attempt to ascertain reason for the unexpected performance. plotted a curve of frequency against e using data obtained from the test 9 llogram starting at 5 cycles before the kv circuit breaker opened and ending 9 cycles after it opened. The resulting ve (Fig. 16) revealed quite unexpected surprising behavior by the motors. tead of starting to slow down imme- ely when their power supply was cut the motors apparently speeded up, ch is most unorthodox. Then, as wn by the curve, they proceeded to lerate in an oscillatory fashion, i.e., alternately slowed down and speeded n a rhythmic pattern. It is impossible to vouch for detailed accuracy of the oscillations shown in the curve because a difference of 1/10 millimeter in scaling the oscillogram made a change of almost a cycle in the calculated frequency. However, the calculations showed a frequency of 60 cycles for the 5-cycle period prior to opening of the 12-kv circuit breaker, and some form of oscillatory pattern showed up regardless of the method of calculating the data, which leads me to believe that the oscillations were real and not due to errors in scaling the oscillogram.

The data for the frequency-time curve were obtained from a glossy silver print of Fig. 12, which is an enlargement of a portion of the test 9 oscillogram. As a means of compensating for nonuniform movement of the film in the oscillogram (evidenced by unequal lengths of the timing-trace cycles), I compared the lengths of 3 cycles of motor 1 and the timing traces on the oscillogram, and multiplied their ratio by 60 cycles. The use of a 3-cycle span, consisting of the cycle involved and the two adjacent ones, seemed the best compromise between 1. minimizing errors resulting from measurement of the length of the spans, and 2. masking the magnitude of single-cycle oscillations. Curves plotted from data calculated on the basis of measuring the span of 1, 2, 3, and 5 cycles showed the same general pattern. Likewise, the patterns were similar for curves calculated from the O-axis and the upper and lower peaks of the traces.

The curve in Fig. 16 was constructed by plotting the calculated frequency at each succeeding cycle of elapsed time and connecting these points by straight lines. The resulting curve is, of course, unrealistic in that it shows abrupt changes in speed, which are physically impossible because of the mechanical inertia of the equipment, but no greater accuracy was possible with the data available.

Believe it or not, as you wish, the "impossible" frequency-time curve in Fig. 16 accounts for:

1. The unexpectedly short over-all operating time recorded, (41 cycles instead of the authors' calculated 49.5 cycles).
2. The faster and nonlinear angular rate of separation below 20 cycles shown in Figs. 13 and 14.

Fig. 16 shows that the shorter over-all

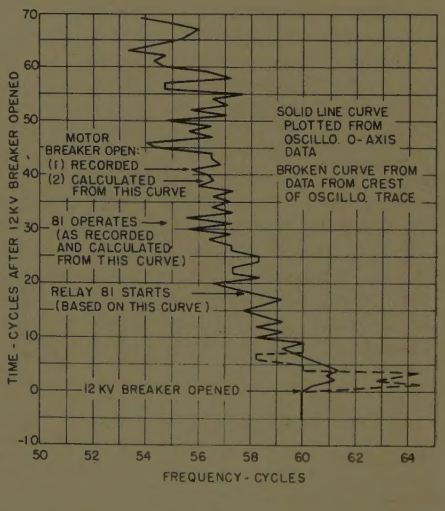

Fig. 16. Frequency-time curve showing behavior of motors based on test 9

operating time resulted because the motors required only 18 cycles to slow down to the 58-cycle setting of the underfrequency relay (device *81*) instead of the calculated 30 cycles. According to Fig. 16 the frequency was constantly fluctuating, and twice during the period from 18 to 30 cycles it even went above the relay's setting of 58 cycles. To determine the relay's operating time for the period, I assumed that the net effect on the relay would be the same as though it had been operating on a constant rate of change of frequency that would have caused the frequency to drop from 58 cycles to the calculated average of 57.3 cycles for the period. Fig. 15 shows that the relay would close its contacts in 12.5 cycles at the 3.5 cps/sec rate of change of frequency calculated on this basis. Adding this to the 18 cycles decelerating time gives a total of 30.5 cycles, which corresponds almost exactly with the recorded operating time of device *81* as shown in Fig. 12. According to the notations of Fig. 12 there was a lapse of 10 cycles from the closing of *81* contacts to the opening of circuit breaker *52-2*. Adding this to the 30.5 cycles gives a total calculated time of 40.5 cycles compared with the recorded 41 cycles reported in the paper.

The curves in Figs. 13 and 14 show that the rate of angular separation during the first 20 cycles was progressively faster as zero time is approached. If the lower end of the separation curve on log-log paper (Fig. 14) is extrapolated at the same slope, the angles of separation at 3 and 4 cycles are 10.7 and 12.8 degrees respectively. The calculated rates of change of frequency during the first 20 cycles based on these extrapolated figures and others taken from the angle of separation curve in Fig. 14 are as follows:

Time, Cycles	Separation Angle, Degrees	Rate of Change, Cycles/Sec/Sec
3	10.7	23.8
4	12.8	16
5	15	12
10	28.5	5.7
20	80	4.0

This pattern of rate of change of frequency corresponds to one that could be calculated from the Fig. 16 curve.

It is my understanding that the angle-of-separation curves in Figs. 13 and 14 did not include allowance for the fact that, when the 12-kv circuit breaker opened the phase angle of the motor, voltage would shift immediately to a position corresponding to that of the motor rotor prior to the interruption. This would mean a backward shift of perhaps 8 degrees for motors carrying about 10% load, as these were doing. Since this shift would have the same effect as motor deceleration, it should be deducted from values shown in Figs. 13 and 14. When this is done,

1. The extrapolation of the Fig. 14 curve would show a negative angle of separation indicating a speed increase rather than decrease in the 0–2 cycle time period.

2. The calculated rate of change of frequency at 20 cycles becomes 3.6 cycles/sec/sec which is essentially the same as the 3.5 value calculated from Fig. 16 for the 18–30 cycle period.

Thus it appears that the curve in Fig. 16 accounts for the performance of the equipment as observed and recorded by the authors. However, we still do not know why the machines behaved that way.

Some of the speculative questions might be:

1. Was the behavior of the machines due to a backward expansion of compressed gas, or to the known fact that synchronous-motor-driven compressors pulsate. In this connection it is interesting to note that the compressor units were in mechanical synchronism during this test, as indicated by the pulsations in the three motor current traces prior to opening of the 12-kv circuit breaker. Consequently, any negative-torque effect would have shown up at its maximum.

2. Was it an isolated incident, or would it happen again to these motors? If so, would it happen regardless of load on the motors?

3. If it was not a freak incident, would it also happen to other motor-driven compressors?

4. Why did the motors slow down so much faster than expected, and would they have behaved proportionately if they had been loaded?

The answers to these questions may have a decided effect on our ability to disconnect compressor motors by means of underfrequency relays fast enough to protect them against out-of-phase re-energization when there is 15–20 cycle reclosing on the power supply.

The authors report that, after these tests were made, the frequency relay was recalibrated to 59.5 cycles to obtain still faster over-all operating time. It was changed again to 58.5 cycles to prevent unnecessary shutdown of the equipment due to power-system frequency fluctuations. That was possible in this case because of ample time for operation of the equipment.

When slowing down of the equipment is not permissible, false operation of the frequency relay can be prevented by using a power relay to monitor it. The contacts of the two relays are connected in series, so that both must operate in order to complete a tripping circuit. With this combination the frequency can fluctuate widely without causing tripping as long as the power relay indicates that the plant is getting power.

Just as a matter of general information, I discovered what was to me a somewhat novel way to scale the oscillogram. Fi I made a pinprick at the points on traces that I wanted to measure, t turned the sheet over and worked on reverse side. It was much easier to l up the scale on the centers of the pinhc than on the oscillographic traces, especia the somewhat unsymmetrical crests of waves.

C. L. Phillips and M. H. Yuen: Becaus is difficult to comment on a field experie without having available the field d being discussed, Mr. Brightman, who h expressed an interest in this subject, v given access to the field data presented the paper. His discussion is a valua extension of the interpretation of data. The authors do not differ w Mr. Brightman's basic views; rather, effort seemingly confirms the autho position as follows:

1. More oscillographic data are needed

2. We do not thoroughly understand w happens to synchronous motor dri within 20 cycles after a power failure.

3. Underfrequency relaying for the p pose of protecting a synchronous mo from a high-speed power reclosure, w apparently the best solution we know to may not permit co-ordination with upstream high-speed reclosing device.

Questions of the character raised Mr. Brightman inherently rest on accuracy of the field data. It should emphasized that these data were taken a professional who had spent a lifetime oscillographer for one of the largest utili in the country. The authors feel sure t data can be relied upon to be accur enough to warrant the paper's conclusi comment, and discussion.

The speculative questions raised rega ing the motors' performance are also in authors' minds; as yet no satisfact answers have been forthcoming.

Regarding Mr. Brightman's suggest to utilize a reverse power relay as a block relay to utility underfrequency excursi certain precautions should be mention If it happens that a true tripping und frequency occurs simultaneously with li or no kilowatt load other than the s chronous motors, then it appears possi that the reverse power relay may fail remove its blocking function prompt thus preventing a legitimate trip. A if the synchronous motors drive normally pulsating load, then, at li loading with high power factor the revers power relay may pulse with the lo negating its blocking function and p mitting false trips on utility frequen excursions. Some more positive block means is desirable for this critical re application.

Power Apparatus and Systems—October 1959

AIEE PUBLICATIONS

	Member Prices	Nonmember Prices: Basic Prices*†	Nonmember Prices: Extra Postage for Foreign Subscription
Electrical Engineering			
Official monthly publication containing articles of broad interest, technical papers, digests, and news sections: Institute Activities, Current Interest, New Products, Industrial Notes, and Trade Literature. Automatically sent to all members and enrolled students in consideration of payment of dues. (Members may not reduce the amount of their dues payment by reason of nonsubscription.) Additional subscriptions are available at the nonmember rates.		annually $12*	$1.00
		Single copies $1.50*	
Bimonthly Publications			
Containing all officially approved technical papers collated with discussion (if any) in three broad fields of subject matter as follows:			
	annually	annually	
Communication and Electronics	$5.00	$8.00*	$0.75
Applications and Industry	$5.00	$8.00*	$0.75
Power Apparatus and Systems	$5.00	$8.00*	$0.75
Each member may subscribe to any one, two, or all three bimonthly publications at the rate of $5.00 each per year. A second subscription to any or all of the bimonthly publications may be obtained at the nonmember rate of $8.00 each per year.			
Single copies may be obtained when available.	$1.50 each	$1.50* each	
AIEE Transactions			
An annual volume in three parts containing all officially approved technical papers with discussions corresponding to six issues of the bimonthly publication of the same name bound in cloth with a stiff cover.			
	annually	annually	
Part I Communication and Electronics	$4.00	$8.00*	$0.75
Part II Applications and Industry	$4.00	$8.00*	$0.75
Part III Power Apparatus and Systems	$4.00	$8.00*	$0.75
Annual subscription to all three parts (beginning with vol. 77 for 1958).	$10.00	$20.00*	$2.25
Annual subscription to any two parts.		$15.00*	$1.50
AIEE Standards			
Listing of Standards, test codes, and reports with prices furnished on request.			
Special Publications			
Committee reports on special subjects, bibliographies, surveys, and papers and discussions of some specialized technical conferences, as announced in ELECTRICAL ENGINEERING.			

*Discount 25% of basic nonmember prices to college and public libraries. Publishers and subscription agencies 15% of basic nonmember prices. For available discounts on Standards and special publications, obtain price lists from Order Department at Headquarters.

†Foreign prices payable New York exchange

Send all orders to:

Order Department
American Institute of Electrical Engineers
33 West 39th Street, New York 18, N. Y.